FLEXURAL BEHAVIOUR OF BEAMS RESTING ON ELASTIC MEDIA

HOSSEIN ATEFI

A THESIS SUBMITTED FOR THE DEGREE OF

DOCTOR OF PHILOSOPHY

Department of Civil Engineering
University of Aston in Birmingham

August 1975

SUMMARY

This thesis is concerned with the analysis of beams resting on elastically deformable media. In particular, the analytical studies are restricted to the treatment of infinite and finite beams subjected to concentrated and distributed loadings. Integral expressions are derived for the plane strain and three dimensional problems of the infinite beam resting on an isotropic homogeneous and non-homogeneous (plane strain) media.

The solution to the problem of the finite beam is obtained by using the solution developed for the infinite beam together with a superposition technique. The numerical values of the integral expressions are tabulated for the finite and infinite beam. The results of contact force distribution, obtained from the superpositon technique, are then compared with the results obtained from Barden's and Ohde's approximate solutions. The influence of the length to width ratio of a beam, subjected to a central concentrated load, on contact force distribution is also investigated.

Laboratory model tests have been conducted on finite beams of different flexibility which rest on a granular subgrade. These tests have been carried out under both two dimensional plane strain, and three dimensional conditions. These experimental results are compared with the theoretical analyses which assume both Winkler and elastic continum behaviour of the granular medium.

ACKNOWLEDGEMENTS

The Author would like to express his gratitude to his tutor, Dr A P S Selvadurai, for his advice and encouragement.

Thanks are also due to the team of technicians in the Department of Civil Engineering for help in the experimental work.

Sincere thanks to Miss D Bailey for carefully typing the script.

The Author would also like to thank the staff of the Aston Computer Centre for their service.

CONTENTS

CONTENTS (contd)

CONTENTS (contd)

CONTENTS (contd)

CONTENTS (contd)

CHAPTER ONE

INTRODUCTION

1.1 Introduction

Shallow foundations are frequently designed and constructed in the form of beams resting on soil media and subjected to external loads. The important step in the design of such foundations is to obtain the manner in which the contact stress is distributed at the beam-soil medium interface. The simple assumption of linear distribution of contact stress disregards the effect of flexibility of the beam and mechanical properties of the soil medium on contact stress distribution.

A rational design approach should take into consideration the influence of factors such as flexibility of the foundation, flexibility of the superstructure, time independent and time dependent deformational characteristics of the soil medium and the nature of external loading. However, there are as yet no efficient techniques which take into account the influence of all the above factors in the design of foundations. The existing techniques for the design of foundations accounts only for the effect of the flexibility of the foundation and the deformational characteristics of the soil medium.

In order to take into consideration the effect of mechanical properties of soil in the analysis of soil foundation interaction problems, it is necessary to have a knowledge of the complete stress-strain characteristics of the soil. A complete stress-strain relationship for soil will furnish the stress and strains

in a soil medium at any particular time under any given loading condition.

Owing to the variety of soils and soil conditions encountered in engineering practice such a generalized stress-strain relationship cannot be developed to fulfil the requirements of every type of soil behaviour.

The inherent complexity in the behaviour of real soil has led to the development of many idealized models of soil behaviour, especially for the analysis of soil foundation interaction problems. The relevant choice of an idealized behaviour of soil for a soil foundation interaction problem will depend primarily on the type of soil and soil conditions, the type of foundation and the nature of external loading. A brief discussion of some idealized models which form the point of view of soil foundation interaction problems is given in the following sections.

1.2 Idealized Soil Models

1.2.1 The Winkler Model

The idealized model of soil media proposed by Winkler (1867) assumes that the soil consists of closely spaced, independent linear springs. The relation between the deflection W of the soil medium at any point on the surface, is then proportional to the stress, p, (applied load per unit area) at that point and independent of stresses at other points.

$$p(x,y) = kw(x,y) \qquad (1.1)$$

where k is termed the modulus of subgrade reaction with units of stress per unit length. For this particular model, the displacement of the loaded area will be constant whether the foundation is subjected to infinitely rigid load or a uniform flexible load (Figure 1.1). In addition, for both types of loading the displacements are zero outside the loaded region.

1.2.2 The elastic solid model

A serious objection can be made to the inability of the Winkler model to produce any deflection outside the loaded area. The simplifying assumptions made in the Winkler's hypothesis restricts its applicability to soil media which possess the slightest amount of cohesion and transmibility of load. It is obvious that in the case of soil media surface deflections will occur not only immediately under the loaded region but also within certain limited zones outside the loaded area. In an attempt to account for this continuous behaviour, the soil media have been treated as an elastic continuum. The problem of semi-infinite homogeneous isotropic linear elastic medium subjected to a concentrated load acting normal to the plane boundary was first analysed by Boussinesq (1885). This basic solution can be used to obtain the response function for the three dimensional elastic soil medium.

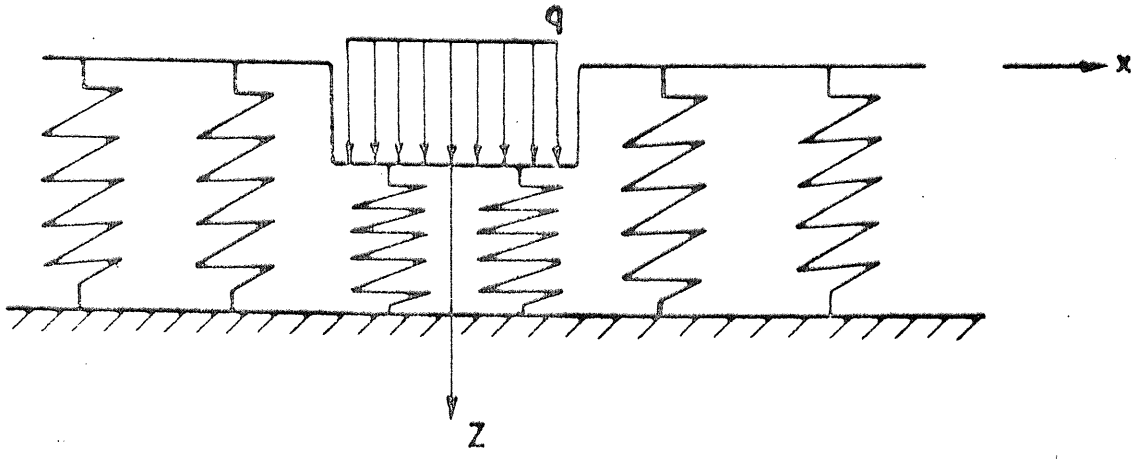

(a.)

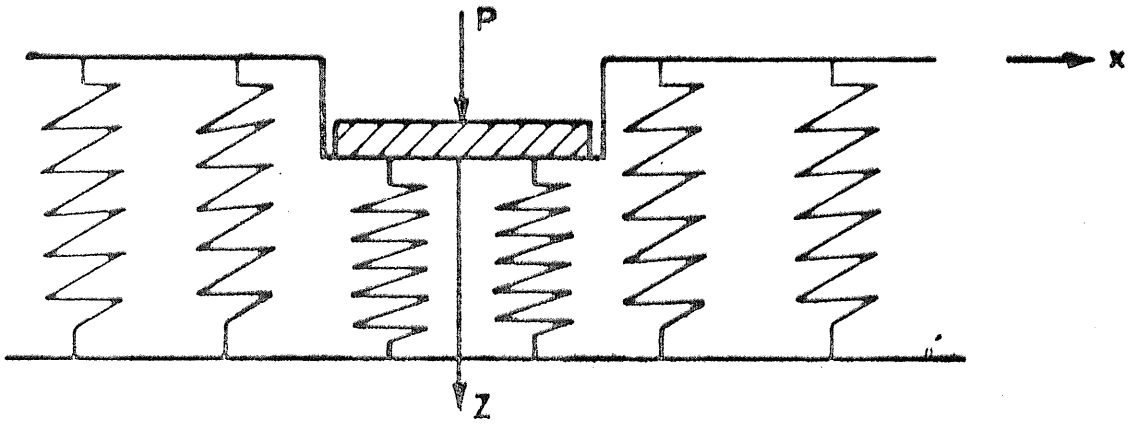

Fig. 1. 1 Deformation of the Winkler model due to

a. uniform flexible load
b rigid load

In general, the application of the theory of classical elasticity to soil-foundation interaction problems presents a complex mathematical problem. References on a number of solutions to boundary value problems of particular interest to soil foundation interaction are given by Selvadurai (1975).

1.2.3 Two parameter models

The inability of the Winkler's model to account for the continuous behaviour of the soil and the mathematical complexities involved in representing the soil medium with an elastic continuum model have led to the development of many other models. In an attempt to find a physically close and mathematically simple representation of a model for the behaviour of the soil medium, one may approach the problem in two ways. In the first approach the discontinuity between the spring elements of Winkler model is eliminated by introducing some kind of interaction between the spring elements. Such physical models of soil behaviour have been proposed by Filanenko-Borodich (1940), Hetenyi (1950) and Pasternak (1954). The second approach starts with the elastic continuum model and introduces simplifying assumptions with respect to the distribution of displacements and stresses. Such a simplification is taken into consideration in the soil models proposed by Reissner (1958) and Vlasov (1966). A comprehensive review of the two parameter models is given by Kerr (1964). Here, a brief discussion of these models is given.

(a) Filonenko-Borodich Model

In this model the interaction between spring elements in the Winkler model is provided by connecting the top ends of the spring elements to a stretched elastic membrane subjected to a constant tension T as shown in Figure (1.2). By considering the equilibrium of the membrane-spring system in the z direction, it can be shown that for the three dimensional problem the load-displacement relation is given by

$$p(x,y) = kw(x,y) - T\nabla^2 w(x,y) \qquad (1.2)$$

where

$$\nabla^2 = \frac{\partial^2}{\partial x^2} + \frac{\partial^2}{\partial y^2}$$

is Laplace's differential operator in rectangular cartesian coordinates. In the case of the two dimensional problem (1.2) reduces to

$$p(x) = k w(x) - T\frac{\partial^2 w}{\partial x^2} \qquad (1.3)$$

From (1.2) and (1.3) it can be seen that this model is characterised by the rigidity of spring elements and the intensity of tension T in the membrane.

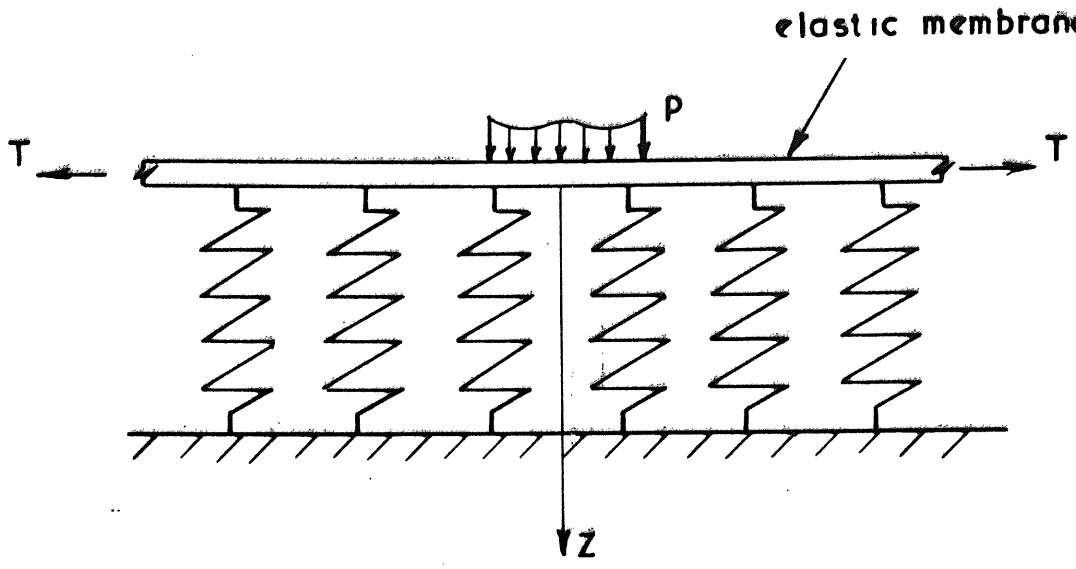

Fig. 1.2 Filonenko – Borodich model

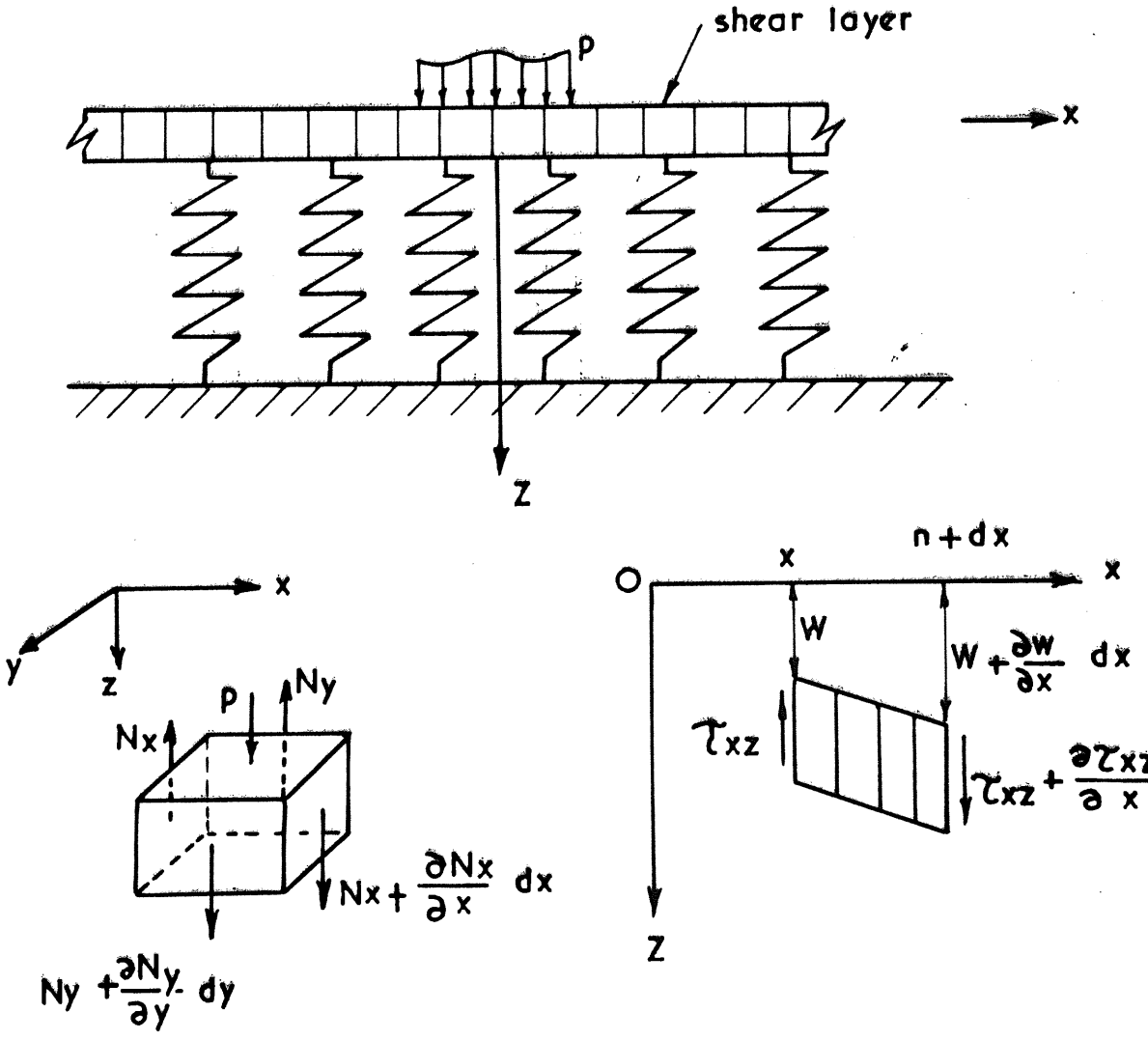

Fig. 1.3 The Pasternak model

(b) Hetenyi Model

In this model which was proposed by Hetenyi (1950), the interaction between spring elements is provided by imbedding, in the two dimensional case an elastic beam and in the three dimensional case an elastic plate, in the material of Winkler foundation. It is assumed that the imbedded beam or plate deforms in bending only. The relation between p and deflection w for the three dimensional case is

$$p(x,y) = kw(x,y) - D\nabla^2\nabla^2 w \qquad (1.4)$$

where

$$D = \frac{Eb^3}{12(1-\nu^2)}$$

and

$$\nabla^2\nabla^2 w = \frac{\partial^4}{\partial x^4} + \frac{2\partial^4}{\partial x^2 \partial y^2} + \frac{\partial^4}{\partial y^4}$$

for the two dimensional problem (1.4) reduces to

$$p(x) = kw(x) + \frac{Eb^3}{12} \frac{\partial^4 w}{\partial x^4}$$

(c) Pasternak Model

The model to represent the soil behaviour proposed by Pasternak (1954) assumes the existence of shear interactions between the spring elements. This can be accomplished by

connecting the ends of the springs to a beam or plate consisting of incompressible vertical elements which deform in transverse shear only (Figure 1.3). Consider the vertical equilibrium of a shear layer element cut out by the surfaces x, x + dx, y and y + dy as shown in Figure (1.3). By assuming that the shear layer is isotropic in the x,y plane with shear modulus $G_x = G_y = G$ we have

$$\tau_{xz} = G_x\gamma_{xz} = G\frac{\partial w}{\partial x}$$

$$\tau_{yz} = G_y\gamma_{yz} = G\frac{\partial w}{\partial y} \qquad (1.5)$$

The shear forces per unit length of the shear layer are

$$N_x = \int_0^1 \tau_{xz}\,dz = G\frac{\partial w}{\partial x}$$

$$N_y = \int_0^1 \tau_{yz}\,dz = G\frac{\partial w}{\partial y} \qquad (1.6)$$

For force equilibrium in the z direction

$$\frac{\partial N_x}{\partial x} + \frac{\partial N_y}{\partial y} + p - kw = 0$$

or

$$p(x,y) = kw(x,y) - G\nabla^2 w(x,y) \qquad (1.7)$$

It can be seen that by replacing G by T, equation (1.7) becomes identical to (1.3).

(d) Vlasov Model

The model of soil response proposed by Vlasov (1949) approaches the problem from an elastic continuum point of view and introduces displacement constraints that simplify the basic equation for a linear elastic medium. By imposing certain restrictions upon the possible distribution of displacements in an elastic layer, Vlasov was able to obtain a soil response function similar in character to (1.3) and (1.7).

(e) Reissner Model

The model which was proposed by Reissner (1958) is derived by assuming that the in plane stresses (in the x,y plane) throughout the soil layer of thickness H are negligibly small

$$\sigma_x = \sigma_y = \tau_{xy} = 0 \qquad (1.8)$$

and the displacement components u, v and w in the rectangular cartesian coordinate directions x, y, z satisfy conditions

$$u = v = w = 0 \quad \text{on } Z = H$$

$$v = u = 0 \quad \text{on } Z = 0$$

It can be shown that the response function for this model is given by

$$c_1 w - c_2 \nabla^2 w = p + \frac{c_2}{4c_1} \nabla^2 p \qquad (1.9)$$

where p is the external load and w is the vertical displacement at Z = 0 and

$$c_1 = \frac{E_f}{H} \qquad c_2 = \frac{HG_f}{3}$$

E_f and G_f are the Young's modulus and shear modulus of the soil layer. For a constant or linearly varying p after redefining of constants $c_1 = k$ and $c_2 = G$ equation (1.9)is identical to (1.7).

A consequence of assumption (1.8) is that the shear stresses τ_{zx} and τ_{zy} are independent of z and hence are constant throughout the layer. Such an assumption is unrealistic particularly for thick soil layers. Since this model is introduced to study the response of the soil surface to loads and not the stresses induced within the layer, this particular deficiency (assumption 1.8) may, in general, be of no serious consequence.

1.3 Beams resting on idealized models of foundations

Assuming that there is no loss of contact at the beam-soil medium interface, the differential equation for the deflection of a beam resting on soil medium is

$$E_b I \frac{d^4 w}{dx^4} + p = q \qquad (1.10)$$

where p is the contact force (contact stress x width of the beam) at the beam medium interface, and q is applied load (load per width, per unit length of the beam). By substituting in (1.10) for p in terms of w from the response function of a particular model. the differential equation can be solved to obtain the deflection of the beam.

Due to limitation of space it is not intended to discuss the analysis of beams resting on all types of idealized models. The analysis of infinite and finite beams resting on two and three dimensional elastic continuum model forms the major part of the thesis and therefore are discussed in separate chapters (chapter 2, 3 and 4). In the following we briefly discuss the analysis of beams resting on Winkler medium.

1.4 Beams resting on Winkler model

The general differential equation governing the deflected shape of a beam resting on Winkler medium is

$$EI \frac{d^4w}{dx^4} + Kw = q \qquad (1.11)$$

where q is the external applied load and EI is the flexural rigidity of the beam.

The solution of (1.11) is

$$w(x) = e^{\lambda x}[c_1 \cos\lambda x + c_2 \sin\lambda x] + e^{-\lambda x}[c_3 \cos\lambda x + c_4 \sin\lambda x] \qquad (1.12)$$

where

$$\lambda = \sqrt[4]{\frac{K}{4EI}}$$

and c_1, c_2, c_3 and c_4 can be determined by making use of boundary conditions at the ends of the beam.

The main difficulty in applying the general solution given by (1.12) to a particular problem arises in the determination of the integration constants which involves a considerable amount of work. To avoid the mathematical difficulties Hetenyi (1947) proposed the method of superposition. In this method the solution for the infinite beam subjected to a concentrated load is used to obtain the solution to the infinite and finite beam subjected to different types of loadings.

The deflected shape of an infinite beam loaded by a concentrated force P applied at the origin (Figure 1.4) is given by

$$w(x) = \frac{P\lambda}{2K} e^{-\lambda x}[\cos\lambda x + \sin\lambda x] \qquad (1.13)$$

where K = Bk and B is the width of the beam.

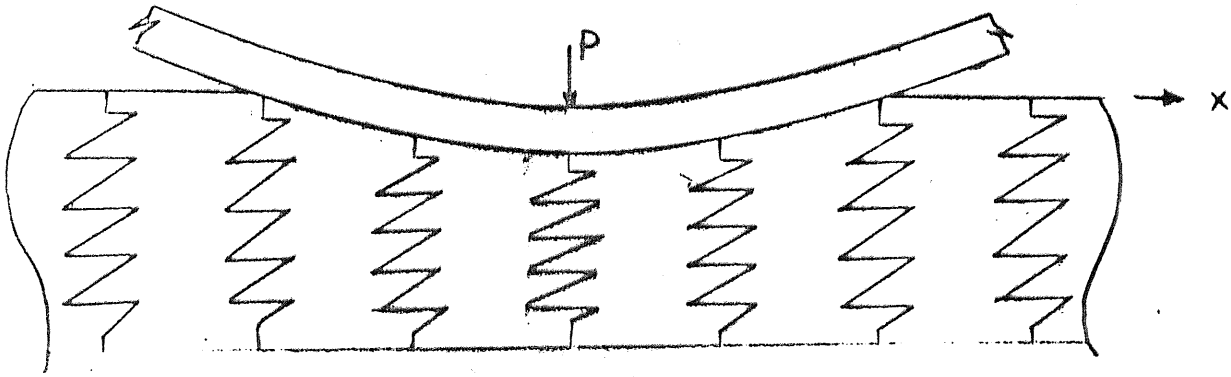

Fig .1.4 Infinite beam on a Winkler medium.

The slope (θ), bending moment (M) and shearing force (V) are related to the deflection of the beam by

$$\theta = \frac{dw}{dx} \quad , \quad M = -E_b I \frac{d^2w}{dx^2} \quad , \quad V = -E_b I \frac{d^3w}{dx^3} \qquad (1.14)$$

By using (1.13) in (1.14) we have

$$\theta(x) = \frac{P\lambda^2}{K} e^{-\lambda x} \sin\lambda x$$

$$M(x) = \frac{P}{4\lambda} e^{-\lambda x} [\cos\lambda x - \sin\lambda x]$$

$$V(x) = -\frac{P}{2} e^{-\lambda x} \cos\lambda x$$

For the details of three and two dimensional analysis of beams on two parameter foundation model see Selvadurai (1975).

1.5 Scope of the Work

The major part of the work is concerned with the analysis of the beams resting on an isotropic homogeneous and non homogeneous elastic medium. The two and three dimensional analysis of an infinite beam resting on an isotropic homogeneous elastic medium and subjected to a concentrated load, a concentrated couple and a uniform distributed load is given in chapter 2. The integral expressions are obtained for the deflection (w), bending moment (M),

shearing force (V) and contact force (Q). The numerical values of these integrals are tabulated in Appendix 1. Analytical expressions are obtained for the maximum deflection, bending moment and contact force of an infinite beam subjected to a concentrated force P. These expressions are then equated to those obtained from the Winkler analysis to obtain values for the modulus of subgrade reaction in terms of the flexural rigidity of the beam and the elastic properties of the medium.

The analysis of the finite beam is discussed in chapter 3. The solution for the infinite beam problem is used, by employing the superposition technique, to analyse the finite beam subjected to a concentrated load, a concentrated couple, and a uniform distributed load at an arbitrary location. The integral expression for W, M, V and Q of the beams with different length subjected to a concentrated load and a concentrated couple, for both two and three dimensional media, are evaluated and given in Appendix 1. The results of the contact force distribution of a beam resting on a three dimensional elastic medium and subjected to a concentrated central load are then compared with the results obtained from the two approximate methods of solution (Barden's and Ohde's methods), and the effect of length to width ratio of the beam on the results discussed.

The differential equation governing the displacement function of a plane strain problem of an isotropic non-homogeneous incompressible elastic medium is developed in chapter 4. The

solution is then used to analyse beams resting on such a non-homogeneous incompressible medium for the case when the shear modulus G is a linear function of the depth. In this chapter the effect of non-homogeneity of the medium on the deflection, bending moment and contact force distribution of the infinite and finite beam subjected to a concentrated load and a concentrated couple is investigated. The numerical results for W, M, V and Q for the finite and infinite beams are given in Appendix 1.

In order to investigate the validity of the theoretical analysis discussed in chapters 2 and 3 for the particular case when the medium is a granular material, a series of model tests with the steel model beams of different stiffness were carried out. The description of apparatus for the three and two dimensional model tests, and experimental procedures are discussed in chapter 5.

The content of chapter 6 is the analysis of experimental results.

In chapter 7 the results of the plate loading tests for the evaluation of the mechanical properties of granular material are given. These properties are used to carry out the theoretical analysis of the beams, assuming Winkler and elastic behaviour of the granular material. The theoretical results are then compared with the experimental results.

CHAPTER TWO

INFINITE BEAM ON ELASTIC MEDIUM

2.1 Introduction

The analysis of an infinite beam resting on a homogeneous isotropic elastic half space and subjected to a concentrated force, was first given by Biot (1937). Vesic (1961) later extended this work to include the case of an infinite beam subjected to a concentrated couple. The analyses given by Biot and Vesic are restricted to the class of slender beams whose bending response is governed by the classical Bernoulli-Euler theory of beams. Briefly, this particular beam theory is based on the following assumptions:

1) The cross sections of the beam remain plane and normal to the axis of bending.

2) The strains and rotations of the beam are small compared to unity.

3) The deflections due to shearing stresses are neglected.

4) The beams are assumed to be straight and prismatic with dimension proportions that will prevent failure by twisting, lateral collapse or local wrinkling.

A more accurate solution of the infinite beam problem can be obtained by treating the beam as an elastic layer of finite thickness (see Hetenyi, 1946).

In this chapter, we shall outline Biot's solution and extend it to the case where the infinite beam is subjected to a uniform distributed load of finite length.

2.2 Semi Infinite Elastic Medium Subjected to a Sinusoidal Load

2.2.1 Plane strain problem of the elastic half space

We consider the plane strain problem (Fig. 2.1) of an isotropic elastic half space which is subjected to a sinusoidal normal load of the form

$$Q(x) = Q_o \cos\lambda x \qquad (2.1)$$

where Q(x) is the intensity of the load per width 2b and unit length (Fig. 2.1). The problem is reduced to obtaining a solution to the biharmonic equation (see Timoshenko and Goodier, 1970).

$$\frac{\partial^4 F}{\partial x^4} + 2\frac{\partial^4 F}{\partial x^2 \partial z^2} + \frac{\partial^4 F}{\partial z^4} = o,$$

subject to the following boundary conditions :

$$\sigma_x = \sigma_z = \tau_{xz} = o, \quad \text{for } z = \infty,$$

$$\sigma_z = -\frac{Q_o}{2b}\cos\lambda x, \quad \tau_{xz} = o, \text{ for } z = o$$

The stress components σ_x, σ_z and τ_{xz}, are given by

$$\sigma_x = \frac{\partial^2 F}{\partial z^2},$$

$$\sigma_z = \frac{\partial^2 F}{\partial x^2}, \qquad (2.2)$$

$$\tau_{xz} = \frac{-\partial^2 F}{\partial x \partial z}$$

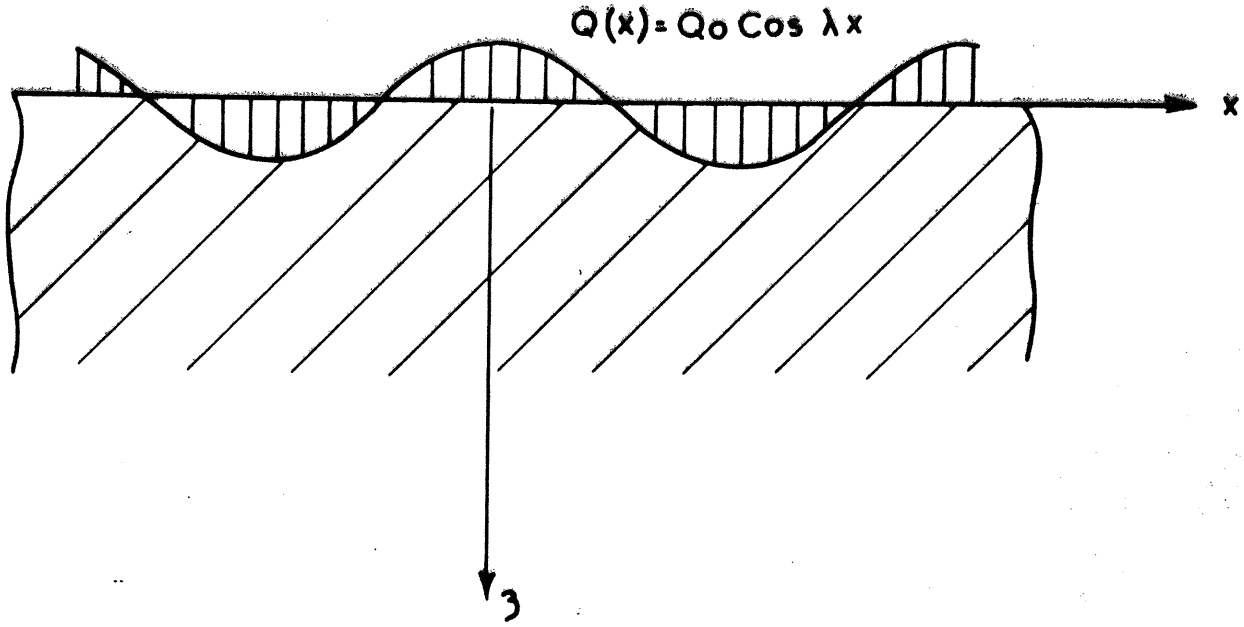

Fig. 2.1 The plane strain problem of infinite half space subjected to a sinusoidal load

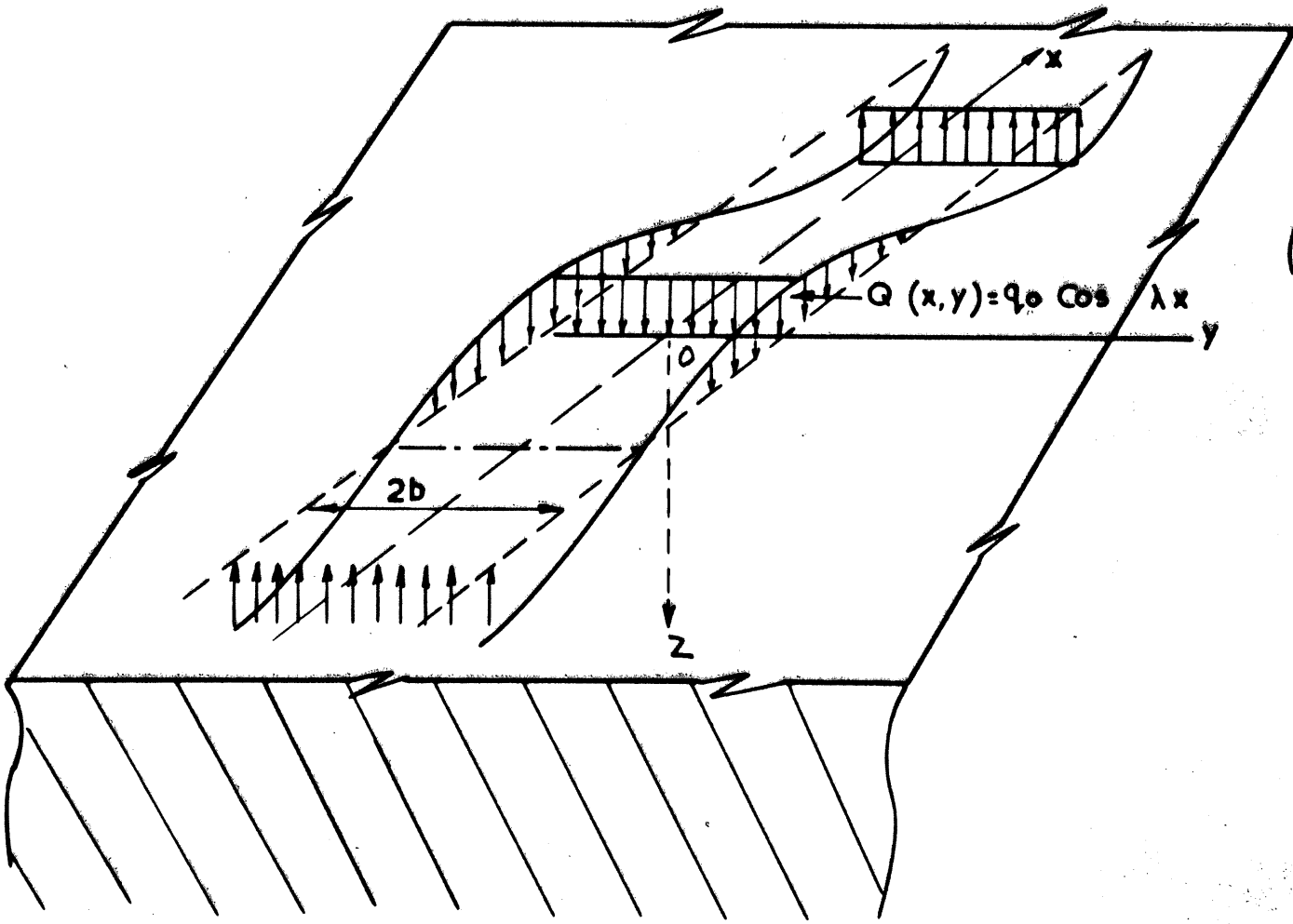

Fig. 2.2. The infinite half space subjected to a sinusoidal load

The complete stress function is given by

$$F = \frac{Q_o}{2b\lambda^2} e^{-\lambda z}(1 + \lambda z)\cos\lambda x \qquad (2.3)$$

By considering the stress-strain relations for an isotropic, homogeneous elastic material, we obtain the following expression for the strain $\varepsilon_z (= \frac{\partial w}{\partial z})$, where w is the displacement in the positive z direction.

$$\frac{\partial w}{\partial z} = \frac{1}{E}[(1-\nu^2)\sigma_z - \nu(1+\nu)\sigma_x], \quad (2.4)$$

In (2.4) E is the modulus of elasticity and ν the Poisson's ratio of the medium. The stress components σ_x, σ_z are obtained by substituting (2.3) in (2.2). By substituting σ_x, σ_z in (2.4) and integrating the resulting expression, we obtain

$$w = \frac{Q_o}{b\lambda E}(1-\nu^2)\cos\lambda x + f(x), \qquad (2.5)$$

where f(x) can be identified as a rigid body motion which can be set equal to zero without loss of generality.

It may be concluded that a sinusoidal loading of the type (2.1) produces a sinusoidal surface displacement

$$w = \frac{(1-\nu^2)}{b\lambda E} Q(x) \qquad (2.6)$$

2.2.2 Three dimensional problem of the elastic half space

Consider a semi infinite homogeneous isotropic elastic half space subjected to the double sinusoidal normal stress

$$q(x) = q_o \cos\lambda x \cos\delta y$$

The equations of equilibrium, in terms of displacements u, v and w (in the positive direction of the rectangular Cartesian coordinate) of a point within the medium, are given by Timoshenko and Goodier, 1970

$$\nabla^2 u + \frac{1}{1-2\nu} \frac{\partial e}{\partial x} = 0 ,$$

$$\nabla^2 w + \frac{1}{1-2\nu} \frac{\partial e}{\partial z} = 0 , \qquad (2.7)$$

$$\nabla^2 v + \frac{1}{1-2\nu} \frac{\partial e}{\partial y} = 0 ,$$

where

$$e = \frac{\partial u}{\partial x} + \frac{\partial w}{\partial z} + \frac{\partial v}{\partial y} , \qquad \nabla^2 = \frac{\partial^2}{\partial x^2} + \frac{\partial^2}{\partial z^2} + \frac{\partial^2}{\partial y^2}$$

A solution of equations (2.7) is to be found in which

1) Shear stresses are zero on the surface (z = 0),
i.e. smooth interface.

2) The stress components σ_x, σ_z tend to zero as $z \to \infty$

In addition, the solution for u, v and w would be doubly sinusoidal in x and y directions. It can be verified (Love, 1944), that the solutions, satisfying these conditions and equations of equilibrium (2.7), are

$$u = \frac{A}{\delta}\left[z - \frac{1-2\nu}{\sqrt{\lambda^2+\delta^2}}\right] e^{-z\sqrt{(\lambda^2+\delta^2)}} \sin\lambda x \cos\delta y$$

$$v = \frac{A}{\lambda}\left[z - \frac{1-2\nu}{\sqrt{(\lambda^2+\delta^2)}}\right] e^{-z\sqrt{(\lambda^2+\delta^2)}} \cos\lambda x \sin\delta y$$

$$w = \frac{A}{\lambda\delta}\left[z\sqrt{(\lambda^2+\delta^2+2(1-\nu)}\right] e^{-z\sqrt{(\lambda^2+\delta^2)}} \cos\lambda x \cos\delta y$$

where A is an arbitrary constant.

The surface displacement in the z direction is

$$w(o) = \frac{2A}{\lambda\delta}(1-\nu)\cos\lambda x \cos\delta y, \qquad (2.8)$$

and the corresponding normal stress is

$$q(x) = -\sigma_z = \frac{AE}{1+\nu}\frac{\sqrt{(\lambda^2+\delta^2)}}{\lambda\delta} \cos\lambda x \cos\delta y \qquad (2.9)$$

From (2.8) and (2.9) we obtain the following relationship between q(x) and w(o)

$$w(o) = 2\frac{1-\nu^2}{E\sqrt{(\lambda^2+\delta^2)}}\, q(x) \qquad (2.10)$$

Consider the isotropic elastic half space acted upon by a sinusoidal normal load

$$q_1(x,y) = q_o(y)\cos\lambda x \tag{2.11}$$

as shown in Fig. 2.2. This load is located within the region $y = \pm b$. In (2.11), $q_o(y)$ is a function of y in such a way that it is equal to zero when $y< -b$, $y>b$ and equal to q_o for all values of y in the interval $+b > y > -b$. We express $q_o(y)$ as a sum of sine functions in the form

$$q_o(y) = \frac{q_o}{\pi}\int_o^\infty \frac{1}{\delta}[\sin\delta(y+b) - \sin\delta(y-b)]d\delta \tag{2.12}$$

The surface displacement of the medium corresponding to the load $q_1(x,y)$ given by (2.11) can be expressed in the form

$$w_1(x,y) = w_o(y)\cos\lambda x, \tag{2.13}$$

where $w_o(y)$ represents the displacement of the medium along any cross section parallel to the y-axis. The value of $w_o(y)$ can be obtained by applying equation (2.10) to each of the elements of the loading given by (2.12), we then obtain

$$w_o(y) = \frac{Q_o}{\pi}\,\frac{1-\nu^2}{E}\,\frac{1}{\beta}\left\{\phi(\gamma_1\beta) - \phi(\gamma_2\beta)\right\} \tag{2.14}$$

where

$$\gamma_1 = \frac{y}{b} + 1, \qquad \gamma_2 = \frac{y}{b} - 1,$$

$$Q_o = 2q_o b, \qquad \beta = \lambda b,$$

and

$$\phi(\xi) = \int_o^\xi k_o(u)\,du \tag{2.15}$$

In (2.15), $k_o(u)$ is the zero-order Bessel function of the second kind, (of modified Hankel's type), given by (see Watson, 1922)

$$k_o(u) = \int_o^\infty \frac{\cos(\gamma\alpha)}{\sqrt{\alpha^2 + \beta^2}}$$

where

$$\alpha = \delta b$$

The average deflection w_{avg} across the width 2b is defined as

$$w_{avg} = \frac{1}{2b} \int_{-b}^{+b} w_o(y)dy \qquad (2.16)$$

By substituting (2.14) in (2.16) and evaluating the integral numerically we obtain the following relationship between Q_o and w_{avg}

$$\frac{Q_o}{w_{avg}} = \frac{E}{1-\nu^2} \beta\psi(\beta) \qquad (2.17)$$

In (2.17), $\psi(\beta)$ may be tabulated as follows, for $\beta > 0.1$

β	0.1	0.5	1.0	3.0	8.0	∞
$\psi(\beta)$	4.80	1.90	1.42	1.13	1.04	1

For $\beta < 0.1$ the function $\psi(\beta)$ takes the asymptotic form (see Biot, 1937).

$$\psi(\beta) = \frac{\pi}{2\beta} \left[\log\frac{1}{\beta} + 0.923\right]^{-1} \qquad (2.18)$$

So far we assumed that the distribution of sinusoidal load across the width 2b is uniform. The effect of changing the distribution of the loading in y direction is now investigated for $\beta = 1$. The average load (Q_{avg}) in the y-direction is

$$Q_{avg} = \frac{1}{2b} \int_{-b}^{+b} q_o(y)dy$$

If the loading is constant ($Q_{avg} = q_o$) across the width 2b ($b > y > -b$), as shown in Fig. (2.2), the corresponding deflection is given by curve a (Fig. 2.3). Now, consider the loading shown in Fig. 2.4. The deflection across the width 2b was found to be nearly uniform (see curve b in Fig. 2.3). It is found that a 3.1 per cent increase in the average loading (Fig. 2.4), causes a 17 per cent increase in the average deflection (Fig. 2.3). That is, the ratio Q_{avg}/w_{avg} can become 1.17/1.03 (= 1.13) times as large, between the case when q_o is a constant across the width of the beam, and the case when $w_o(y)$ is nearly constant, when $\beta = 1$. Equation (2.17) can now be written as (see Biot, 1937)

$$\frac{Q_{avg}}{w_{avg}} = \frac{Q_o}{Cw_{avg}} = \frac{E}{C(1-\nu^2)} \beta\psi(\beta) \qquad (2.19)$$

where C is a coefficient which varies from unity for a constant pressure distribution q_o across the width of the beam to 1.13 for uniform deflection w_o across the width of the beam. The effects of changing the distribution of the loading across the width 2b was investigated for a special case $\beta = 1$. The margin of variation of C in (2.19) is generally much smaller for $o < \beta < 1$ and $\infty > \beta > 1$, and tends to zero for $\beta = o$, or $\beta = \infty$.

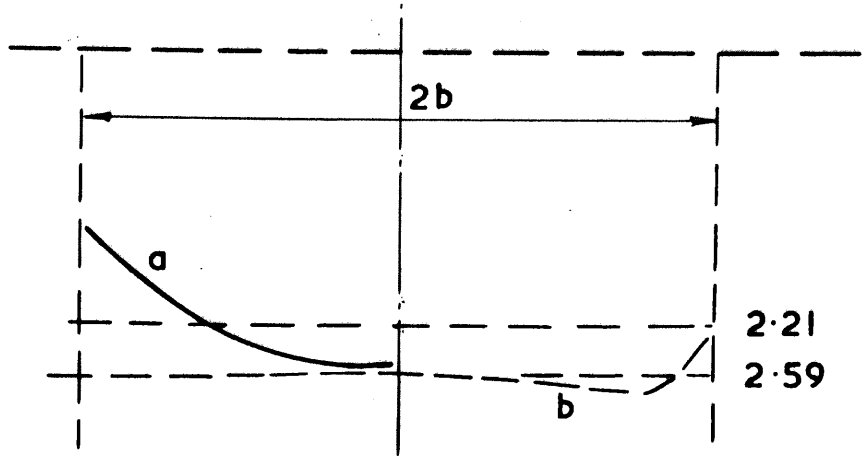

Fig. 2.3. The displacements corresponding to the loadings shown in fig 2.4

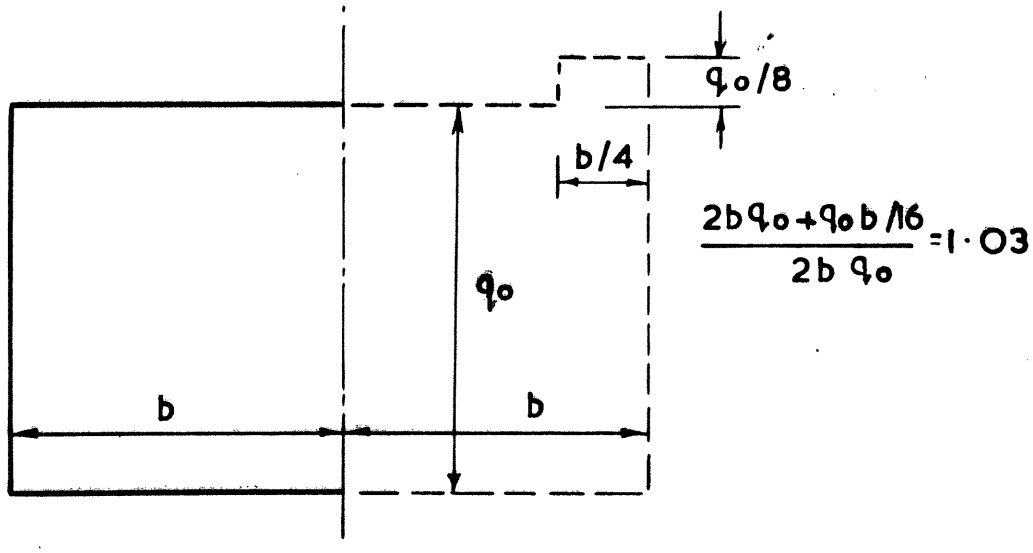

Fig. 2.4. The corresponding loadings for displacements a & b. of fig 2.3

2.3 The Infinite Beam Problem

Consider an infinite beam, resting on an elastic, homogeneous and isotropic medium (Fig. 2.5a), and subjected to a sinusoidal external load p(x) per unit length

$$p(x) = p_o \cos\lambda x \tag{2.20}$$

where p_o is a constant.

It is assumed that there is no loss of contact at the beam-elastic medium interface. The reactive force Q(x) is assumed to be in the form of a sinusoidal distribution (Fig. 2.5b) of the type

$$Q(x) = Q_o \cos\lambda x \tag{2.21}$$

where Q_o is the constant.

The relationship between the deflection W(x) of the beam and the reactive force Q(x) is

$$W(x) = \frac{Q_o}{F} \cos\lambda x \tag{2.22}$$

where for the plane strain problem of the elastic half space, from (2.6) F is given by

$$F = \frac{bE\lambda}{(1-\nu^2)}$$

From (2.19) it is evident that for the three-dimensional problem of the elastic half space

$$F = \frac{E}{C(1-\nu^2)} \beta\psi(\beta)$$

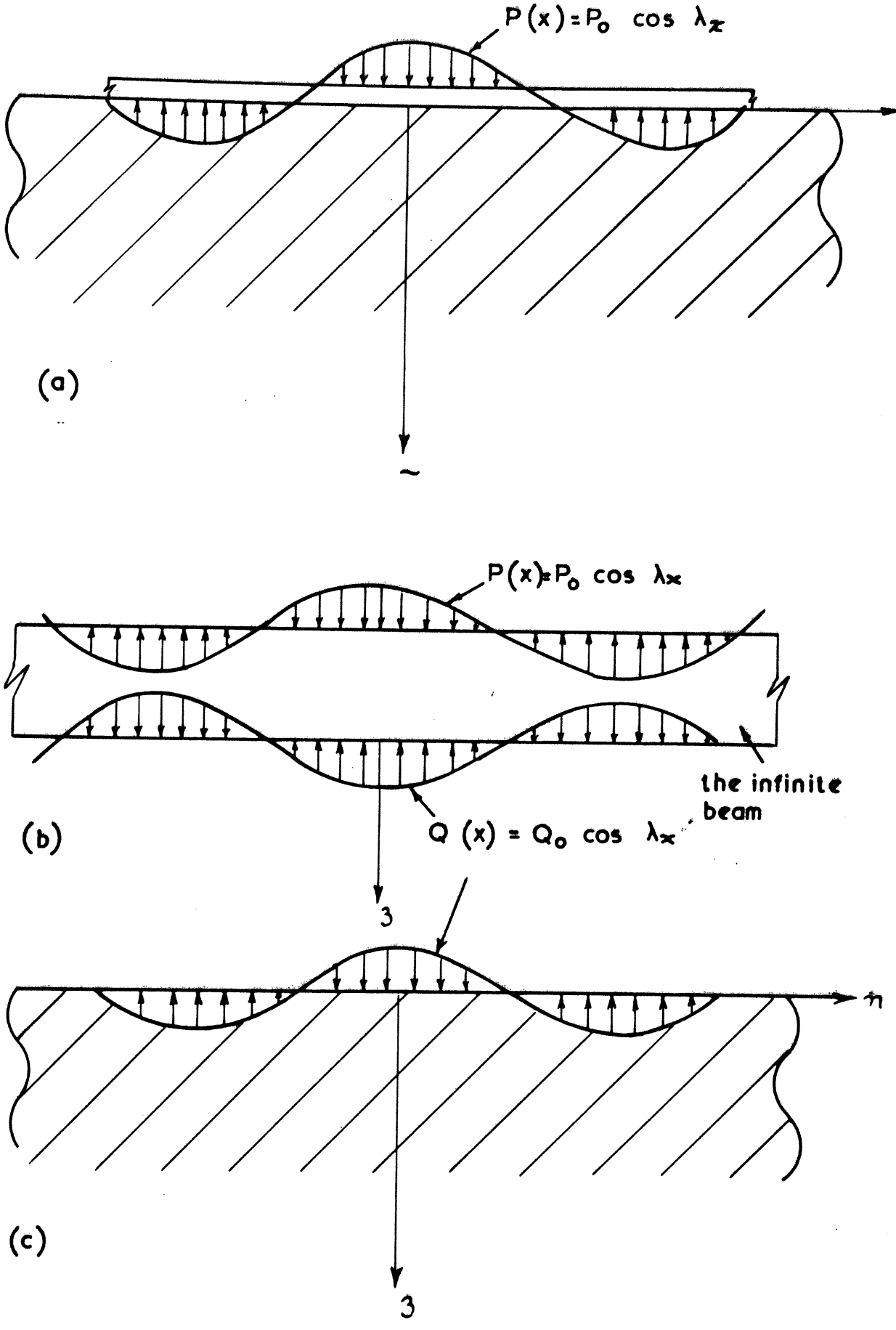

Fig. 2.5. The infinite beam subjected to a sinusoidal load

The differential equation governing the deflection W(x) of the beam is

$$E_b I \frac{d^4 W(x)}{dx^4} = P(x) - Q(x) \qquad (2.23)$$

where $E_b I$ is the flexural rigidity of the beam.

By making use of (2.20), (2.21), (2.22) and (2.23) it can be shown that the deflection W(x) of the beam due to sinusoidal external loading P(x) is given by

$$W(x) = \frac{P_o \cos\lambda x}{\lambda^4 E_b I + F} \qquad (2.24)$$

By a superposition of the external loads of the type (2.20) any arbitrary loadings P(x), symmetrical about the y-axis, can be expressed as a Fourier integral, in the following form :-

$$P(x) = \int_o^\infty \bar{P}(\lambda) \cos\lambda x \, d\lambda \qquad (2.25)$$

where

$$\bar{P}(\lambda) = \frac{2}{\pi} \int_o^\infty P(\xi) \cos\lambda\xi \, d\xi$$

2.4 Infinite beam loaded by a uniform load of finite length

Consider the problem of an infinite beam which is subjected to a uniform load of intensity p per unit length, and of length 2a. In this case expression (2.25) for this external loading reduces to

$$P(x) = \frac{2p}{\pi} \int_o^\infty \frac{\sin\lambda a}{\lambda} \cos\lambda x \, d\lambda \qquad (2.26)$$

From (2.24) we note that each element of this loading

$$\frac{2p}{\pi} \frac{\sin\lambda a}{\lambda} \cos\lambda x d\lambda$$

produces a deflection

$$dW(x) = \frac{2p}{\pi} \frac{\sin\lambda a}{\lambda(\lambda^4 E_b I+F)} \cos\lambda x d\lambda$$

The total deflection W(x) due to the uniform strip load can be obtained as an integral of these deflections, i.e.

$$W(x) = \frac{2p}{\pi} \int_o^\infty \frac{\sin\lambda a}{\lambda(\lambda^4 E_b I+F)} \cos\lambda x d\lambda$$

or

$$W(x) = \frac{2pc^4}{E_b I\pi} J_{ou}(X) \qquad (2.27)$$

where

$$J_{ou}(X) = \int_o^\infty \frac{\sin(\alpha a')}{\alpha^2(\alpha^3+\Omega)} \cos(\alpha X) d\alpha \qquad (2.27a)$$

In (2.27a) $a' = a/c$, $X = x/c$,

for the plane strain problem of the elastic half space, we have

$$c = \left[\frac{E_b I(1-\nu^2)}{Eb}\right]^{1/3}$$

$$\Omega = 1 \qquad (2.28)$$

for a three dimensional problem of the elastic half space

$$c = \left[C(1-\nu^2)\frac{E_b I}{Eb}\right]^{1/3}$$

$$\Omega = \psi(\beta) \qquad (2.29)$$

The flexural moments in the beam are given by

$$M(x) = -EI\frac{d^2W(x)}{dx^2} \tag{2.30}$$

Similarly, the shearing force V(x) and the contact force, Q(x) are given by

$$V(x) = \frac{dM(x)}{dx} \quad , \quad Q(x) = p(x) - EI\frac{d^4W(x)}{d^4x} \tag{2.31}$$

By using (2.27), (2.30) and (2.31) respectively, we obtain the following expressions for M(x), V(x) and Q(x) (reaction per width 2b and unit length of the beam).

$$M(x) = \frac{2pc^2}{\pi} J_{2u}(X),$$

$$V(x) = \frac{2pc}{\pi} J_{3u}(X), \tag{2.32 a-c}$$

$$Q(x) = \frac{2p}{\pi} J_{4u}(X)$$

where

$$J_{2u}(X) = \int_o^\infty \frac{\sin(\alpha a')}{\alpha^3+\Omega} \cos(\alpha X)d\alpha$$

$$J_{3u}(X) = \int_o^\infty \frac{\alpha\sin(\alpha a')}{\alpha^3+\Omega} \sin(\alpha X)d\alpha \tag{2.33 a-c}$$

$$J_{4u}(X) = \int_o^\infty \frac{\Omega\sin(\alpha a')}{\alpha(\alpha^3+\Omega)} \cos(\alpha X)d\alpha$$

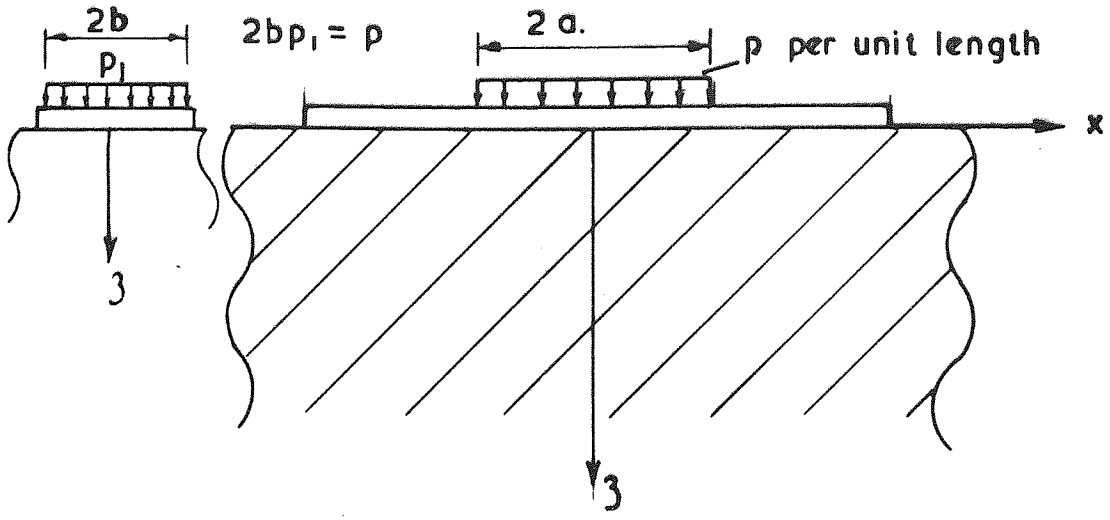

Fig. 2.6 The infinite beam subjected to a uniform load.

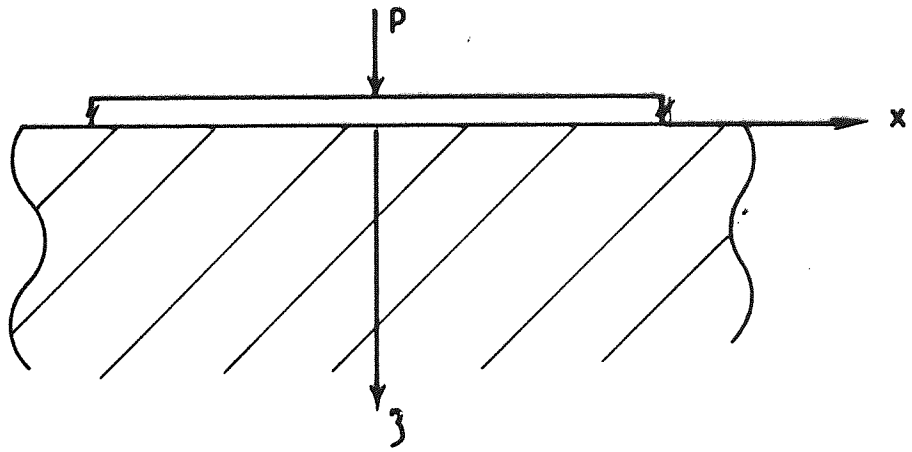

Fig 2.7 The infinite beam subjected to a concentrated force

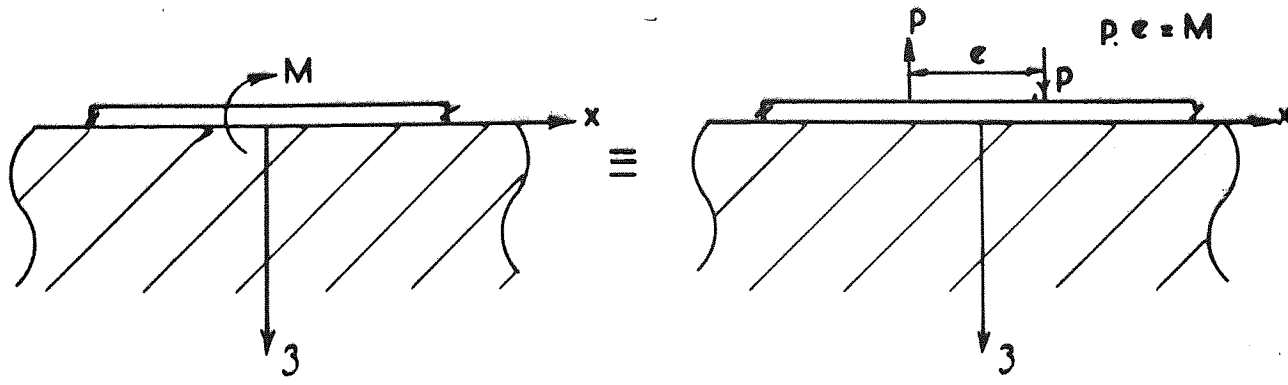

Fig. 2.8. The infinite beam subjected to a concentrated couple

2.5 Infinite beam subjected to a concentrated force

The solution to the problem of an infinite beam loaded by a concentrated line force of intensity P (total load across the width of the beam) at the origin (Fig. 2.7) can now be obtained as a limit of the case, where the width of the strip load $2a \to o$, and the total load per unit length $2pa \to P$. Considering that

$$\underset{\alpha a' \to o}{\text{Lt}} \frac{\sin(\alpha a')}{\alpha\, a'} = 1$$

from (2.27) and (2.32 a-c), the expressions for W(x), M(x), V(x) and Q(x) are given by

$$W(x) = \frac{Pc^3}{\pi E_b I} J_{op}(X)$$

$$M(x) = \frac{Pc}{\pi} J_{2p}(X) \qquad (2.34\ a\text{-}d)$$

$$V(x) = -\frac{P}{\pi} J_{3p}(X)$$

$$Q(x) = \frac{P}{c\pi} J_{4p}(X)$$

where

$$J_{op}(X) = \int_o^\infty \frac{\cos(\alpha X)}{\alpha(\alpha^3+\Omega)}\, d\alpha, \qquad J_{2p}(X) = \int_o^\infty \frac{\alpha\cos(\alpha X)}{\alpha^3\ \Omega}\, d\alpha$$

$$J_{3p}(X) = \int_o^\infty \frac{\alpha^2 \sin(\alpha X)}{\alpha^3+\Omega}\, d\alpha, \qquad J_{4p}(X) = \int_o^\infty \frac{\Omega\cos(\alpha X)}{\alpha^3+\Omega}\, d\alpha$$

(2.35 a-d)

2.6 Infinite beam loaded by a concentrated couple

A couple, M, acting on the infinite beam can be represented as a limiting case of a combination of two concentrated forces acting a small distance (e) apart, as shown in Fig. 2.8. It is assumed that as $e \to o$, Pe approaches the value, M. Using (2.34a), the equation of the deflected shape can be written as

$$W(x) = \frac{Pc^3}{\pi E_b I} \left[J_{op}(X+e/c) - J_{op}(X) \right] \tag{2.36}$$

Using the condition $Pe \to M$ as $e \to o$ (2.36) is expressed as

$$W(x) = \frac{M c^2}{\pi E_b I} \frac{dJ_{op}(X)}{dX}$$

By differentiating $J_{op}(x)$ (equation 2.35a) with respect to X, the expression for W(x) can be given by

$$W(x) = \frac{Mc^2}{\pi EI} J_{1p}(X) \tag{2.37}$$

where

$$J_{1p}(X) = \int_o^\infty \frac{\sin(\alpha X)}{\alpha^3 + \Omega} d\alpha \tag{2.38}$$

The expressions for M(x), V(x), and Q(x) are

$$M(x) = \frac{M}{\pi} J_{3p}(X),$$

$$V(x) = \frac{M}{c\pi} J_{4p}(X), \tag{2.39 a-c}$$

$$Q(x) = \frac{M}{c^2 \pi} J_{5p}(X)$$

where

$$J_{5p}(X) = \int_o^\infty \frac{\alpha\Omega \sin(\alpha X)}{\alpha^3 + \Omega} d\alpha \tag{2.40}$$

2.7 The integrals involved in the analysis

In order to evaluate the deflections, bending moments, shearing forces, etc., for the case of the infinite beam, and the finite beam, subjected to a concentrated load, a concentrated couple, and a uniform distributed load, it becomes necessary to evaluate the integrals $J_{np}(X)$ and $J_{nu}(X)$ given by equations (2.35 a-d), (2.38), (2.27a), and (2.32a-c). These integrals, however, cannot be expressed in an explicit form. Therefore approximate numerical techniques are generally employed for their evaluation (see Biot, 1937; Vesic, 1961; Drapkin, 1955).

2.7.1 The function $\psi(\beta)$

We note that for the three dimensional problem of the elastic half space all these integrals are dependent upon the function $\psi(\beta)$. The function $\psi(\beta)$ takes into account the three dimensional effect of the supporting medium (see section 2.2.2). This function is tabulated by Biot, 1937, for $\infty > \beta > 0.1$ and given by a logarithmic expression (equation 2.18) for $\beta < 0.1$. The numerical evaluation of the integrals requires an explicit expression for $\psi(\beta)$, which represents this function for the whole range of $\alpha(\infty > \alpha > 0)$. Drapkin, 1955, suggests a hyperbolic curve for this function in the form of

$$\psi(\beta) = 1 + \frac{a}{\beta} \qquad (2.41)$$

in which a is a constant and is obtained by fitting the hyperbolic representation (2.41) to Biot's logarithmic expression for $\beta < 0.1$.

Using the method of least squares, Drapkin found a = 0.34. It was found that for upper range of β ($\infty > \beta > 0.1$), the corresponding values for $\psi(\beta)$ from (2.41) is in close agreement with Biot's tabulated values. The hyperbolic representation of $\psi(\beta)$ (equation 2.41) and Biot's values for the function (logarithmic representation for $\beta < 0.1$ and tabulated values for $\infty > \beta > 0.1$) are shown in Fig. 2.9. In evaluation of the integrals, the hyperbolic representation given by (2.41) is used for the function $\psi(\beta)$ for the whole range of β ($\infty > \beta > 0$).

2.7.2 Evaluation of Integrals $J_{np}(X)$

A technique which was used by Vesic, 1961, is employed for the evaluation of the integrals $J_{op}(x)$, $J_{1p}(x)$ ..... $J_{5p}(x)$, involved in the analysis of infinite beam resting on a three dimensional medium. Since the same procedure is used for evaluation of all the above integrals, the method is explained in detail for one of these integrals. $J_{1p}(x)$ is given by

$$J_{1p}(X) = \int_{o}^{\infty} \frac{\sin(\alpha X)}{\alpha^3 + \psi(\beta)}$$

is chosen as a typical example. The integrand of this integral is a convergent oscillating curve which is shown in Fig. 2.10. First the integral is divided into two parts, i.e.

$$\left| J_{1p}(X) \right|_{o}^{\infty} = \left| J_{1p}(X) \right|_{o}^{\alpha_m} + \left| J_{1p}(X) \right|_{\alpha_m}^{\infty} \qquad (2.42)$$

where α_m is the value of α for point M (Fig. 2.10).

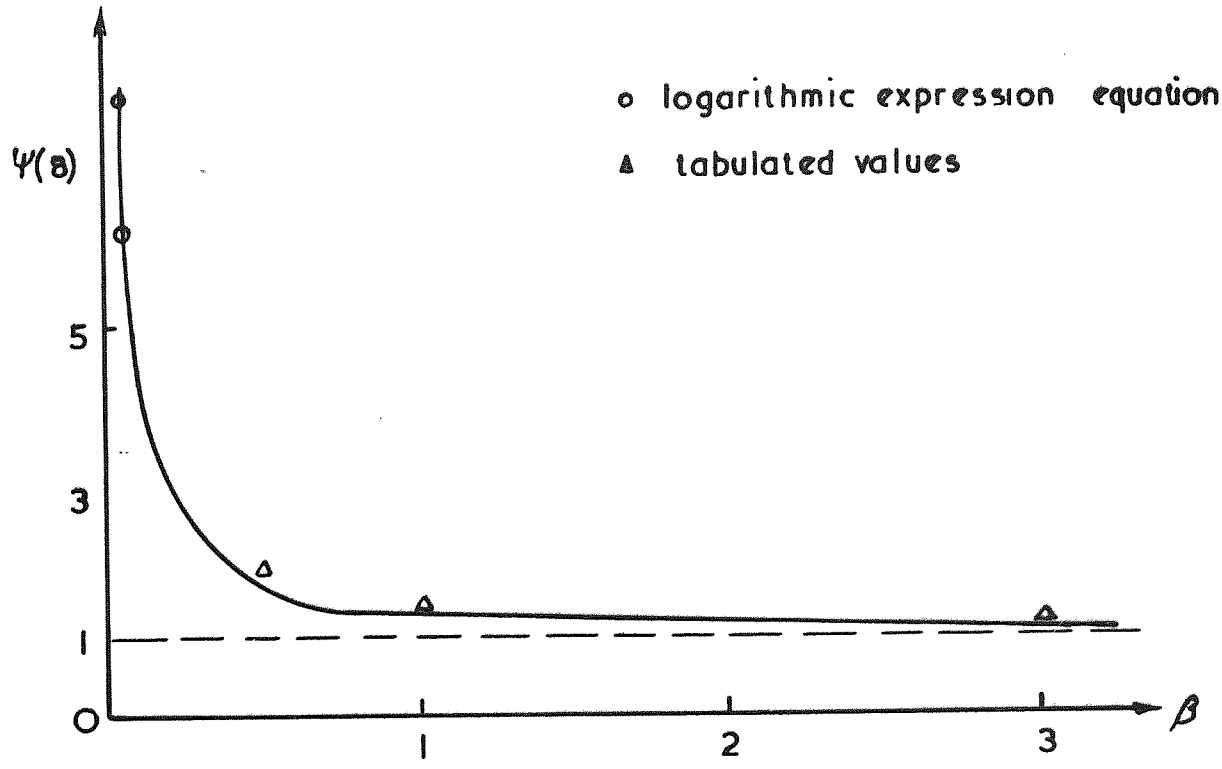

Fig 2.9. Variation of $\psi(\beta)$ with β (after Drapkin 1955)

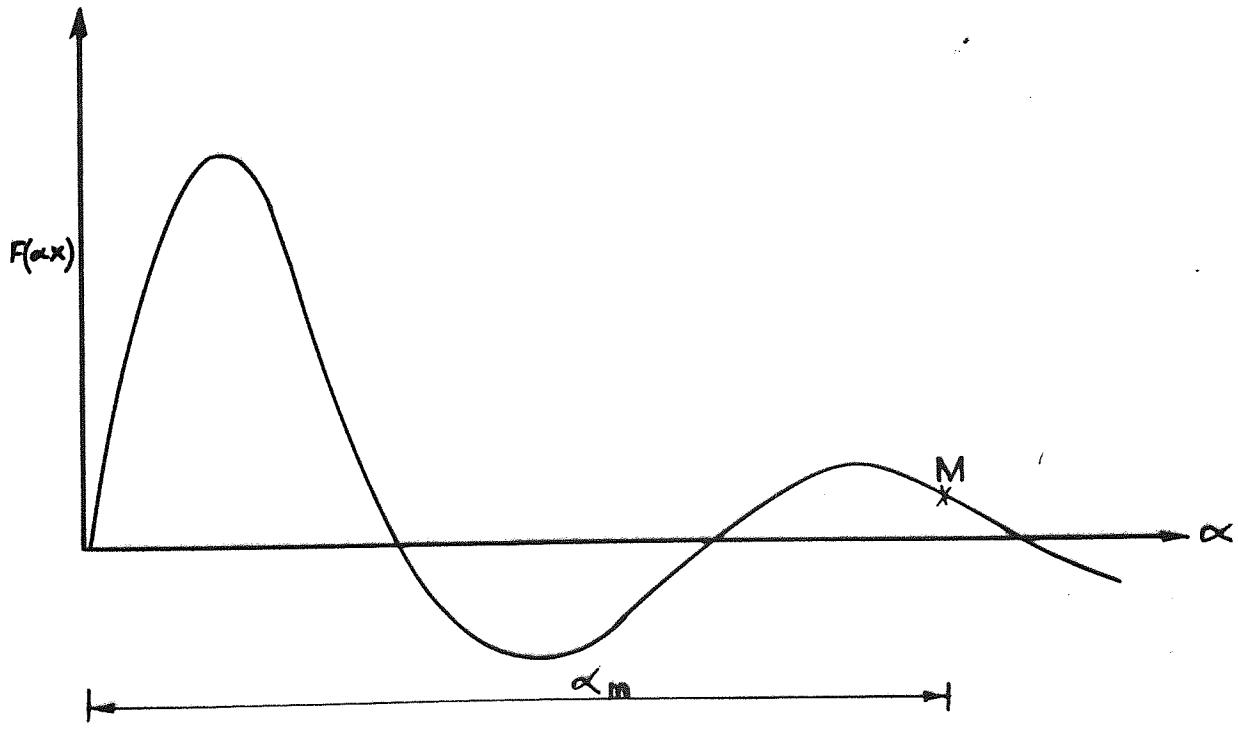

Fig. 2.10. Variation of the integrand of $J_{1p}^{(x)} = \int_0^{\infty} (\alpha x)$ with α

The first part of the integral ($|J_{1p}(X)|_{o}^{\alpha_m}$) is integrated by interpolation, using Simpson's rule. The second part ($|J_{1p}(X)|_{\alpha_m}^{\infty}$) can be integrated, partly numerically, and partly analytically, by employing the following approximation

$$|J_{1p}(X)|_{\alpha_m}^{\infty} = \int_{\alpha_m}^{\infty} \frac{\sin(\alpha X)}{\alpha^3+\psi(\beta)}\, d\alpha \simeq \int_{\alpha_m}^{\infty} \frac{\sin(\alpha X)}{\alpha^3}\, d\alpha \qquad (2.43)$$

The amount of error involved in making the above approximation will be discussed in a later section (section 2.9). Integrating (2.43) by parts we obtain

$$\int_{\alpha_m}^{\infty} \frac{\sin(\alpha X)}{\alpha^3}\, d\alpha = \frac{\sin(\alpha_m X)}{2\alpha_m^2} + x/2 \left[\frac{\cos(\alpha_m X)}{\alpha_m} - \frac{\pi x}{2} + xSi(\alpha_m X)\right]$$

where $Si(\alpha_m X)$ is a sine integral given by

$$Si(\alpha_m X) = \int_{o}^{\alpha_m x} \frac{\sin\nu}{\nu}\, d\nu \qquad (2.44)$$

The same procedure is followed for the evaluation of integrals $J_{2p}(X)$ ..... $J_{5p}(X)$, that is; up to a certain point, M, these integrals are evaluated numerically and from point M onwards, i.e. $\infty > \alpha > \alpha_m$ (α_m is the value of α at point M), the approximation similar to (2.43) is made. For the rest of the integrals $|J_{np}(X)|_{\alpha_m}^{\infty}$ is given as follows

$$|J_{2p}(X)|_{\alpha_m}^{\infty} = \int_{\alpha_m}^{\infty} \frac{\alpha\cos(\alpha X)}{\alpha^3+\psi(\beta)}\, d\alpha \simeq \int_{m}^{\infty} \frac{\cos(\alpha X)}{\alpha^2}\, d\alpha,$$

or

$$|J_{2p}(X)|_{\alpha_m}^{\infty} \simeq \frac{\cos(\alpha_m X)}{\alpha_m} - x\pi/2 + xSi(\alpha_m X) \qquad (2.45)$$

$$\left| J_{3p}(\chi) \right|_{\alpha_m}^{\infty} = \int_{\alpha_m}^{\infty} \frac{\alpha^2 \sin(\alpha X)}{\alpha^3 + \psi(\beta)}\, d\alpha \simeq \int_{\alpha_m}^{\infty} \frac{\sin(\alpha X)}{\alpha}\, d\alpha$$

or

$$\left| J_{3p}(X) \right|_{\alpha_m}^{\infty} \simeq \pi/2 - Si(\alpha_m X) \tag{2.46}$$

$$\left| J_{4p}(X) \right|_{\alpha_m}^{\infty} = \int_{\alpha_m}^{\infty} \frac{\psi(\beta)\cos(\alpha X)}{\alpha^3 + \psi(\beta)}\, d\alpha \simeq \int_{\alpha_m}^{\infty} \frac{\cos(\alpha X)}{\alpha^3}\, d\alpha$$

or

$$\left| J_{4p}(X) \right|_{\alpha_m}^{\infty} \simeq \frac{\cos(\alpha_m X)}{2\alpha^2{}_m} + X/2 \left[\frac{\sin(\alpha_m X)}{\alpha_m} + X Ci(\alpha_m X) \right] \tag{2.47}$$

Where in (2.47) $Ci(\alpha_m X)$ is a cosine integral

$$Ci(\alpha_m X) = \int_{\infty}^{\alpha_m X} \frac{\cos\nu}{\nu}\, d\nu \tag{2.48}$$

For $J_{op}(X) = \int_{o}^{\infty} \frac{\cos(\alpha X)}{\alpha(\alpha^3+\psi(\beta))}\, d\alpha$, due to the infinite value of the integrand of this integral, the procedure is slightly different. The integral is divided into three parts, as follows

$$\left| J_{op}(X) \right|_{o}^{\infty} = \left| J_{op}(X) \right|_{o}^{\varepsilon} + \left| J_{op}(X) \right|_{\varepsilon}^{\alpha_m} + \left| J_{op}(X) \right|_{\alpha_m}^{\infty} \tag{2.49}$$

where ε is an abscissa, small in comparison with unity ($\varepsilon = 0.00001$). To evaluate $\left| J_{op}(X) \right|_{o}^{\varepsilon}$ it should be noted that, for small enough value of α, $\cos(\alpha X) \simeq 1$, and α^4 becomes negligible compared with $\alpha\psi(\beta)$.

Therefore,

$$|J_{op}(X)|_{o}^{\varepsilon} = \int_{o}^{\varepsilon} \frac{\cos(\alpha X)}{\alpha[\alpha^3+\psi(\beta)]}\, d\alpha \simeq \int_{o}^{\varepsilon} \frac{d\alpha}{\alpha\psi(\beta)} \qquad (2.50)$$

By substituting for $\psi(\beta)$ from (2.41), we have

$$|J_{op}(X)|_{o}^{\varepsilon} \simeq \log_e[(b/c)(\varepsilon + 0.34/b/c)/0.34] \qquad (2.51)$$

The second part of integral (ie $|J_{op}(X)|_{\varepsilon}^{\alpha_m}$) can only be evaluated numerically. For the third part (ie $|J_{op}(X)|_{\alpha_m}^{\infty}$) the following approximation is employed.

$$|J_{op}(X)|_{\alpha_m}^{\infty} = \int_{\alpha_m}^{\infty} \frac{\cos(\alpha X)}{\alpha(\alpha^3+\psi(\beta))}\, d\alpha \simeq \int_{\alpha_m}^{\infty} \frac{\cos(\alpha X)}{\alpha^4}\, d\alpha \qquad (2.52)$$

Integrating (2.51) by parts we have

$$|J_{op}(X)|_{\alpha_m}^{\infty} \simeq \frac{\cos(\alpha_m X)}{3\alpha_m^3} - \frac{x^2\cos(\alpha_m X)}{6\alpha_m} + \frac{X^3}{6}[\pi/2 - Si(\alpha_m X)] - \frac{X\sin(\alpha_m X)}{6\alpha_m^2} \qquad (2.53)$$

For the case of the two dimensional analyses, the procedure for the evaluation of integrals is the same as the three dimensional case, except $\psi(\beta)$ is replaced by unity. The integrals $J_{op}(X)$ and $J_{ou}(X)$ in the case of two dimensional problems are infinite (the integrands

of these integrals are infinite at $\alpha = 0$) for all values of X. It is therefore impossible to represent absolute values for the integrals $J_{op}(X)$ and $J_{ou}(X)$. To overcome this difficulty, the integrals $J_{op}(X)$ and $J_{ou}(X)$ are evaluated relative to their values at X = 0, (i.e. $J_{op}(o)$ and $J_{ou}(o)$) as follows

$$J_{op}(X) - J_{op}(o) = \int_o^\infty \frac{[\cos(\alpha X) - 1]}{\alpha(\alpha^3 + 1)} \, d\alpha$$

$$J_{ou}(X) - J_{ou}(o) = \int_o^\infty \frac{[\cos(\alpha X) - 1]}{\alpha(\alpha^3 + 1)} \sin(\alpha a) \, d\alpha \qquad (2.54)$$

It can be shown that the integrands of the integrals (2.54), are zero at $\alpha = 0$, and have finite values for $\infty > \alpha > 0$.

2.7.3 Evaluation of integrals $J_{nu}(X)$

In evaluating the integrals $J_{nu}(X)$ (equations 2.27a and 2.33 a-c), the integrals are first divided into two parts as follows :

$$\left| J_{nu}(X) \right|_o^\infty = \left| J_{nu}(X) \right|_o^{\alpha_m} + \left| J_{nu}(X) \right|_{\alpha_m}^\infty$$

The first part of the integral $\left(\left| J_{nu}(X) \right|_o^{\alpha_m} \right)$ is evaluated numerically using Simpson's rule. For the second part $\left(\left| J_{nu}(X) \right|_{\alpha_m}^\infty \right)$, the integrals can not be further simplified by employing an approximation similar to that given by (2.43). The first part of the integrals can then be taken as the value of integral with the value of α_m such that a further increase in the value of α_m does not change the value of

$|J_{nu}(X)|_{o}^{\alpha_m}$ significantly. The effect of a change in α_m on the value of $|J_{nu}(X)|_{o}^{\alpha_m}$ is discussed in a later section (section 2.9).

2.8 Numerical Results

The University's ICL 1905E computer was used to obtain numerical values for the integrals $J_{np}(X)$ and $J_{nu}(X)$. In the programme which was developed for this purpose, the standard routines F4INTSMP, S12ABA, and S13ACA, were used (see ref.[21]). The first routine (i.e. F4INTSMP) employs Simpson's rule to evaluate the integrals between the limits zero and α_m (α_m refers to the abscissa of point M in Fig. 2.10). This upper limit was chosen to be twenty (i.e. $\alpha_m = 20$). The effect of a change in the value of α_m on the numerical values of integrals $J_{np}(X)$ and $J_{nu}(X)$ is discussed in a later section (section 2.9). The maximum error in the values of the integrals due to numerical integration is limited to $\pm$ 0.1%. The routines S13ABA and S13ACA evaluate the sine and cosine integrals (equations 2.44 and 2.48). The numerical values for the integrals $J_{np}(X)$ for both three and two dimensional problems of an infinite beam are tabulated in appendix 1. The distribution of deflection, bending moment and contact force for an infinite beam resting on an isotropic homogeneous elastic medium and subjected to a concentrated load, a concentrated couple and a uniform load, for both three and two dimensional media for different values of B/2c are given in Figures (2.11) to (2.16). For the two dimensional problem, since the integrals involved in the expressions for the deflection of the beam subjected to concentrated and uniform load are infinite for all values of X (integrals 2.27a and 2.35a with the function $\Omega = 1$), the deflected shape of the beam is evaluated [W(0)-W(x)] instead of absolute values of deflections (Figures 2.13 and 2.16a).

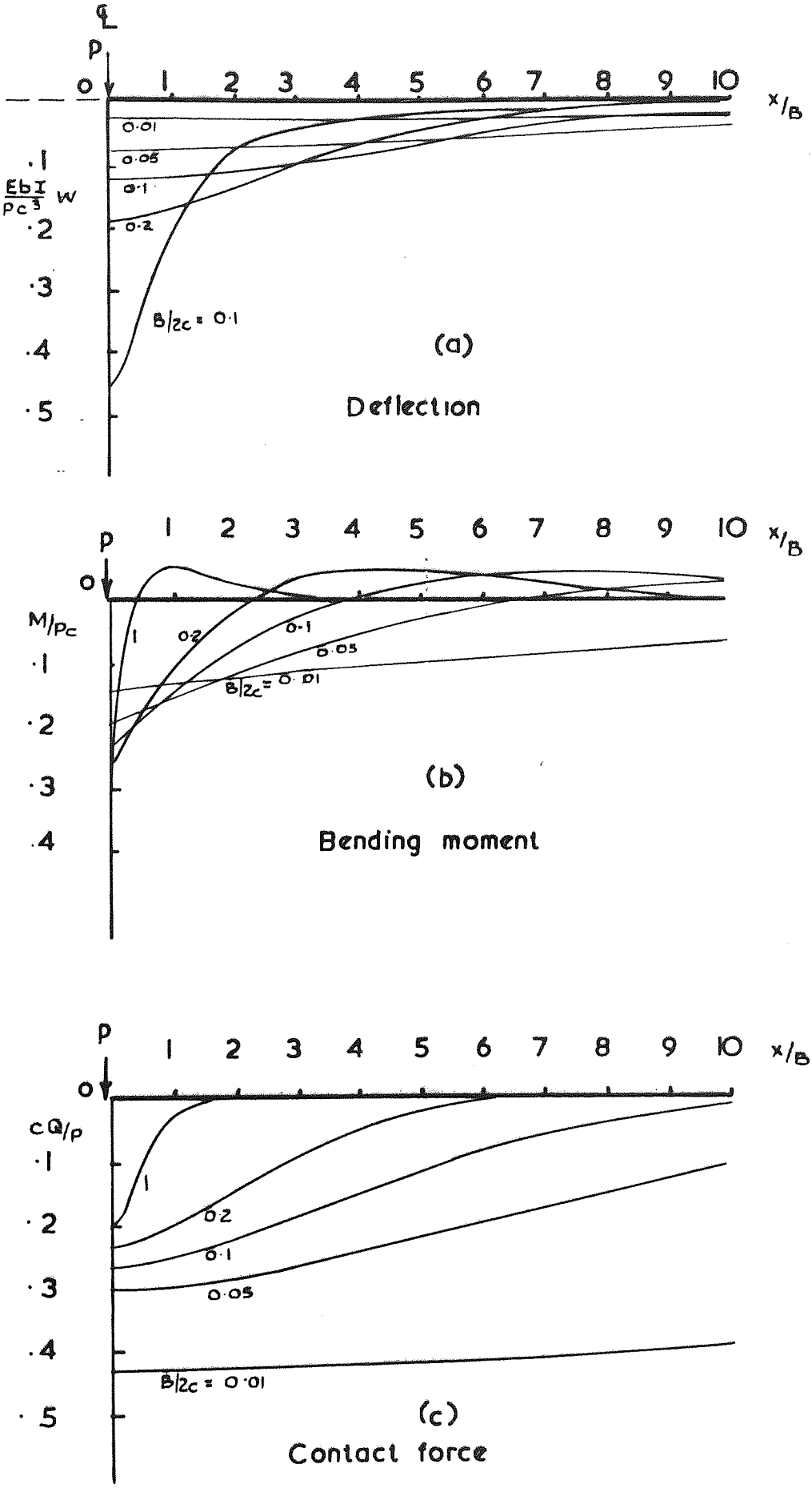

Fig. 2.11. Infinite beam subjected to a concentrated load (Three Dimensional Problem)

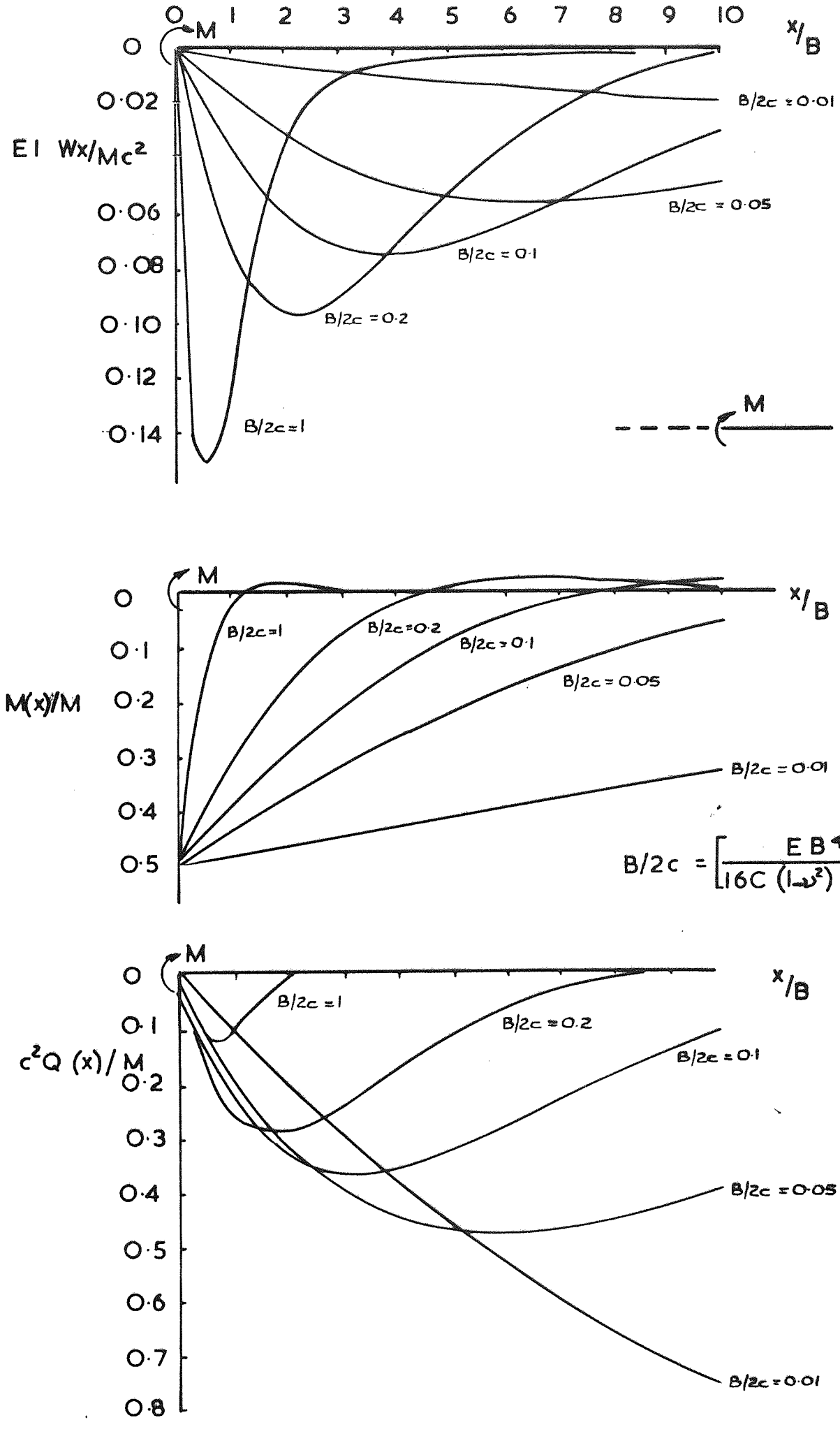

Fig 2.12 Three dimensional problem of an infinite beam subjected to a concentrated couple

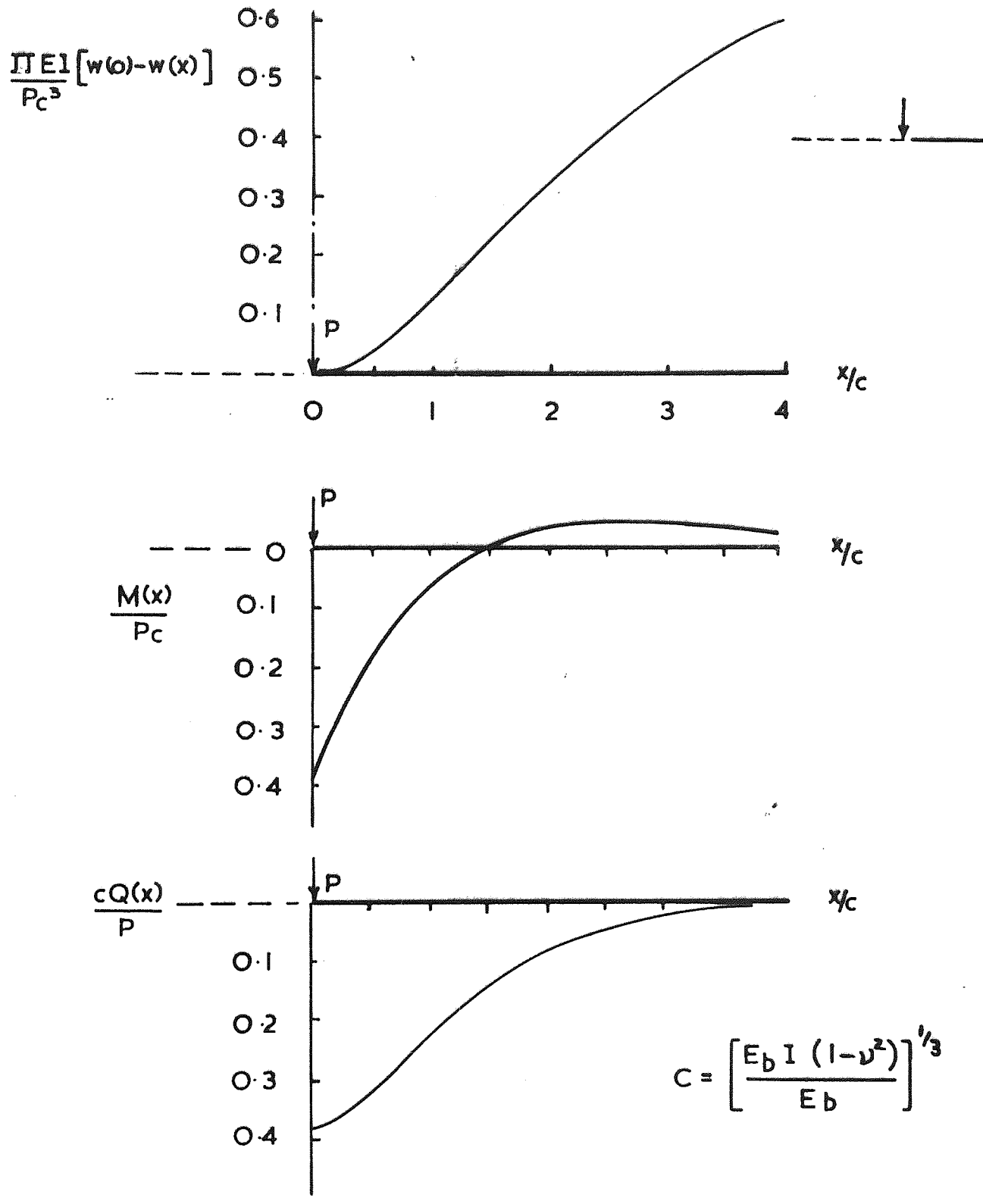

Fig. 2.13 Plane strain problem of an infinite beam subjected to a concentrated load

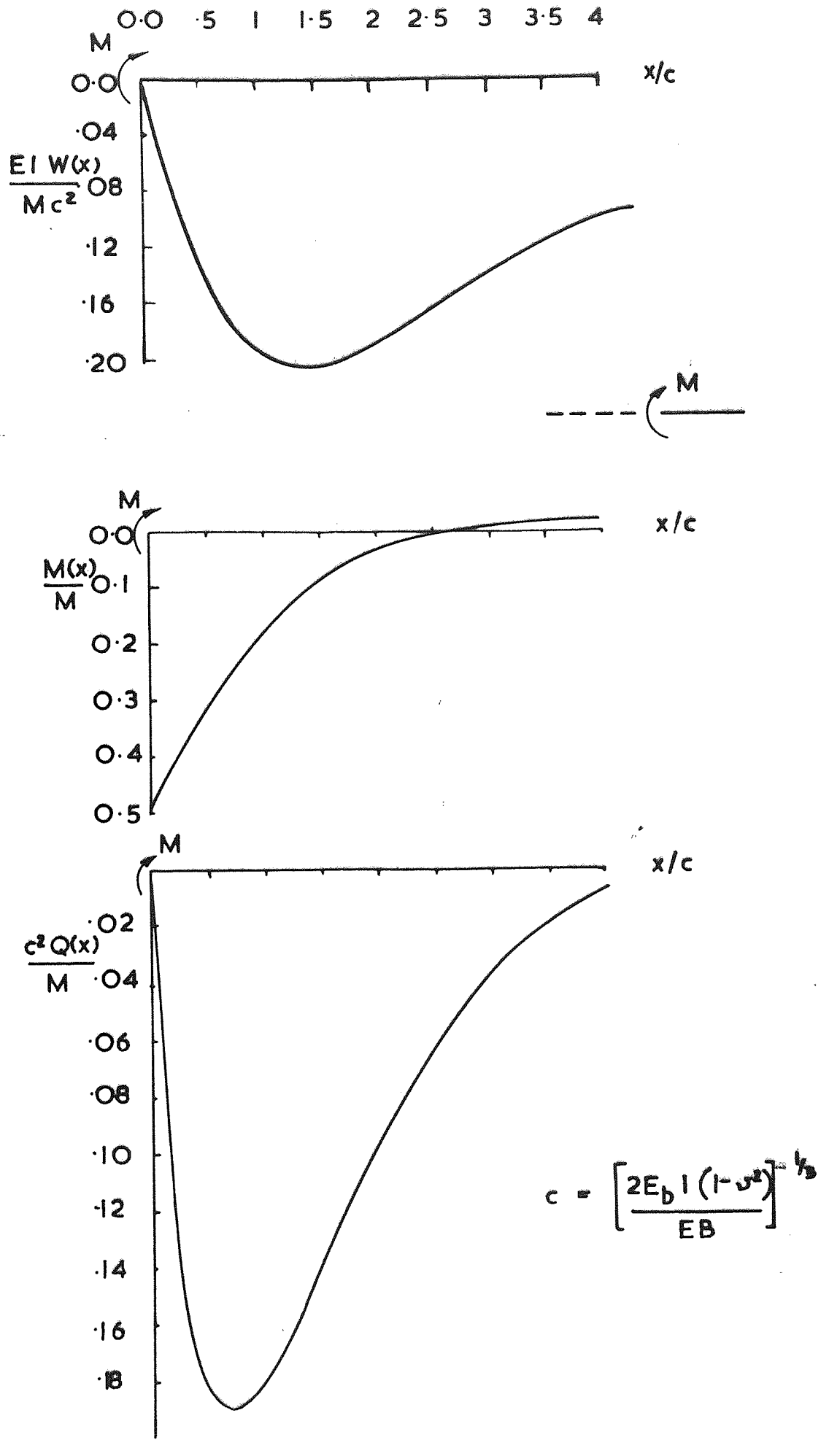

Fig. 2.14. Two - dimensional problem of an infinite beam subjected to a concentrated couple.

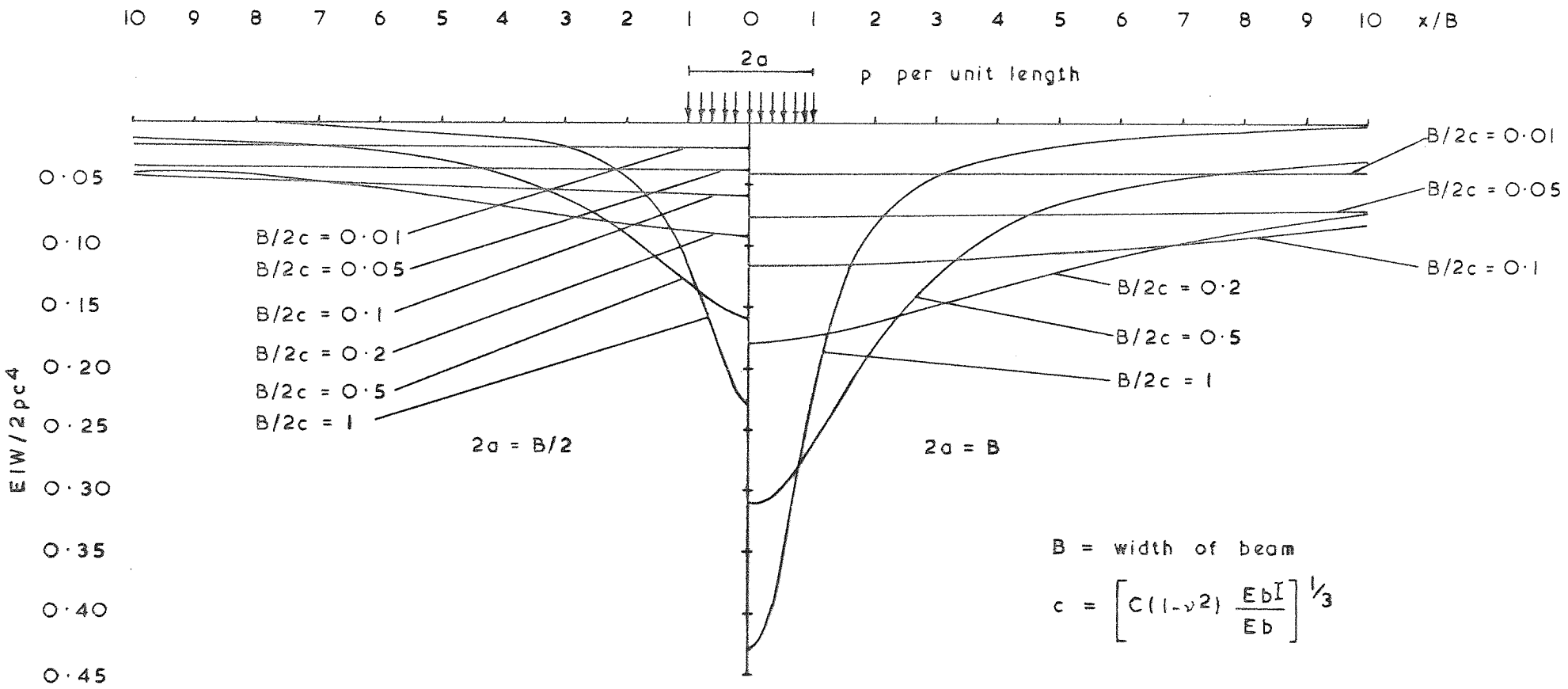

FIG. 2.15a Infinite beam subjected to uniform load (Deflection), Three Dimensional problem

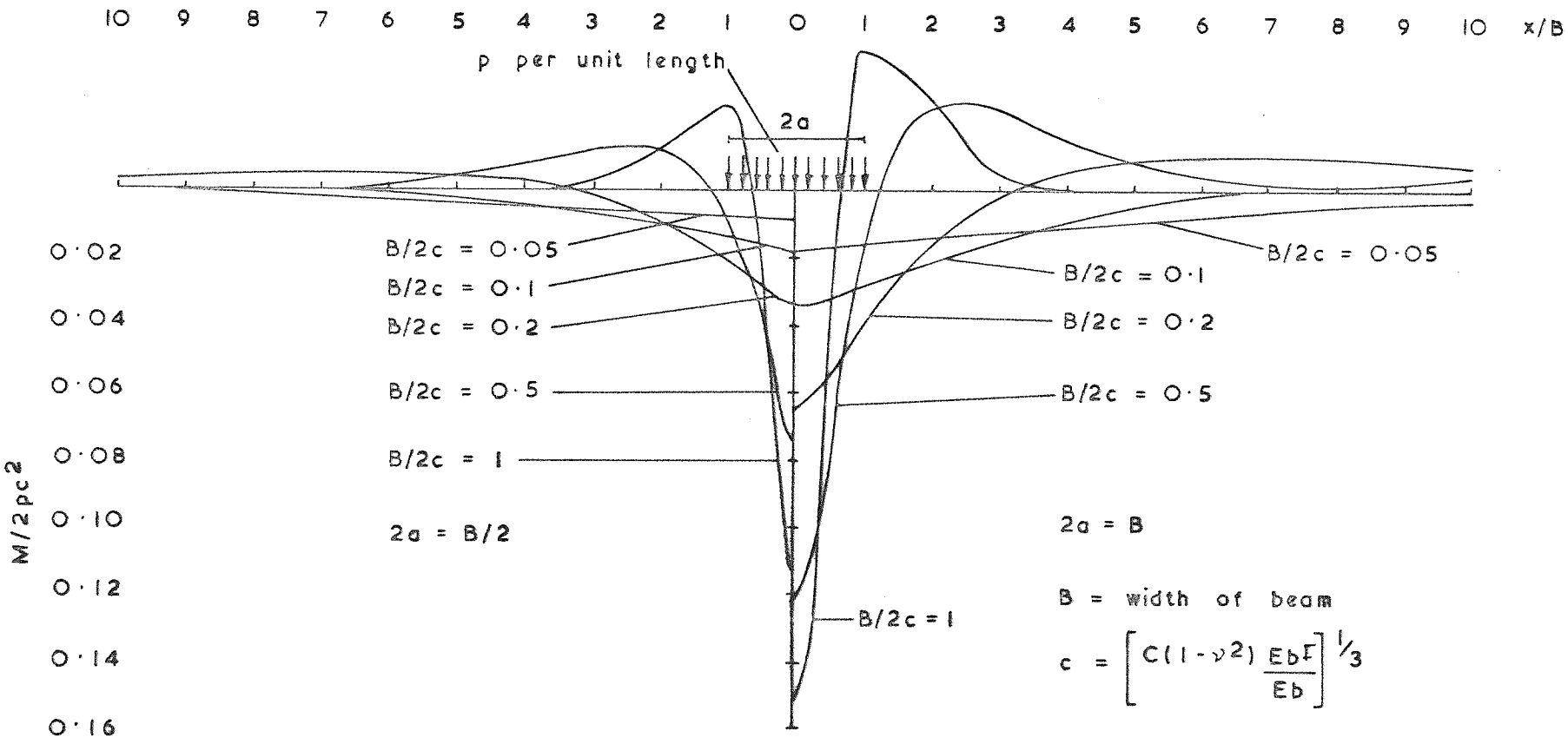

FIG. 2.15b Infinite beam subjected to uniform load

(Bending moment)

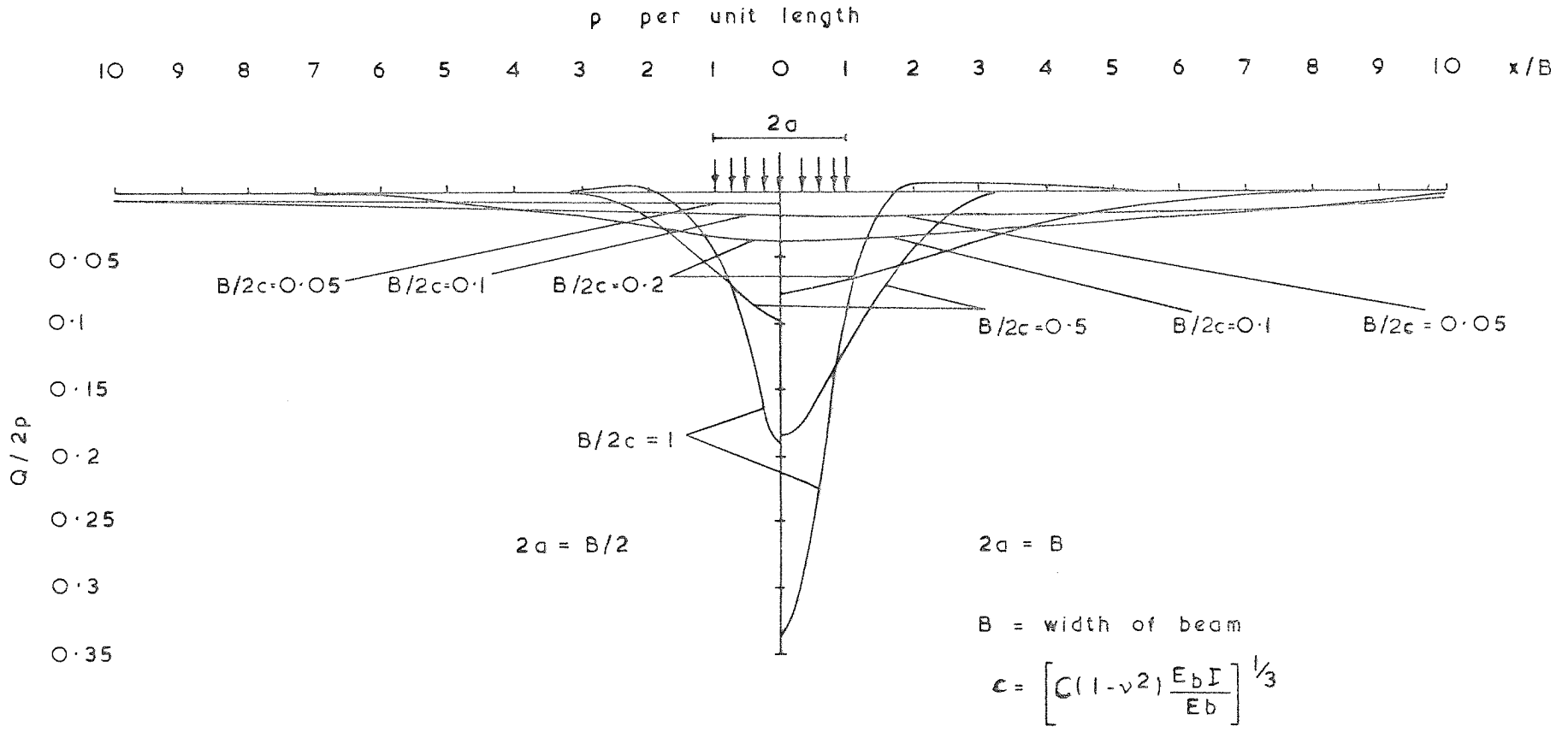

FIG. 2.15c Infinite beam subjected to uniform load (contact force)

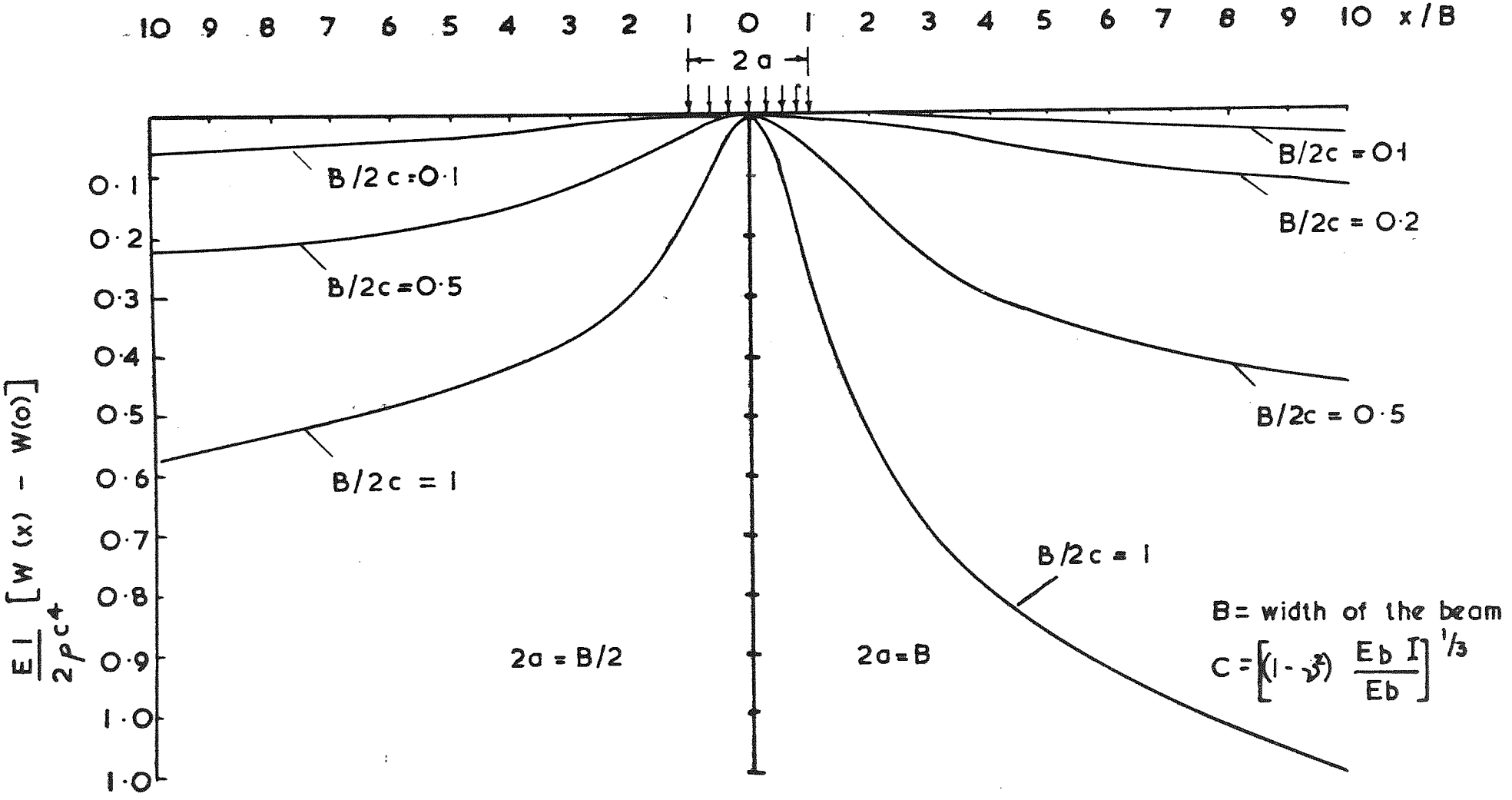

Fig. 2.16a. Infinite beam subjected to a uniform load (two dimensional) deflected shape of the beam.

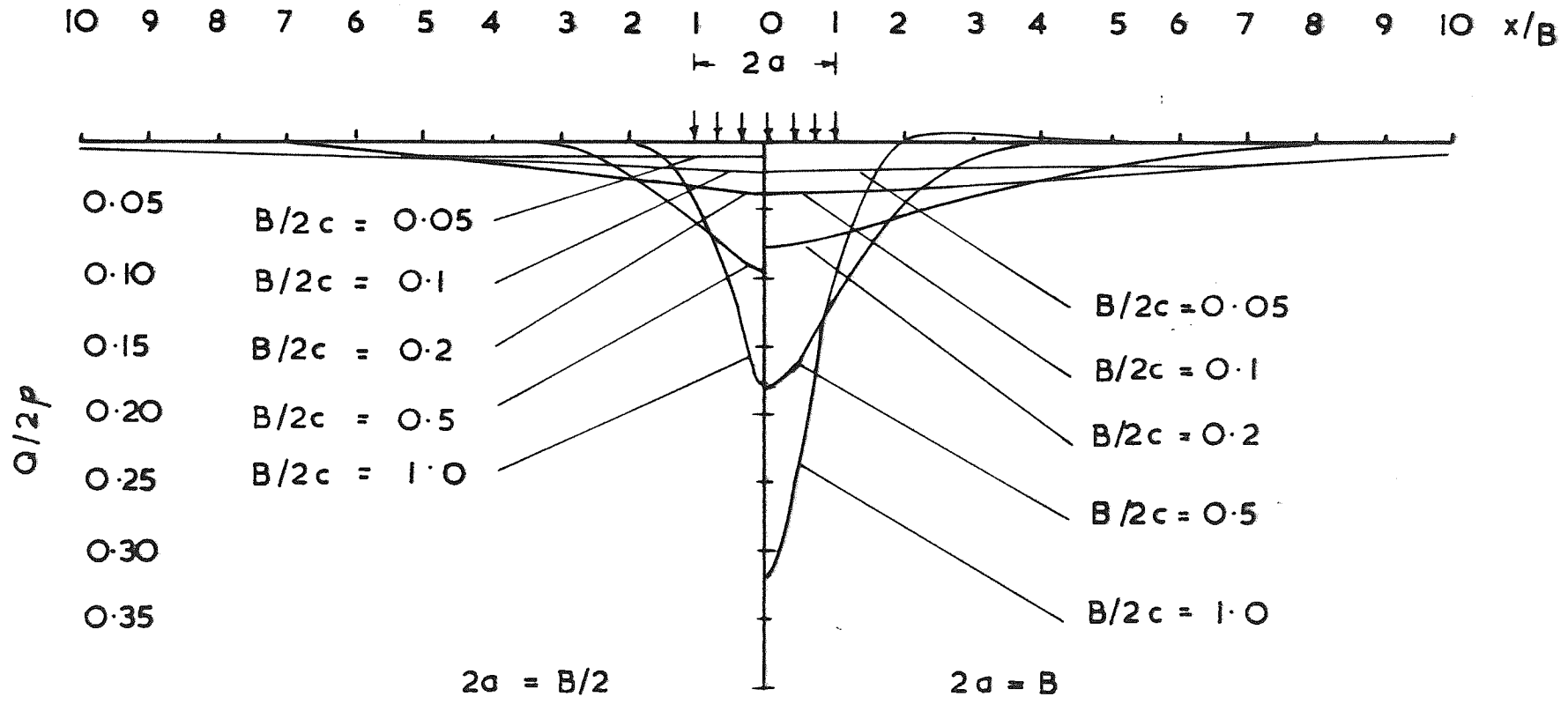

Fig. 2.16 b Infinite beam subjected to uniform load (two dimensional) contact force distribution

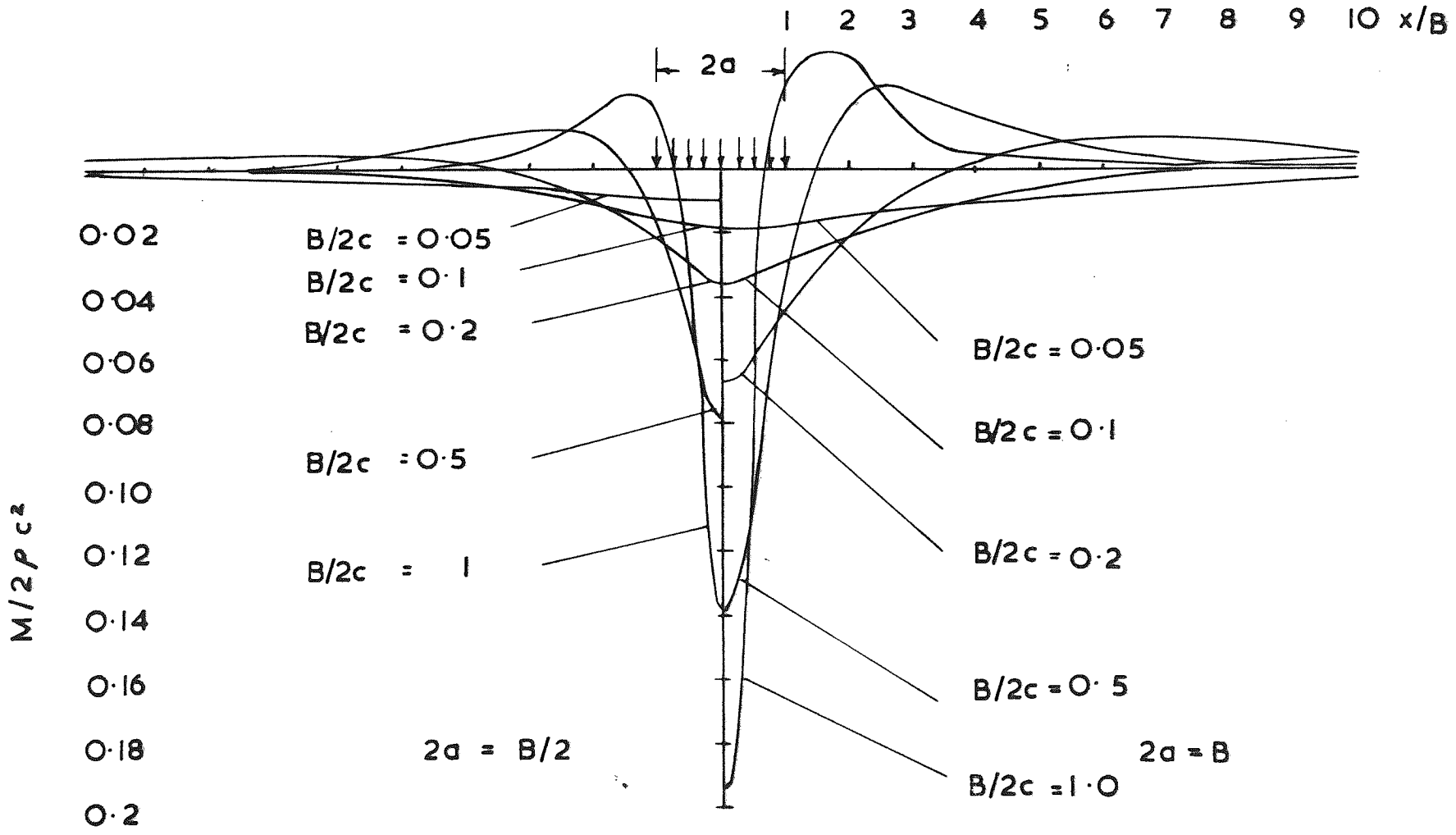

Fig .2.16c Infinite beam subjected to a uniform (two dimensional) bending moment distribution

2.9 The accuracy of the values of integrals

In the previous section, it was mentioned that the amount of error in the values of integrals $J_{np}(X)$ is limited to $\pm 0.1\%$. There is a second source of error which results from the approximation of the type given by (2.43). This approximation implies that in the integrals $J_{np}(X)$ for values of $\alpha > \alpha_m$, the function $\Omega = 0$ instead of its real value $\Omega = \psi(\beta)[\psi(\beta) = 1 + \frac{0.34}{\alpha b/c}]$, for the three dimensional, and $\Omega = 1$ for the two dimensional problem. To obtain the amount of error due to this approximation, the upper limit α_m was doubled (i.e. $\alpha_m = 40$), and the integrals were evaluated for different values of x/B (x/B = 0 to 10). The maximum percentage difference between the values obtained with $\alpha_m = 20$ and those with $\alpha_m = 40$ were as follows

less than -0.001% for $J_{op}(X)$, $J_{1p}(X)$, $J_{2p}(X)$,

" " -0.01% " $J_{3p}(X)$, and (2.55)

" " -0.1% " $J_{4p}(X)$ and $J_{5p}(X)$.

An increase in the value of α_m beyond $\alpha_m = 40$ did not have a significant effect on the values of the integrals $J_{np}(X)$. The maximum error is therefore the sum of errors given by (2.55) and that due to numerical integration. It can be seen that the maximum error occurs for $J_{4p}(X)$ and $J_{5p}(X)$, which is -0.2%. In order to investigate the accuracy of the values of integrals $J_{4u}(X)$, the integrals were first evaluated numerically between zero and twenty ($\alpha_m = 20$). The upper limit of the integrals was then doubled ($\alpha_m = 40$)

and the integrals were evaluated. The maximum difference in the values of integrals obtained with the upper limits α_m = 20 and 40 was less than -1%.

2.10 Analytical expressions for M_{max}, W_{max}, and Q_{max} in an infinite beam

The maximum value of the bending moment (M_{max}), deflection (W_{max}), and contact force (Q_{max}) in an infinite beam, subjected to a concentrated load P (total load across the width of the beam), and resting on an homogeneous elastic isotropic medium occurs at the point of application of the load (i.e. x = 0). From the equations (2.34 a-d) the values of M_{max}, W_{max}, and Q_{max} are then given by

$$
\begin{aligned}
M_{max} &= \frac{Pc}{\pi} \int_o^\infty \frac{\alpha d\alpha}{\alpha^3+\psi(\beta)} = \frac{Pc}{\pi} J_{2p}(o), \\
W_{max} &= \frac{Pc^3}{\pi E_b I} \int_o^\infty \frac{d\alpha}{\alpha[\alpha^3+\psi(\beta)]} = \frac{Pc^3}{\pi E_b I} J_{op}(o), \\
Q_{max} &= \frac{P}{c\pi} \int_o^\infty \frac{\psi(\beta)}{\alpha^3+\psi(\beta)} = \frac{P}{c\pi} J_{4p}(o).
\end{aligned}
\tag{2.56}
$$

The values of $J_{np}(o)/\pi$ (see Appendix 1) are plotted against B/2c (Fig. 2.17). It was found that the values of $J_{np}(X)/\pi$ at X = 0 can be represented by the following analytical expressions

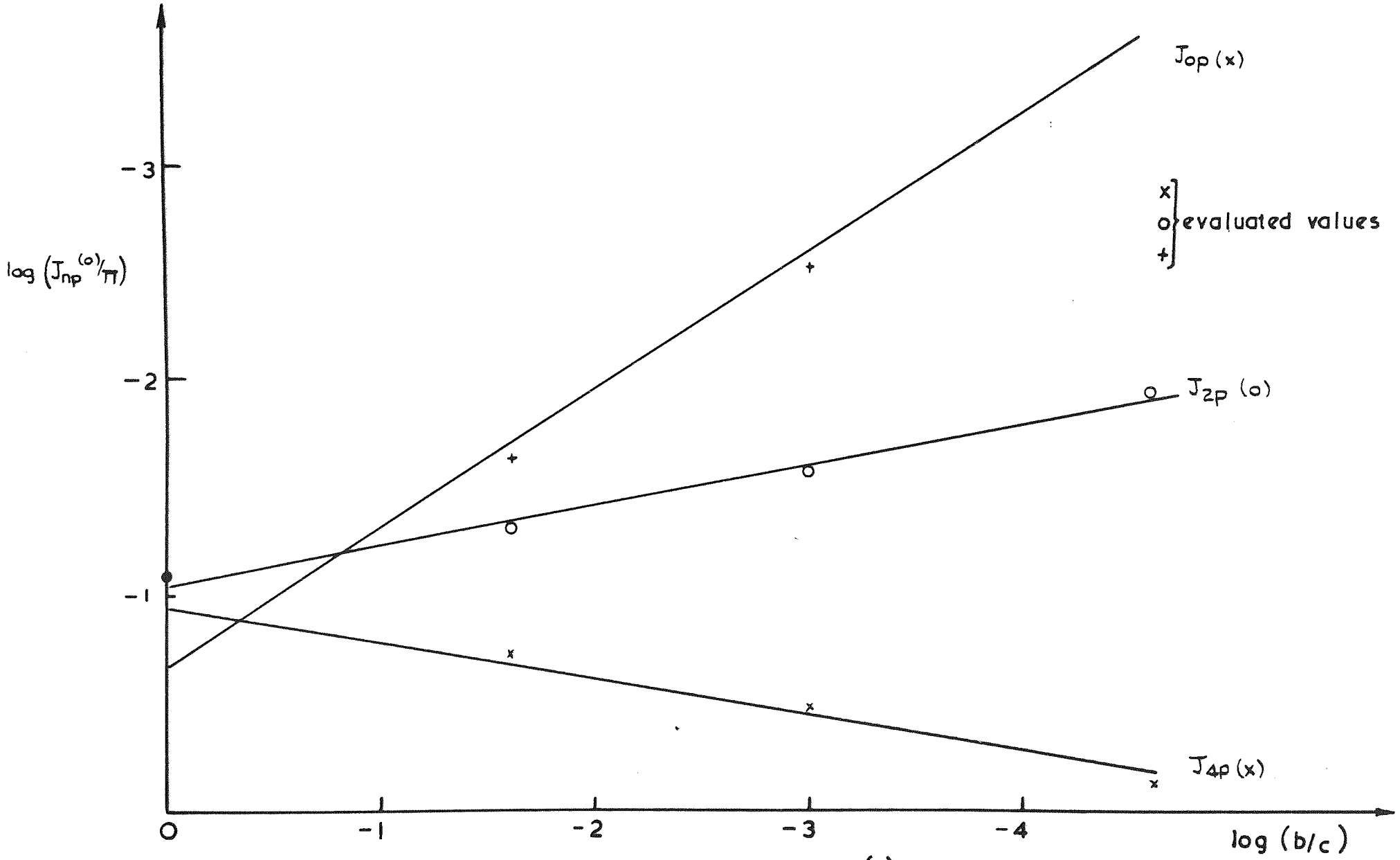

Fig . 2.17 Analytical representation of $J_{np}^{(o)}/\pi$

$$J_{2o}(o) = 0.352 \left[\frac{B}{2c}\right]^{0.188},$$

$$J_{op}(o) = 0.515 \left[\frac{B}{2c}\right]^{0.649}, \qquad (2.57)$$

$$J_{4p}(o) = 0.390 \left[\frac{B}{2c}\right]^{0.166}.$$

By substituting (2.57) in (2.56) we obtain

$$M_{max} = 0.352\ Pc \left[\frac{B}{2c}\right]^{0.188},$$

$$W_{max} = 0.515 \frac{Pc^3}{E_b I} \left[\frac{B}{2c}\right]^{0.649}, \qquad (2.58)$$

$$Q_{max} = 0.390 \frac{P}{c} \left[\frac{B}{2c}\right]^{-0.166}.$$

Depending on the value of B/2c, the maximum error in representing the above analytical expressions for $J_{np}(o)$, can be positive or negative (see Fig. 2.17). This error is ±8% for W_{max}, ±4.5% for M_{max}, and ±5.5% for Q_{max}. Biot (1937) gives an expression for the maximum bending moment as follows

$$M_{max} = 0.332\ Pc \left[\frac{2c}{B}\right]^{0.831}.$$

This expression appears to be in error, the correct form is as follows

$$M_{max} = 0.166\ PB \left[\frac{2c}{B}\right]^{0.831}$$

or

$$M_{max} = 0.332\ Pc \left[\frac{2c}{B}\right]^{-0.169}$$

2.11 Comparison with the solution for an infinite beam resting on a Winkler medium

The analysis of beams resting on a Winkler medium (see Chapter 1) is sometimes referred to as "conventional analysis" (see Vesic, 1961). This definition is adopted here in our discussion. In the conventional analysis, the expressions for the deflection (W), bending moment (M), and contact force Q are given by (see Hetenyi, 1947).

$$W = \frac{P\lambda}{2K} e^{-\lambda x}(\cos\lambda x + \sin\lambda x),$$

$$M = \frac{P}{4\lambda} e^{-\lambda x}(\cos\lambda x - \sin\lambda x), \qquad (2.59)$$

$$Q = \frac{P\lambda}{2} e^{-\lambda x}(\cos\lambda x + \sin\lambda x),$$

where

$$\lambda = \left[\frac{K}{4E_b I} \right]^{1/4}$$

The value of the modulus of subgrade reaction (K) may be determined from in-situ tests (e.g. plate loading tests). A comprehensive account of the evaluation of the modulus of subgrade reaction from plate loading tests is given by Terzaghi (1955).

It is also possible to find a value for K in terms of E and ν of the elastic medium, by a comparison of the solutions for an infinite beam in conventional and rigorous (Biot's solution) method of analysis. By comparing the maximum bending moments in two methods

of solution, Biot obtained the following expression for K

$$K = 1.23\left[\frac{B}{2c}\right]^{0.33} \quad \frac{E}{C(1-\nu^2)} \tag{2.60}$$

Expressions similar to (2.58) can be obtained by comparing the maximum deflections, and contact forces of an infinite beam in the two methods of analysis (Biot's solution and conventional analysis). The maximum values of W, M and Q in conventional analysis (equations 2.57 a-c) occurs at x = 0.

$$W_{max} = \frac{p\lambda}{2K} \ ,$$

$$M_{max} = \frac{P}{2\lambda} \ , \tag{2.61}$$

$$Q_{max} = \frac{P\lambda}{2} \ .$$

By equating W_{max}, M_{max}, and Q_{max} in conventional analysis (equations 2.61) with those of rigorous method (Biot's method) represented by analytical expressions (equations 2.58), we obtained three values for K defined as K_W, K_M, and K_Q as follows

$$K_W = 0.606 \left[\frac{B}{2C}\right]^{0.135} \quad \frac{E}{C(1-\nu^2)} \ ,$$

$$K_M = 1.018 \left[\frac{B}{2C}\right]^{0.248} \quad \frac{E}{C(1-\nu^2)} \ , \tag{2.62}$$

$$K_Q = 1.481 \left[\frac{B}{2C}\right]^{0.336} \quad \frac{E}{C(1-\nu^2)} \ .$$

Where C is defined by (2.29).

The distribution of deflections, bending moments and contact forces for an infinite beam subjected to a concentrated load for both rigorous method of analysis (with B/2C = 0.01, 1.0) and conventional analysis (with K = K_W, K_M, K_Q) are shown in Fig. 2.18 a-c. Table 2.1 shows the percentage difference in the values of W_{max}, M_{max}, and Q_{max} of a infinite beam subjected to a concentrated load, and resting on a semi infinite elastic medium, and those of conventional analysis.

	W_{max}		M_{max}		Q_{max}	
B/2C	0.01	1.0	0.01	1.0	0.01	1.0
K_W	0	0	0	-14	1	20
K_M	0	31	0	0	1	9
K_Q	-3	49	-1	9	0	0

Table 2.1 Difference in % in the values of maximum deflection, bending moment, and contact force

2.12 Conclusions

Biot's solution for an infinite beam resting on an homogeneous, isotropic elastic half space was extended to include the case of loading by a uniform strip load.

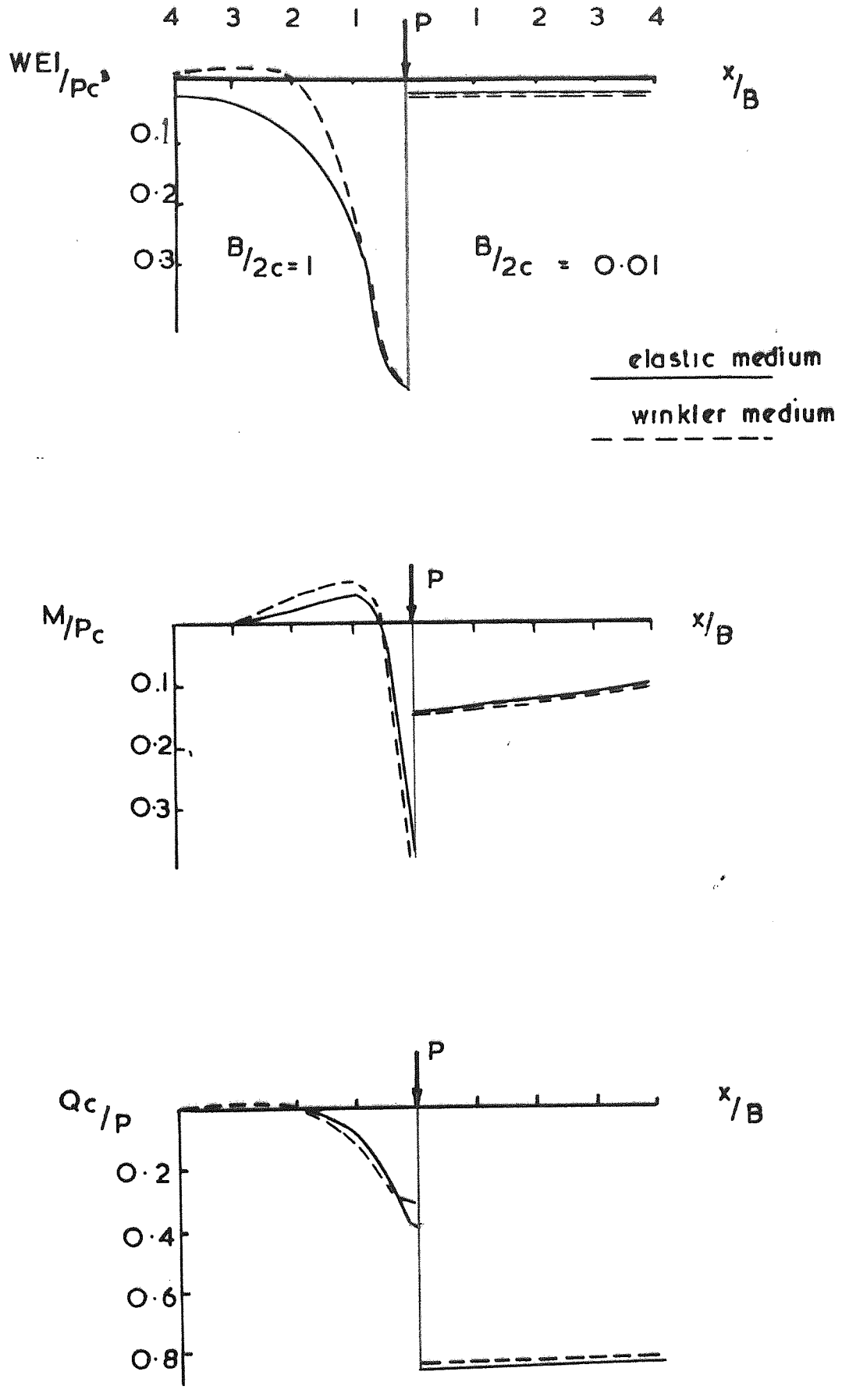

K = Kw

Fig .2.18 a_c Comparison of the results for an infinite beam resting on Winkler and elastic medium

a. $K = K_W$ b. $K = K_M$ c. $K = K_Q$

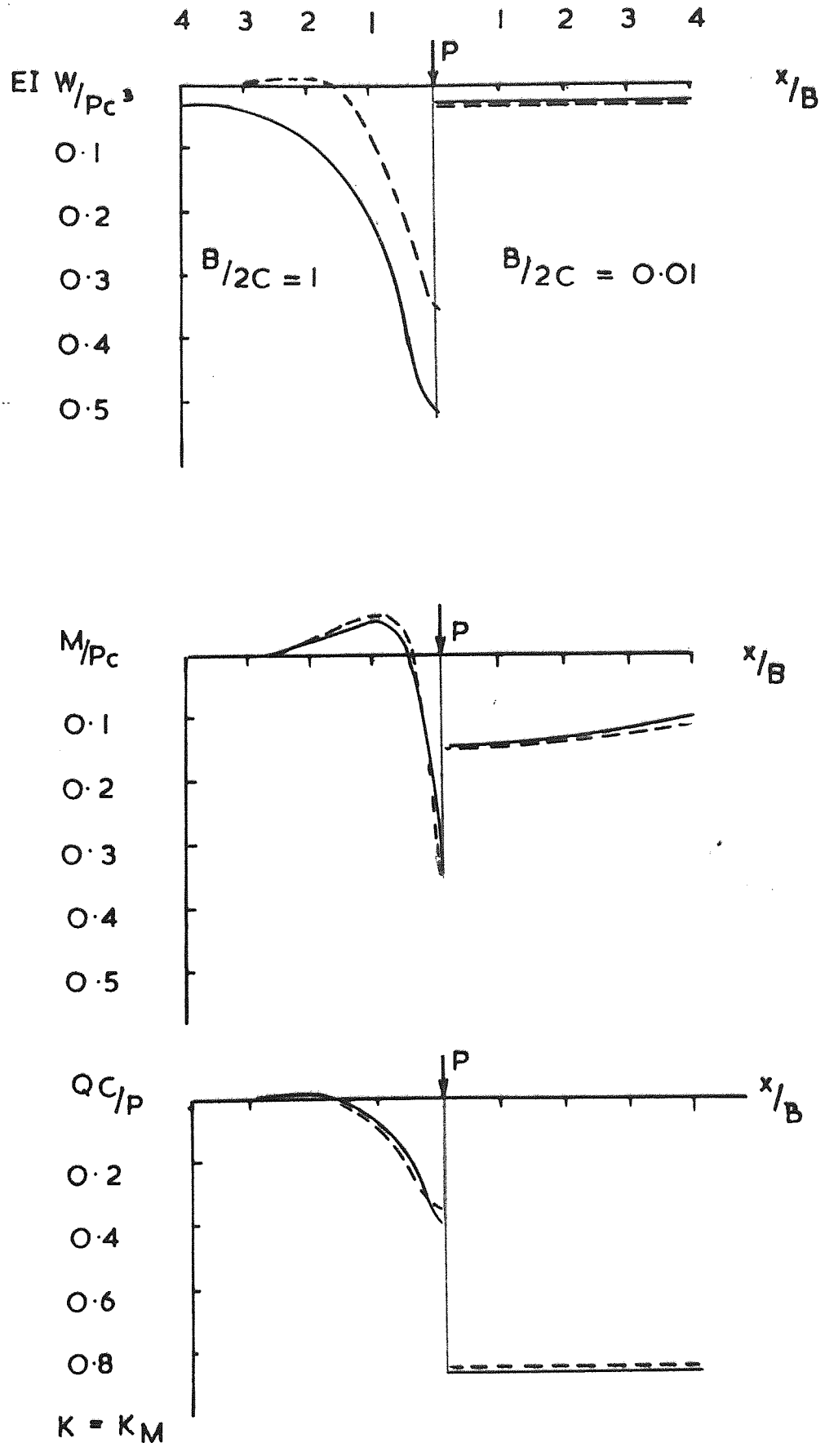
4 3 2 1 1 2 3 4
P
EI W/Pc³
x/B
0·1
0·2
0·3
0·4
0·5
B/2C = 1
B/2C = 0·01
M/Pc
P
x/B
0·1
0·2
0·3
0·4
0·5
QC/P
P
x/B
0·2
0·4
0·6
0·8
K = KM

Fig. 2.18 b

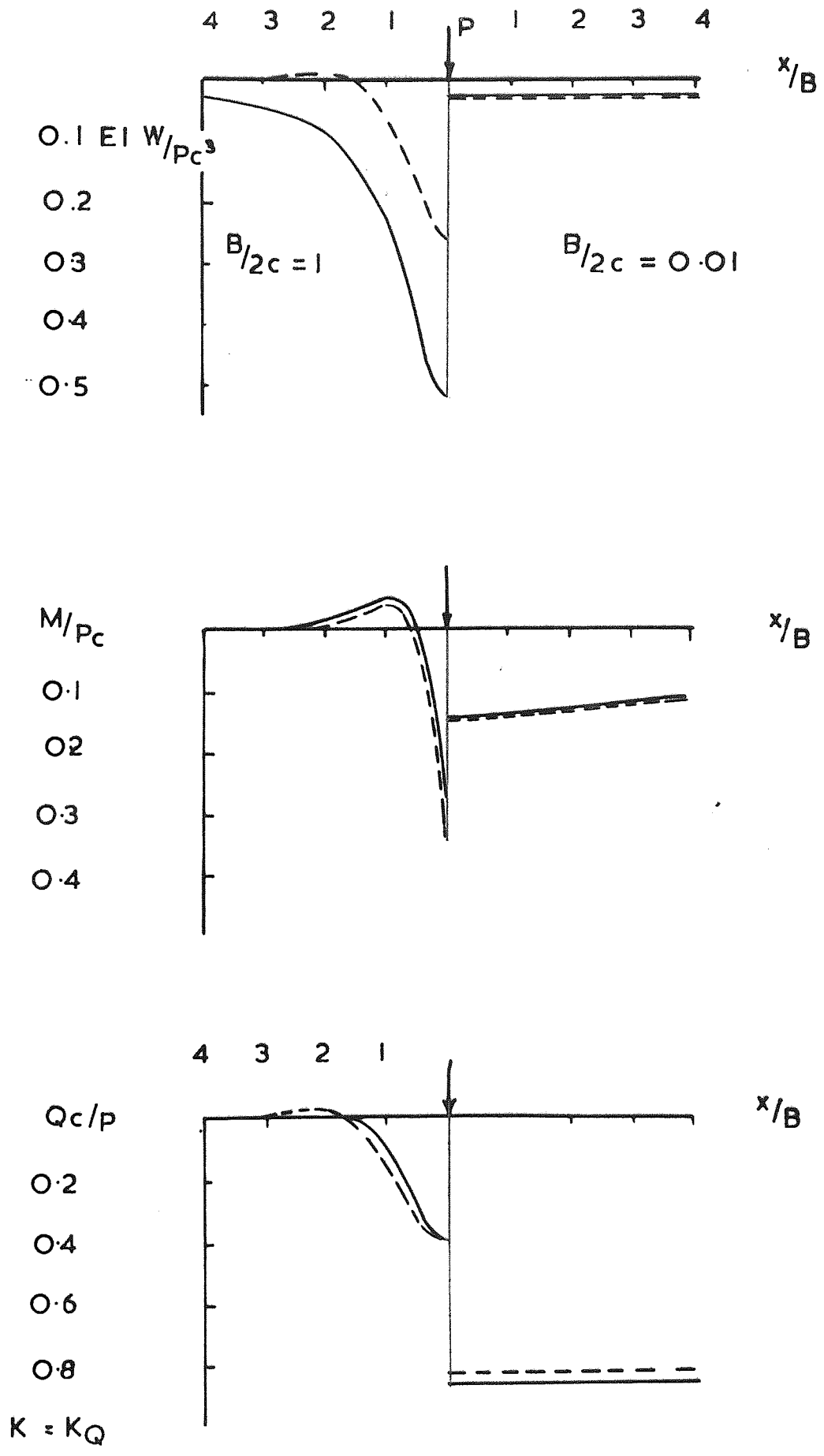
4 3 2 1 P 1 2 3 4
x/B
0.1 EI W/Pc³
0.2
0·3
0·4
0·5
B/2c = 1
B/2c = 0·01
M/Pc
0·1
02
0·3
0·4
x/B
4 3 2 1
Qc/P
0·2
0·4
0·6
0·8
K = KQ
x/B

Fig . 2.18c.

The distribution of deflection, bending moment and contact force of a beam subjected to a concentrated load, a concentrated couple, and a uniform load were plotted for different B/2c values (Figures 2.11 to 2.16). Numerical values for the integrals involved in the expressions for deflections, slopes, bending moments, shearing forces, and contact forces of the infinite beam resting on both three and two dimensional elastic media, subjected to a concentrated load, and a concentrated couple are given in Appendix 1.

The maximum error involved in evaluation of integrals is limited to -0.2% (for $J_{np}(X)$), and +1% (for $J_{nu}(X)$). The analytical expressions for the maximum value of deflection, bending moment, and contact force of a beam subjected to a concentrated load and resting on a three dimensional medium were obtained (equations 2.38). By equating W_{max}, M_{max} and Q_{max} in the rigorous method (Biot's solution) with that of the Winkler problem, it is possible to obtain three values for the subgrade modules identified as K_W, K_M and K_Q (equations 2.62). These values of K are used for the purpose of comparing the distribution of displacements, bending moments, and contact forces for both types of supporting media (i.e. elastic half space and Winkler).

CHAPTER THREE

FINITE BEAMS ON ELASTIC MEDIUM

3.1 Introduction

The analytical solution of a finite beam resting on a semi-infinite isotropic homogeneous elastic medium is complicated due to the fact that both continuity and boundary conditions must be satisfied simultaneously. There exist several methods of analysis which overcome the mathematical complexity involved in the problem.

The approximate methods of analysis of a finite beam resting on a semi-infinite isotropic homogeneous elastic medium are given by Ohde (1942), and Barden (1962). In these methods it is assumed that the contact forces are made up from a number of blocks of uniform loads. By satisfying the continuity of slope (Ohde's method), or deflection (Barden's method) at the beam-medium interface, the contact forces are obtained by solving a set of simultaneous equations.

A superposition technique (the technique was first used by Hetenyi, 1946 to analyse the problem of a finite beam resting on Winkler medium) was employed by Drapkin (1955) for the analysis of centrally loaded finite beam.

In this chapter, we adopt a superposition technique for the solution of a finite beam resting on an isotropic homogeneous elastic medium. The solution is given for the following loadings :

1) finite beam subjected to a concentrated force at an arbitrary point,

2) finite beam subjected to a uniform load at an arbitrary location, and

3) finite beam subjected to a concentrated couple at an arbitrary point.

3.2 Finite beam with free ends

We develop here the superposition technique for the analysis of finite beams resting on an isotropic elastic homogeneous half space, and subjected to an arbitrary external loading. First, the finite beam with free ends to be analysed is assumed to occupy a region of the infinite beam with the same external loading (see Fig. 3.1a). Referring to Fig. 3.1a, points A and B in the infinite beam will in general have non zero bending moments and shearing forces. The object of the superposition technique is to reduce the bending moments and shearing forces at locations A and B, (Fig. 3.1a) to zero simultaneously. For this purpose we utilise the solutions, developed earlier for the problem of an infinite beam which is subjected to a concentrated force, and a concentrated moment.

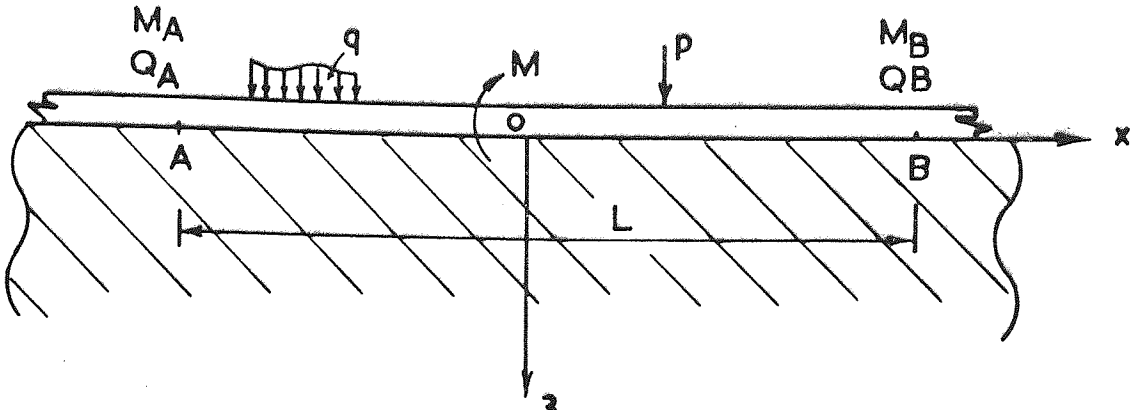

a. Infinite beam subjected to an arbitrary system of loading.

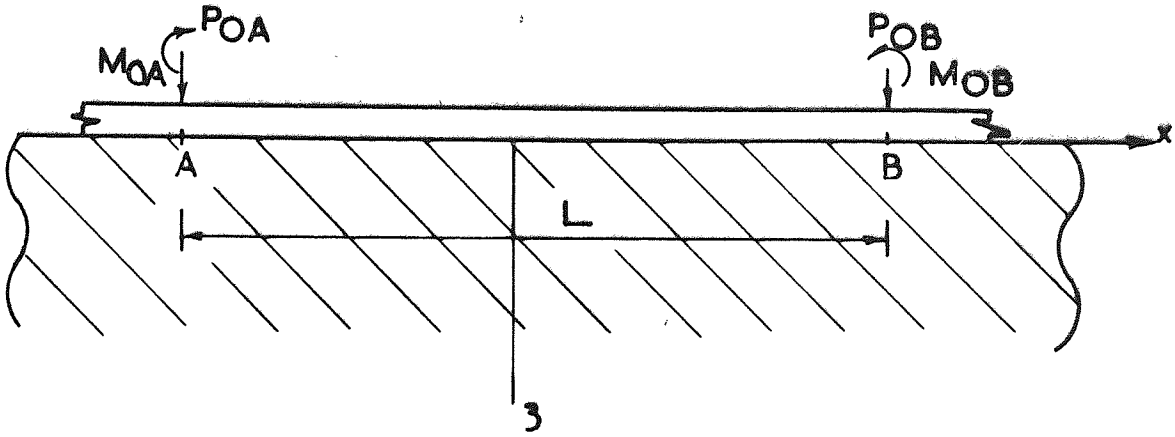

b. Infinite beam subjected to end conditioning loads

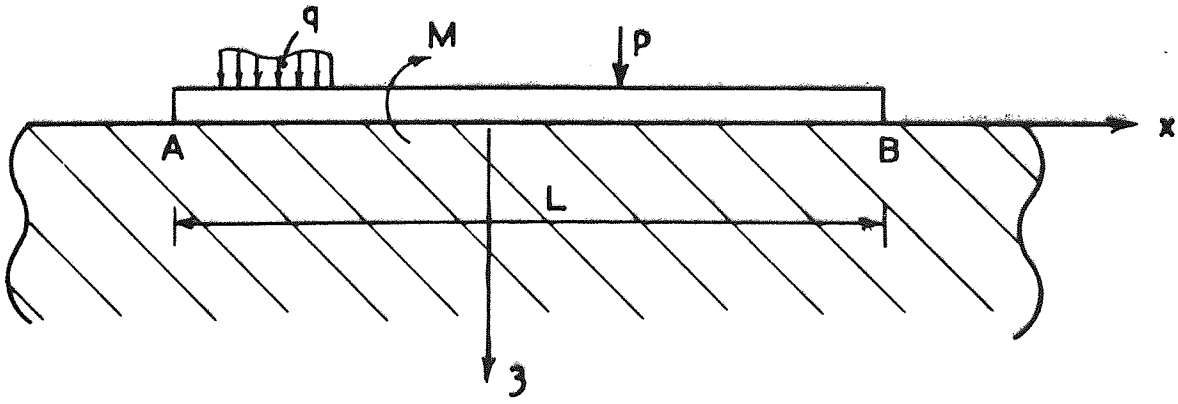

c. Finite beam subjected to an arbitrary system of loading

Fig. 3.1

Let the bending moment and shearing forces at points A and B of the infinite beam, due to loadings shown in Fig. 3.1a, be M_A, Q_A, and M_B, Q_B. Next consider an infinite beam, subjected to a system of loading P_{OA} and M_{OA} at A, and P_{OB}, M_{OB} at B (Fig.3.1b). In order that the superpostion of the solutions for infinite beams shown in Fig. (3.1a) and (3.1b) give the solution for the finite beam with free end (Fig. 3.1c), it is necessary that the loadings P_{OA}, M_{OA}, P_{OB} and M_{OB} produce bending moments and shearing forces $-M_A$, $-Q_A$, and $-M_B$, $-Q_B$ at A and B respectively, i.e.

$$\begin{aligned} \Sigma M_{atA} &= -M_A , & \Sigma M_{atB} &= -M_B \\ \Sigma Q_{atA} &= -Q_A , & \Sigma Q_{atB} &= -Q_B \end{aligned} \tag{3.1}$$

or

$$\begin{aligned} M_{A1} + M_{A2} + M_{A3} + M_{A4} &= -M_A \\ Q_{A1} + Q_{A2} + Q_{A3} + Q_{A4} &= -Q_A \\ M_{B1} + M_{B2} + M_{B3} + M_{B4} &= -M_B \\ Q_{B1} + Q_{B2} + Q_{B3} + Q_{B4} &= -Q_B \end{aligned} \tag{3.2}$$

where M_{An}, Q_{An} and M_{Bn}, Q_{Bn} are bending moments and shearing forces at A and B due to loadings P_{OA}, M_{OA}, P_{OB} and M_{OB}. The four quantities P_{OA}, M_{OA}, P_{OB} and M_{OB} are referred to as end conditioning forces (Hetenyi, 1946). By making use of the

solutions for infinite beam subject to a concentrated load and couple, given by (2.34 a-d), and (2.39 a-c), equations (3.2) can be written in matrix form as

$$\underset{\sim}{\{F\}} = \underset{\sim}{[C]}\ \underset{\sim}{\{R\}}\ , \tag{3.3}$$

where, $\underset{\sim}{\{F\}}$ and $\underset{\sim}{\{R\}}$ are column vectors given by

$$\underset{\sim}{\{F\}} = \begin{vmatrix} -M_A \\ -Q_A \\ -M_B \\ -Q_B \end{vmatrix}\ , \qquad \underset{\sim}{\{R\}} = \begin{vmatrix} P_{OA} \\ P_{OB} \\ M_{OA} \\ M_{OB} \end{vmatrix}\ , \tag{3.4}$$

and $\underset{\sim}{[C]}$ is the coefficient matrix given by

$$\underset{\sim}{[C]} = \begin{vmatrix} (C/\pi)J_{2PO} & (C/\pi)J_{2PL'} & 1/2 & (1/\pi)J_{3PL'} \\ -1/2 & (1/\pi)J_{3PL'} & -(1/C\pi)J_{4PO} & (1/C\pi)J_{4PL'} \\ (C/\pi)J_{2PL'} & (C/\pi)J_{2PO} & (1/\pi)J_{3PL'} & 1/2 \\ (-1/\pi)J_{3PL'} & 1/2 & -(1/C\pi)J_{4PL'} & (1/C\pi)J_{4PO} \end{vmatrix} \tag{3.5}$$

In the coefficient matrix, J_{nPr} refers to $J_{nP}(X)$ evaluated at $X = r$, and $L' = L/C$.

The superposition technique, as outlined here, only satisfies the boundary conditions at the ends of the beam and continuity conditions at the interface. For the complete solution of the problem it is necessary to satisfy the zero traction boundary condition on the surface of the half space exterior to the beam. Consider beam

AB in Fig. 3.2. Suppose the solution for this beam is obtained by applying the superposition technique. There might exist a contact stress distribution outside region AB, such that produce zero bending moment and shearing forces at A and B. Therefore when the superposition technique is used to find the solution for the finite beam, the solution is not valide unless the traction on the surface of the half space (at z = 0) exterior to the beam is zero.

3.3 Finite beam subjected to a concentrated force at an arbitrary point

In this section we apply the superposition technique, outlined earlier, to the special case of a finite beam, subjected to a concentrated force P at an arbitrary location (Fig. 3.1). The solution of the problem can be further simplified by resolving the load P into its symmetric and antisymmetric parts (see Hetenyi, 1946). Using such a decomposition, the number of unknown end conditioning forces for each loading are reduced to two. We denote the end conditioning forces, in symmetric case, P_0, M_0, and P_0, M_0 in antisymmetric case (Fig. 3.3 b-c). These end conditioning forces are related to P_{OA}, P_{OB}, M_{OA} by (Fig. 3.5)

$$P_{OA} = P_0' + P_0'' \qquad P_{OB} = P_0' - P_0''$$
$$M_{OA} = M_0' + M_0'' \qquad M_{OB} = M_0' - M_0'' \tag{3.6}$$

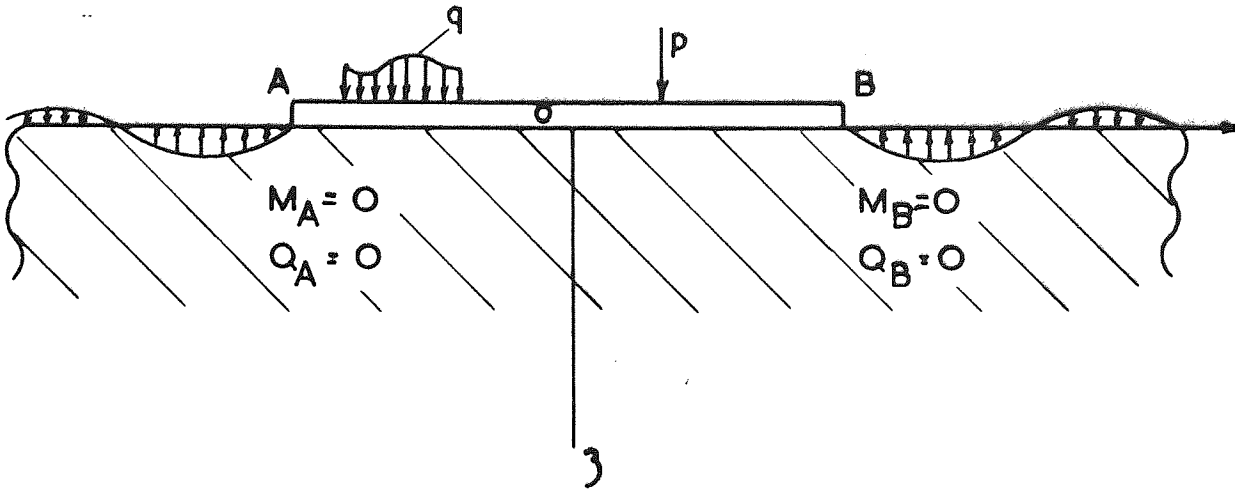

Fig .3.2 Non zero traction at the surface of the half space exterior to the beam

In the symmetric loading, P_0' and M_0' produce $-M_A'$, $-Q_A'$ at A, and $-M_A'$, $+Q_A'$ at B (Fig. 3.4). By making use of infinite beam solution for the concentrated force and the concentrated couple (equations 2.34 a-d, 2.37, 2.39 a-c), the zero moment and zero shearing forces boundary conditions at A and B are given by

$$\frac{P_0' C}{\pi} (J_{2PO} + J_{2PL'}) + \frac{M_0'}{\pi} (J_{3PO} + J_{3PL'}) + M_A' = 0 ,$$

$$\frac{-P_0'}{\pi} (J_{3PO} - J_{3PL'}) - \frac{M_0'}{C\pi} (J_{4PO} - J_{4PL'}) + Q_A' = 0, \tag{3.7}$$

where J_{nPr} is the value of $J_{nP}(X)$ evaluated at $X = r$ and $L' = L/c$.

For the antisymmetric case P_0'' and M_0'' produces $-M_A''$, Q_A'' at A and M_A'', $-Q_A''$ at B (Fig. 3.4). The boundary conditions give

$$\frac{P_{0C}''}{\pi} \left[J_{2PO} - J_{2PL}\right] + \frac{M_0''}{\pi} \left[J_{3PO} - J_{3PL'}\right] + M_A'' = 0 ,$$

$$\frac{-P_0''}{\pi} \left[J_{3PO} + J_{3PL'}\right] - \frac{M_0''}{C\pi} \left[J_{4PO} + J_{4PL'}\right] + Q_A'' = 0 \tag{3.8}$$

The relationship between M_A', Q_A', M_A'' and Q_A'', and M_A, M_B, Q_A and Q_B (Fig. 3.4) are given by the following :

$$M_A' = 1/2(M_A + M_B) , \quad M_A'' = 1/2 (M_A - M_B) ,$$

$$Q_A' = 1/2(Q_A - Q_B) , \quad Q_A'' = 1/2 (Q_A + Q_B) \tag{3.9}$$

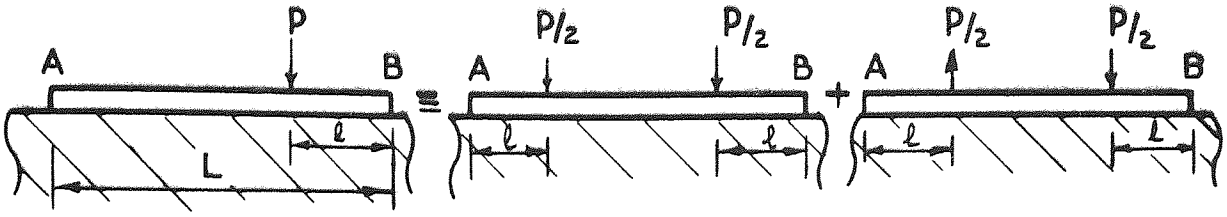

a. The loading resolved into symmetric & unsymmetric part

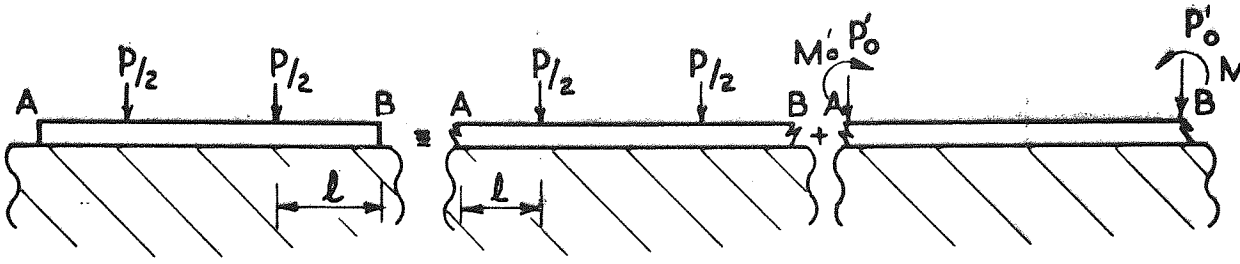

b. symmetric part

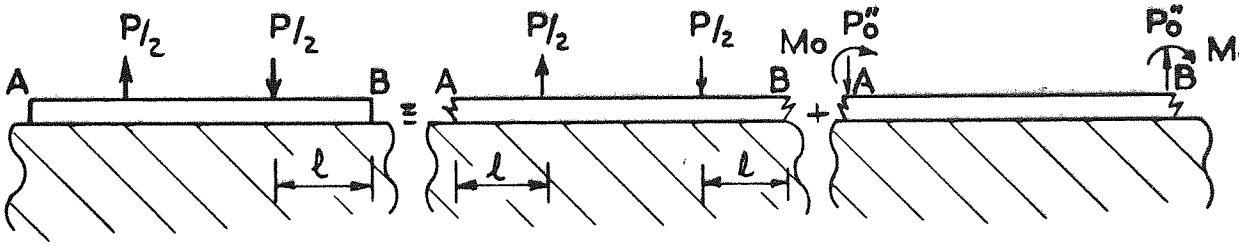

c. unsymmetric part

Fig. 3.3

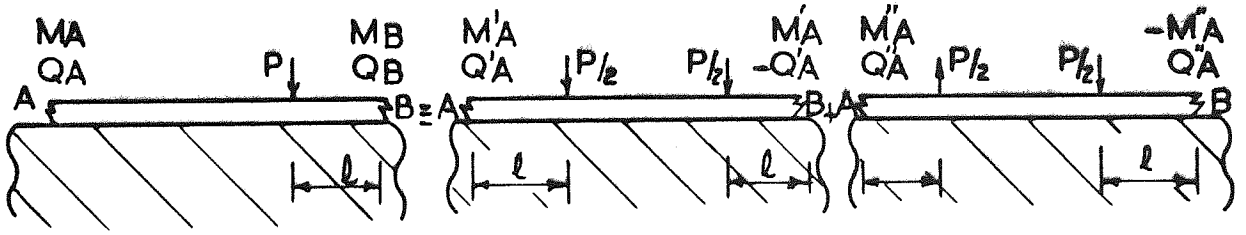

Fig. 3.4. Bending moment and shearing forces produced at A and B for original symmetric and unsymmetric loading.

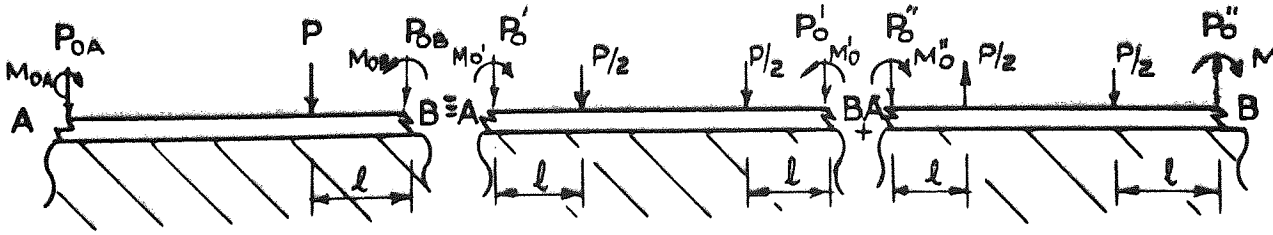

Fig. 3.5. End conditioning forces for original, symmetric and unsymmetric part

By solving (3.7) and (3.8) for P_0', M_0', P_0'' and M_0'', and making use of (3.6) and (3.9), we obtain the following expressions for the end conditioning forces P_{OA}, M_{OA}, P_{OB}, M_{OB}

$$P_{OA} = P(\alpha_1 + \alpha_2) \ , \qquad M_{OA} = P(\alpha_3 + \alpha_4) \ ,$$
$$P_{OB} = P(\alpha_1 - \alpha_2) \ , \qquad M_{OB} = P(\alpha_3 - \alpha_4) \ . \tag{3.10}$$

where

$$\alpha_1 = \frac{A+B}{C} \ , \qquad \alpha_2 = \frac{A_1+B_1}{C_1} \ ,$$
$$\alpha_3 = \frac{F+H}{C} \ , \qquad \alpha_4 = \frac{F_1+H_1}{C_1} \ , \tag{3.11}$$

and

$$A = -1/2 \left[J_{2Pg'} + J_{2P\ell'}\right] \left[J_{4p0} - J_{4PL'}\right] \ ,$$
$$B = -1/2 \left[J_{3Pg'} + J_{3P\ell'}\right] \left[J_{3P0} + J_{3PL'}\right] \ ,$$
$$A_1 = -1/2 \left[J_{2Pg'} - J_{2P\ell'}\right] \left[J_{4P0} + J_{4PL'}\right] \ ,$$
$$B_1 = -1/2 \left[J_{3Pg'} - J_{3P\ell'}\right] \left[J_{3P0} - J_{3PL'}\right] \ ,$$
$$C = \left[J_{2P0} + J_{2PL'}\right] \left[J_{4P0} - J_{4PL'}\right] - \left[(J_{3P0})^2 - (J_{3PL'})^2\right]$$
$$C_1 = \left[J_{2P0} - J_{2PL'}\right] \left[J_{4P0} + J_{4PL'}\right] - \left[(J_{3P0})^2 - (J_{3PL'})^2\right]$$

(3.12 a-j)

$$F = 1/2 \left[J_{3Pg'} + J_{3P\ell'}\right] \left[J_{2PO} + J_{2PL'}\right] ,$$

$$F_1 = 1/2 \left[J_{3Pg'} - J_{3P\ell'}\right] \left[J_{2PO} - J_{2PL'}\right] ,$$

$$H = 1/2 \left[J_{2Pg'} + J_{2P\ell'}\right] \left[J_{3PO} - J_{3PL'}\right] ,$$

$$H_1 = 1/2 \left[J_{2Pg'} - J_{2P\ell'}\right] \left[J_{3PO} + J_{3PL'}\right] .$$

where $L' = L/C$, $\ell' = \ell/C$, $g' = L' - \ell'$.

The solutions for the finite beam shown in Fig. 3.6a are then obtained by superpostion of the solutions for an infinite beam, subjected to concentrated force P (Fig. 3.6b), and system of loadings P_{OA}, M_{OA}, P_{OB}, M_{OB} (Fig. 3.6c), given by equation (3.10).

The expressions for deflection, bending moment, shearing force, and contact force [(contact stress) x B] are given by

$$W(X) = \frac{P c^3}{\pi E_b I} G_{OP}(X) ,$$

$$M(X) = \frac{Pc}{\pi} G_{2P}(X) ,$$

$$V(X) = -\frac{P}{\pi} G_{3P}(X) ,$$

$$Q(X) = \frac{P}{c\pi} G_{4P}(X) .$$

(3.13 a-d)

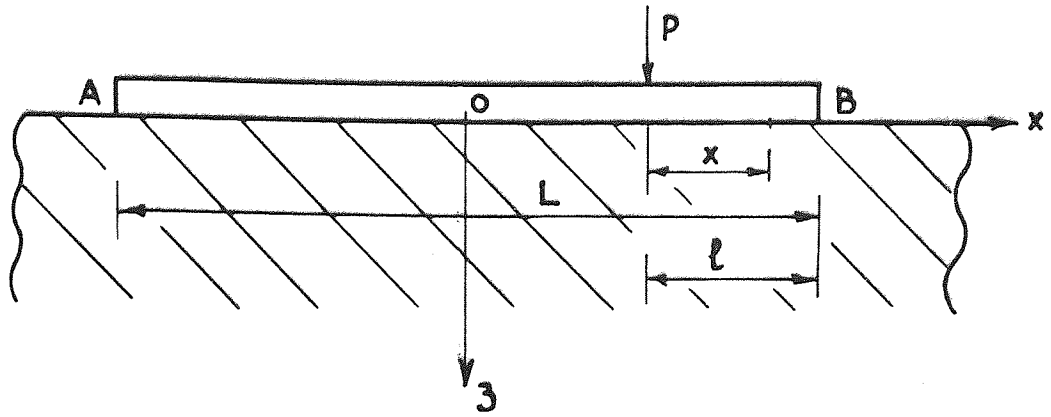

a. Finite beam subjected to a concentrated load

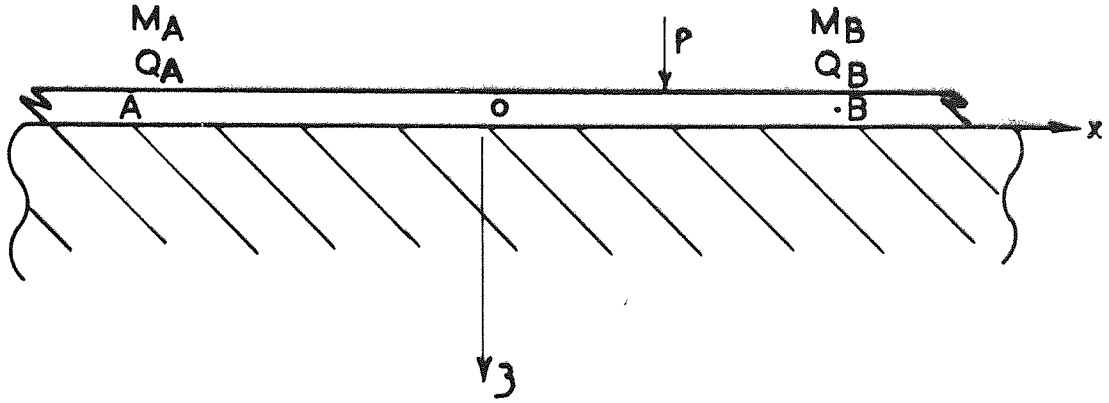

b. Infinite beam subjected to a concentrated load.

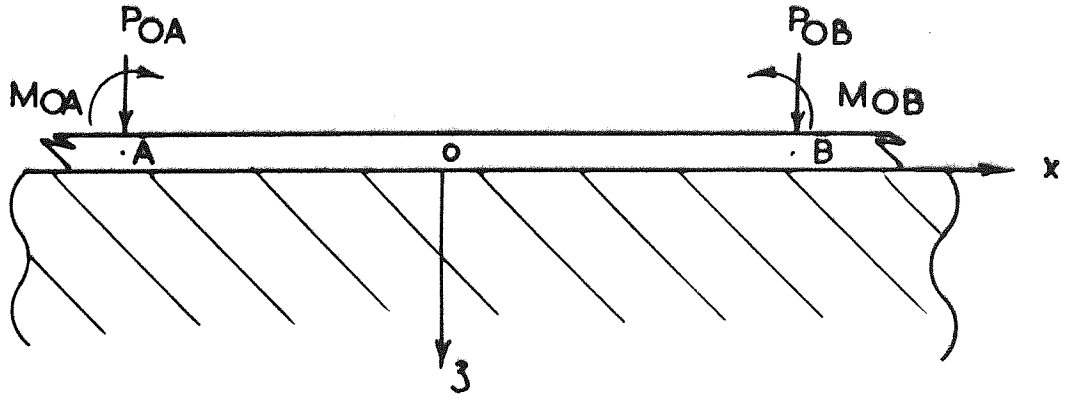

c. Infinite beam subjected to end conditioning forces

Fig . 3.6

where

$$G_{0P}(X) = J_{0PX} + (\alpha_1 + \alpha_2)J_{0PX_1} + (\alpha_1 - \alpha_2)J_{0PX_2} + (\alpha_2 + \alpha_3)J_{1PX_1} + (\alpha_2 - \alpha_3)J_{2PX_2}$$

$$G_{2P}(X) = J_{2PX} + (\alpha_1 + \alpha_2)J_{2PX_1} + (\alpha_1 - \alpha_2)J_{2PX_2} + (\alpha_2 + \alpha_3)J_{3PX_1} + (\alpha_2 - \alpha_3)J_{3PX_2}$$

$$G_{3P}(X) = J_{3PX} + (\alpha_1 + \alpha_2)J_{3PX_1} + (\alpha_1 - \alpha_2)J_{3PX_2} + (\alpha_2 + \alpha_3)J_{4PX_1} + (\alpha_2 - \alpha_3)J_{4PX_2}$$

$$G_{4P}(X) = J_{4PX} + (\alpha_1 + \alpha_2)J_{4PX_1} + (\alpha_1 - \alpha_2)J_{4PX_2} + (\alpha_2 + \alpha_3)J_{5PX_1} + (\alpha_2 - \alpha_3)J_{5PX_2}$$

(3.14 a-d)

and

J_{nPr} is the value of $J_{np}(X)$ evaluated at $X = r$,

$X_1 = L' - \ell' + X$, $X_2 = \ell' - X$, $X = x/C$

3.4 Finite beam subjected to a uniform distributed load acting at an arbitrary location

The superposition analysis of this problem (Fig. 3.7) can be approached in a manner similar to that outlined in the previous section. The deflection, bending moment, shearing forces, and contact forces are given by

$$W(X) = \frac{2pc^4}{\pi E_b I} G_{0U}(X) \quad ,$$

$$M(X) = \frac{2pc^2}{\pi} G_{2U}(X) \quad ,$$

$$V(X) = -\frac{2pc}{\pi} G_{3U}(X) \quad , \qquad (3.15\ a\text{-}d)$$

$$Q(X) = \frac{2p}{\pi} G_{4U}(X) \quad .$$

Where

$$G_{0U}(X) = J_{0UX} + (\alpha_5 + \alpha_6)J_{0PX_1} + (\alpha_5 - \alpha_6)J_{0PX_2} + (\alpha_7 + \alpha_8)J_{1PX_1} + (\alpha_7 - \alpha_3)J_{1PX_2} \quad ,$$

$$G_{2U}(X) = J_{2UX} + (\alpha_5 + \alpha_6)J_{2PX_1} + (\alpha_5 - \alpha_6)J_{2PX2} + (\alpha_7 + \alpha_8)J_{3PX_1} + (\alpha_7 - \alpha_8)J_{3PX_2} \quad ,$$

$$G_{3U}(X) = J_{3UX} + (\alpha_5 + \alpha_6)J_{3PX_1} + (\alpha_5 - \alpha_6)J_{3PX_2} + (\alpha_7 + \alpha_8)J_{4PX_1} + (\alpha_7 - \alpha_8)J_{4PX_2} \quad ,$$

$$G_{4U}(X) = J_{4UX} + (\alpha_5 + \alpha_6)J_{4PX_1} + (\alpha_5 - \alpha_6)J_{4PX_2} + (\alpha_7 + \alpha_8)J_{5PX_1} + (\alpha_7 - \alpha_8)J_{5PX_2} \qquad (3.16\ a\text{-}d)$$

In (3.16 a-d), J_{nUr} and J_{nPr} are the values of $J_{nU}(X)$ (equations 2.27a and 2.33 a-c) and $J_{nP}(X)$ evaluated at $X = r$.

$$X_1 = L' - \ell' + X \ , \quad X_2 = \ell' - X \ ,$$

$$L' = L/C \ , \quad \ell' = \ell/C \ , \quad X = x/C$$

$$\alpha_5 = \frac{A'+B'}{C'} \ , \qquad \alpha_6 = \frac{A_1'+B_1'}{C_1'} \ , \tag{3.17}$$

$$\alpha_7 = \frac{F'+H'}{C'} \ , \qquad \alpha_8 = \frac{F_1'+H_1'}{C_1'}$$

The values of A', B', C', C_1', F', H', F_1' and H_1' are obtained by making the following substitution in (3.12 a-j) :

$$J_{2P\ell'} \rightarrow J_{2U\ell'} \ ,$$

$$J_{2Pg'} \rightarrow J_{2Ug'} \ ,$$

$$J_{3P\ell'} \rightarrow J_{3U\ell'} \ ,$$

$$J_{3Pg'\ell} \rightarrow J_{3Ug'\ell} \ .$$

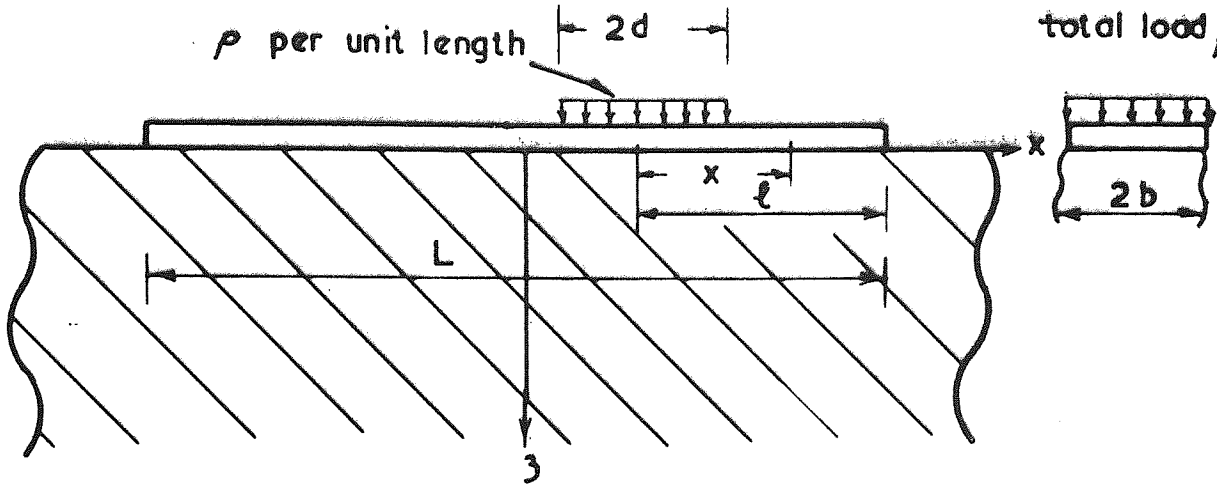

Fig .3.7 Finite beam subjected to a uniform distributed load at an arbitrary location.

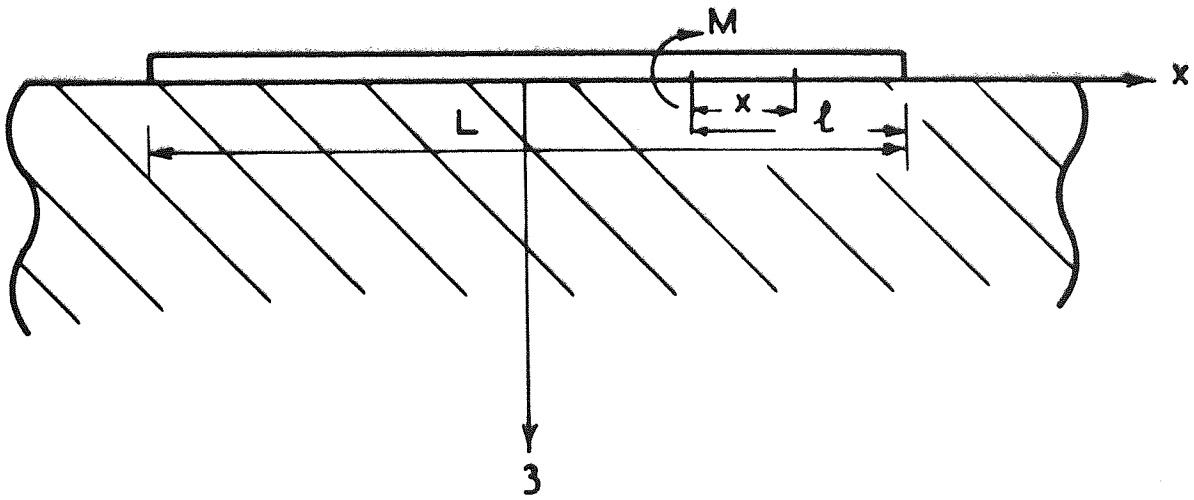

Fig. 3.8. Finite beam subjected to a concentrated couple at an arbitrary location

3.5 Finite beam subjected to a concentrated couple acting at an arbitrary location

The solution to the problem of a concentrated couple acting at an arbitrary location (Fig. 3.8), can be written in the form

$$W(X) = \frac{Mc^2}{\pi E_b I} G_{0M}(X) \ ,$$

$$M(X) = \frac{M}{\pi} G_{2M}(X) \ ,$$

$$V(X) = -\frac{M}{c\pi} G_{3M}(X) \ ,$$

$$Q(X) = \frac{M}{c^2\pi} G_{4M}(X) \ . \qquad (3.18\ a\text{-}d)$$

Where

$$G_{0M}(X) = J_{1PX} + (\alpha_9 + \alpha_{10})J_{0PX_1} + (\alpha_9 - \alpha_{10})J_{0PX_2} + (\alpha_{11} + \alpha_{12})J_{1pX_1} + (\alpha_{11} - \alpha_{12})J_{1PX_2} \ ,$$

$$G_{2M}(X) = J_{3PX} + (\alpha_9 + \alpha_{10})J_{2PX_1} + (\alpha_9 - \alpha_{10})J_{2PX_2} + (\alpha_{11} + \alpha_{12})J_{3PX_1} + (\alpha_{11} - \alpha_{12})J_{3PX_2} \ ,$$

$$G_{3M}(X) = J_{4PX} + (\alpha_9 + \alpha_{10})J_{3PX_1} + (\alpha_9 - \alpha_{10})J_{3PX_2} + (\alpha_{11} + \alpha_{12})J_{4PX_1} + (\alpha_{11} - \alpha_{12})J_{4PX_2} \ ,$$

$$G_{4M}(X) = J_{5PX} + (\alpha_9 + \alpha_{10})J_{4PX_1} + (\alpha_9 - \alpha_{10})J_{4PX_2} + (\alpha_{11} + \alpha_{12})J_{5PX_1} + (\alpha_{11} - \alpha_{12})J_{5PX_2} \ . \qquad (3.19a\text{-}d)$$

In (3.19 a-d)

$$\alpha_9 = \frac{A'' + B''}{C''} \quad , \qquad \alpha_{10} = \frac{A''_1 + B''_1}{C''_1} \quad ,$$

$$\alpha_{11} = \frac{F'' + H''}{C''} \quad , \qquad \alpha_{12} = \frac{F''_1 + H''_1}{C''_1} \quad . \tag{3.20}$$

In (3.20) A'', B'', A''_1, B''_1, C'', C''_1, F'', H'', F''_1 and H''_1 are obtained by making the following substitution in (3.12 a-j):

$$J_{2P\ell'} \rightarrow J_{3P\ell'}$$

$$J_{2Pg'} \rightarrow -J_{3Pg'} \tag{3.21}$$

$$J_{3P\ell'} \rightarrow J_{4P\ell'}$$

$$J_{3Pg'} \rightarrow -J_{4Pg'}$$

3.6 Numerical Results

Numerical values are obtained for the deflections W(X), bending moments M(X), shearing forces V(X), and contact forces Q(X) of a finite beam subjected to a concentrated unit load and a concentrated unit couple, resting on a three dimensional elastic medium (the numerical results for the two dimensional medium are given in chapter 4). In order to evaluate the above

values, it is necessary to obtain values for $G_{0P}(X)$, $G_{2P}(X)$, $G_{3P}(X)$, and $G_{4P}(X)$ (defined in 3.14a-d), and $G_{0M}(X)$, $G_{2M}(X)$, $G_{3M}(X)$ and $G_{4M}(X)$ (defined in 3.19a-d). A method for the evaluation of integrals $J_{nP}(X)$ occuring in expressions $G_{nP}(X)$ and $G_{nM}(X)$ was discussed in chapter 2. The numerical results for L/B = 5, 10, 20 and B/2c = 0.01, 0.05, 0.1, 0.2 and 1.0 are given in Appendix 1. These results are for the following eccentricities of concentrated load and concentrated couple :

ℓ = 0, B, 2B, 2.5B	for L/B = 5
ℓ = 0, 2B, 4B, 5B	" 10
ℓ = 0, 4B, 8B, 10B	" 20

where ℓ is the distance from the point of application of external load to the end of the beam, L is the length of the beam, and B is its width.

Figures 3.9 and 3.10 show the contact force and bending moment distribution for beams with L/B ratios of 5, 10 and 20, and B/2c = 0.01, 0.05, 0.1, 0.2, 1.0, subjected to a central concentrated unit load. The full lines are the results obtained for the infinite beam.

Figure 3.11 shows the distribution of contact force for a finite beam (L/B = 10) subjected to a concentrated unit load of different eccentricities. From Figure 3.11 it can be seen that for B/2c = 1.0, the finite beam can be treated as an infinite beam, as long as the concentrated load acts at ℓ > B (i.e. the

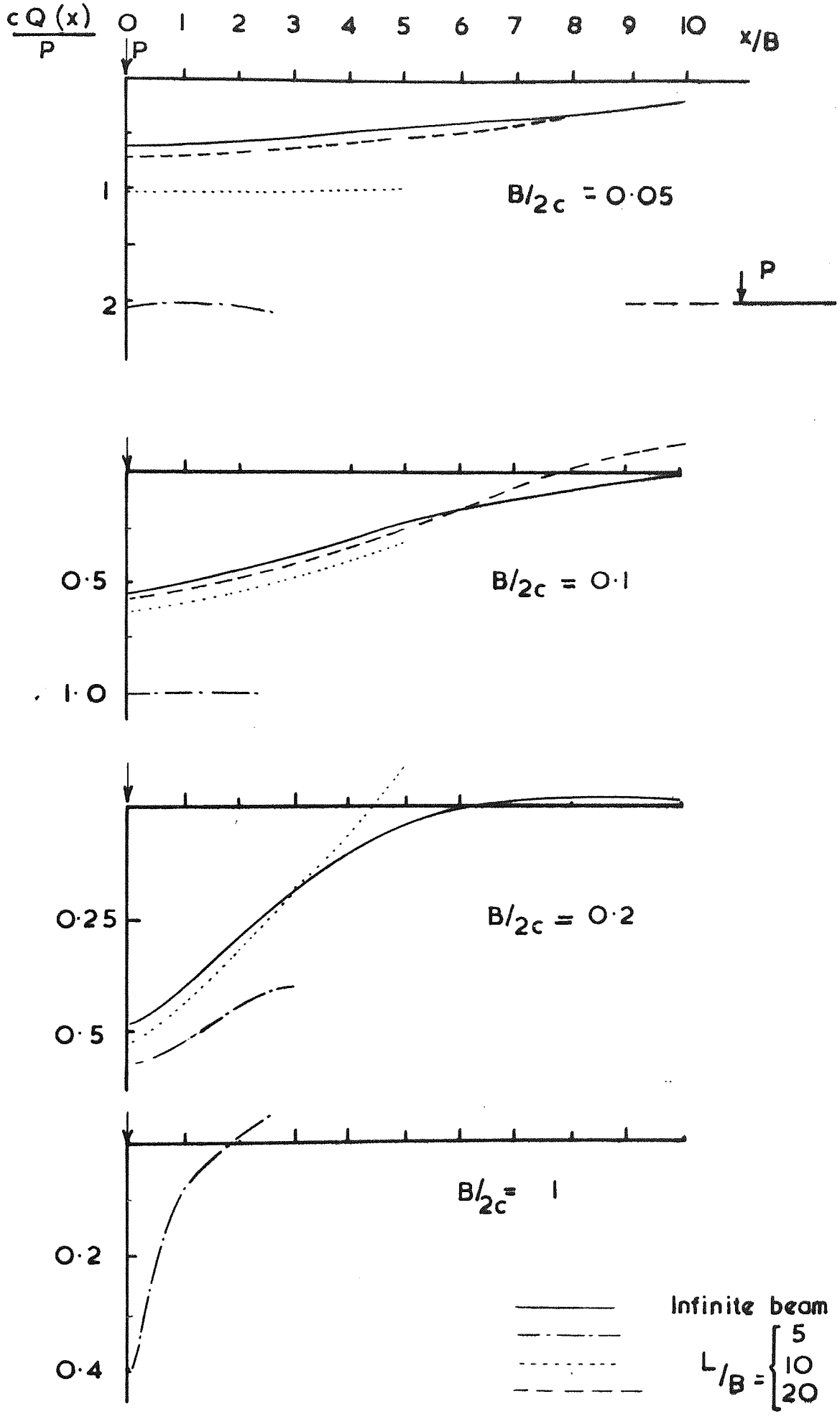

Fig .3.9 Contact force distribution for centrally loaded beam

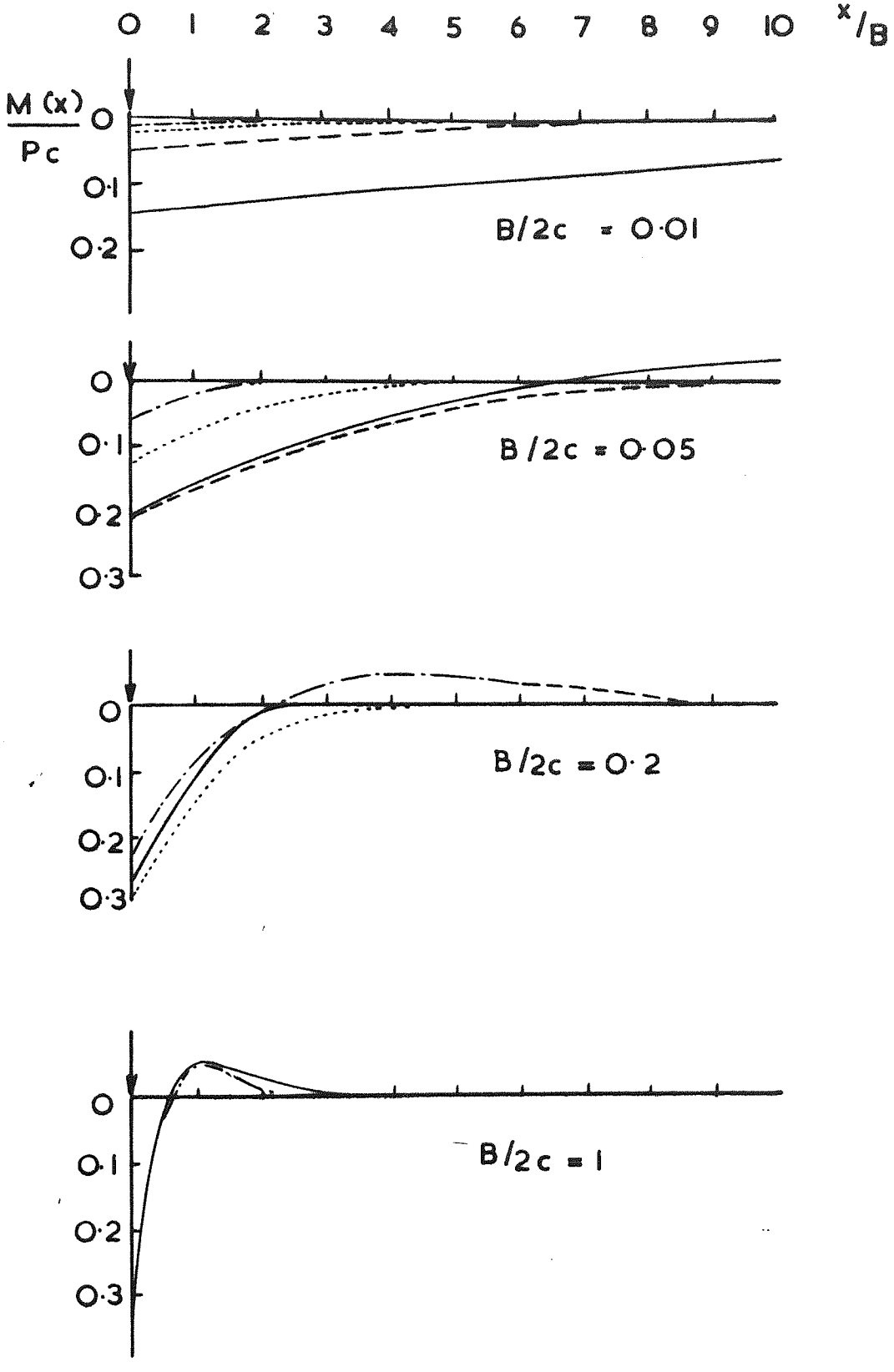

Fig . 3.10 Bending moment distribution for a finite beam subjected to a concentrated load in the middle

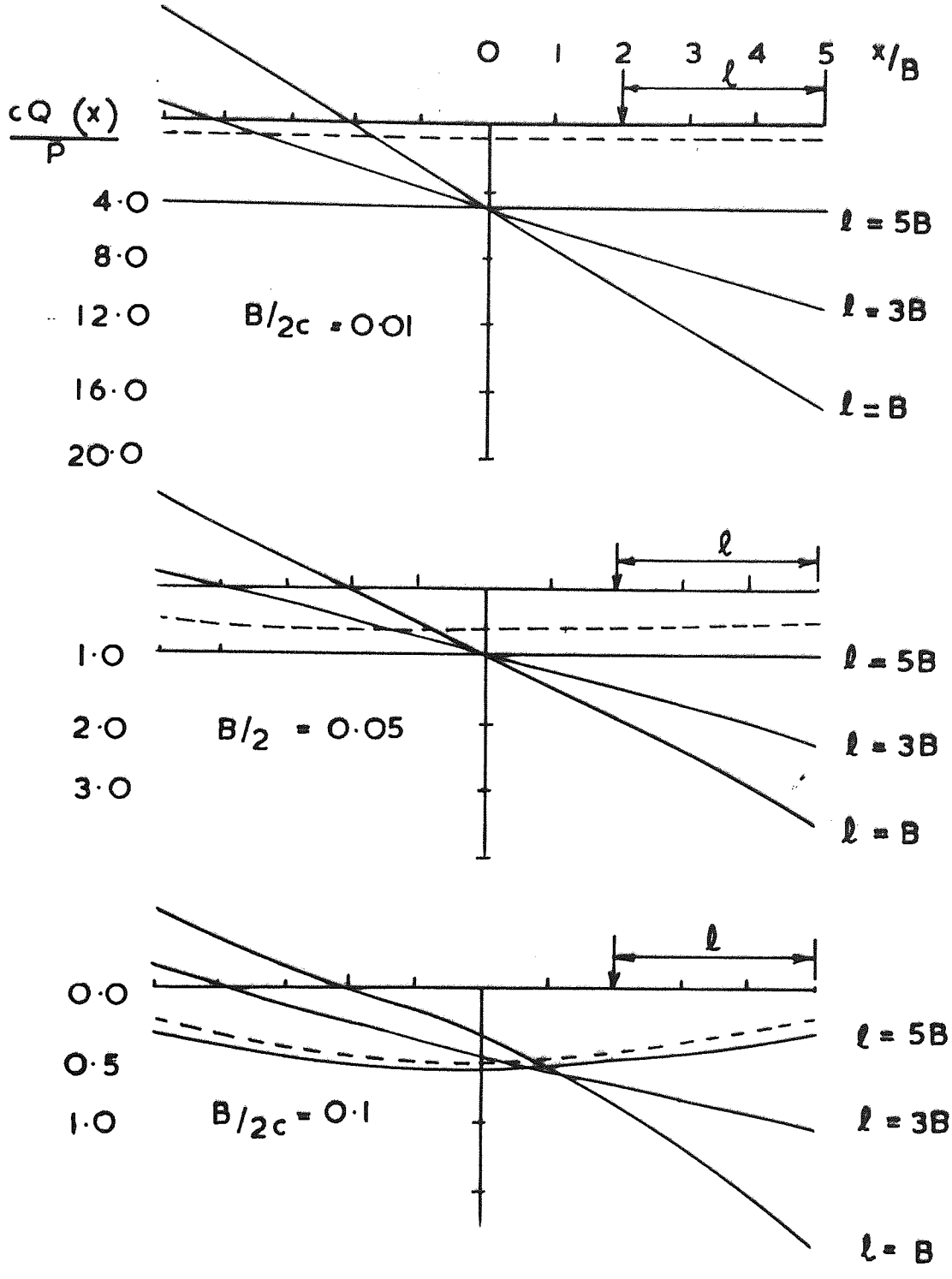
0 1 2 3 4 5 x/B
ℓ
cQ (x)/P
4·0
8·0
12·0
16·0
20·0
B/2c = 0·01
ℓ = 5B
ℓ = 3B
ℓ = B
1·0
2·0
3·0
B/2 = 0·05
ℓ = 5B
ℓ = 3B
ℓ = B
0·0
0·5
1·0
B/2c = 0·1
ℓ = 5B
ℓ = 3B
ℓ = B

Fig . 3 . 11

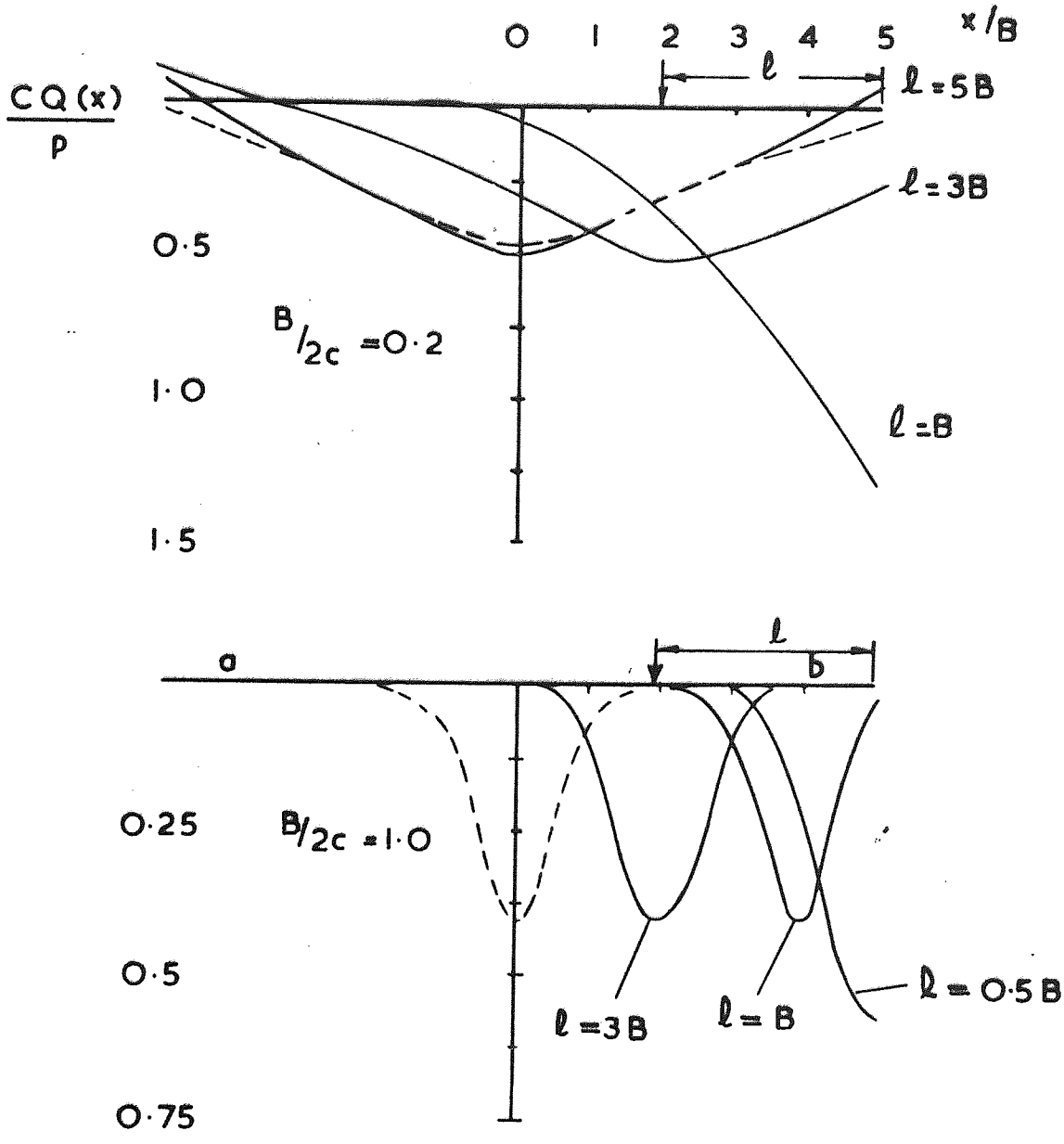

Fig. 3.11 Finite beam subjected to a concentrated load contact force distribution L/B = 10

---- Infinite beam

——— Finite beam

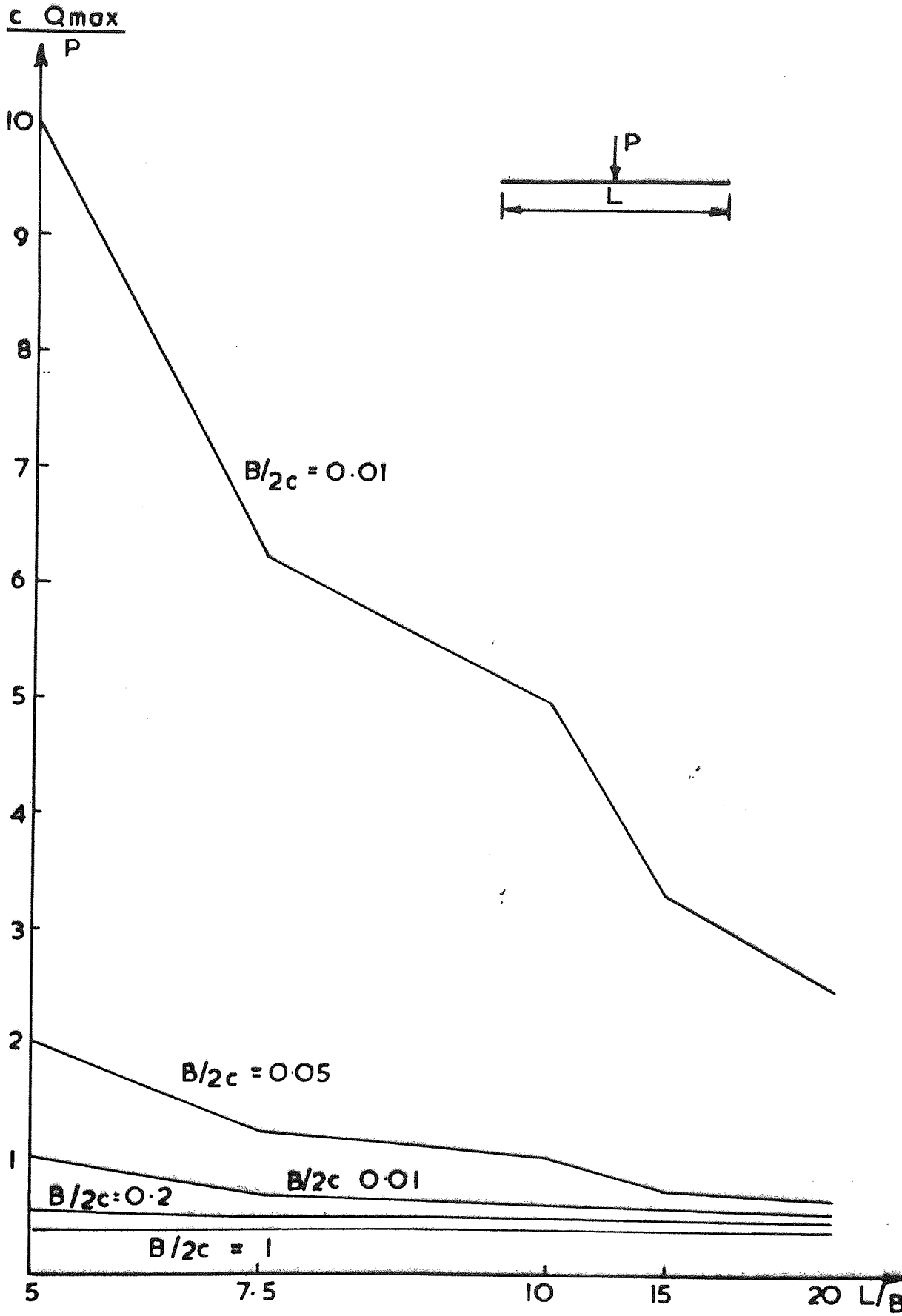

Fig.3.12 Variation of maximum contact force against L/B

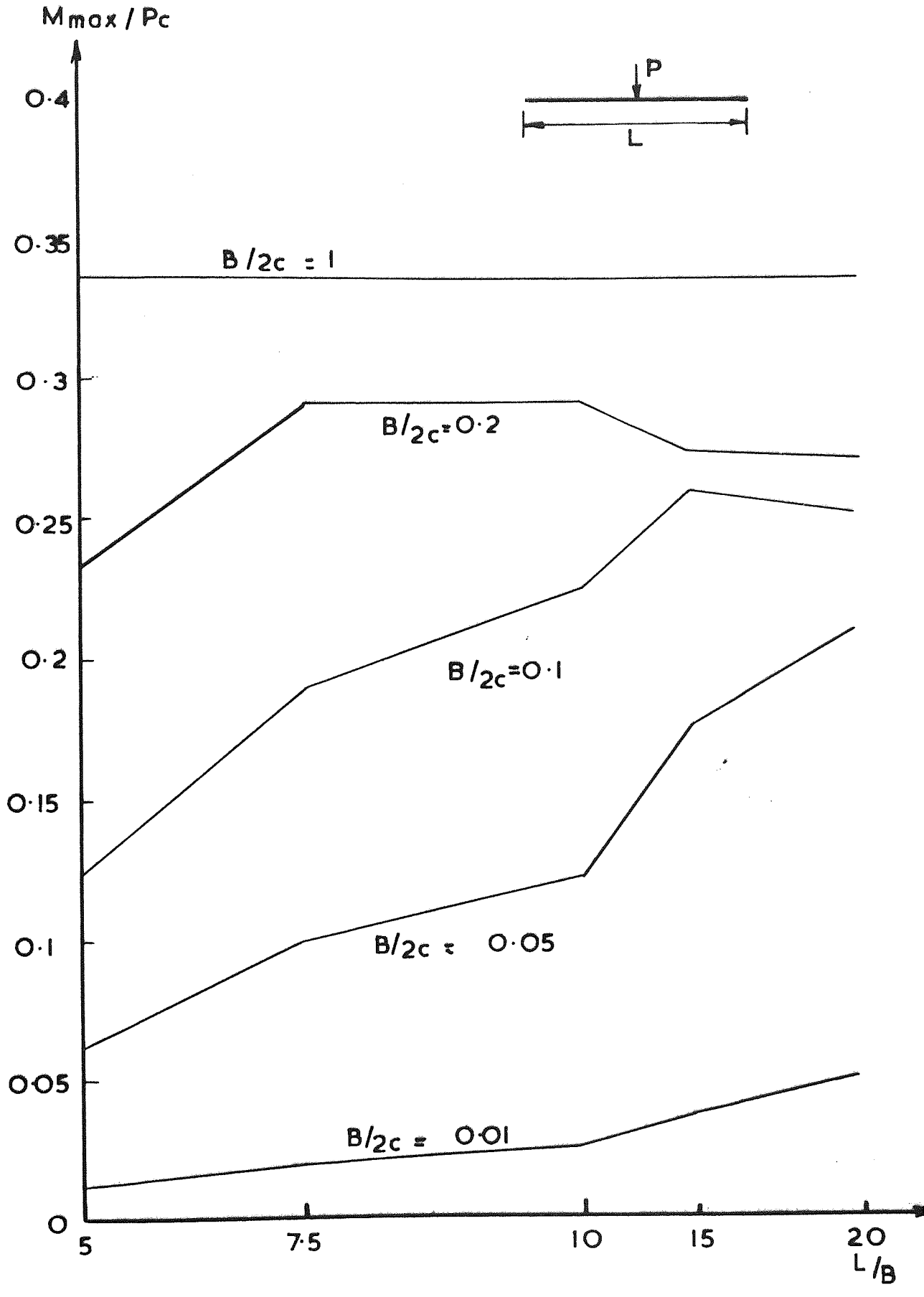

Fig. 3.13 Variation of maximum bending moment against L/B

load acts at region ab). From Appendix 1 it can be seen that the beam with L/B = 5 behaves similarly to L/B = 10 for B/2c = 1.0; i.e. when the concentrated load acts at a distance $4B > \ell > B$, the beam can be treated as an infinite beam. In Figures 3.12 and 3.13 the variation of maximum contact force and bending moments for beams with L/B = 5, 10, 20 subjected to a central concentrated load P for different values of B/2c are given. It can be see that for a flexible beam (B/2c = 1), the maximum contact force and bending moments are almost the same for L/B = 5, 10 and 20.

3.7 Comparison with approximate methods of analysis

Barden (1962) gives an approximate method of obtaining contact force distribution beneath finite beams resting on an elastic medium. The solution is governed by a dimensionless parameter ϕ given by

$$10^4\phi = \frac{\pi E L^4}{4E_b I(1-\nu^2)} \qquad (3.22)$$

In this method it is assumed that the contact force distribution is made up from a number of steps or blocks of uniform vertical loads. The beam will deflect under the action of the known external applied loads and the unknown contact force distribution. The elastic medium will also deflect under the equal and opposite reaction to the contact force. Assuming that the beam does not lift, the deflected shapes of the beam and soil must coincide; hence the unknown contact pressure distribution may be solved.

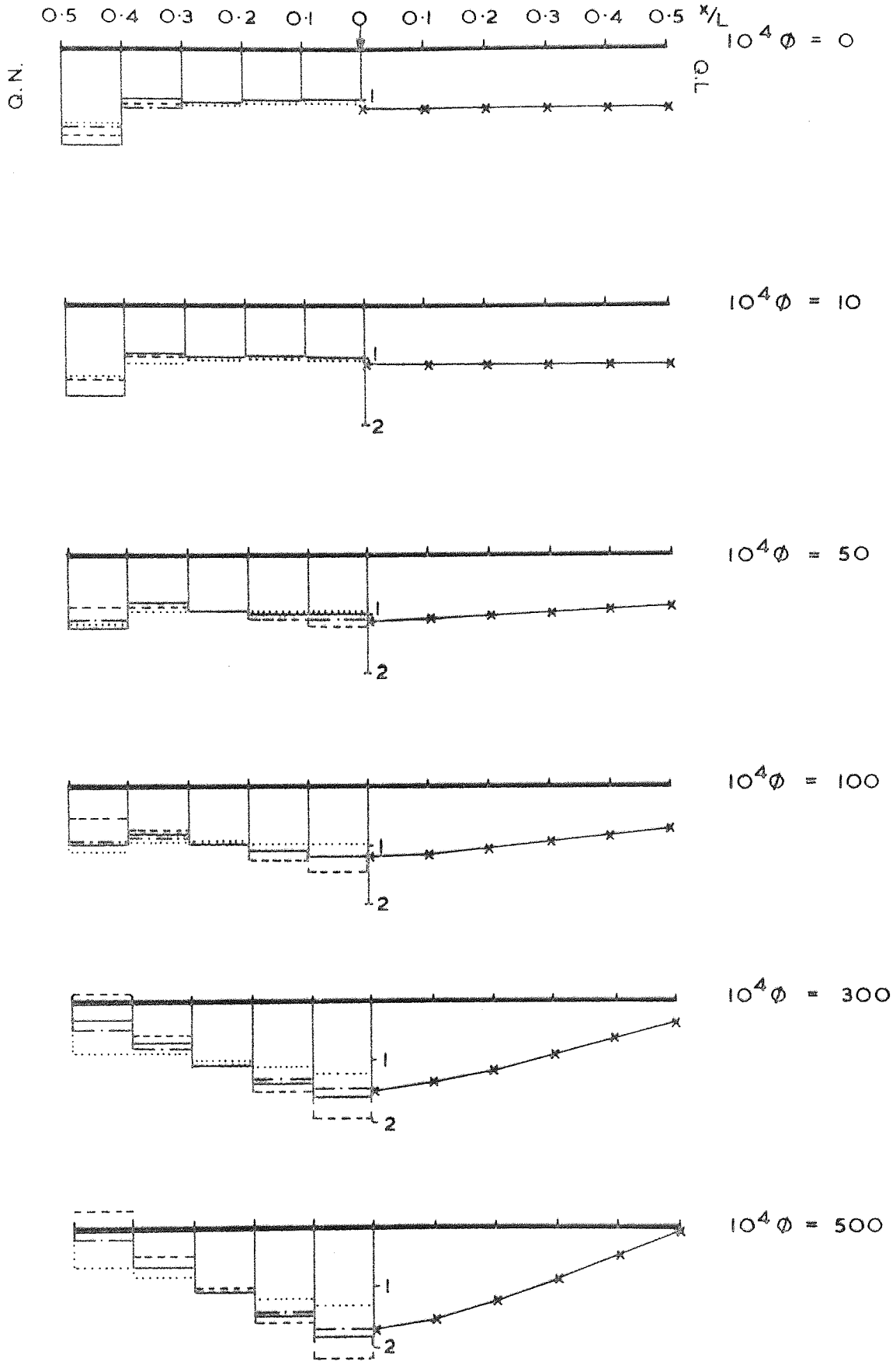
0·5 0·4 0·3 0·2 0·1 0 0·1 0·2 0·3 0·4 0·5 x/L
Q.N.
G.L.
1
2
$10^4\phi = 0$
$10^4\phi = 10$
$10^4\phi = 50$
$10^4\phi = 100$
$10^4\phi = 300$
$10^4\phi = 500$

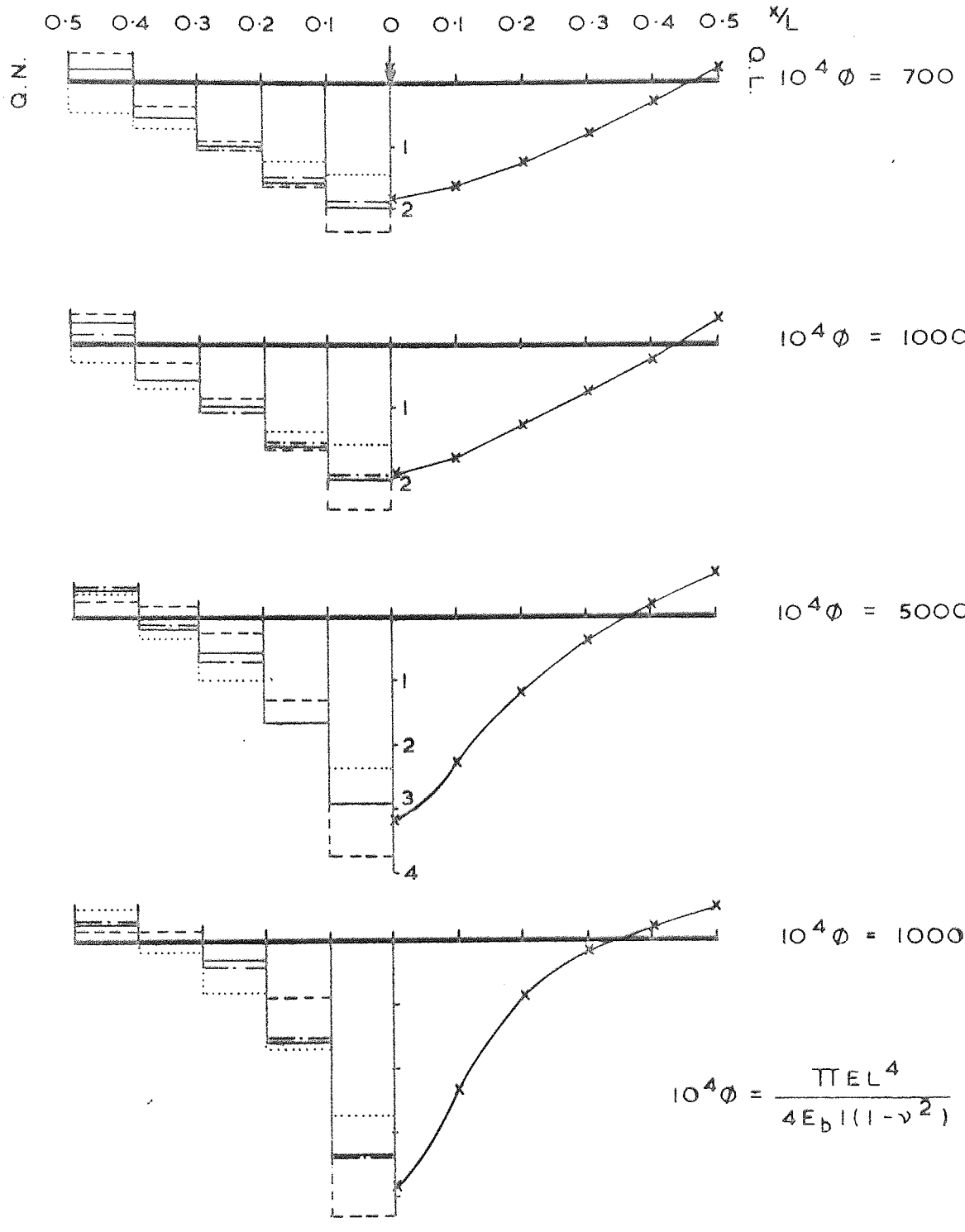

FIG. 3.14 Contact force distribution using

a) Superposition method
b) Ohde s method
c) Bardens method

Number of blocks of pressure n = 10

Barden gives Tables of influence coefficients of the contact force distribution for different values of $10^4\phi$ (= 0, 10, 50, 100, 300, 500, 700, 1000, 5000, 10000) for a beam with L/B = 10 with different eccentricities of applied load. Barden concludes that the influence coefficients for the contact force obtained in the case of beams with L/B = 5 and 20 are fairly close to the corresponding values obtained with L/B = 10. However, the extent of error involved due to a variation of L/B is not explicitly evaluated.

In this section we investigate the influence of L/B on the contact force distribution of a finite beam resting on an elastic medium, subjected to a central unit load, using the following methods of analysis :

(i) Ohde's Method

(ii) Solution obtained by using superposition technique.

A summary of Ohde's method is given in Appendix 2. In this method the solution is governed by an influence coefficient given by

$$\beta = \frac{a^3 BE}{E_b I(1-\nu^2)} \qquad (3.23)$$

This method is used to obtain the contact stress distribution of the beams with L/B = 5, 10, 20, subjected to a central concentrated load. The contact force distribution for different values of β (equation 3.23) corresponding to $10^4\phi$ values (Table 3.1) are given in Appendix A.2, Tables (A.2.2a-c). Fig. 3.14 shows the contact force distribution obtained for L/B = 5, 10, and 20, for different $10^4\phi$ values by using Ohde's method. The results given by Barden are also shown in solid lines.

The relation between B/2c values of superposition technique and Barden's $10^4\phi$ values can be written as follows :

$$B/2c = \left[\frac{10^4\phi}{4\pi(L/B)^4} \right]^{1/3} \qquad (3.24)$$

From (3.24) it can be seen that B/2c is not independent of L/B. Since the integrals $J_{nP}(X)$ occuring in the expression for the contact force distribution (equation 3.13d) are dependent on B/2c, therefore a change in L/B would have an effect on the distribution of contact force. The corresponding values of B/2c for different values of $10^4\phi$ are given in Table (3.1). By using superposition technique the contact force distribution of the beams with L/B = 5, 10, 20 subjected to a central unit load are obtained for different values of B/2c. The maximum contact forces for the beams with different L/B ratios obtained from different methods of analysis (superposition, Barden's and Ohde's method) are compared in Table (3.2). It can be seen that for rigid beams

L/B	$10^4\phi$	0.01	10	50	100	300	500	700	1000	5000	10000
5	B/2c	0.011	0.108	0.185	0.233	0.337	0.399	0.447	0.503	0.860	1.084
	β	0.000	0.002	0.013	0.025	0.076	0.127	0.178	0.255	1.273	2.546
10	B/2C	0.004	0.043	0.073	0.093	0.134	0.158	0.177	0.20	0.341	0.430
	β	0.000	0.001	0.006	0.013	0.038	0.064	0.089	0.127	0.637	1.273
20	B/2c	0.002	0.017	0.029	0.037	0.053	0.063	0.070	0.079	0.135	0.171
	β	0.000	0.001	0.003	0.006	0.019	0.032	0.044	0.064	0.318	0.636

Table (3.1) values of B/2c and β corresponding to $10^4\phi$ values

$$B/2c = \left[\frac{EB^4}{16C(1-\nu^2)E_b I} \right]^{1/3}$$

$$10^4\phi = \frac{\pi E L^4}{4E_b I(1-\nu^2)}$$

$$\beta = \frac{a^3 BE}{E_b I(1-\nu^2)}$$

$10^4\phi$	L/B = 5			L/B = 10			L/B = 20		
	O/B	S/B	S/O	O/B	S/B	S/O	O/B	S/B	S/O
0.0	1.02	1.20	1.10	1.06	1.20	1.13	1.09	1.20	1.18
10	1.07	1.16	1.10	1.04	1.15	1.10	1.04	1.15	1.08
50	1.16	1.09	1.13	0.99	1.06	1.07	0.93	1.05	0.94
100	1.21	1.05	1.14	0.96	1.00	1.04	0.85	0.97	0.87
300	1.22	1.03	1.19	0.93	0.94	1.01	0.75	0.89	0.84
500	1.21	1.04	1.20	0.94	0.94	1.00	0.73	0.88	0.86
700	1.21	1.06	1.20	0.95	0.95	1.00	0.74	0.89	0.88
1000	1.22	1.08	1.20	0.96	0.98	1.02	0.75	0.90	0.88
5000	1.27	1.23	1.22	0.99	1.07	1.08	0.80	0.98	0.97
10000	1.29	1.34	1.26	1.01	1.15	1.14	0.81	1.02	1.04

Table (3.2) Comparison of the maximum contact stress of a finite beam subjected to a concentrated load in the middle, using different methods of analysis

O = Ohde's method

B = Barden's method

S = Superposition

($10^4\phi < 50$), the superposition method gives greater values for the maximum contact force for the three values of L/B. This is because the methods fails to predict the concentration of the stresses at the ends of the beam. From Table (3.2) it can be seen that for L/B = 10 and $10^4\phi > 50$ the results obtained from different methods are in good agreement.

In order to investigate the effect of L/B on the results, the ratio between the maximum contact forces of the beams with L/B = 5 and those of L/B = 10, and 20 are obtained for different $10^4\phi$ and given in Table (3.3). The maximum contact force for beams with L/B ratios of 5, 10 and 20 referred to as Q_5, Q_{10} and Q_{20} respectively. It can be seen that a decrease in L/B increases the maximum contact force. This increase depends on the flexural rigidity of the beam and elastic properties of the medium. The ratios of maximum contact forces of L/B = 5 and those of L/B = 10 and 20 for a flexible beam ($10^4\phi = 1000$) are

$$\frac{Q_5}{Q_{10}} = 1.28 \qquad \frac{Q_5}{Q_{20}} = 1.59$$

using Ohde's approximate method and

$$\frac{Q_5}{Q_{10}} = 1.16 \qquad \frac{Q_5}{Q_{20}} = 1.32$$

using superposition method.

$10^4\phi$	Q_5/Q_{10}		Q_5/Q_{10}	
	OH	SU	OH	SU
0.01	0.96	1	0.93	1
10	1.03	1.01	1.03	1.01
50	1.18	1.03	1.25	1.04
100	1.27	1.05	1.43	1.07
300	1.32	1.10	1.64	1.16
500	1.28	1.11	1.67	1.19
700	1.28	1.11	1.64	1.19
1000	1.27	1.10	1.64	1.20
5000	1.28	1.15	1.59	1.25
10000	1.28	1.16	1.59	1.32

Table (3.3) The ratios Q_5/Q_{10} and Q_5/Q_{20} for a beam subjected to a concentrated central unit load

Q_5 = Maximum contact force for L/B = 5

Q_{10}= " " " L/B = 10

Q_{20}= " " " L/B = 20

OH = Ohde's method

SU = Superposition method

3.8 Validity of the solution

A serious objection which can be made on the solution obtained from the superposition technique is that the method fails to predict the concentration of contact forces at the ends of the beam. It was thought that the reason for this peculiar behaviour might be due to one of the following :

(a) The no zero tractions which might exist on the surface of the medium exterior to the beam (see section 3.2)

(b) It was assumed that the deflection of the beam is governed by equation (2.23) which is restricted to the class of slender beams.

It is however possible to compare the results for contact forces obtained from this method and those of an approximate method of solution to obtain a criteria for the validity of the solution. Numerical results were obtained for contact force distribution of a beam with L/B = 10 subjected to a concentrated unit load with different eccentricities for different values of B/2c (equation 3.24) corresponding to $10000 > 10^4\phi > 0$. The results were compared with the values given by Barden. It was observed that the two results are in good agreement for

$$10^4\phi > 100 \quad \text{or} \quad B/2c > 0.09 \qquad (3.25)$$

The relation between L/2c, L/B and B/2c is

$$L/2c = L/B \cdot B/2c \tag{3.26}$$

The limit given by (3.25) in terms of L/2c is

$$L/2c > 0.9 \tag{3.27}$$

By using (3.25), (3.26) and (3.27) the limit of B/2c for the validity of the superposition method for beams with L/B = 5 and 20 are

$$\begin{aligned} B/2c &= 0.18 \quad \text{for } L/B = 5 \\ B/2c &= 0.045 \quad \text{for } L/B = 20 \end{aligned} \tag{3.28}$$

3.9 Conclusions

The expressions for the deflection, bending moment, shearing force and contact force were obtained for a finite beam subjected to a concentrated load, a concentrated couple and a uniform load acting at an arbitrary location. Numerical results for L/B = 5, 10, 20 and B/2c = 0.01, 0.05, 0.1, 0.2, 1, for the case of concentrated force and a concentrated couple are given in Appendix 1. The results show that beams with L/B = 5, 10 and 20 and B/2c = 1 can be treated as an infinite beam provided the concentrated force or couple is acting at a distance $\ell > B$ from the end of the beam.

The results for contact force distribution showed that the solution is not valid for rigid beams. By comparing the results for the contact force distribution obtained from superposition method and those given by Barden, a criteria was given for the validity of the superposition method as follows :

$B/2c > 0.18$	for	$L/B = 5$
$B/2c > 0.09$	"	" 10
$B/2c > 0.045$	"	" 20

The influence of L/B on the maximum contact force distribution of a finite beam with different flexibilities subjected to a central load was investigated.

CHAPTER FOUR

BEAMS ON NON-HOMOGENEOUS ELASTIC MEDIUM

4.1 Introduction

In the analysis of the infinite and the finite beam problem (Chapters 2 and 3) elastic properties of the medium were treated as being constant throughout the medium. There is experimental evidence which indicates that the elastic properties of the soil vary with depth. A series of plate loading tests at different depths were performed on Middle Chalk in Norfolk (Burland and Lord, 1970). The values obtained for Young's modulus increased as the depth increased. Marsland (1971) obtained values for Young's modulus of London clay at different levels to a depth of 25m from the in situ plate loading tests and laboratory triaxial tests. These values indicate that Young's modulus increases with depth as a result of increase in overburden pressure. Simons (1971) in his investigation on the effect of non-homogeneity of London clay in the settlement calculations, concludes that the elastic modulus of soil varies with depth as a consequence of increasing effective stresses. An example of settlement calculation given by Simons indicates that the immediate settlement (elastic settlement) in a foundation is over-estimated if the elastic properties are assumed to be constant with depth. Triaxial tests on samples, taken from different depths of London clay, were carried out by Wroth (1971). The results obtained from these tests showed that the values of Young's modulus increased with depth. The above evidence suggests that a deposit of soil can be treated as a non-homogeneous medium. A non-homogeneous medium is one whose mechanical properties at a point are functions of the spatial

coordinates at that point, i.e. $G = G(x,z)$ and $\nu = \nu(x,z)$.

In this chapter, the differential equation governing the displacement function of an isotropic non-homogeneous incompressible elastic medium is developed. The problem is then solved for the special case when shear modulus G is a linear function of depth in the form $G = G(o) + mz$. The solution is used to analyse beams resting on such non-homogeneous incompressible medium. The effect of a linear variation with depth of shear modulus on the stresses and displacements in an isotropic non-homogeneous incompressible ($\nu = 0.5$) elastic medium subjected to a uniform distributed load was first investigated by Gibson (1967). The work was later extended to include all values of Poisson's ratio (Gibson and Sills, 1971).

4.2 Basic equations

Consider a plane strain problem of an isotropic non-homogeneous incompressible ($\nu = 0.5$) elastic medium, where shear modulus G is a function of x and z (Fig. 4.1); i.e. $G = G(x,z)$

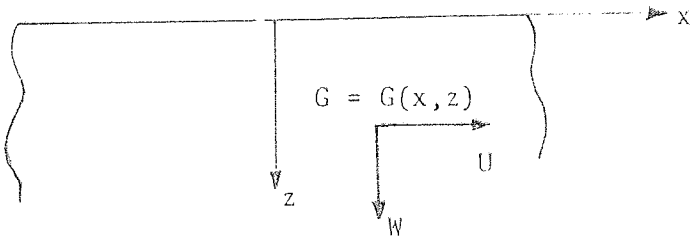

Fig. 4.1

For such a non-homogeneous elastic medium, the stress components are related to displacements U and W by the relations

$$\sigma_x = p(x,z) + 2G \frac{\partial U}{\partial x} \quad ,$$

$$\sigma_z = p(x,z) + 2G \frac{\partial W}{\partial z} \quad , \qquad (4.1)$$

$$\tau_{xz} = G \left(\frac{\partial U}{\partial z} + \frac{\partial W}{\partial x} \right) \quad ,$$

Where

$$p(x,z) = (\sigma x + \sigma z)/2$$

is an arbitrary hydrostatic pressure which should be determined by the boundary conditions of the particular problem.

In the absence of body forces, the equations of equilibrium in the x and z directions are

$$\frac{\partial \sigma_x}{\partial x} + \frac{\partial \tau_{xz}}{\partial z} = 0$$

$$\qquad (4.2)$$

$$\frac{\partial \sigma_z}{\partial z} + \frac{\partial \tau_{xz}}{\partial x} = 0$$

By substituting (4.1) in (4.2) we obtain

$$\frac{\partial p(x,z)}{\partial x} + \frac{\partial}{\partial x} \left(2G \frac{\partial U}{\partial x} \right) + \frac{\partial}{\partial z} \left[G \frac{\partial U}{\partial z} + \frac{\partial W}{\partial x} \right] = 0$$

$$\frac{\partial p(x,z)}{\partial z} + \frac{\partial}{\partial z} \left(2G \frac{\partial W}{\partial z} \right) + \frac{\partial}{\partial x} \left[G \frac{\partial U}{\partial z} + \frac{\partial W}{\partial x} \right] = 0$$

(4.3)

4.2.1 Displacement function

We introduce a displacement function ζ such that

$$U = \frac{\partial \zeta}{\partial z} \quad , \qquad W = - \frac{\partial \zeta}{\partial x} \tag{4.4}$$

which satisfies the condition of incompressibility

$$\frac{\partial U}{\partial x} + \frac{\partial W}{\partial z} = 0 \tag{4.5}$$

Using (4.4), (4.3) can be expressed in terms of $p(x,z)$ and $\zeta(x,z)$; by eliminating $p(x,z)$ from the resulting equations we obtain

$$G\nabla^4\zeta + 2\frac{\partial G}{\partial x}\frac{\partial}{\partial x}(\nabla^2\zeta) + 2\frac{\partial G}{\partial z}\frac{\partial}{\partial z}(\nabla^2\zeta) + 4\frac{\partial^2 G}{\partial x \partial z}\frac{\partial^2 \zeta}{\partial x \partial z} + \left(\frac{\partial^2 G}{\partial x^2} - \frac{\partial^2 G}{\partial z^2}\right)\left(\frac{\partial^2 \zeta}{\partial x^2} - \frac{\partial^2 \zeta}{\partial z^2}\right) = 0 \tag{4.6}$$

It can be shown that the hydrostatic stress should satisfy the following equation :

$$\nabla^2 p(x,z) + 2\frac{\partial^2 \zeta}{\partial x \partial z}\left(\frac{\partial^2 G}{\partial x^2} - \frac{\partial^2 G}{\partial z^2}\right) + 2\frac{\partial G}{\partial x}\frac{\partial}{\partial z}\left(\frac{\partial^2 \zeta}{\partial x^2} + \frac{\partial^2 \zeta}{\partial z^2}\right) - 2\frac{\partial G}{\partial z}\frac{\partial}{\partial x}\left(\frac{\partial^2 \zeta}{\partial z^2} + \frac{\partial^2 \zeta}{\partial x^2}\right) + 2\frac{\partial^2 G}{\partial x \partial z}\left(\frac{\partial^2 \zeta}{\partial z^2} - \frac{\partial^2 \zeta}{\partial x^2}\right) = 0$$

4.2.2 Linear variation of G(x,z)

We now consider the particular case where the shear modulus varies linearly with depth according to

$$G = G(o) + mz/c \qquad (4.7)$$

Where G(o) is the shear modulus at z = 0, c is a typical length parameter and m is a positive constant. By substituting (4.7) in (4.6) we obtain

$$\nabla^4\zeta(X,Z) + \frac{2}{Z}\frac{\partial}{\partial Z}\nabla^2\zeta(X,Z) = 0 \qquad (4.8)$$

or

$$\nabla^2[Z\nabla^2\zeta(X,Z)] = 0 \qquad (4.9)$$

Where

$$Z = z/c + \rho \quad , \quad \rho = \frac{G(o)}{m} \quad , \quad X = x/c$$

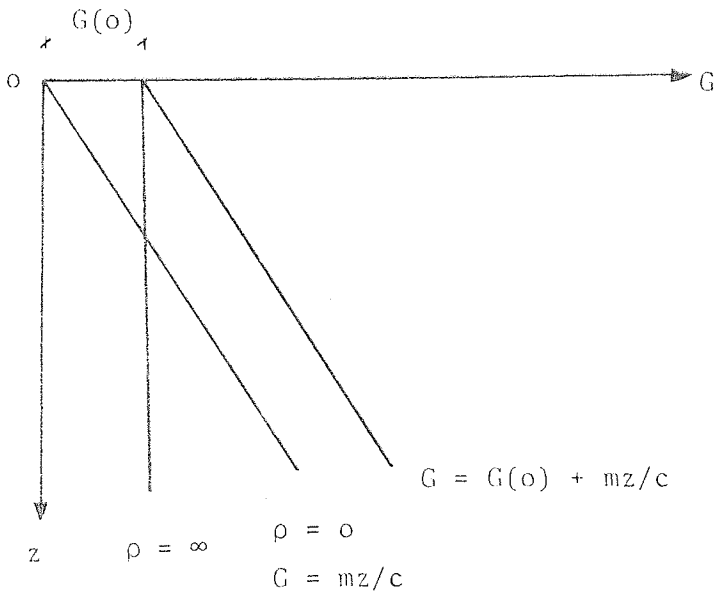

Fig. 4.2

4.2.3 Sinosuidal Loading

Consider the plane strain problem of an isotropic non-homogeneous incompressible medium which is subjected to a sinosuidal load $Q(X) = Q_o \cos\lambda X$ shown in Fig. 4.3 (Total load per width 2b)

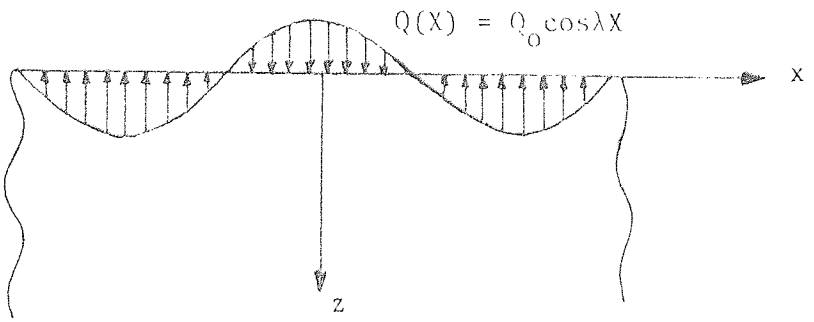

Fig. 4.3

A solution for ζ obtained from (4.8) and substituted in the stress displacement relationship (equation 4.1) should satisfy the following boundary condition

$$\text{at} \quad Z = \rho(z=0) \qquad \sigma_z = \frac{-Q_o}{2b} \cos\lambda X, \qquad \tau_{xz} = 0 \tag{4.10}$$

In addition, the stresses should tend to zero when $Z \to \infty$. A solution for equation (4.8) which is appropropriate to the sinosuidal loading $Q(x) = Q_o \cos\lambda x$ and satisfies the condition of zero stresses where $Z \to \infty$, is of the form

$$Z\nabla^2\zeta(X,Z) = k_1 e^{-\lambda Z} \sin \lambda X \tag{4.11}$$

Where k_1 is a constant which is determined from the boundary conditions.

The displacement function $\zeta(X,Z)$ has the form of

$$\zeta(X,Z) = H(Z)e^{-\lambda Z} \sin\lambda X \tag{4.12}$$

By substituting (4.12) in (4.11) we obtain

$$\frac{d}{dZ}\left[\frac{dH(Z)}{dZ} - 2\lambda H(Z)\right] = \frac{k_1}{Z} \tag{4.13}$$

or

$$\frac{dH(Z)}{dZ} - 2\lambda H(Z) = k_1 \log Z + C \tag{4.14}$$

A solution of (4.14) is

$$H(Z) = k_1\left[-\frac{1}{2\lambda}\log Z - \frac{e^{2\lambda Z}}{2\lambda} Ei(-2\lambda Z)\right] + k_2 \tag{4.15}$$

where $k_2 = -C/2\lambda$, and $Ei(-\theta)$ is the exponential integral defined by

$$Ei(-\theta) = -\int_o^\infty \frac{e^{-t}}{t}\,dt$$

By substituting (4.15) in (4.12), we obtain

$$\zeta = \left\{ k_2 + k_1\left[-\frac{1}{2\lambda}\log Z - \frac{e^{-2\lambda Z}}{2\lambda} Ei(-2\lambda Z)\right] e^{-\lambda Z} \right\}\sin\lambda X \tag{4.16}$$

This displacement function directly gives the displacement components U and W, we have

$$U = \left\{ -\alpha k_2 + k_1 \left[\frac{1}{2} \log Z - \frac{e^{-2\lambda Z}}{2} Ei(-2\lambda Z) \right] \right\} e^{-\lambda Z} \sin\lambda X \qquad (4.17)$$

$$W = -\lambda \left\{ k_2 + k_1 \left[-\frac{1}{2\lambda} \log Z - \frac{e^{-2\lambda Z}}{2} Ei(-2\lambda Z) \right] \right\} e^{-\lambda Z} \cos\lambda X \qquad (4.18)$$

By substituting (4.17) and (4.18) in the first (or second) of equations (4.3) we obtain for p(X,Z) the following expression :

$$p(X,Z) = \frac{G}{\lambda} \left\{ -k_1 \left[\frac{\lambda}{Z} + \frac{1}{Z^2} \right] + \frac{2k_2\lambda^2}{\rho} + \right. \qquad (4.19)$$

$$\left. + \frac{k_1}{\rho} \left[-\lambda \log Z - \lambda e^{2\lambda Z} Ei(-2\lambda Z) + \frac{1}{Z} \right] \right\} e^{-\lambda Z} \cos\lambda X$$

The constants k_1 and k_2 are obtained by satisfying the boundary conditions (4.10).

$$k_1 = \frac{Q_o}{4bG(o)} \frac{e^{\lambda\rho}}{\frac{1}{\rho} + \frac{1}{2\lambda\rho^2} + \lambda e^{2\lambda\rho} Ei(-2\lambda\rho)} \qquad (4.20)$$

$$k_2 = k_1 \left[\frac{1}{2\lambda} \log\rho + \frac{1}{2\lambda} e^{2\lambda\rho} Ei(-2\lambda\rho) - \frac{1}{2\lambda^2\rho} \right]$$

The expressions for U and W are obtained by substituting (4.20) in (4.17) and (4.18). By superposition of the external loads of the type $Q = Q_o \cos\lambda X$ (see Chapter 2, sections 2.4 and 2.5), it is also possible to obtain the expressions for the displacements U and W of the half space subjected to a uniform distributed load (Fig. 4.4)

or a concentrated load. For the uniform distributed loading it can be shown that

$$W(X,Z) = \frac{q}{2\pi G(o)} \int_{o}^{\infty} e^{-\lambda Z} \frac{\sin(\lambda b)\cos(\lambda X)}{\lambda^2} \left[\frac{1+\lambda\rho\eta(\lambda\rho)-\lambda\rho\eta(\rho Z)}{\lambda\rho e^{2\lambda\rho} Ei(-2\lambda\rho)+ \frac{1}{2\lambda\rho} + 1} \right] d\lambda \qquad (4.21)$$

Where

$$\eta(\omega) = e^{2\omega} Ei(-2\omega) - \log \omega$$

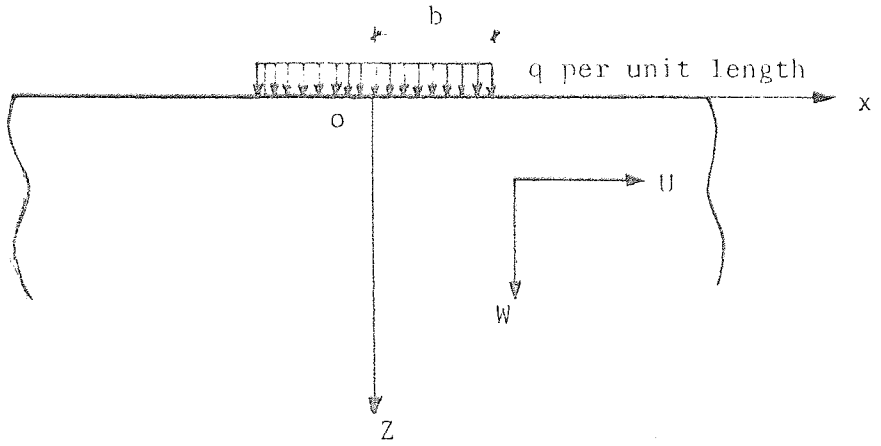

Fig. 4.4

Equation (4.21) is identical to that obtained by Gibson (1967). By substituting (4.21) in (4.18), the surface displacement [W(X,0)] in the Z direction is given by

$$W(X,0) = \frac{Q_o}{4\lambda bG(0)} \left[\frac{1}{F(\lambda\rho)} \right] \cos\lambda X \qquad (4.22)$$

where

$$F(\lambda\rho) = 2 \left[1 + \frac{1}{2\lambda\rho} + \lambda\rho \; e^{2\lambda\rho} Ei(-2\lambda\rho) \right] \qquad (4.23)$$

For large values of θ, $Ei(\theta)$ can be approximated by the following :

$$Ei(-\theta) = -\frac{1}{\theta} e^{-\theta} [1 + O(\theta^{-1})] \qquad (4.24)$$

With this value of $Ei(-\theta)$, we obtain (from (4.23))

$$F(\lambda\rho) = 2 \left\{ 1 + \frac{1}{2\lambda\rho} - \frac{1}{2} [1 + O(\theta^{-1})] \right\} \qquad (4.25)$$

The solution for the homogeneous case is obtained as the limiting case when $\rho \to \infty$

$$\text{Lt}_{\rho \to \infty} F(\lambda\rho) = 1$$

With $F(\lambda\rho) = 1$, equation (4.22) becomes

$$W = \frac{Q_o}{4\lambda bG(0)} \cos\lambda X \qquad (4.26)$$

This is identical to the expression found earlier [equation (2.6) with $\nu = 0.5$]. The values of function $F(\lambda\rho)$, evaluated for different $\lambda\rho$ are as follows :

$\lambda\rho$	0.0001	0.001	0.01	0.1	1.0	5	10	20	50
$F(\lambda\rho)$	10002	1002	101.9	11.70	2.27	1.28	1.14	1.07	1.03

4.3 Beams resting on an isotropic non-homogeneous incompressible medium where shear modulus is a linear function of depth

The solutions of the infinite and the finite beam subjected to a uniform distributed load, a concentrated load, and a concentrated couple, are similar to the case where the medium was treated as an isotropic homogeneous elastic medium (Chapters 2 and 3). The expressions for W(X), M(X), V(X) and Q(X) are identical to those given in Chapters 2 and 3, except the function Ω in the integrals $J_{nu}(X)$ and $J_{np}(X)$ is equal to $\Omega = F(\lambda\rho)$. And the typical length parameter in this case is

$$c = \left[\frac{E_b I}{4bG(o)} \right]^{1/3}$$

4.4 Numerical Results

The numerical values of expressions for the deflections, bending moment, shearing forces, and contact forces for an infinite beam subjected to a concentrated load, and a concentrated couple were obtained. The method for the evaluation of the integrals involved in these expressions is similar to the homogeneous case which is given in chapter 2. Since in the two dimensional analysis the deflection of an infinite beam subjected to a concentrated load is infinite for all values of x

$$W(X) = \frac{Pa^3}{\pi E_b I} \int_0^\infty \frac{\cos(\alpha X)}{\alpha[\alpha^3 + F(\lambda\rho)]}\, d\alpha = \frac{Pa^3}{\pi E_b I} J_o(X)$$

it is not therefore possible to obtain an absolute value for the deflection of the beam. It is however possible to obtain the deflected shapes of the beam (deflection relative to the point of application of load).

$$W(o) - W(X) = \frac{Pa^3}{\pi E_b I} \int_0^\infty \frac{1 - \cos(\alpha X)}{\alpha[\alpha^3 + F(\lambda\rho)]}$$

The integral in the above expression is zero for $\alpha = 0$.

In Figure 4.5 the deflected shapes of the beam for different values of $\rho = \frac{G(o)}{m}$ are shown. These results suggest that as non-homogeneity increases (increase in m) the deflection of the beam under the load is also increased. The distribution of bending moment, shearing forces, and contact forces are given

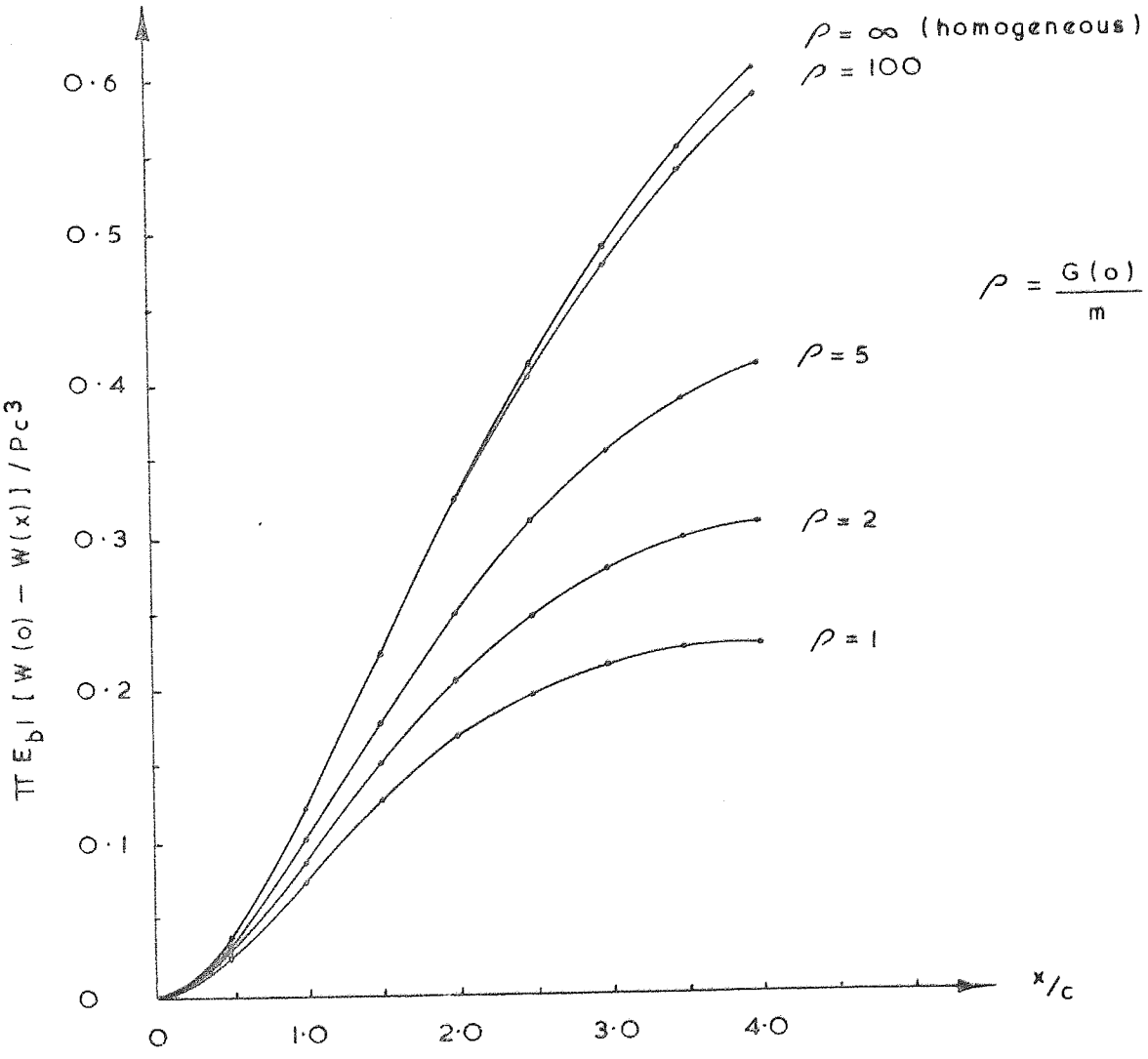

FIG. 4.5 Deflection of the beam relative to the point of application of the concentrated load.

in Figures (4.6), (4.7) and (4.8). It can be seen that an increase in m (decrease in ρ) increases the maximum bending moment. The shearing forces along the beam (Figure 4.7) decrease as non-homogeneity of the medium increases. Table (4.2) gives the maximum values of bending moment, contact force, and relative deflection [W(o) - W(x)] of the beam (at x/c = 0) for different values of ρ.

ρ	1	2	5	100	Homogeneous
$\frac{\pi E_b I}{Pc^3} W^*$	0.23028	0.31129	0.41739	0.59045	0.60844
$\frac{M}{Pc}$	0.28640	0.31390	0.34342	0.38205	0.38490
$\frac{cQ}{P}$	0.46969	0.43726	0.41039	0.38544	0.38490

Table (4.2)

From Table (4.2) it can be seen that for ρ = 100 the results are very close to those obtained by treating the medium as being homogeneous. Figure 4.8a shows the variation of maximum bending moments and contact forces against ρ for an infinite beam subjected to a concentrated load.

Since the integrals occuring in the expressions for the shearing and contact force distribution of an infinite beam subjected to a concentrated force [$J_{3p}(X)$ and $J_{4p}(X)$] are similar to the integrals in the expressions for bending moment and shearing forces

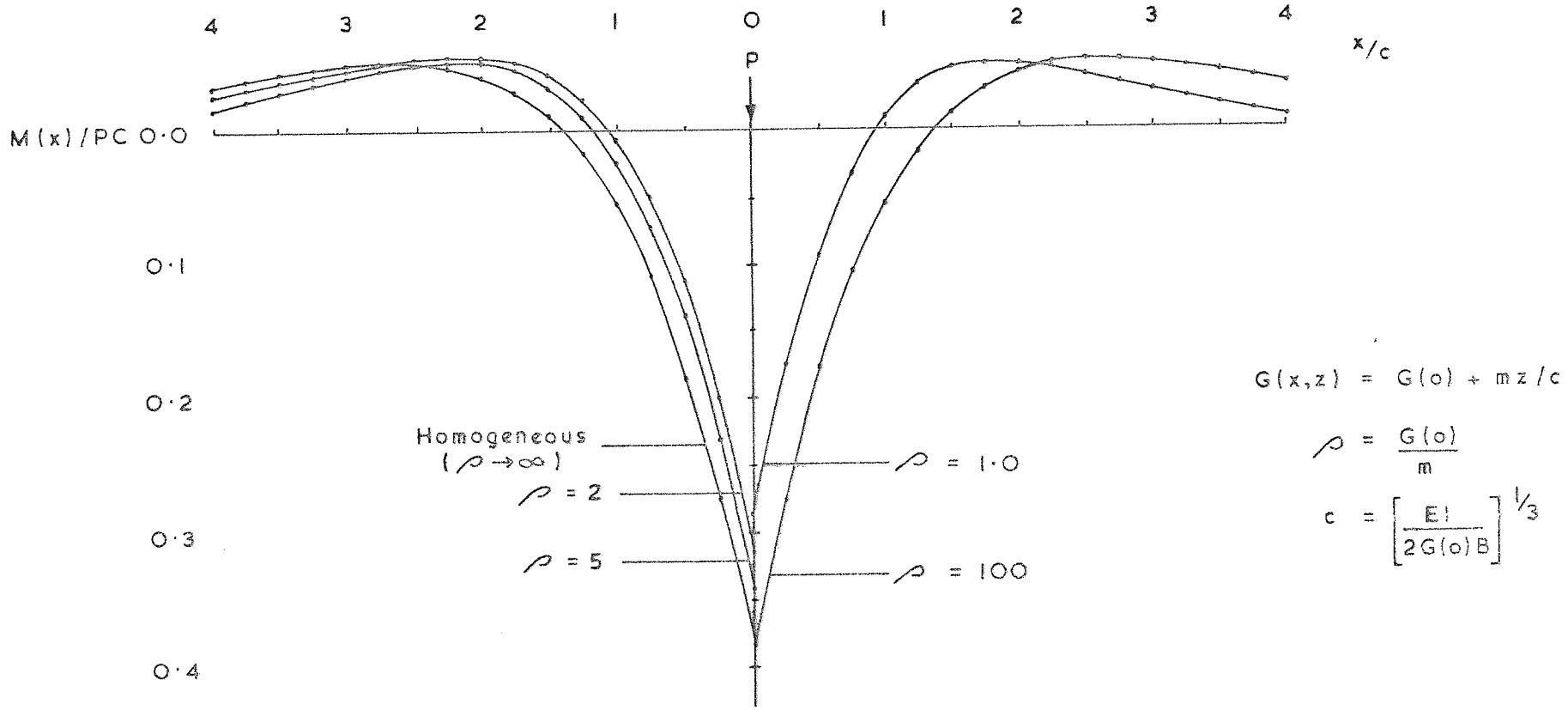

FIG. 4.6 Infinite beam subjected to a concentrated load – bending moment distribution.

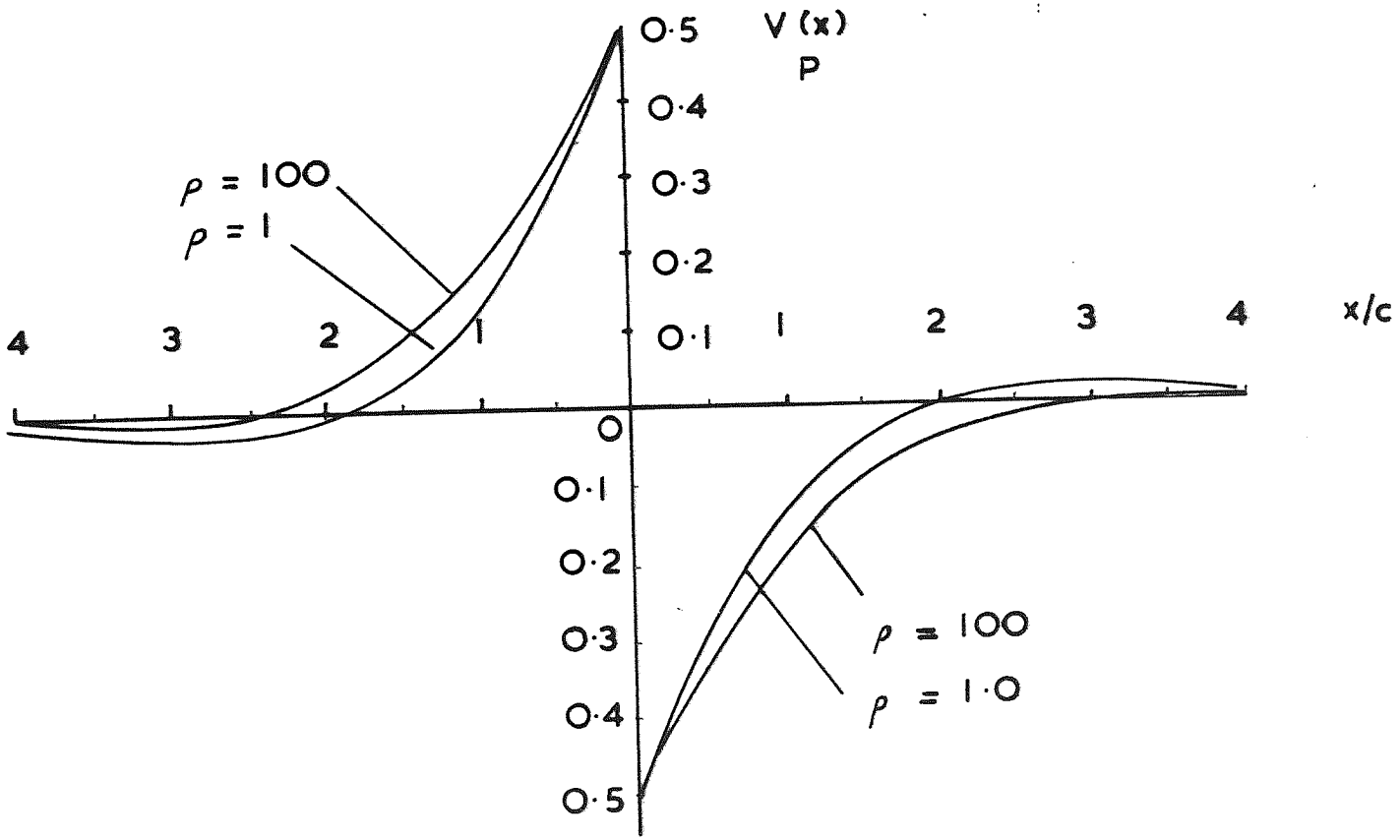

Fig. 4.7 Infinite beam - shear force distribution for a concentrated load

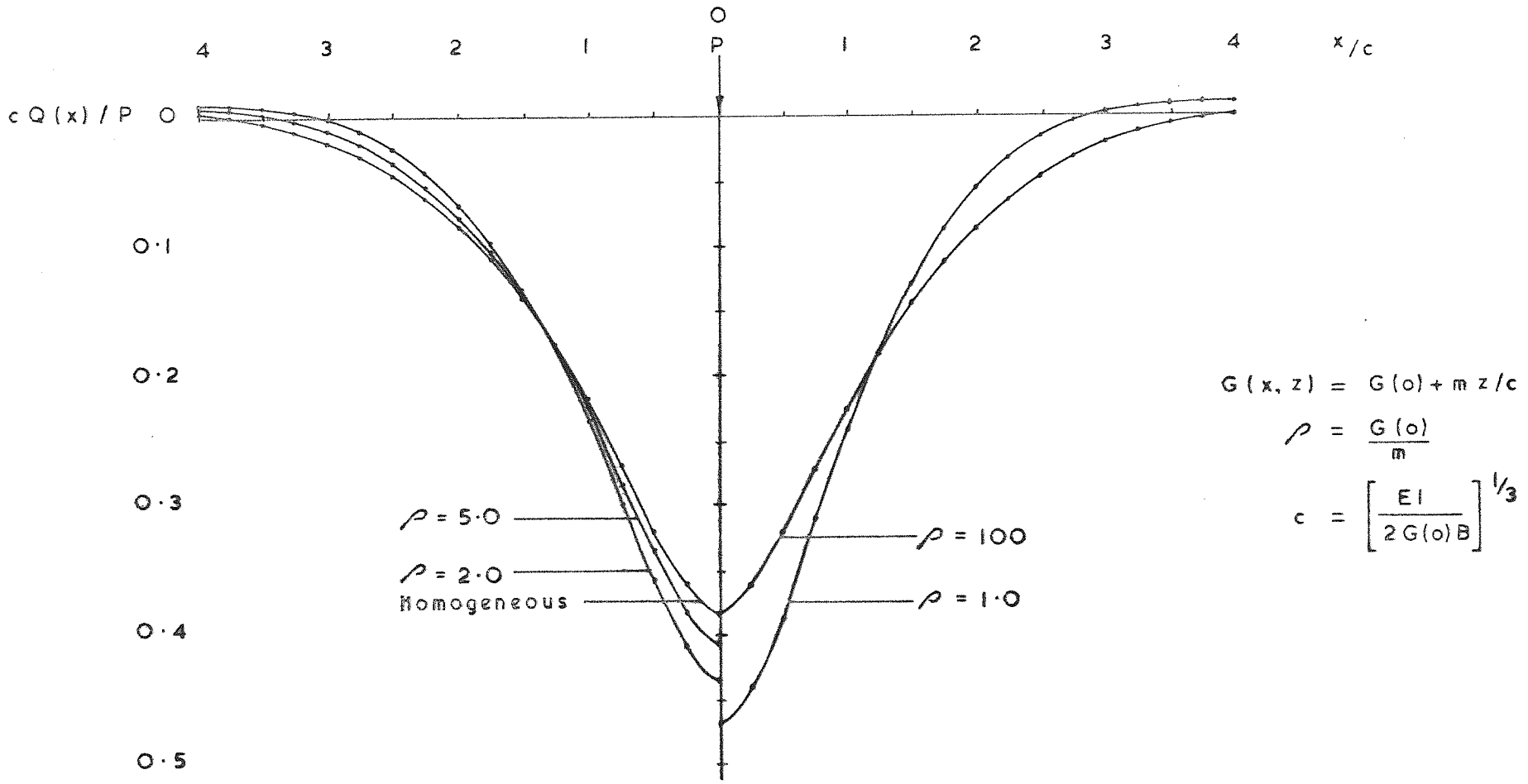

FIG. 4.8 Infinite beam subjected to a concentrated load, contact force distribution.

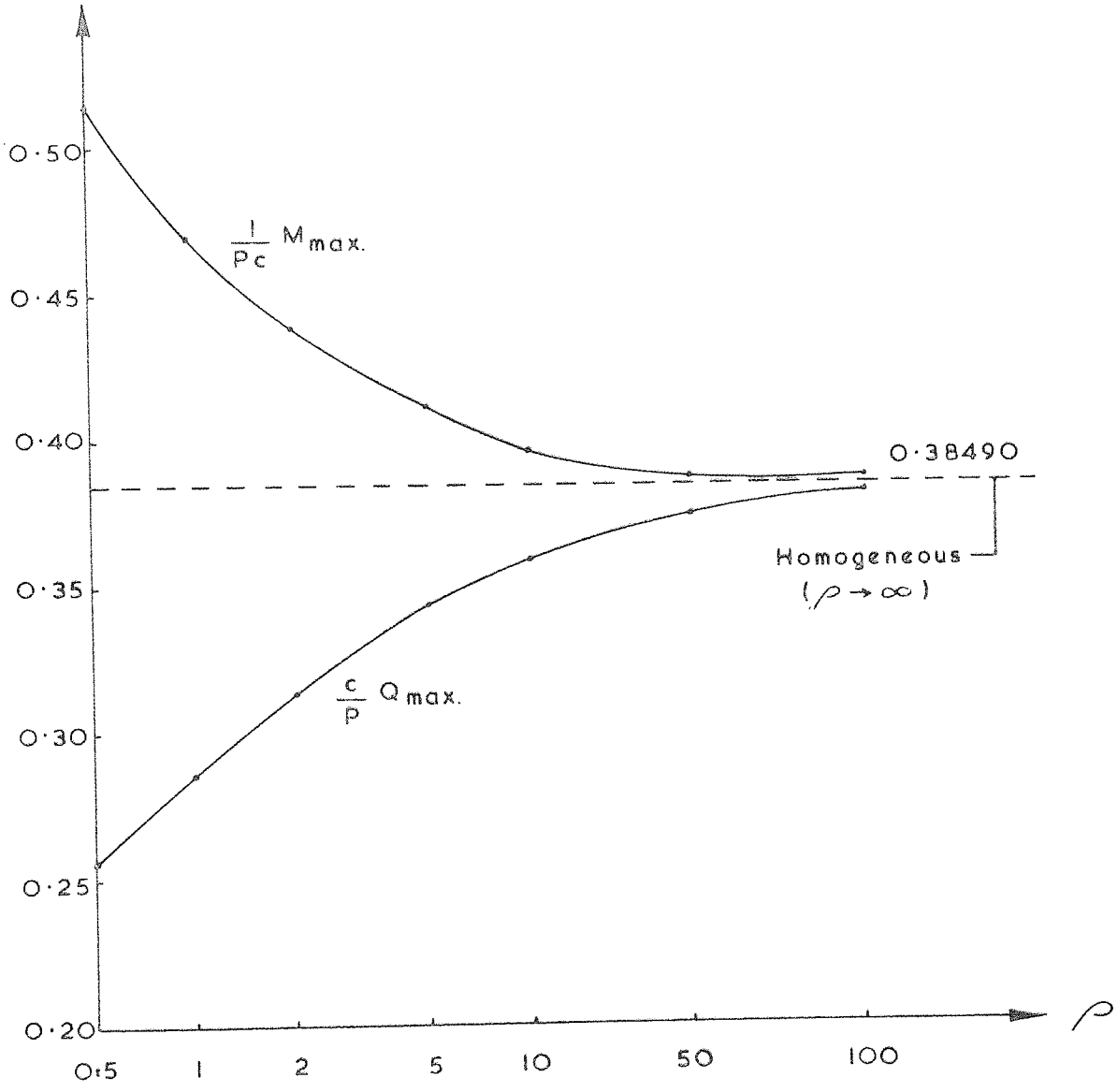

FIG. 4.8d Variation of maximum bending moment and contact force with ρ

of an infinite beam subjected to a concentrated couple, (see chapter 2), therefore the curves in Figures 4.7 and 4.8 can be considered as curves for bending moments and shearing forces for the loading by a concentrated couple (replacing the vertical axis in Figure 4.7 by $\frac{M(X)}{M}$, and in Figure 4.8 by $\frac{cV(X)}{M}$). The deflection and contact force distribution for loading by a concentrated couple are given in Figures (4.9) and (4.10).

The solution to the finite beam was obtained by using the infinite beam solution and applying a superposition technique (see chapter 3). The numerical values for bending moments, shearing and contact forces were obtained for beams with L/c = 0.5, 1, 2, 4, subjected to a concentrated load or a concentrated couple at distances 0.25L and 0.5L from the end of the beam for both homogeneous and non-homogeneous medium (ρ = 0.5, 1, 2, 100). The results are tabulated in Appendix 1. These results are for three locations on the beams (two ends and the point under the load). In Figure 4.11 the distribution of contact force and bending moment for a finite beam (L/c = 0.5, 1, 2, 4) subjected to a central concentrated load are given for different values of ρ. Similar to the three dimensional case (chapter 3), it can be seen that the solution fails to give concentration of stresses at the ends of the rigid beam. The results for the rigid beams contrast with the theory of elasticity which states that concentration of stresses must exist at the edges of a rigid stamp resting on elastic medium.

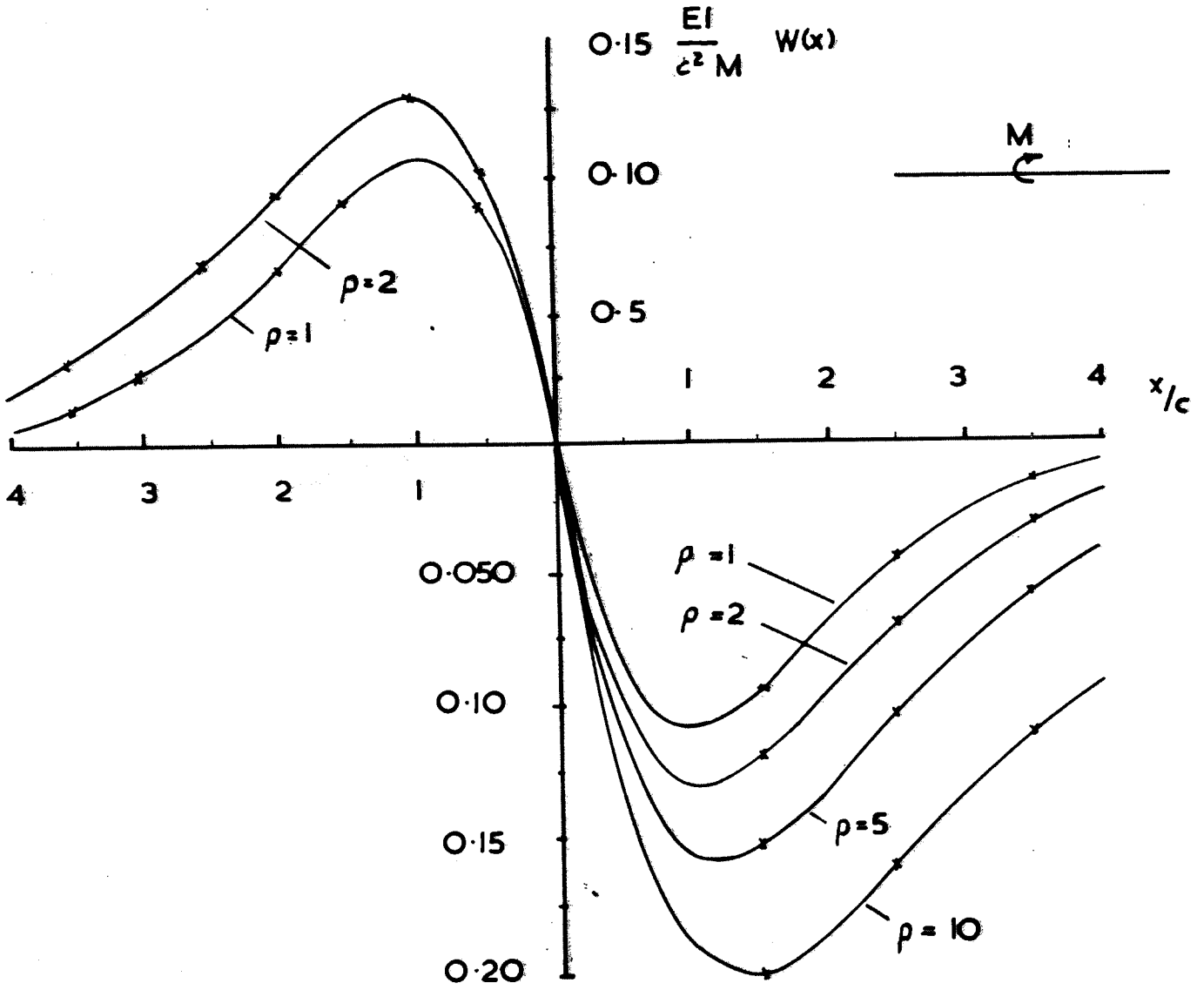

Fig . 4.9 Infinite beam subjected to a concentrated couple-deflection curve

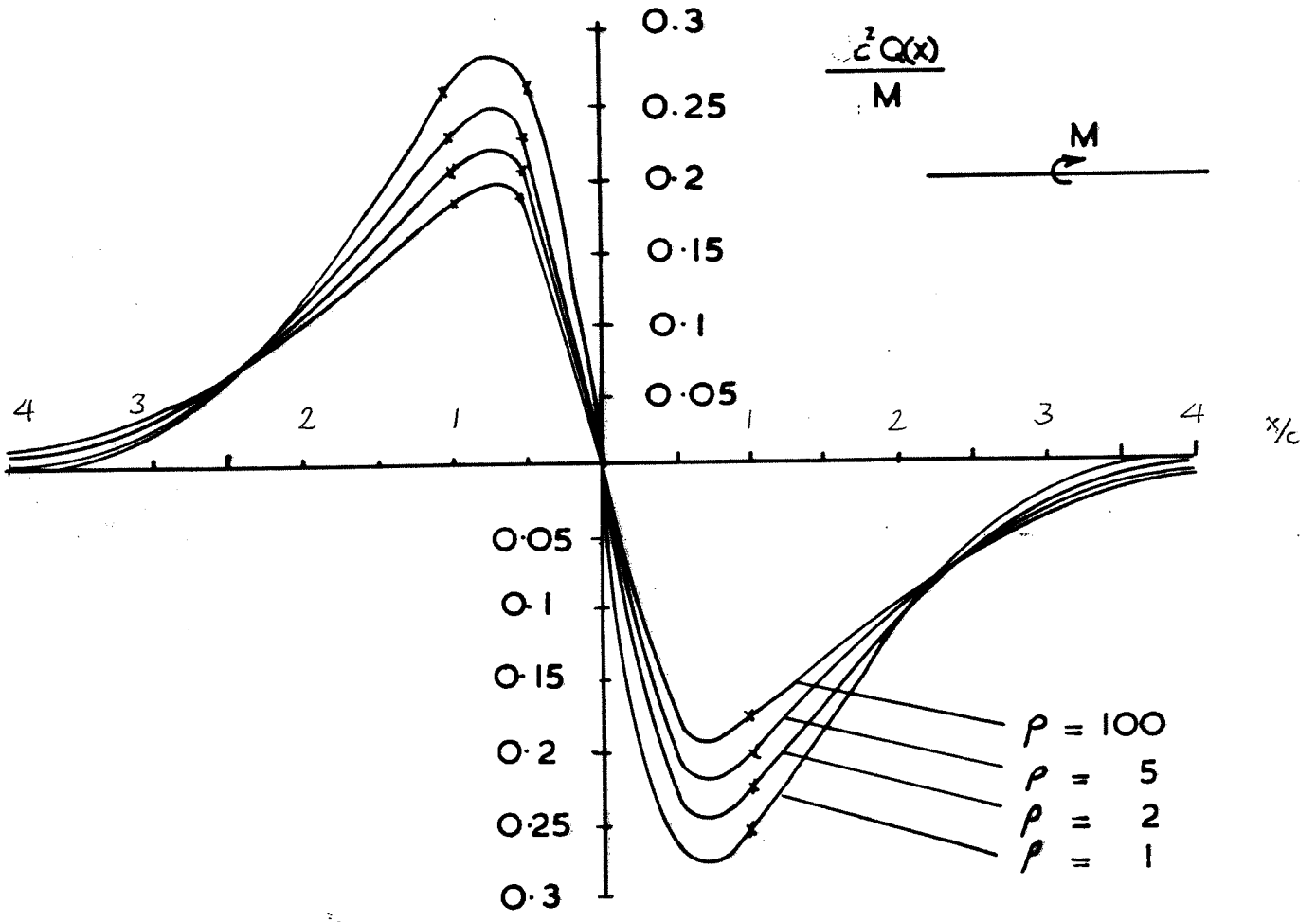

Fig. 4.10 Infinite beam subjected to a concentrated couple - contact force distribution

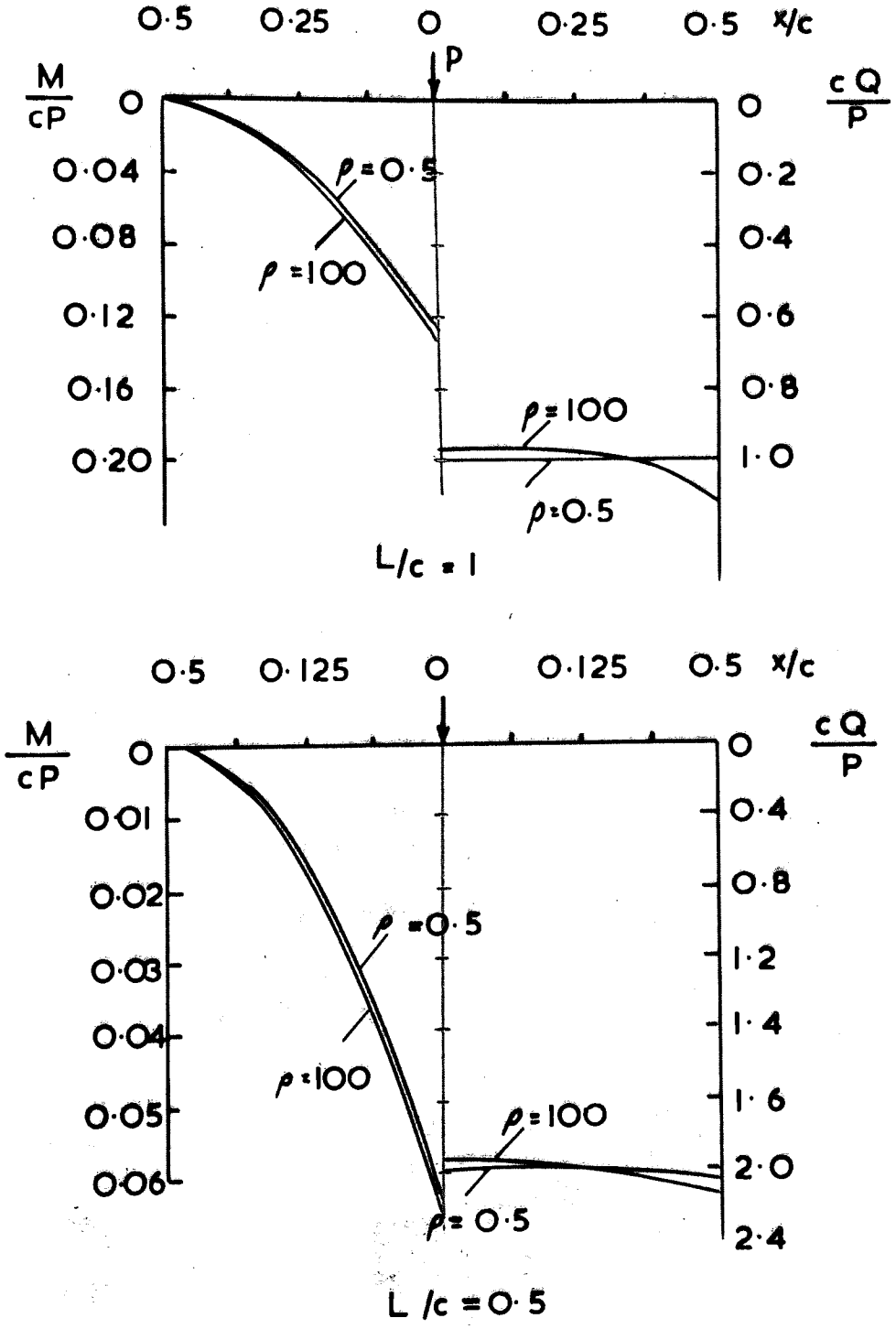

Fig. 4.11 Bending moment and contact force distribution

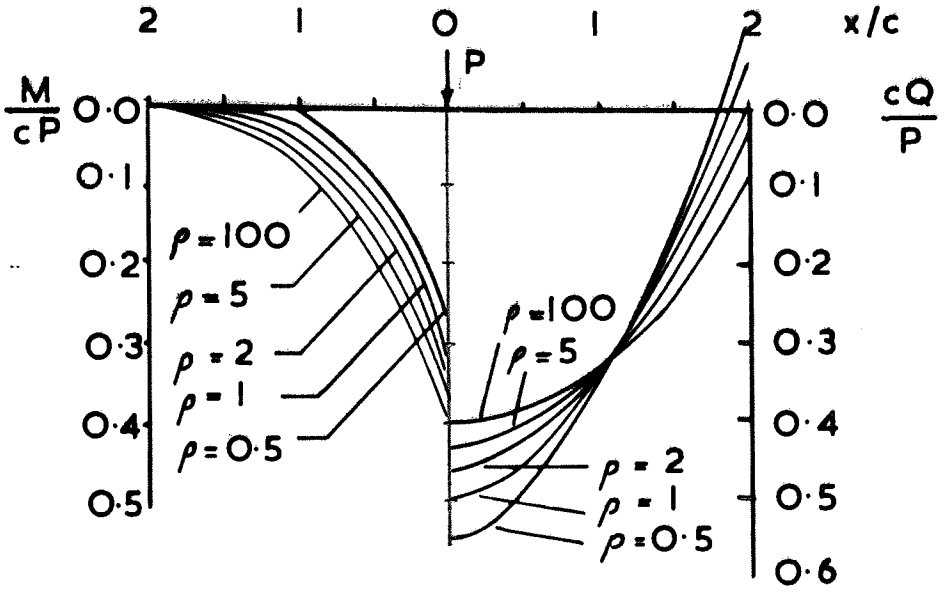

L/c = 4

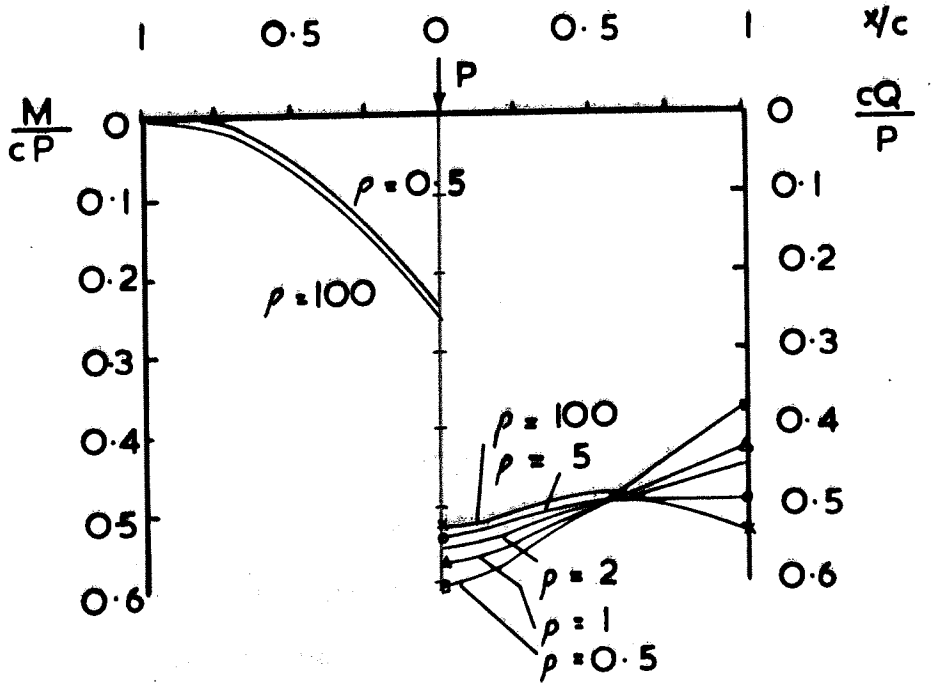

L/c = 2

Fig. 4.11

Figures 4.12 and 4.13 show the variation of maximum contact force and bending moment (for a beam subjected to a central concentrated load) against ρ. For a particular value of ρ, the maximum contact force decreases as L/c increases, (Figure 4.12). The values of maximum contact force for L/c = 8 with different values of ρ showed that these results are equal to those of infinite beam (up to third decimal place). From Figure (4.13) it can be seen that for a particular value of ρ maximum bending moment increases as L/c increases. The maximum value of bending moment for a finite beam with L/c = 4 can be greater than that of an infinite beam. This is due to negative contact forces which exist for an infinite beam. The negative values of contact force produces negative bending moment and hence the maximum value of bending moment for an infinite beam might be less than that of a finite beam.

4.5 Conclusions

The two dimensional problem of an infinite beam resting on a non-homogeneous elastic half space where shear modulus is a linear function of z, $G(Z) = G(o) + mZ$ was analysed. The maximum deflection of a beam resting on such medium is over-estimated if the analysis is based on the assumption of homogeneous behaviour of the medium. As far as maximum bending moments and contact forces are concerned, the effect of non-homogeneity is to reduce the former and increase the latter. For values of

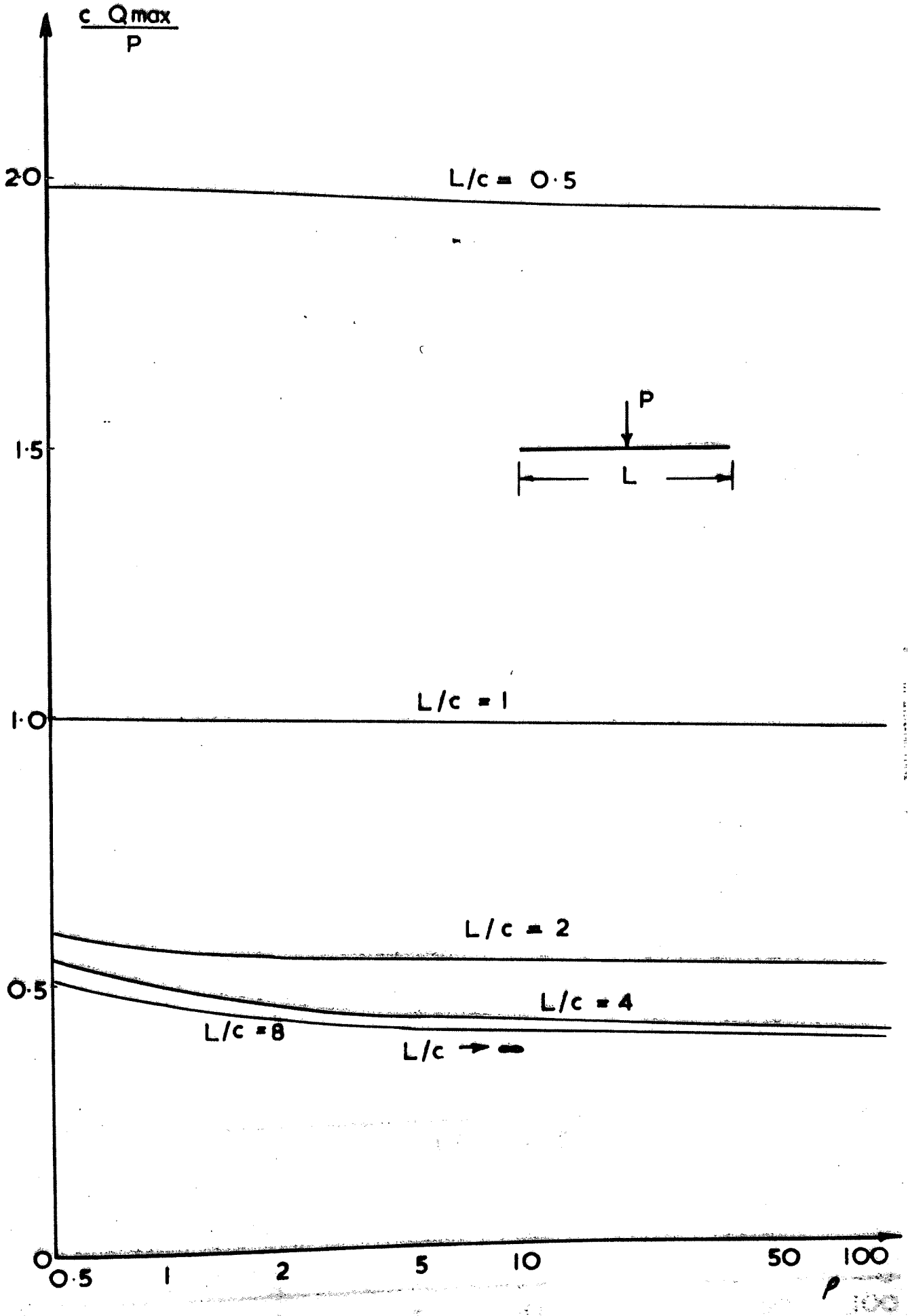

Fig .4.12 Variation of maximum contact force against ρ

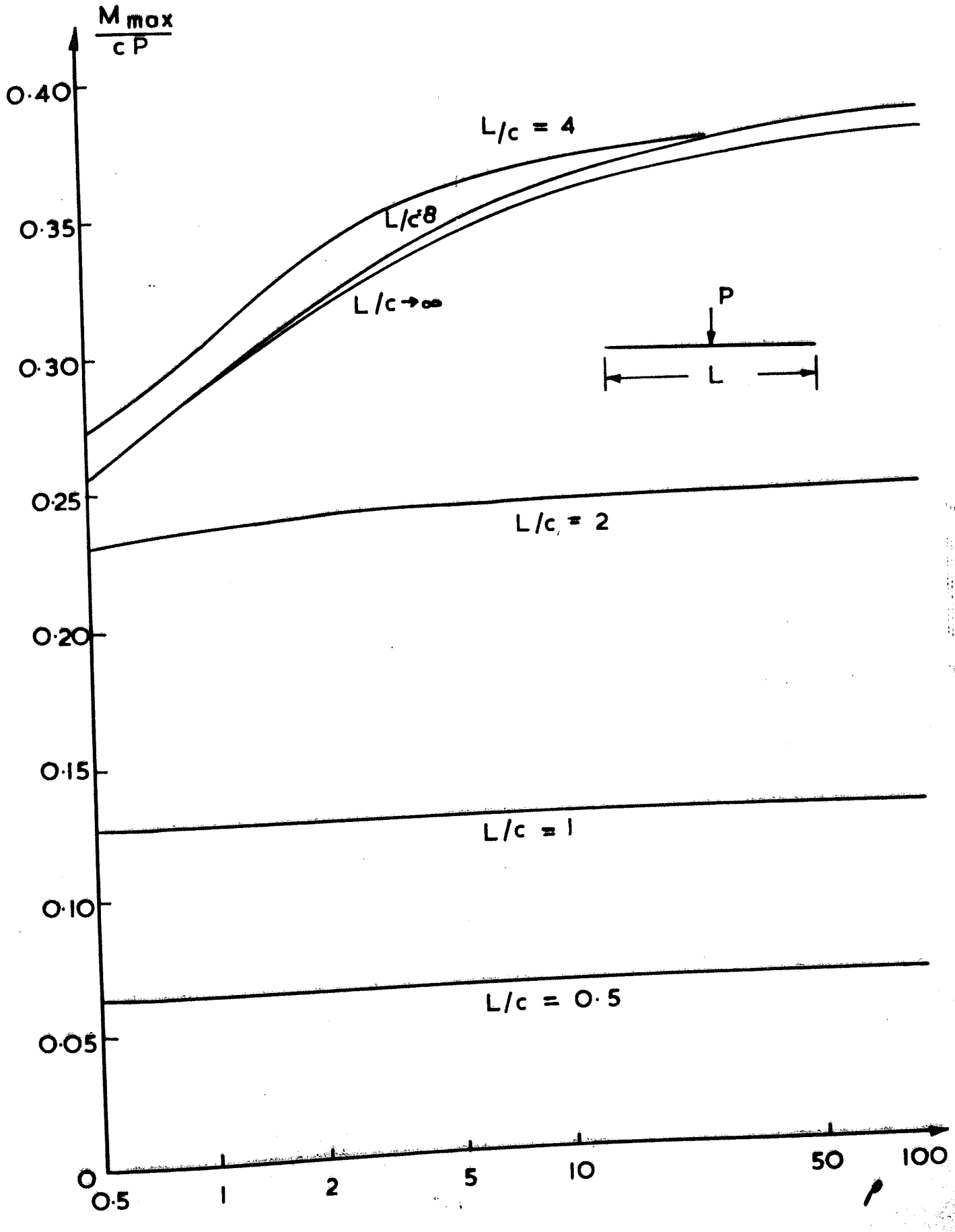

Fig. 4.13 Variation of maximum bending moment against ρ

$\rho > 100$ [$\rho = \frac{G(o)}{m}$] the results obtained from non-homogeneous solution are practically the same as those obtained from classical solution.

The solution for the finite beam was obtained by employing a superposition technique and using the infinite beam solution. The numerical results for finite beams subjected to a concentrated load and a concentrated couple at distances 0.25L and 0.5L from the end of the beam are given in Appendix 1. It was shown (Figure 4.12, 4.13) that for a particular value of ρ for values of $L/c > 8$ the finite beam subjected to a concentrated load can be treated as an infinite beam. As in the case of the infinite beam problem, the effect of non-homogeneity of the medium with $\rho > 100$ on the results obtained for the finite beams is insignificant and the medium can be treated as being homogeneous. Finally, the results obtained for the rigid beams show that the finite beam solution is only valid for flexible beams.

CHAPTER FIVE

MODEL TEST DESCRIPTION

5.1 Introduction

In the previous chapters (chapters 2, 3 and 4), the analytical solution of the infinite and finite beam, resting on a two, or three dimensional elastic medium, were given. These solutions can be applied to analyse the foundation of a structure resting on natural deposits of soils. Owing to the variety of soils and soil conditions that can be encountered in engineering practice, the applicability of the analytical solutions (chapters 2, 3 and 4) should be investigated from tests on full scale prototype structures. These tests, although necessary, are expensive and time consuming. For this reason the laboratory scale model tests are more attractive.

A series of model tests were performed to investigate the behavior of steel beams resting on a granular subgrade. The model tests were designed so that the stress conditions in the underlying foundation material were two dimensional (plane strain) and three dimensional.

In this chapter the material used in model tests, the detail of apparatus, and experimental procedure are described. The analysis of the experimental results and their comparison with the theoretical results are given in chapters 6 and 7.

5.2 Materials used in the model test

5.2.1 The Beams

Three steel beams were used as beam models. The beams have the same length (L = 140 cm), but different moments of inertia. The moment of inertia of the beams were chosen so that, according to Hetenyi's classification of the beams (Hetenyi, 1946), they present a short, a medium and a long beam.

Hetenyi's classification of the beams, resting on Winkler medium is based on their "λL" values given by

$$\lambda L = \sqrt[4]{\frac{KL^4}{4E_bI}} \tag{5.1}$$

where,

L is the length of the beam

K is modulus of subgrade reaction

E_bI is flexural rigidity of the beam

Hetenyi's classifications are as follows :

a)	Short beams	$\lambda L < \pi/4$
b)	Beams of medium length	$\pi/4 < \lambda L < \pi$
c)	Long beams	$\lambda L > \pi$

(5.2)

From (5.1) the moment of inertia is given by

$$I = \frac{L^4K}{4E_b(\lambda L)^4} \tag{5.3}$$

In order to choose the I values for the beams, so that they present the classification given by (5.2), the values of E_b and K in (5.3) are required. For Young's modulus of steel, a value of $E_b = 2.1 \times 10^6$ Kg/cm^2 was chosen. From the plate loading tests on a square plate 16cm x 16cm x 1.2cm (see chapter 7) k = 0.454 Kg/cm^3. An approximate value of 16cm was chosen for the width of the beams. The value of K is then K = 0.454 x 16 = 7.2 Kg/cm^2. For this particular case ($E_b = 2.1 \times 10^6$, K = 7.2 Kg/cm^2) in terms of moment of inertia, the classification given by (5.2) can be written as follows :

d)	Short beams	I > 803 cm^4	
e)	Beams of medium length	803 > I > 3.4 cm^4	(5.3)
f)	Long beams	I < 3.4 cm^4	

The beam sections were chosen so that each beam has a moment of inertia in one of the limits given by (5.3). These sections are rectangular, channel, and two channels welded toe to toe to form a box section. Some data on beam sections are given in Table 5.1.

Table 5.1 Some data on beam sections

Section (1)	Width (2) in cm	Depth (3) in cm	Area (4) in cm^2	Moment of (5) Inertia, I, in cm^4
Flat	15.2	1.2	18	2.16
Channel	15.7	6.5	24.5	113
Box	15.7	13.0	49.0	1600

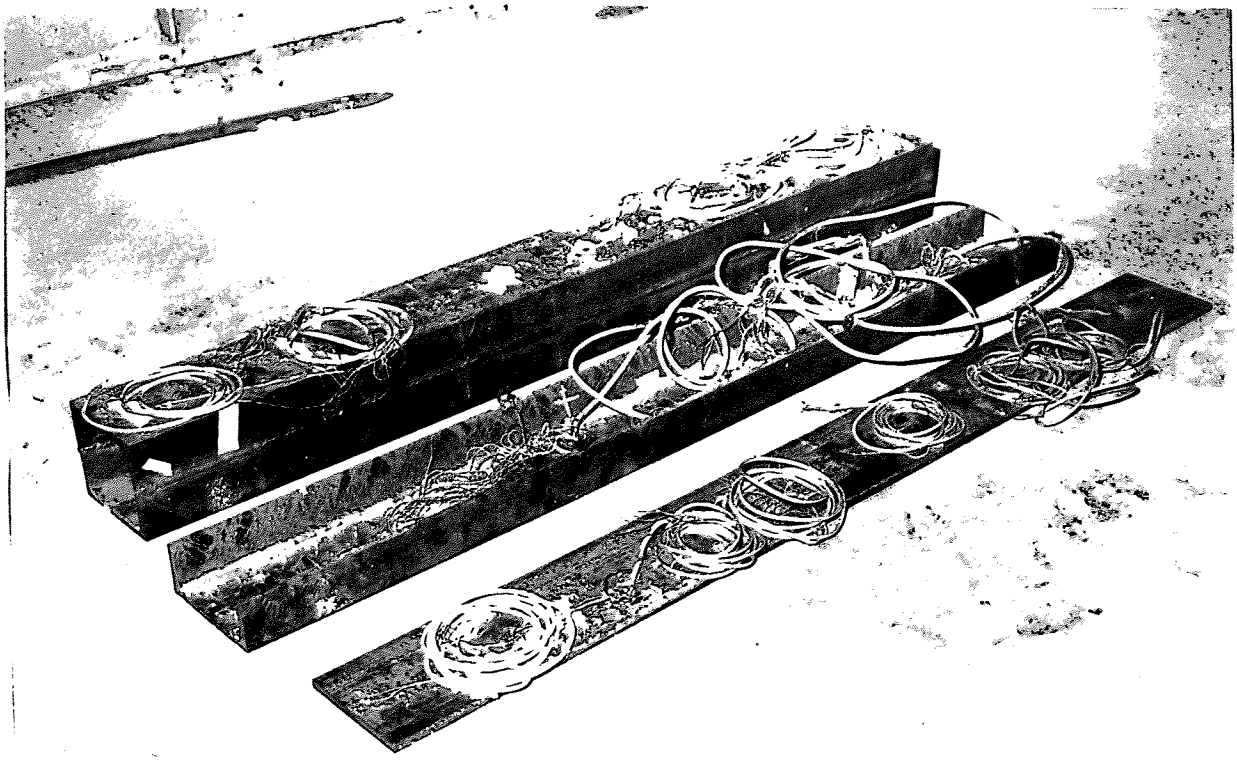

PLATE 5.1 THE MODEL BEAMS

Strain gauges of the type FLA-6-11 are fixed on the surfaces of the beams to measure the surface strain due to bending. Twenty-nine strain gauges were located 5cm apart. For the case of loading by two concentrated loads, two extra strain gauges were fixed to the beam at the points of application of loads. Plate (5.1) shows the beam sections with the attached strain gauges.

5.2.2 The Sand

A Leighton Buzzard sand was used as the subgrade. Particle size distribution of the sand, obtained from a standard sieve analysis, is shown in Figure (5.1). The sieve analysis gave D_{10} = 0.34mm, D_{60} = 0.48mm and uniformity coefficient μ = 1.40. The maximum and minimum porosities measured, using methods of tilting and vibrating table, suggested by Kolbuszewski (1948). The values obtained are n_{max} = 45.5% and n_{min} = 33.7%. The specific gravity of grains, which was measured according to procedure in BS1377 was G_s = 2.66.

5.3 The Test Tank

5.3.1 The Three Dimensional Tank

The test tank for three dimensional test is a 2400mm x 1200mm x 1200mm rectangular box (see plates 5.5 and 5.6).

PARTICLE SIZE DISTRIBUTION

British Standard Sieve Sizes

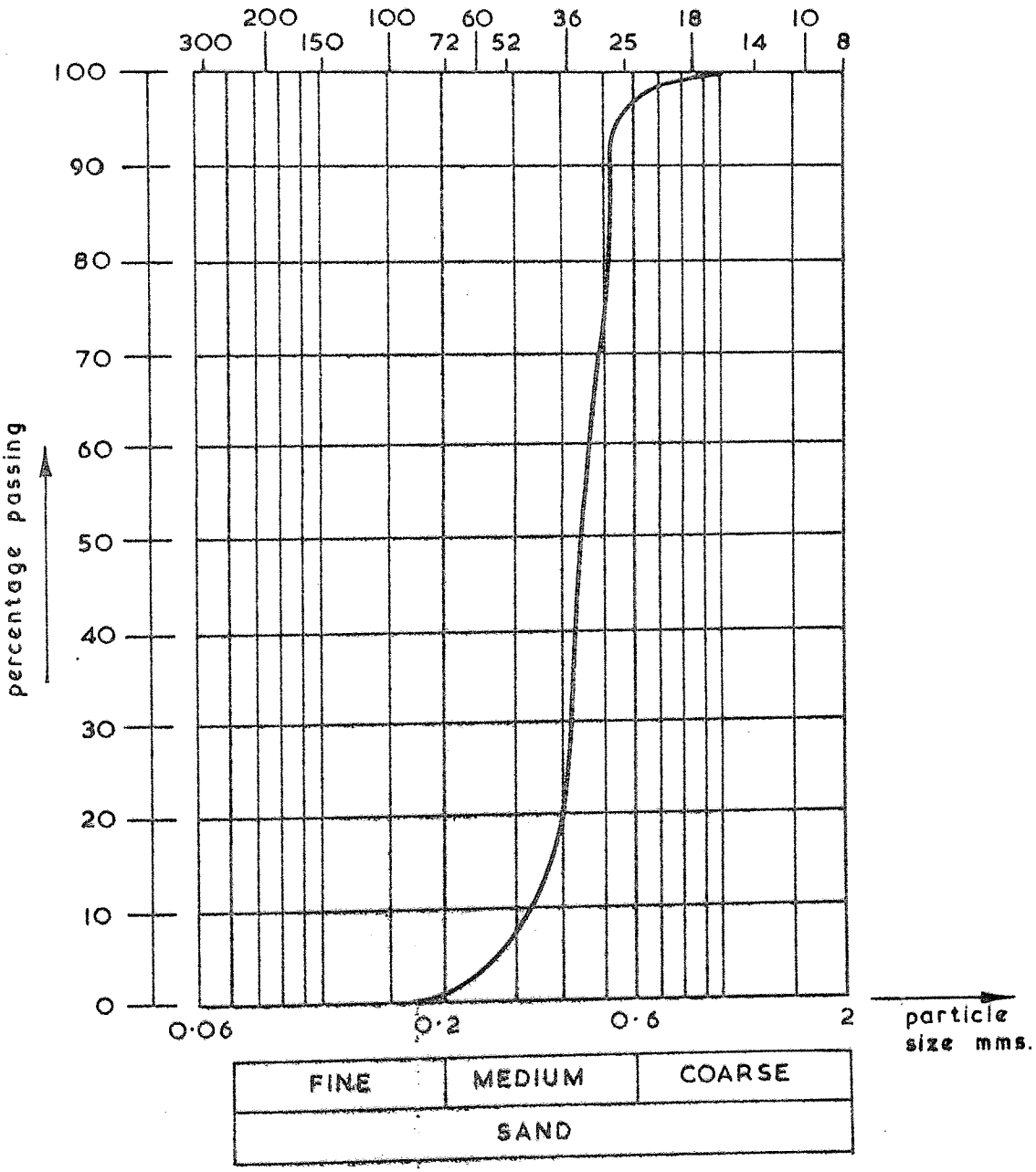

FIG. 5.1

The sides of the box consist of 6mm perspex inside a steel frame, the steel frame was restrained by three 75mm x 37mm x 95mm steel angle section, which went round the perimeter of the box. Three 12.5mm reinforcing bars restrained the top of the box across the width. The diagonal restraints were provided by 50mm x 50mm x 5mm steel angle sections. The maximum deflection of the sides during the test, for maximum applied load on the beam, (1600 Kg), did not exceed 1mm. The box rests on the base beam of the rig (see plate 5.11).

5.3.2 The Two Dimensional Test Tank

For two dimensional test tank a reinforced concrete box was constructed (Fig. 5.2). The inside dimensions of the box were 2100mm x 165mm x 1200mm. The tank is constructed in four sections: side S_1 and base B were constructed as one element, side S_2, end columns C_1 and C_2. To minimise the friction between the sand and the surfaces of the sides (S_1 and S_2) of the box, these surfaces were levelled with sheets of smooth formica, 3mm thick. A strong adhesive (Araldite) was used to stick the formica sheets. The elements C_1 and C_2 and sides S_2 were then mounted to their position on the base B. The columns C_1 and C_2 were fixed to the sides S_1 and S_2 by eight bolts (Fig. 5.2). The bolts passed through the holes which were provided in S_1, S_2, C_1 and C_2, during the casting. In order to provide space for the base beam of the loading frame, the tank was placed on four 170mm x 100mm x 1000mm concrete beams.

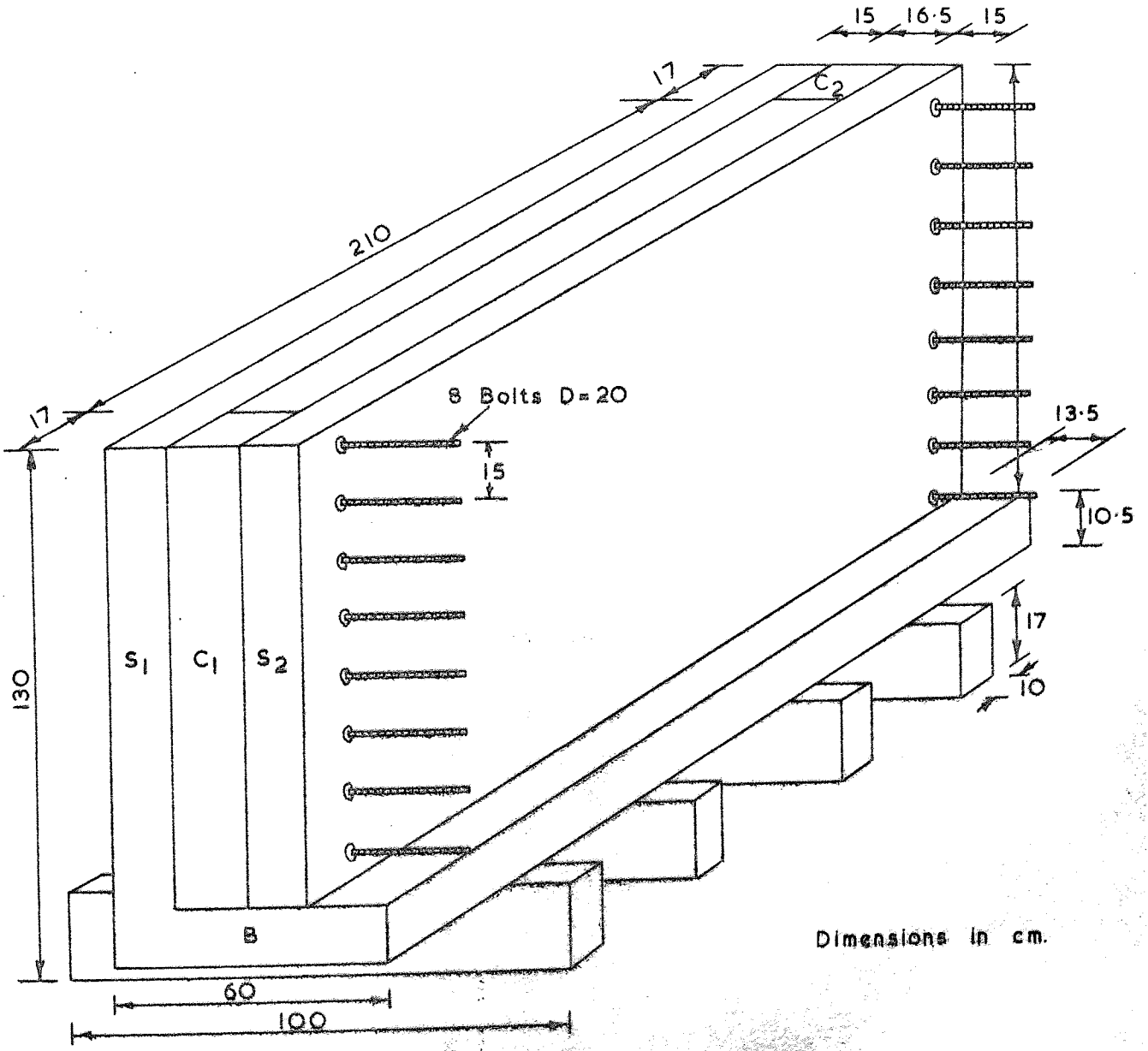

FIG. 5. 2 The test bed for two dimensional model test.

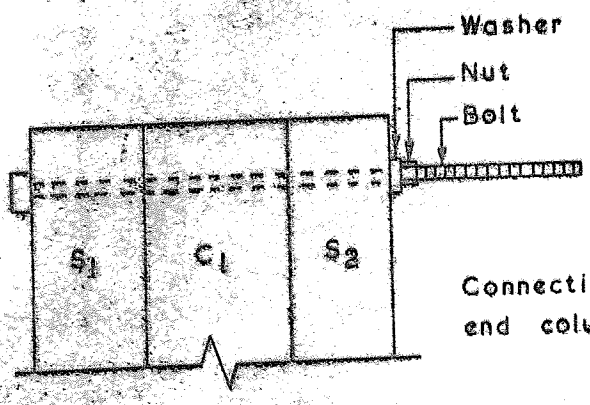

Connection of sides with end columns

The maximum deflection of the sides, for the maximum single concentrated load of 2400 Kg applied on the beam, did not exceed 0.1mm. The smoothness of the sides and their high rigidity fulfills the requirement for the existance of plane state of strain in sand during the test.

5.4 Deposition of sand

When sand is used in laboratory model testing, the fundamental problem is the formation of sand beds with constant porosity throughout the deposit. The methods for preparation of sand deposits can be divided into two major groups, depending on the technique used to achieve the desired porosity. The first method is where the porosity of sand is adjusted after deposition. The sand is deposited in layers, the porosity of each layer is adjusted by mechanical means (tamping, vibrating). The method is only suitable for preparation of dense deposits. A sand layer prepared in this manner has a non-homogeneous distribution of porosity. Barden (1962a), used vibration techniques to prepare deposits of dense sand. Feda (1961) observed that deposits of dense sand obtained by compaction, had different porosities at different locations in the layer.

In the second method, the porosity is controlled by adjusting the rate (the weight deposited per unit area in unit time) and velocity (height of fall) of the sand rain during the deposition.

Kolbuszewski (1948), investigating the methods of determining the limiting porosities of sand, (maximum and minimum porosities), concluded that the porosity of a sand deposit increases with increasing intensity and decreasing velocity of deposition. With this method, two techniques of deposition are commonly used. The first technique is where the sand is deposited over the whole plan area of the tank (Kolbuszewski and Jones, 1961). In the second technique the sand is deposited, using a sand curtain which travels backwards and forwards across the length of the tank (James, 1967; Walker and Whitaker, 1967). The porosity of the deposits, obtained by the first technique, is affected by the turbulence in the region of deposition (i.e. a non-homogeneous deposit). With the second technique, since the displaced air can move away in front of the sand curtain, the deposit exhibits relatively homogeneous porosities. It can be concluded that the best available method for the preparation of homogeneous deposits of sand at a certain known porosity is the depostion, using a controlled intensity sand curtain traversing along the area of the test tank. This technique is adopted here for preparation of the deposits.

5.4.1a Description of Hopper

For the depositon of sand in three dimensional model tests, an apparatus designed by Cunnell (1974) was used. The apparatus which is a travelling hopper is shown in plate (5.2). It consists of a steel frame chassis and a wooden panel to give a capacity of

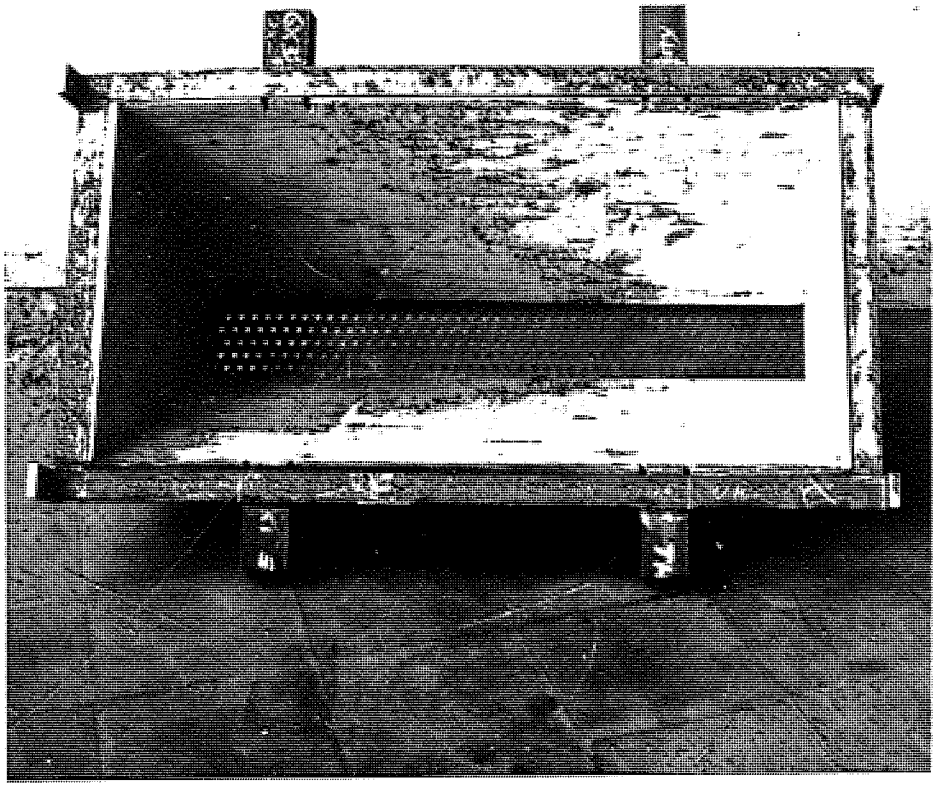

PLATE (5.2) THE HOPPER

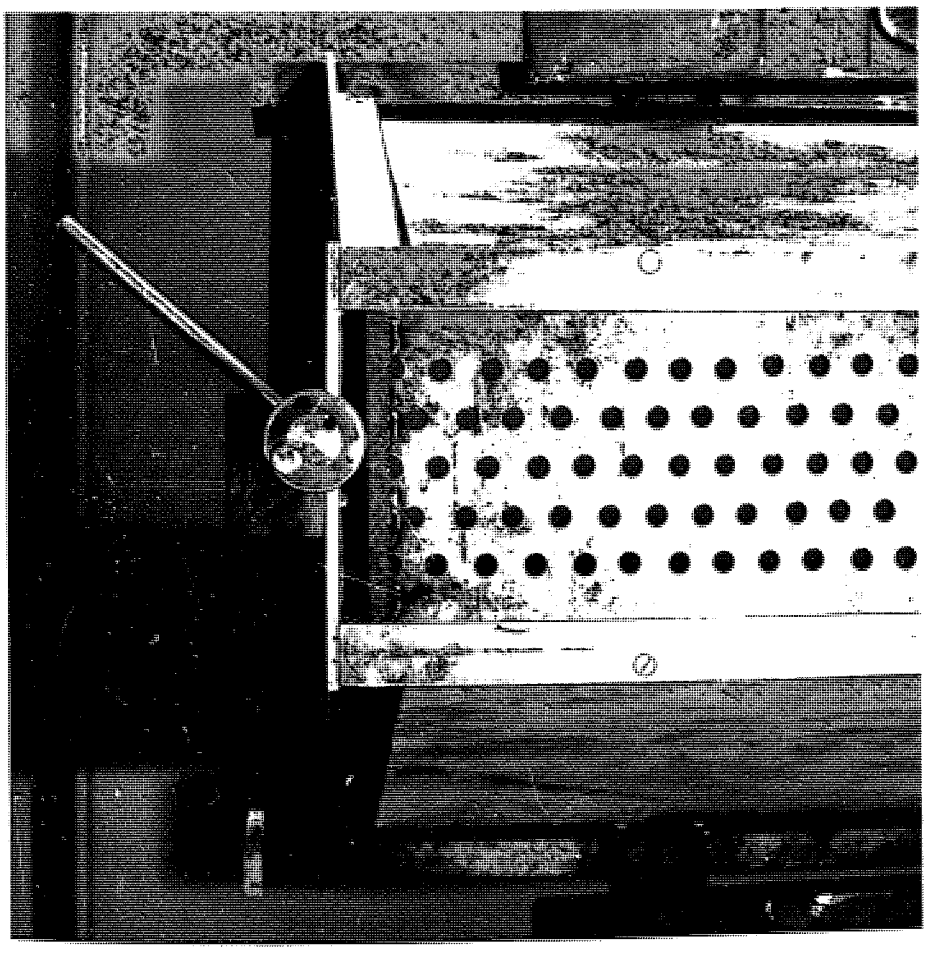

PLATE (5.3) THE BASE PLATE AND ADJUSTING CAM

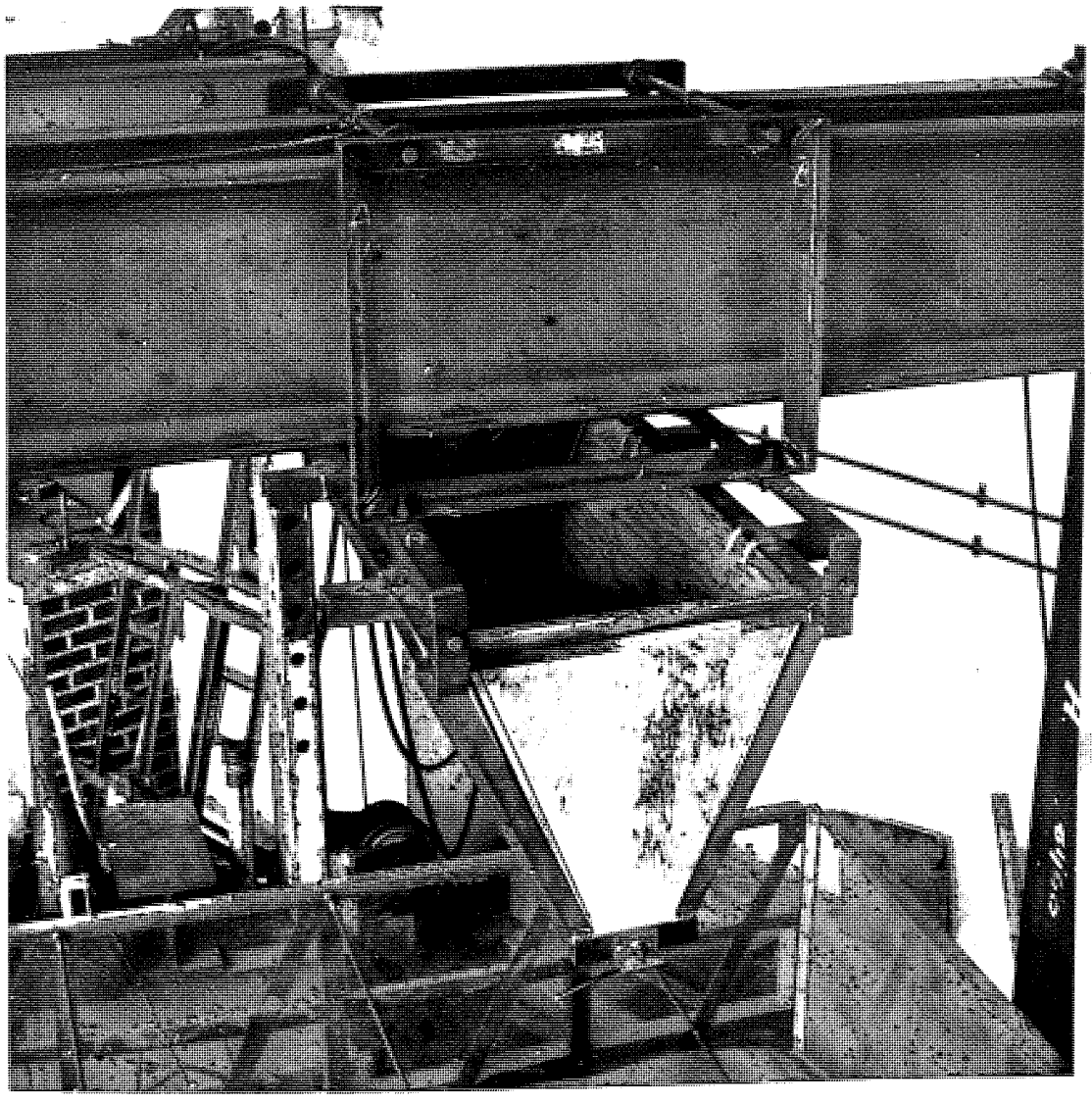

PLATE (5.4) THE HOPPER MOUNTED ON THE TROLLEY

PLATE (5.5) POURING AT APERTURE POSITION 1

PLATE (5.6) POURING AT APERTURE POSITION 4

$0.28m^3$. The base of the hopper consists of two plates, the inner plate which is welded to the hopper chassis and the outer plate which can move in a groove along the length of the base. Both base plates are drilled with a regualr pattern of holes, 11mm diameter, at 25mm centre. In a closed position, the holes of the base plates coincide with the solid spaces in the outer plate. A partial or full coincidence of the holes can be provided by displacement of the outer plate, an adjusting cam, shown in plate (5.3) was used for this purpose. The cam was calibrated for three positions between closed positions and full coincidence of the holes. These positons correspond to zero, 3mm, 6mm, 9.5mm and 22mm displacements of outer plate, as shown in Figure (5.4a), as position 0, 1, 2, 3 and 4. The shaded area in these positions shows the coincidence of the holes. A second cam, which was provided on the other side of the base, could bring the outer plate to zero position (closed position).

The hopper filled with sand, lifted by a fork lift truck and attached to the trolley which consists of a steel frame, two axles and four wheels as shown in plate (5.4). The trolley, with the hopper attached to it, could travel along the top flange of the cross beam of the rig. The manner in which the hopper travels is shown in Figure (5.3a). The speed of the travel was adjusted so that the hopper was empty when it reached the other end. The hopper was then lifted to ground level, filled with sand, lifted and attached to the trolley. The process was continued, until the sand reached the required level in the test tank.

5.4.1b Measurement of Porosity

Cylindrical density tins were placed at different points of the receiver to obtain the porosity of the sand. The tins, which are 50mm in diameter and 37mm high were made from brass tubing. To allow the displaced air to expel from the tins, the base of each tin was perforated by a number of 12.5mm diameter holes and had gauze stuck inside the face of it.

5.4.1c Calibration of the Hopper

The variation in porosity of sand, deposited by the hopper, depends both on height of fall (velocity of sand rain) and aperture size (intensity of sand rain). Cunnell (1974) showed that; (a) for a particular aperture size, the difference between average porosity, measured at the bottom and surface level of the bed was nor more than a random variation, and (b) a change in the level of sand in the hopper had no significant effect on the porosity of the deposit. Figure 5.4b shows the variation in the average porosity with the aperture set shown as positions 1, 2, 3 and 4 in Figure (5.4a). The varying intensity of the sand rain at positions 1 and 4 are shown in plates (5.5) and (5.6).

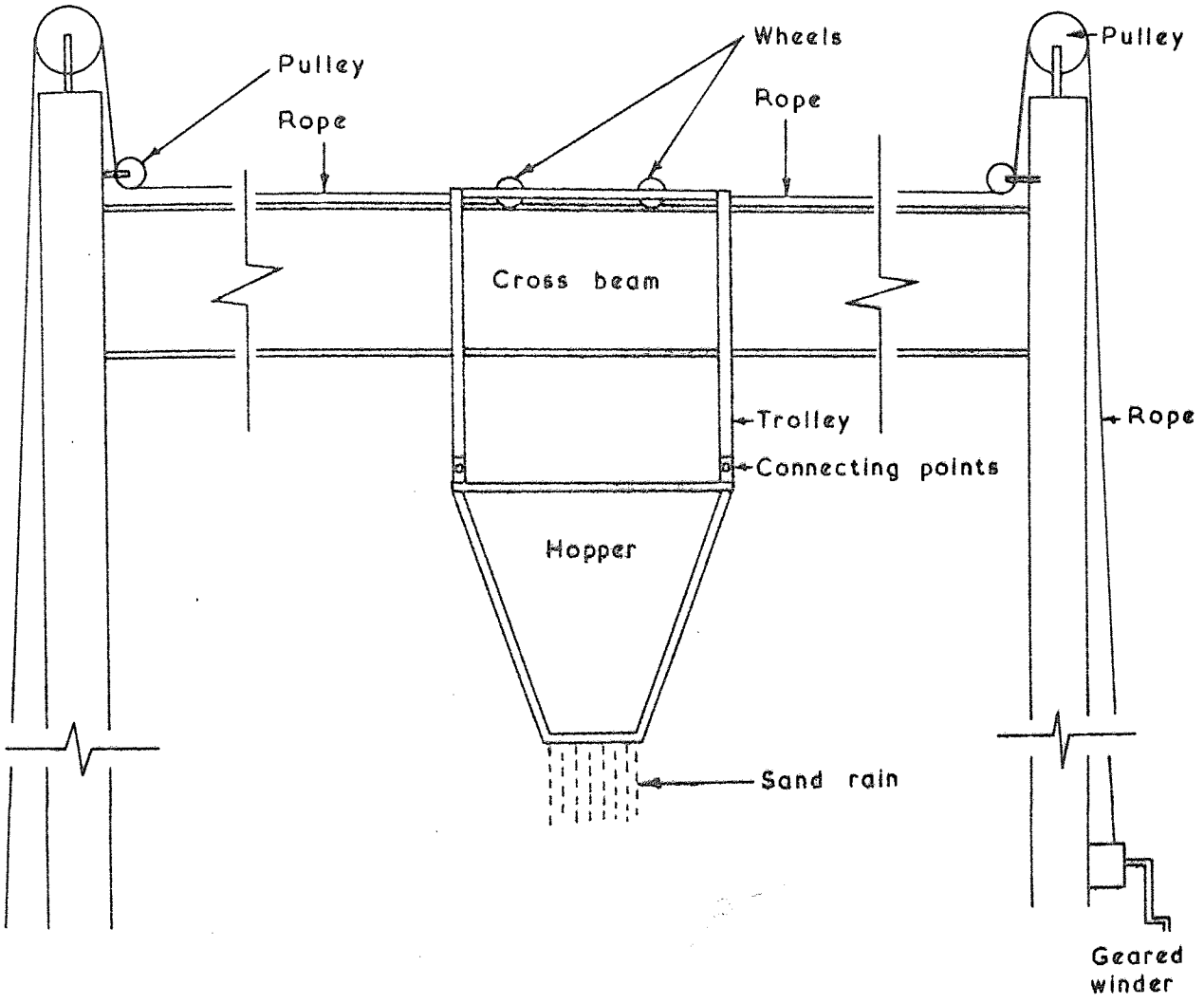

FIG. 5. 3a

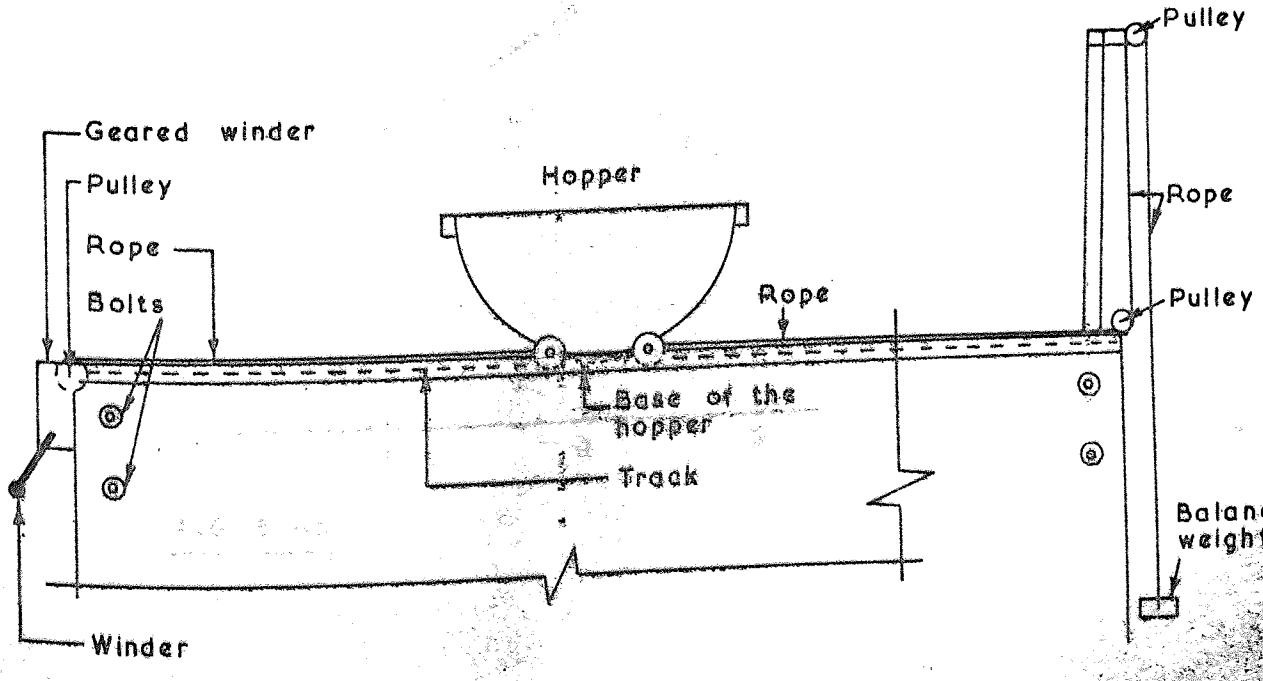

FIG. 5. 3b

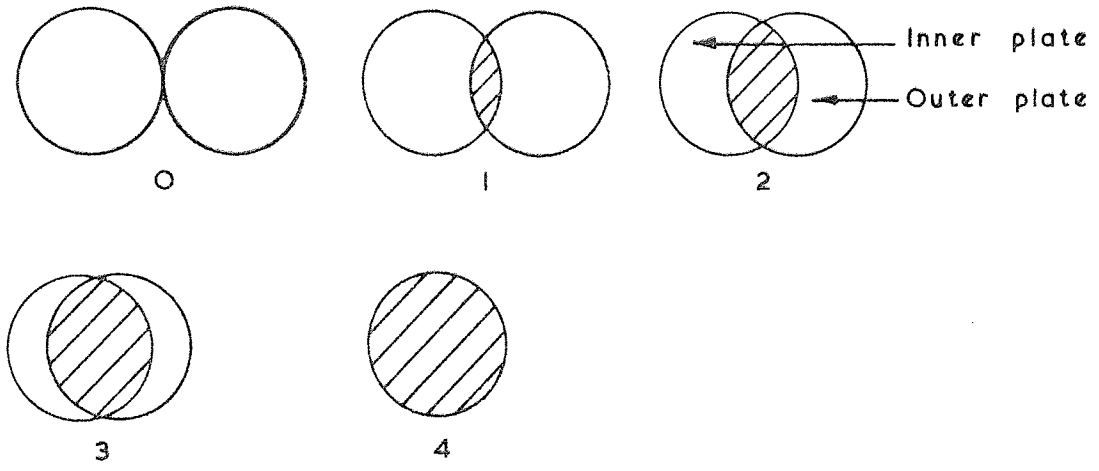

FIG. 5.4a The aperture corresponding to 3, 6, 9·5, 22 m-m displacement of outer plate.

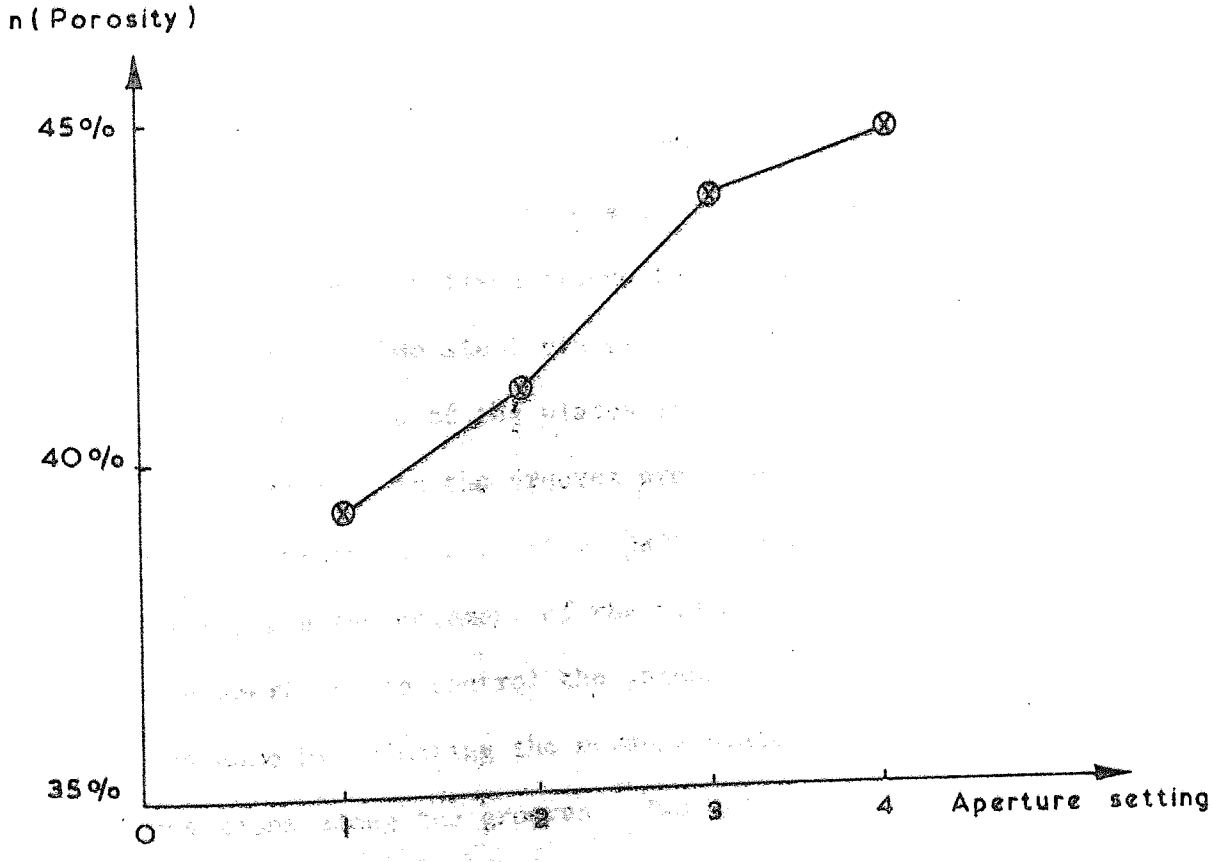

FIG. 5.4b

5.4.2 Deposition of sand for the Two Dimensional Model Test

5.4.2a Description of Hopper

The apparatus is on the same principles as that of the hopper for a three dimensional test. The intensity of a traversing sand curtain is adjusted to obtain a deposit with required porosity.

The hopper trolley, used for this purpose, is shown in plate (5.7). The capacity of the hopper trolley is $0.102m^3$, and it is composed of; two semi circle sides, 580mm in diameter, which are made from 19mm ply wood. A semi circle surface, 390mm wide, which was made from a plastic faced flexible hard board, 3mm thick, with the smooth surface facing inside the hopper. This part had a hole 170mm x 75mm at its bottom. A wooden frame is fixed around the perimeter of this hole (plate 5.7). Two steel plates 3mm thick form the base of the hopper. One of the plates is fixed to the frame, the other can move in the grooves provided on the frame. The movable plate had a vertical part (see plate 5.7) to facilitate the movement of the plate. The setting of the apertures to control the intensity of the sand rain, was made by adjusting the movable plate at different positions along the grooves. Two bolts, each having two adjusting nuts, were fixed to the base frame. By

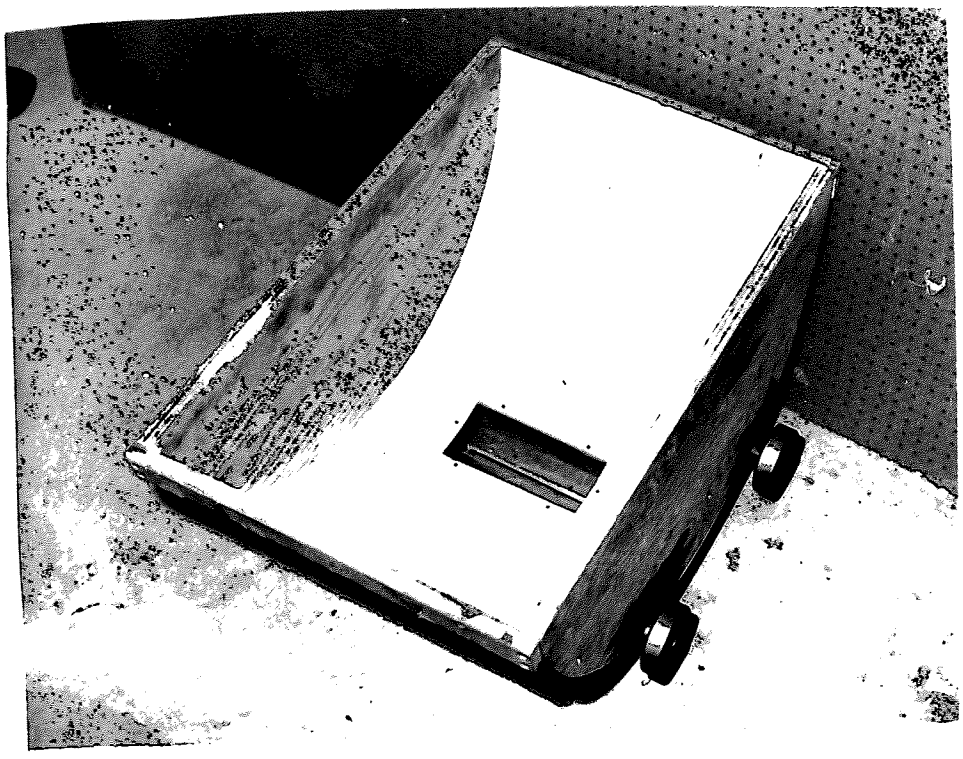

PLATE (5.7a) GENERAL VIEW OF THE HOPPER

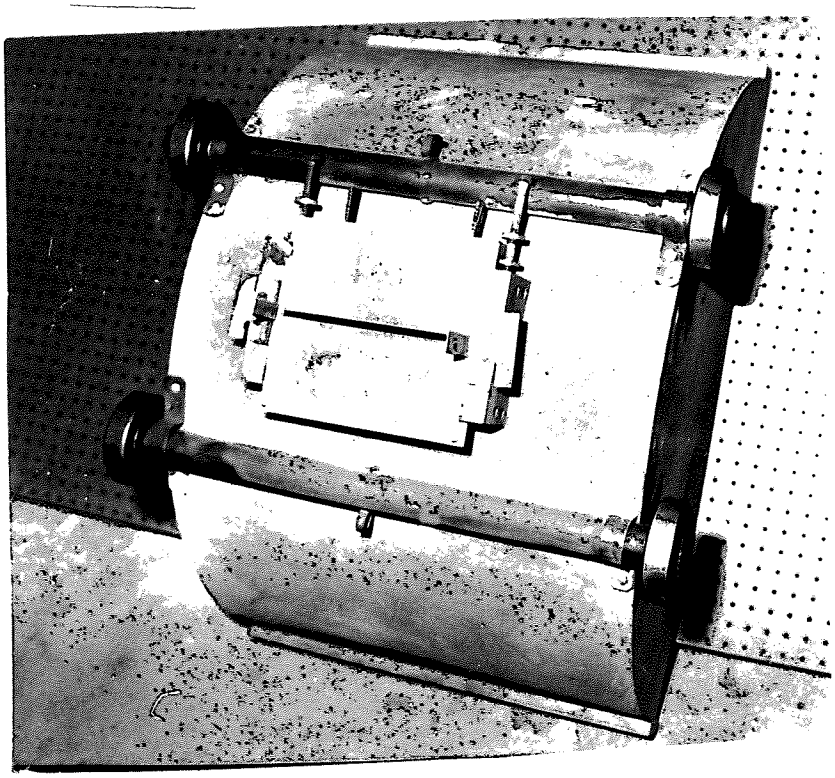

PLATE (5.7b) BASE OF THE HOPPER

THE HOPPER USED FOR DEPOSITION IN THE TWO DIMENSIONAL TEST

turning the adjusting nuts against the vertical part of the movable plate, the plate was moved along the grooves of the frame to give the required aperture size. To measure the size of the aperture the vertical part of the movable plate moved along two graduated bars which are fixed to the base frame. To prevent the sand pouring out when the hopper is not in operation, a square wooden plate, 180mm x 100mm was slid in the grooves, on the outside surface of the adjustable plate to shut the aperture. The trolley of the hopper consists of two axles with four wheels attached to them, the axles were fixed to the hopper by four support clips.

The manner in which the hopper moves along the tank is shown in Figure (5.3b). A rope was attached to a hook which was fixed on the axle, the rope passed over a pulley which was connected to a hand operated geared winder. In a trial fill a considerable duning effect was observed, this was due to jerking of the hopper. A balance weight as shown in Figure (5.3b) was used to minimise this effect.

The alignment of the hopper during deposition was insured by two channel guides. These channels had one side each fixed to the frame, and the other side inside the tank to act as a guide (see plate 5.7).

5.4.2b Calibration of hopper

In order to deposit a layer of sand to a predetermined porosity, it was necessary to find the porosity of sand rain at different heights of the tank for different sizes of hopper aperture. Density tins were placed at different positions along a wooden platform, 2080mm x 160mm in plan. This platform, which is supported by two ropes at its ends, is suspended inside the tank at different levels. The supporting ropes passed over two pulleys at the ends of the tank. The pulleys (Fig. 5.3b) are fixed on slotted angles which rest on the edges of the end columns. The height of fall, which is from the top of the tank to the surface of the platform, is measured by a graduated wooden bar. The hopper was filled and the aperture was adjusted to the required size. The hopper ran along the tank by winding the geared winder manually. When the density tins were filled, the platform was pulled up, the tins were screeded level, weight and porosity calculated. This was repeated for different heights and different sizes of aperture.

Figures (5.5a-d) show the variation of porosity with aperture size for different heights of fall. In contrast with the hopper for the three dimensional test, it can be seen that the height of fall affects the porosity of deposit, i.e. the porosity increases as the height of fall decreases.

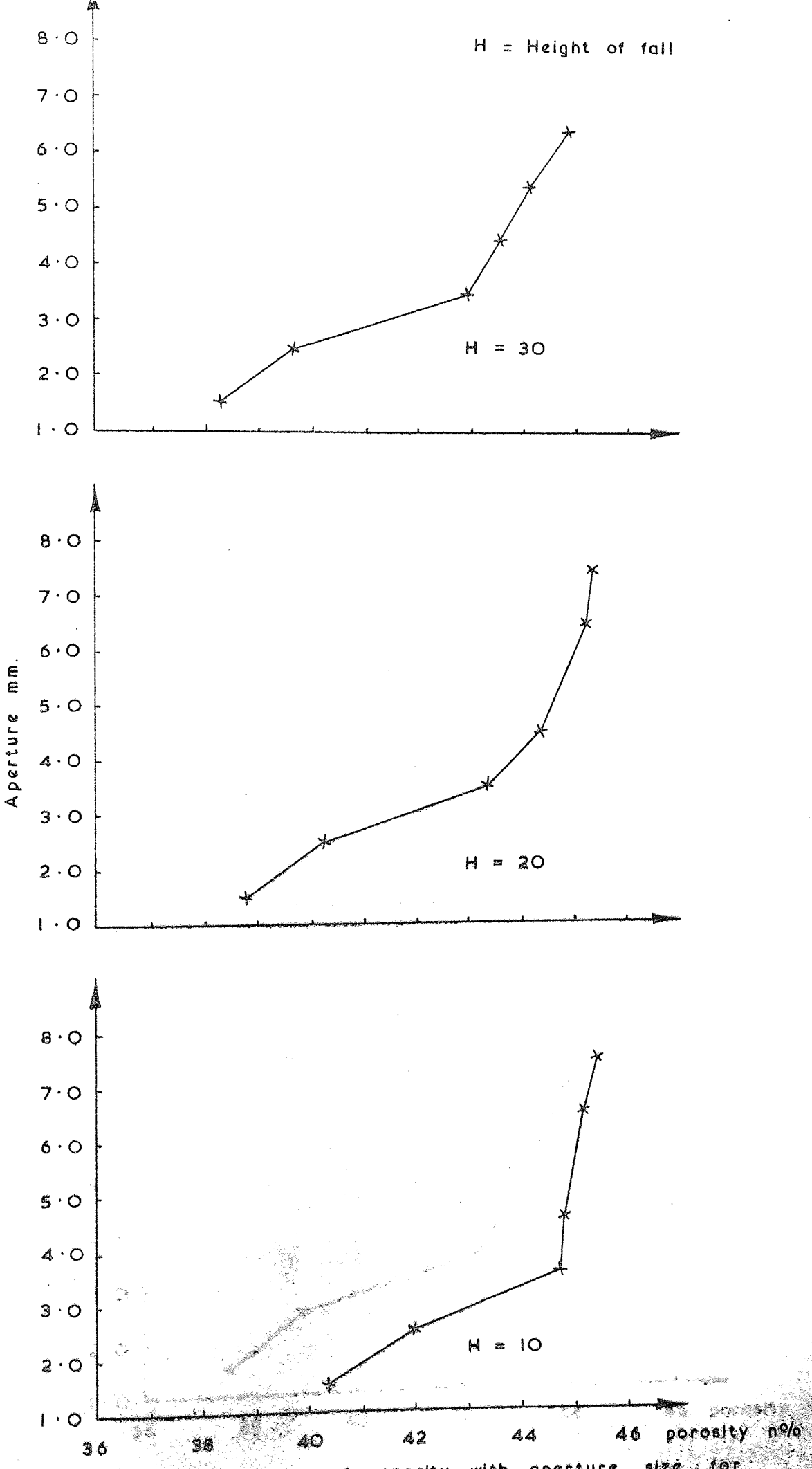

FIG. 5.5.a-d. Variation of porosity with aperture size for different height of fall.

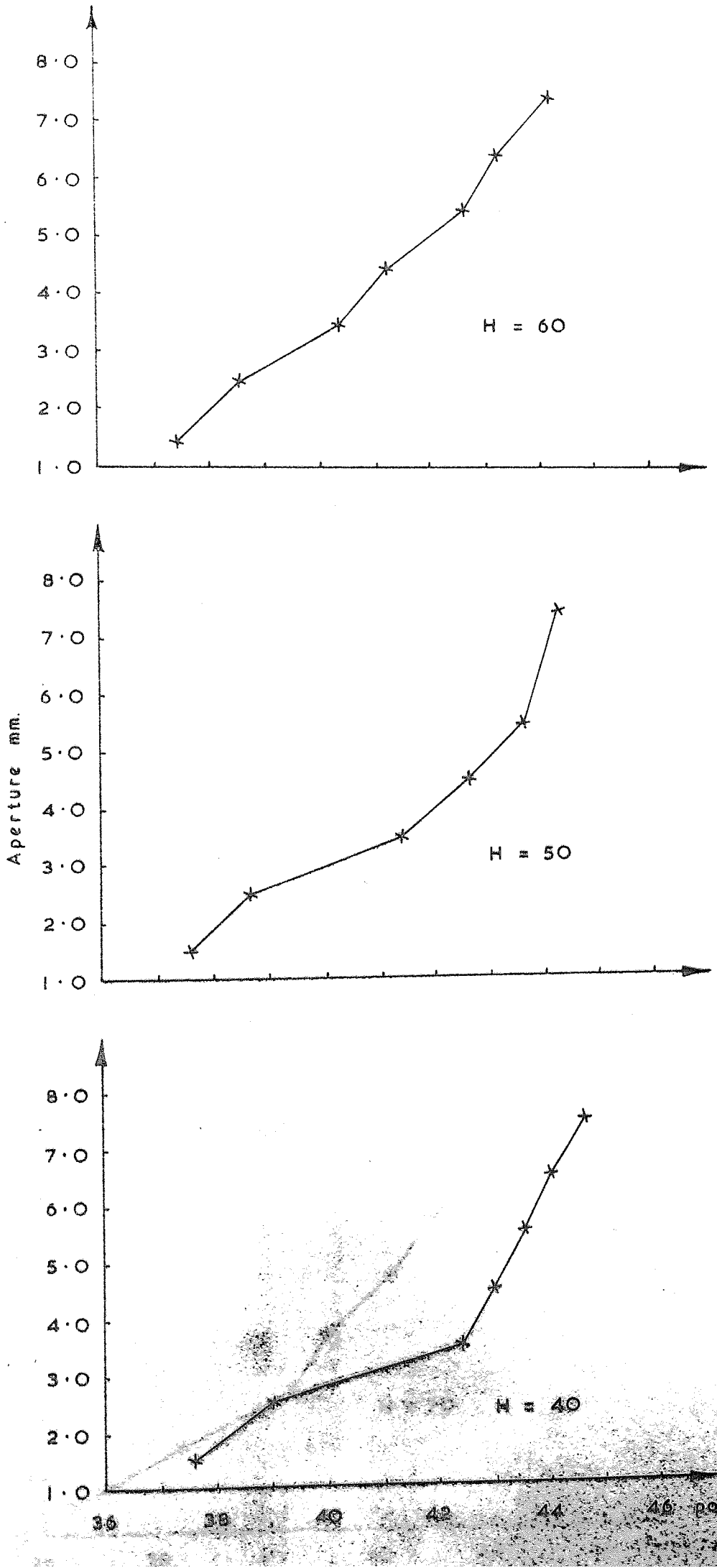
8·0
7·0
6·0
5·0
4·0
3·0
2·0
1·0
H = 60
Aperture mm.
H = 50
H = 40
36
38
40
42
44
46
porosity n%

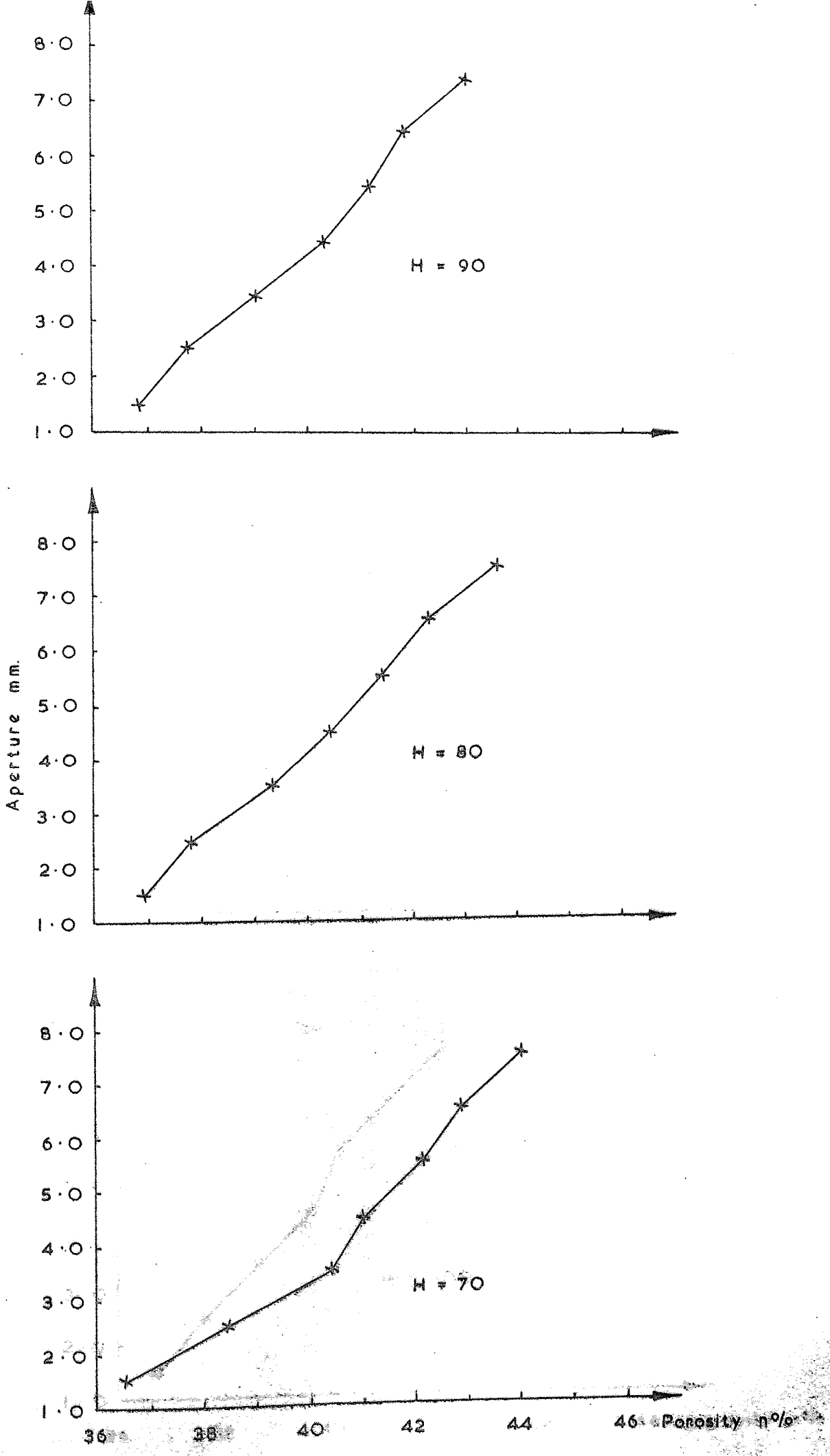
8·0
7·0
6·0
5·0
4·0
3·0
2·0
1·0
H = 90
H = 80
H = 70
Aperture mm.
36
38
40
42
44
46
Porosity n°/o

FIG. 5.5c

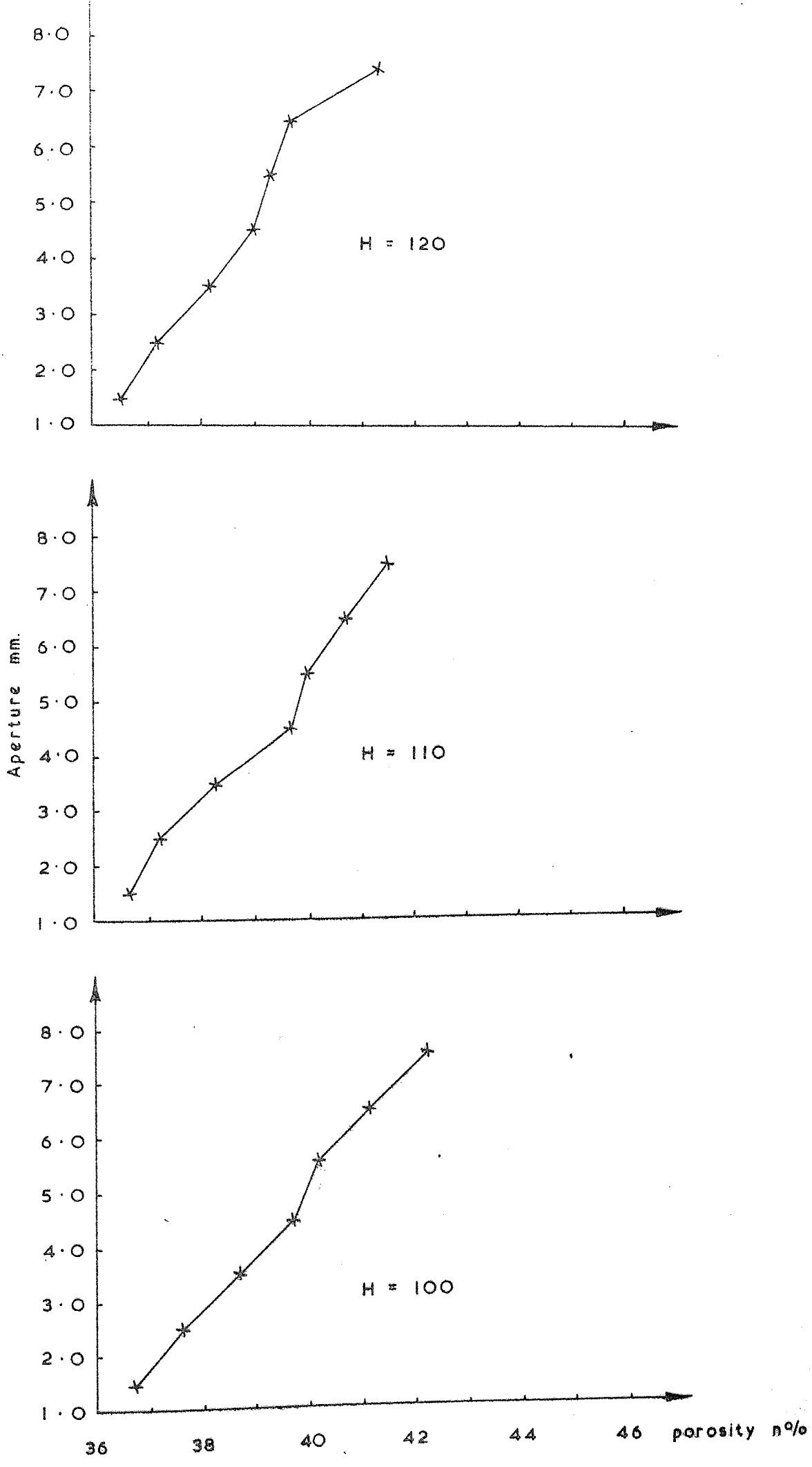
8·0
7·0
6·0
5·0
4·0
3·0
2·0
1·0
H = 120
H = 110
H = 100
Aperture mm.
36
38
40
42
44
46
porosity n%

FIG. 5.5d

5.5 Loading System

Initially it was intended to use a hydraulic jack for the application of the load to the experimental beams. The base of the jack was fixed to the bottom flange of the cross beam of the loading frame of the two dimensional model. A steel proving ring was used to measure the applied load. The proving ring was fixed to a knife edge which was located at the point of application of the load on the beam model. The settlement of the beam which was largely irrecoverable, caused the load to decrease. The hydraulic pump had to be continuously readjusted to maintain a constant reading on the proving ring. To eliminate this problem, it was decided to adopt a dead load system. The loading system used for this purpose is shown in Figure (5.6a). It consists of a loading arm, a restraining bar, and an inverted "T" knife edge through which the load is applied on the beam. The lever arm, which is 150cm long, is made from two 75 mm x 75mm x 25mm steel angle sections. The angles are 25mm apart and accommodate two steel blocks 25mm x 25mm x 25mm The steel blocks are welded to the angles and have "V" shape seatings to receive the knife edges of the restraining part, and inverted "T" (Fig. 5.6a). The horizontal part of the inverted "T" is a knife edge which rests across the width of the beam and transfers the applied load on the beam. The restraining part for the three dimensional tests (which is different than that of the two dimensional loading system) is shown in Figure 5.6b. The magnification of the loading arm was approximately five.

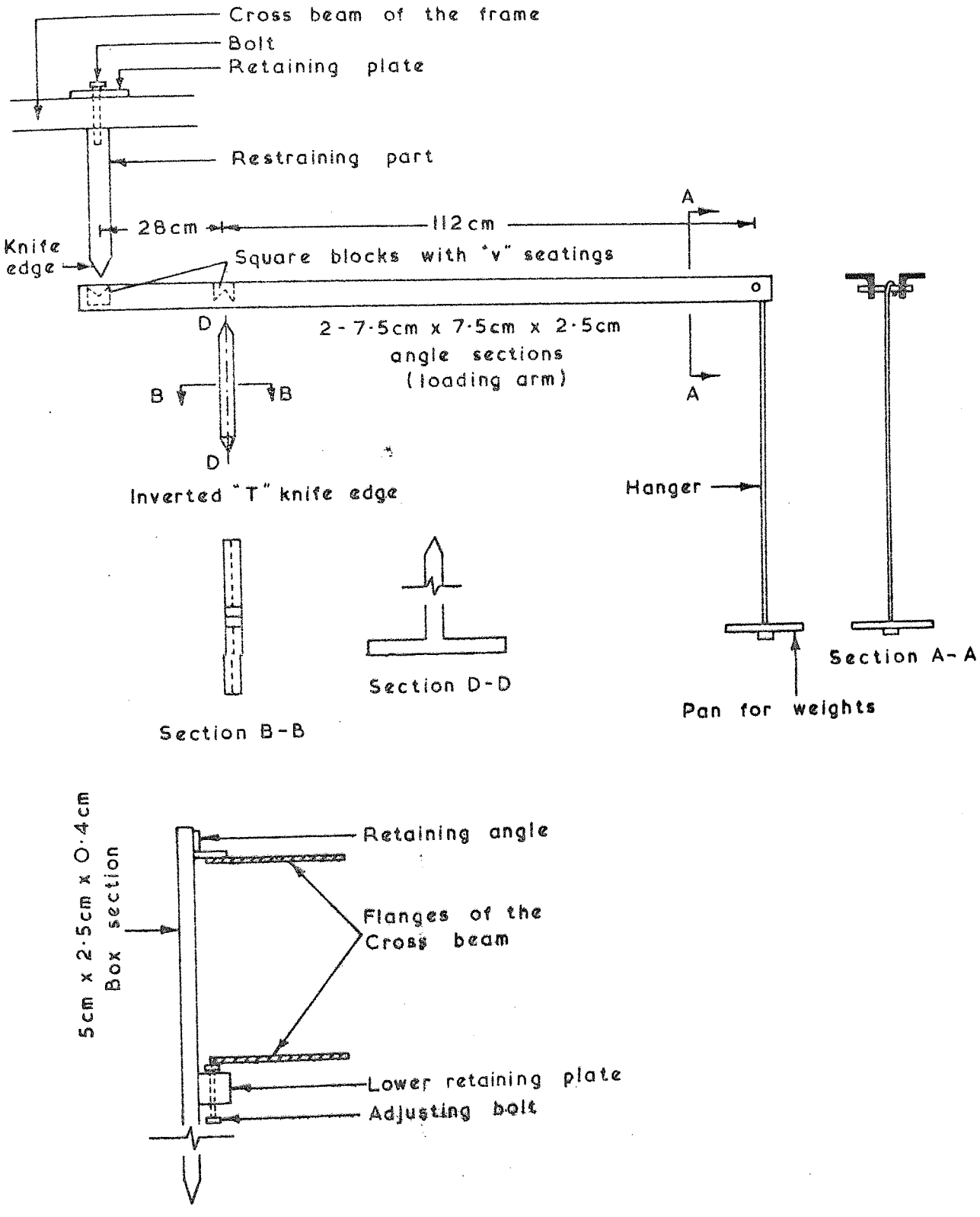

FIG.(5. 6)

a) Layout of the loading system

b) Restraining part for the loading in three dimensional test

5.6 Experimental Procedure

5.6.1 Experimental Procedure for Three Dimensional Test

Experiments of Cunnell (1974) showed that, when depositing sand, the surface of the sand at the edges is lower than the centre of the bed. This problem has been overcome by placing the sand at the bottom of the test bed and banking it round the edges. Four density tins were placed on sand and their positions and numbers were noted. Using a fork lift truck, the hopper which was filled at ground level, (see plate 5.8a-b) was lifted and connected to the trolley. The hopper was brought to the starting position which was marked on the cross beam of the loading frame. The aperture was set and the hopper was drawn along the bed by winding the crank of the worm gear, the speed of the pulling was adjusted so that the hopper was empty when it reached the other end. When the hopper reached the other end, the aperture was closed and the hopper was pulled back to its starting position. The hopper was lifted down and filled. Before the next layer is deposited, density tins are placed on sand. The deposition was continued until the required level of sand (approximately 90cm) was reached. The surface of the bed was then levelled by using a board, the same width of the bed. The board, with its two handles resting on the frame of the bed, was pulled along the bed to level its surface.

The beam was then placed centrally on the bed (the manner in which the beams were handled and placed on the bed is shown in Figure 5.7). The frame for dial gauges was built. This frame

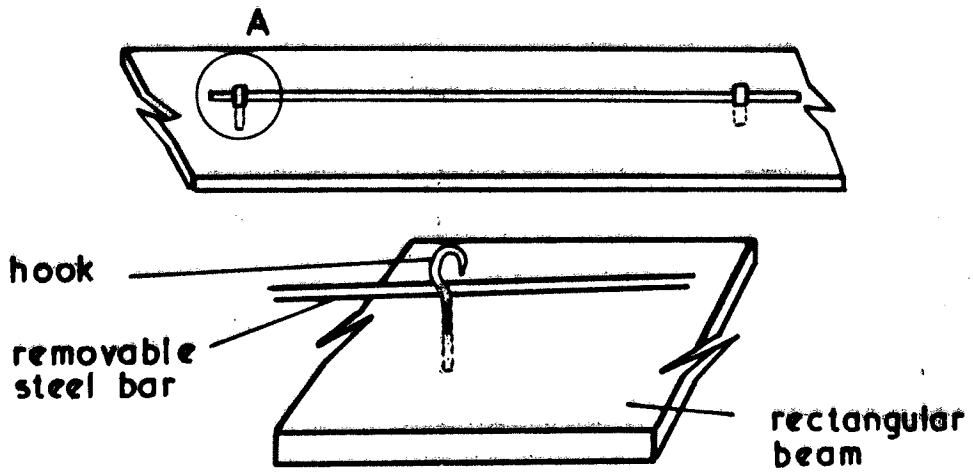

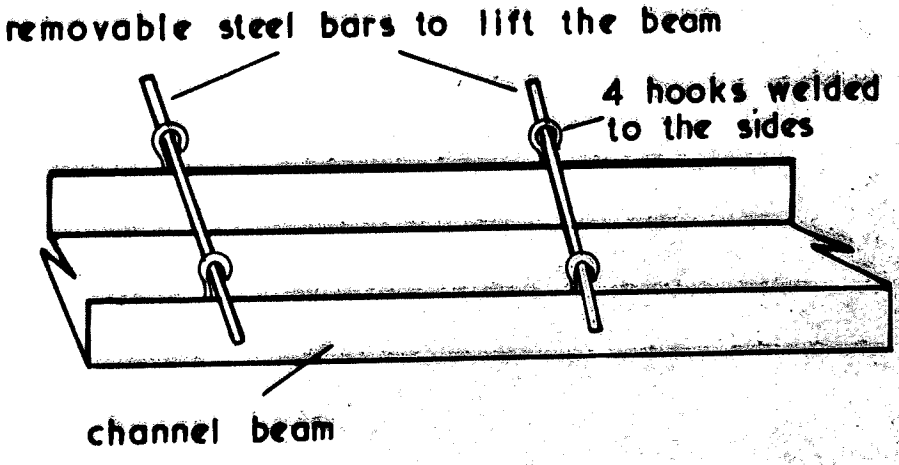

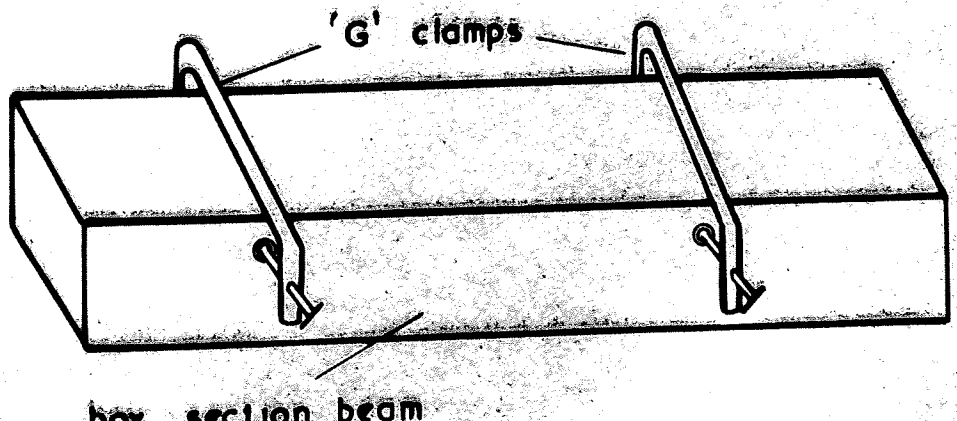

Fig. 5.7. The manner in which the beams were lifted.

PLATE (5.8a) THE FILLED HOPPER AT GROUND LEVEL

PLATE (5.8b) THE HOPPER BEING ATTACHED TO THE TROLLEY

rested on two sides of the test bed and was fixed in position by "G" clamps. The loading system was then assembled and strain gauges were connected to the extension box. The strains were recorded by Compuleg Alpha 16 Computer; reading time for each strain gauge was approximately 0.1 second. Plates (5.9) and (5.10) show the channel beam under a concentrated load, and the flat beam under two point loads.

After completion of the test, the loading arm, the dial gauges frame, and the beam, were removed. Finally, the sand was emptied into plastic containers, through two openings at the base of the tank (plate 5.11). The density tins were removed as soon as they appeared, and their weights were recorded.

The three dimensional model tests were carried out with two different porosities of sand corresponding to aperture set 1 (n = 39.3%) and 3(n = 43.8%) of Figure 5.4a. The range of porosity measured by density tins, for different tests, were between 43.4% and 44.3% for opening 3, and between 39.1%, 39.9% for opening 1 (n_{max} = 45.5%, n_{min} = 33.7%).

5.6.2 Experimental procedure for Two Dimensional Test

The hopper was lifted and placed in position with its channel guides inside the tank and the wheels on the tracks (Fig. 5.3b). The hopper was filled with sand, and the aperture was adjusted (see section 5.4.2b). The shutter was removed and the hopper was

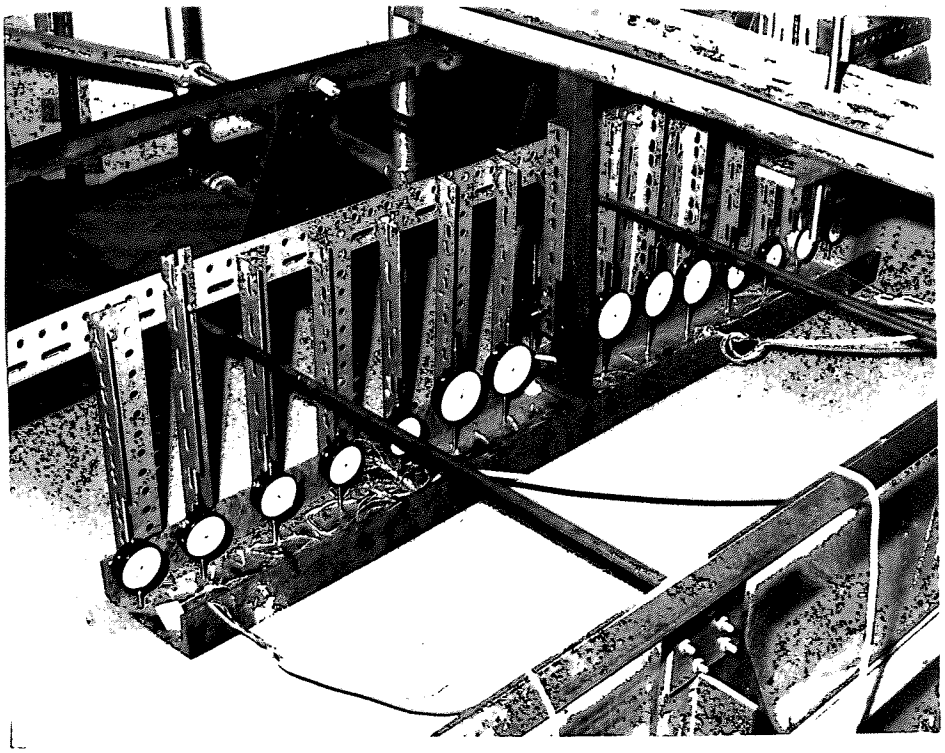

PLATE 5.9 THE CHANNEL BEAM UNDER CONCENTRATED LOAD (THREE DIMENSIONAL TEST)

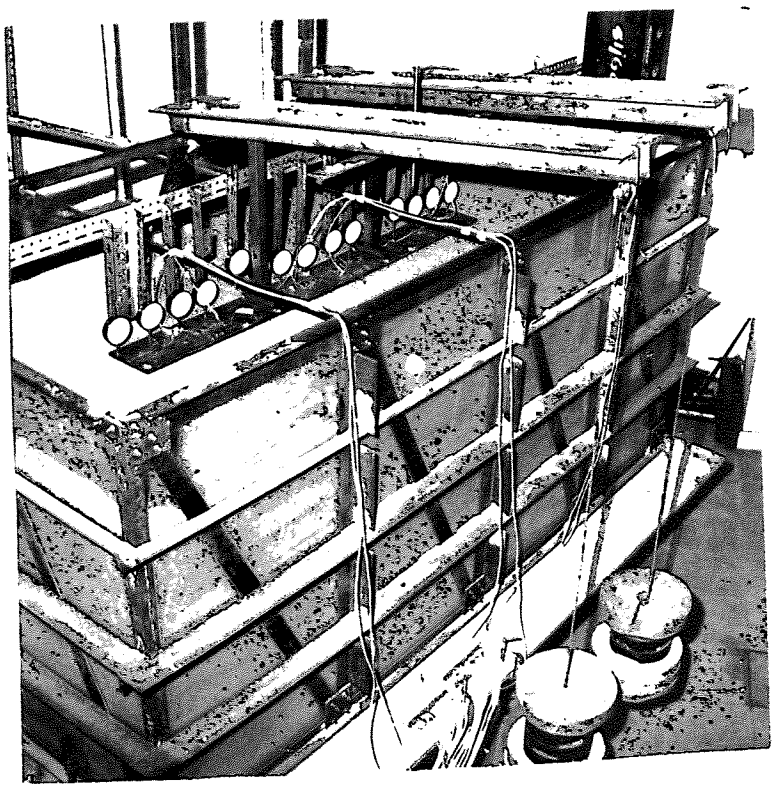

PLATE 5.10 THE FLAT BEAM UNDER TWO POINT LOADS (THREE DIMENSIONAL TEST)

PLATE 5.11 EMPTYING THE SAND

pulled along the tank (Fig. 5.3b). The tests were performed on the deposits of sand in their densest possible state which could be prepared by the hopper. From the calibration curves (Fig. 5.5a-d), it can be seen that the densest homogeneous deposit which can be prepared, has a porosity n = 40.5%. The size of aperture to give this porosity at different levels was obtained from Figures (5.5a-d). With each aperture size, 10cm of sand was deposited. The speed of the geared winder, to pull the hopper, was adjusted so that 5cm of sand was deposited for each travel of the hopper along the tank.

When the hopper reached the end of the bed, the shutter was pushed in to stop the sand rain. The rope was disconnected from the axle and the hopper was pushed back to the other end. The process was repeated until the tank was filled to a level approximately 50mm below the top of the walls. The hopper was lifted down and the surface of the sand was then levelled by a scraper which ran along the tests bed (plate 5.12) as the scraper is made of a plate 3mm thick fixed to an angle section 25mm x 25mm. In order to ensure that the thickness of the bed is the same throughout the bed, the angles rested on two supports, which were fixed to the frame at the top of the tank, and levelled carefully. The scraper was drawn from the middle to the ends, the extra sand was then removed from the ends.

The beam, which was marked at the point of application of load, was lifted and placed on the bed with its mark in coincidence with the mark on the top of the wall, indicating the line of action of the load. The loading arm was then placed on the supporter with the

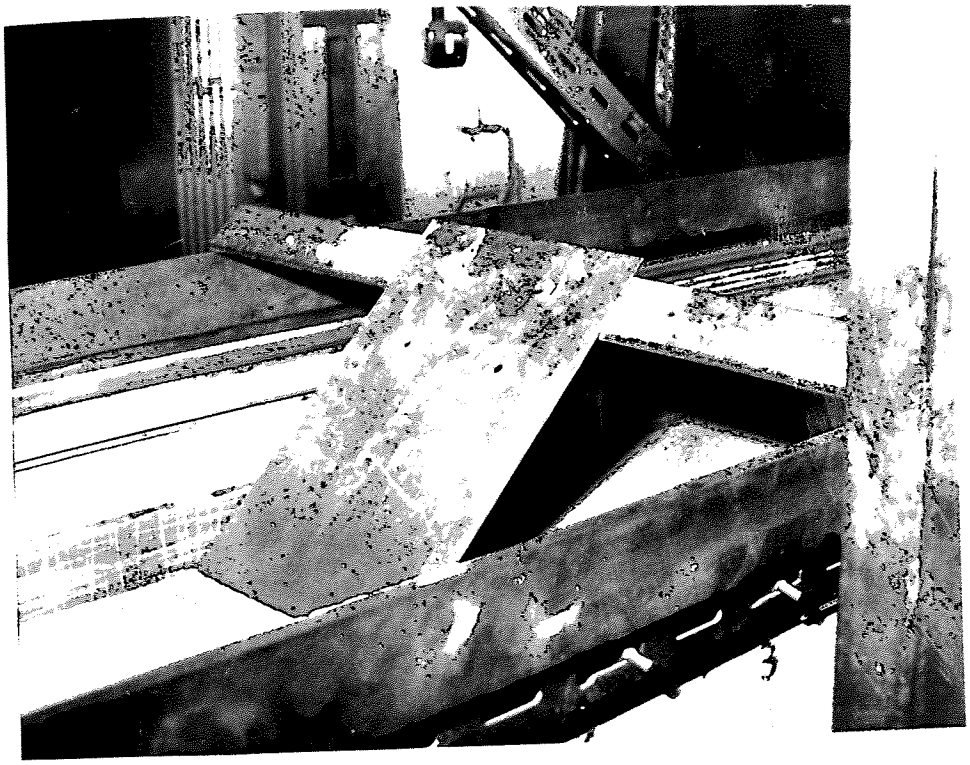

PLATE 5.12 THE SCRAPER USED TO LEVEL THE SAND IN THE TWO DIMENSIONAL TEST

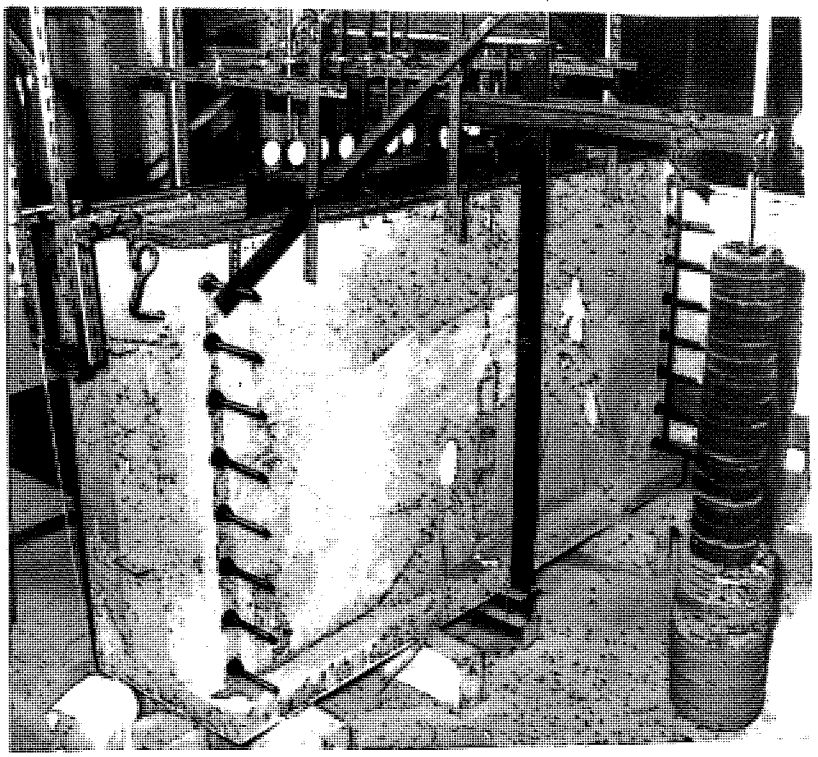

PLATE 5.13 THE BOX SECTION BEAM UNDER CONCENTRATED LOAD (TWO DIMENSIONAL TEST)

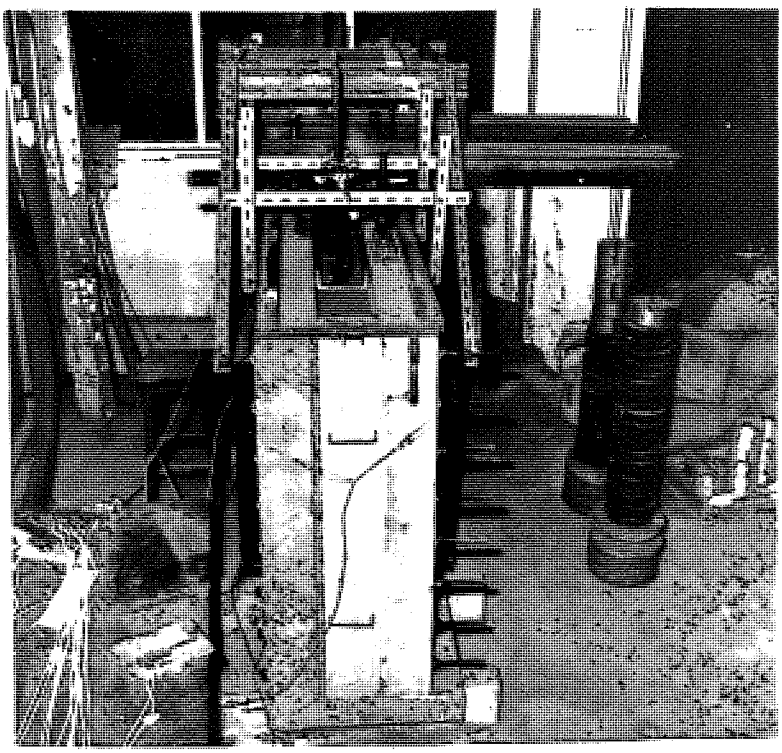

PLATE 5.14 THE CHANNEL BEAM UNDER TWO LOADS (TWO DIMENSIONAL TEST)

knife edge of the restraining bar inside the "V" shape. The inverted "T" was placed at the point of application of load with the knife edge of the vertical part of it located in the "V" shape of the lever arm.

The strain gauges were connected to an extension box by multi-core electric cables. A strain indicator 'peekle" was used to record the induced surface strains. The deflection of the beam at different points were measured by dial gauges located at 10cm intervals. The "V" shape of the lever arm was then brough in contact with the vertical knife edge of the inverted "T" by lowering the plate which supports the lever arm. The loading was then started by gently placing the weights on the pan of the loading hanger. The load increment was continued until the deflection at the point under the load reached 25mm. Plates (5.13) and (5.14) show the box section beam under a point load and channel beam under two point loads. When the test was completed, the loading system, the dial gauges frame and the beam were removed. Finally, the sand was emptied (using a vacuum cleaner) and weighed. The porosity of the sand was calculated for each test. The range of porosity for different tests was between n = 43.4% and n = 44.2%.

CHAPTER SIX

EXPERIMENTAL RESULTS

6.1 Introduction

The description of the apparatus and the testing procedure, for both two and three dimensional model tests were given in Chapter 5. The results of experiments are presented in this chapter. A series of experiments were performed with the different beams which were subjected to either a concentrated central load or two concentrated loads. The number of tests with different beams in the two and three dimensional conditions are shown in Table (6.1).

In the three dimensional tests, the experiments were performed with two different porosities of sand. These porosities were obtained by setting the aperture size at settings 1 or 3 of the hopper (Chapter 5 Section 5.41c). These deposits are referred to as medium dense, and medium loose, respectively (n_{max} = 45.5%, n_{min} = 33.7%). The range of the average porosity of the deposits in different tests were

n = 39.0% to n = 40.2% aperture setting 1

n = 43.4% to n = 44.3% " " 3

In the two dimensional tests, the deposits for different tests were prepared with the same aperture settings (Chapter 5, Section 5.4.2b). The range of porosity in different tests was between n = 43.4% and n = 43.9%. The bending moments along the beams were obtained, using the relationship

$$M = \epsilon E_b \frac{I}{y}$$

where

ϵ is the recorded strain

E_b is Young's modulus of the beams (E_b= 2100000 Kg/cm^2)

I is the moment of inertia

and y is the distance from the neutral axis of the section to a level where the strain gauges are located. The value of I/y for each beam section is as follows

I/y = 3.6 cm^3 flat beam

" = 75.7 " channel "

" = 246 " box "

Since the loading is concentrated, the contact force distribution (contact stress x width of the beam) along the beams can be obtained through double differentiation of the bending moment distribution curves.

Table 6.1

Section	No. of Tests	Single load 3D	Single load 2D	Two Loads 3D	Two Loads 2D
Box	3	2	1	-	-
Channel	4	2	1	-	1
Flat	6	2	1	1	1

6.2 The results

The variation of the load against the central deflection of the beams (subjected to a concentrated load) in the two and three dimensional tests (shown as 2D and 3D) are given in Figures (6.1ac). In the three dimensional tests the load increment for each test was up to a point (final load) where a rapid increase in the deflection of the beam was observed. The load deflection curves of the beams, resting on medium dense subgrade (n = 39% to 40.2%) were linear over a considerable initial range. At higher loads (exceeding half the final load), the rate of deflection incrased (Figures 6.1ac). For the medium loose subgrade (n = 43.4% to 44.3%), for the first initial loadings, (60% of the final load), the slope of the load-central deflection curve decreased, and at higher loads (up to the final loading), the deflections were proportional to the applied load.

The corresponding curves in the two dimensional tests (shown as 2D in Figures 6.1ac) on medium loose sand (n = 43.4% to 43.3%), were linear for the whole range of applied load.

The results of surface strains showed a linear increase with applied load. The central strain against the applied load for the flat beam is shown in Figure (6.2). Because of the linear increase of strains and deflections with the applied loads (in the three dimensional tests with medium loose sand, the deflection curves are linear after some initial loadings), as shown in Figures (6.1ac) and (6.2), the distribution of deflection, bending moment and contact force along the beams are obtained for a particular load in the linear part of load-central deflection curve. These are shown in Figures (6.3ac) and (6.4ac).

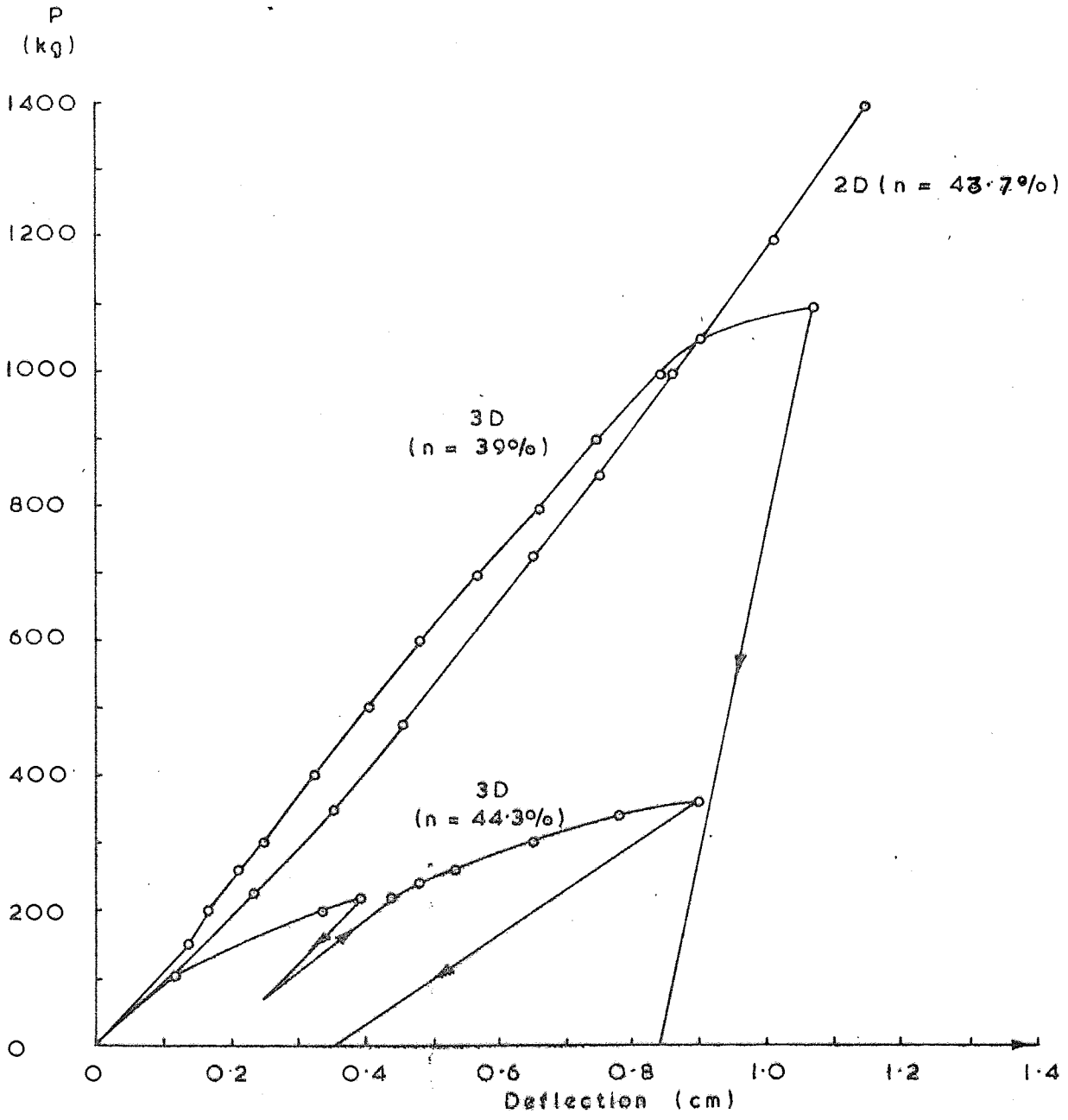

FIG. 6. 1a Load - versus central deflection curves (flat beam)

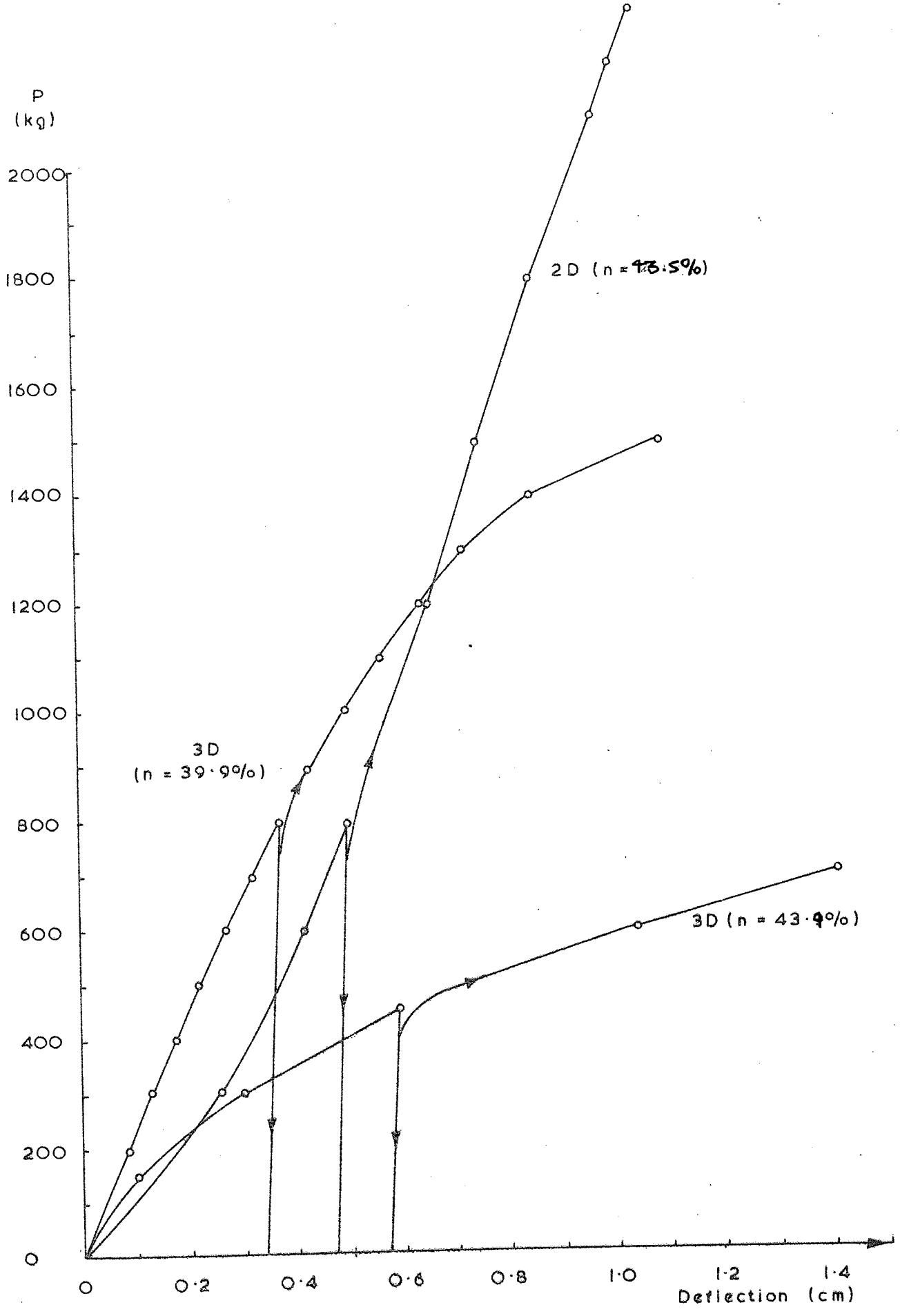

FIG. 6. 1b Load - versus central deflection curves (Channel beam)

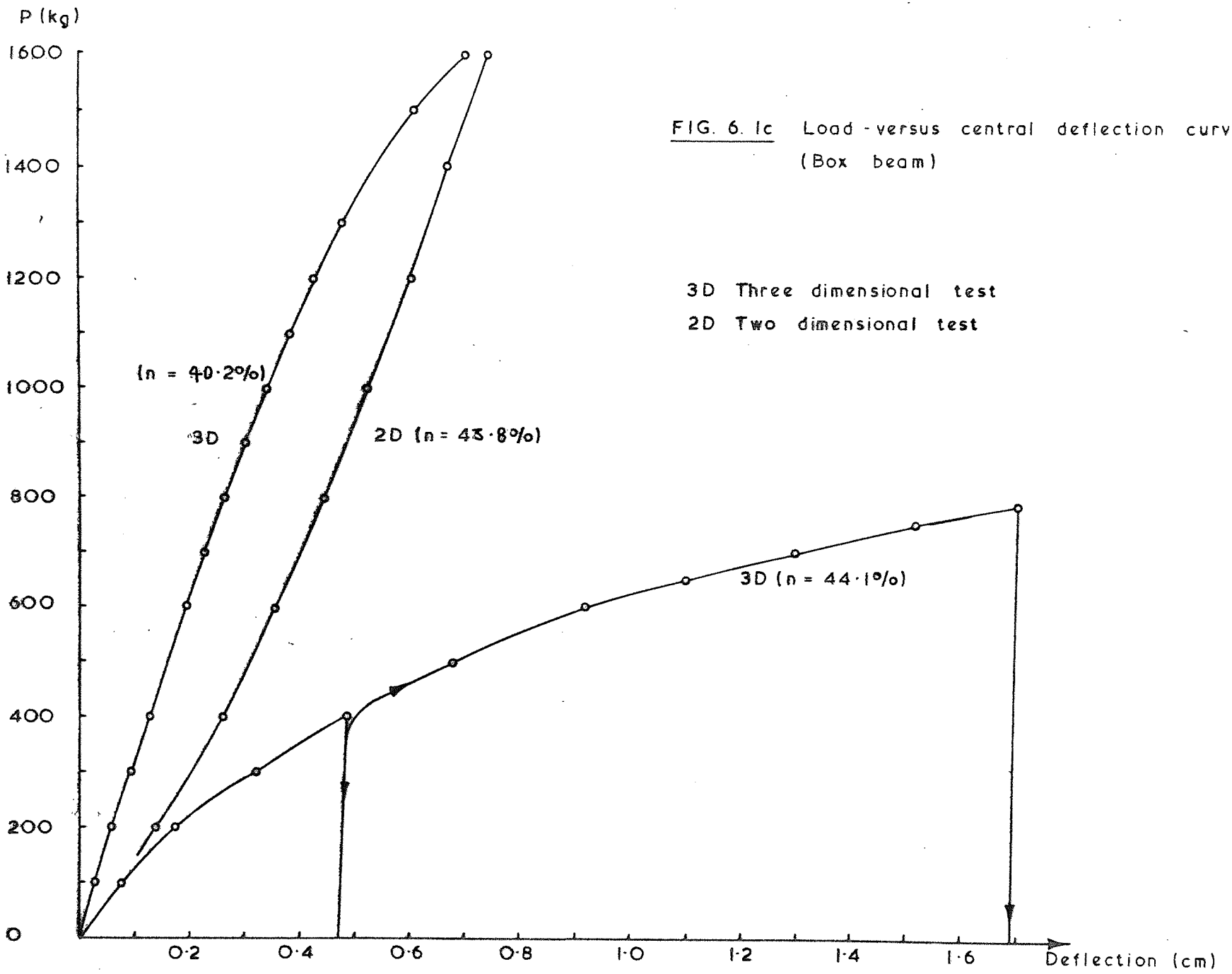

FIG. 6. Ic Load - versus central deflection curves (Box beam)

3D Three dimensional test

2D Two dimensional test

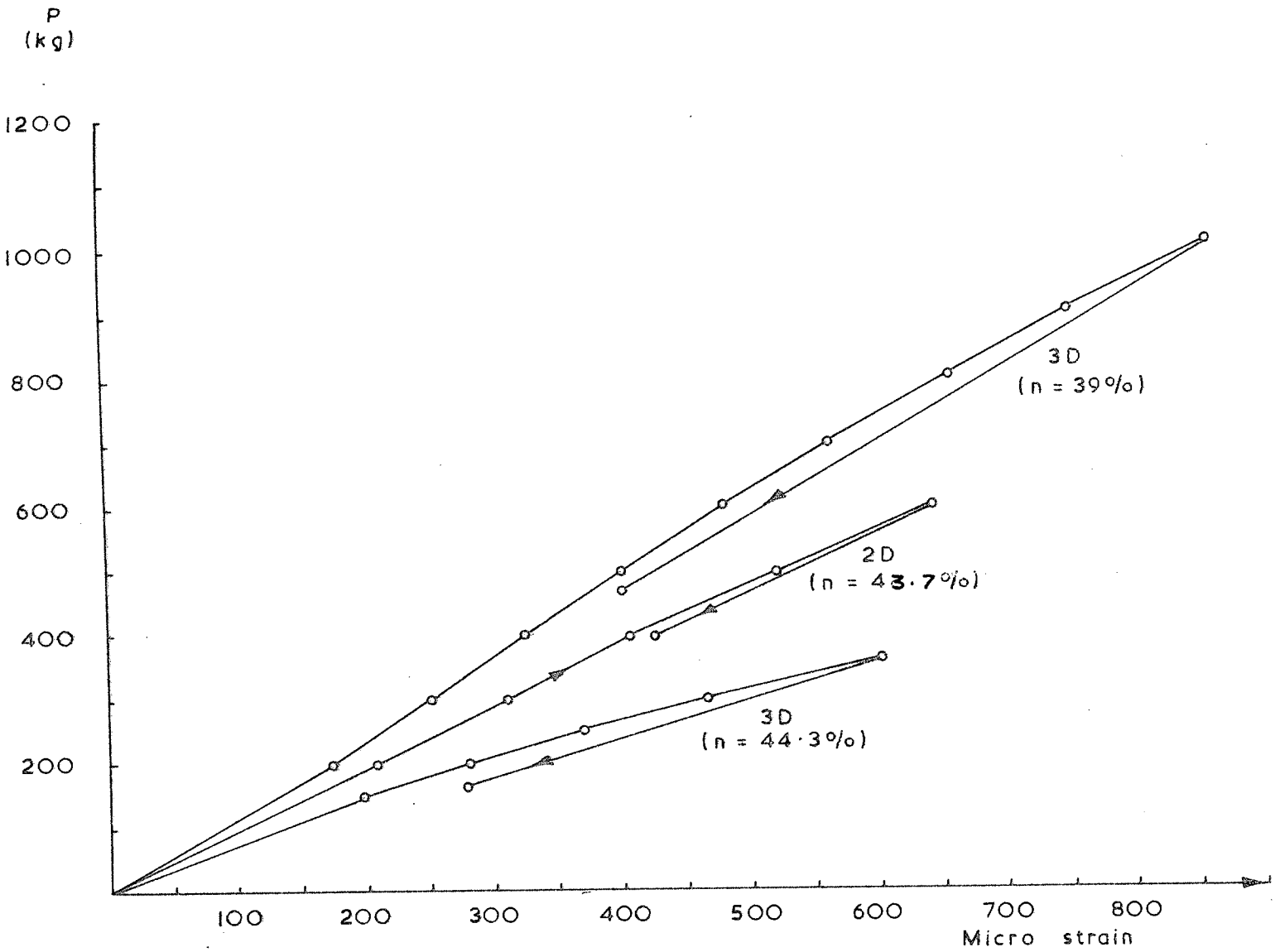

FIG. 6. 2 Load – versus central strain
(flat beam)

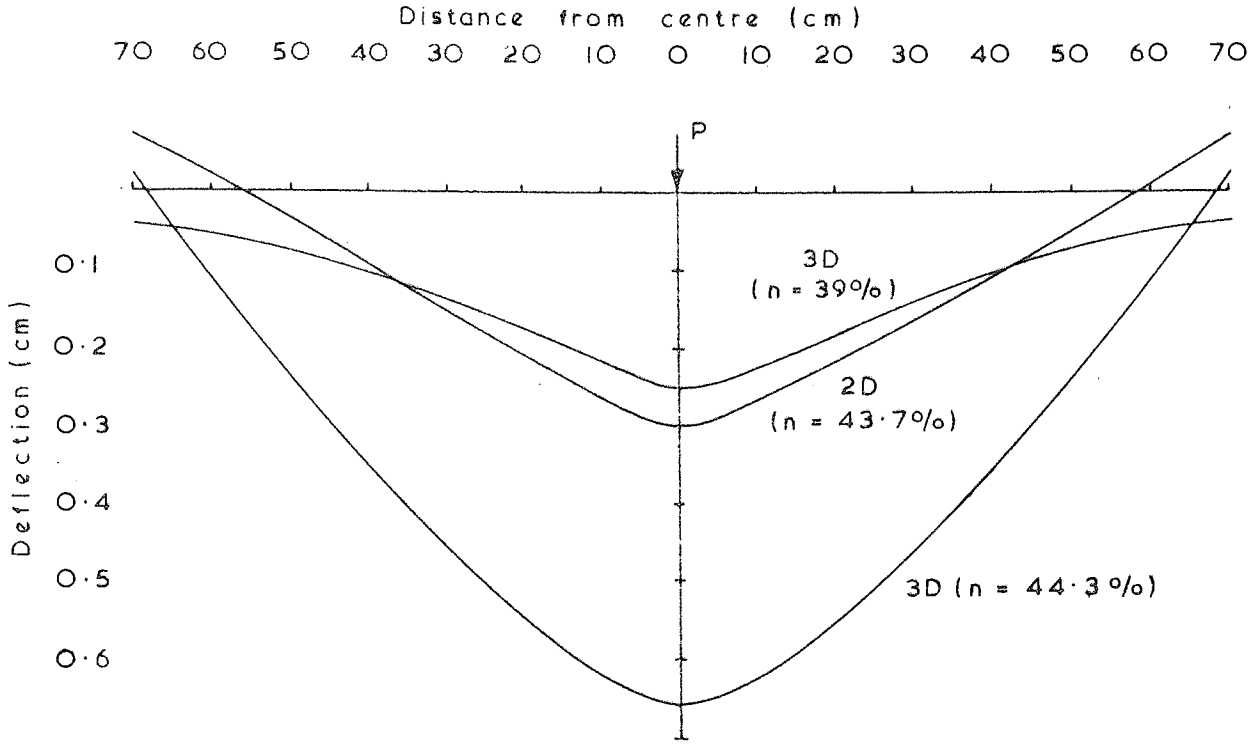

FIG. 6. 3a Flat beam - deflection curve

P = 300 kg

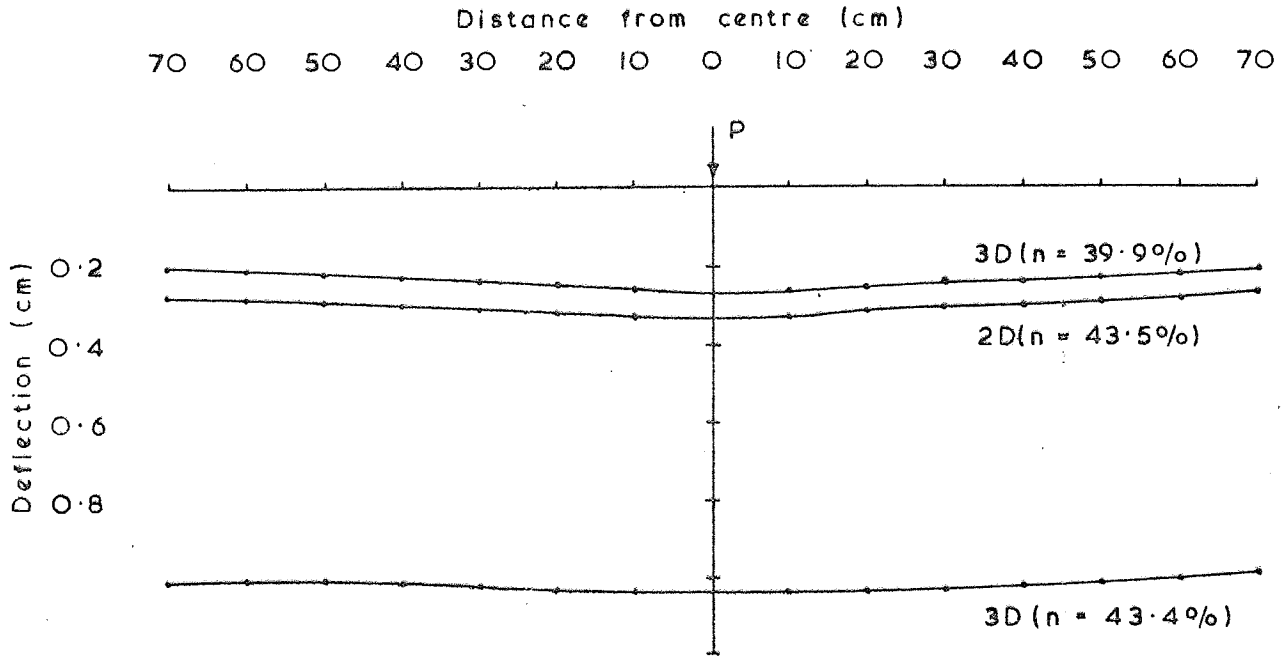

FIG. 6. 3b Channel beam deflection curve

P = 600 kg

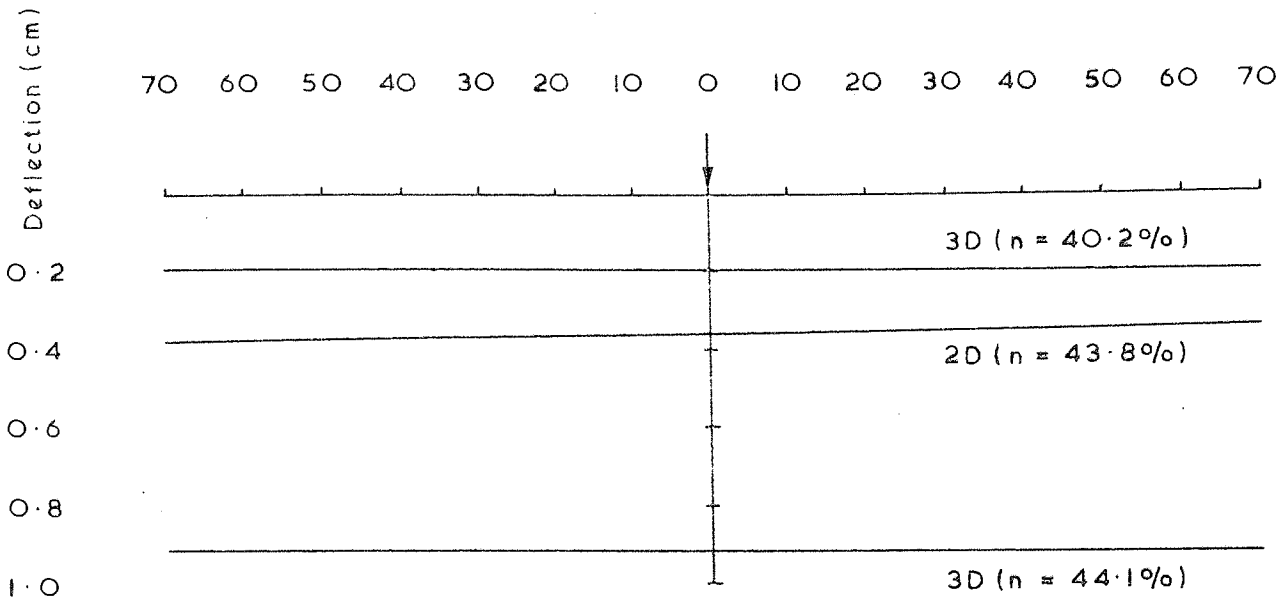

FIG. 6. 3c Box beam Deflection curve
(P = 600 kg)

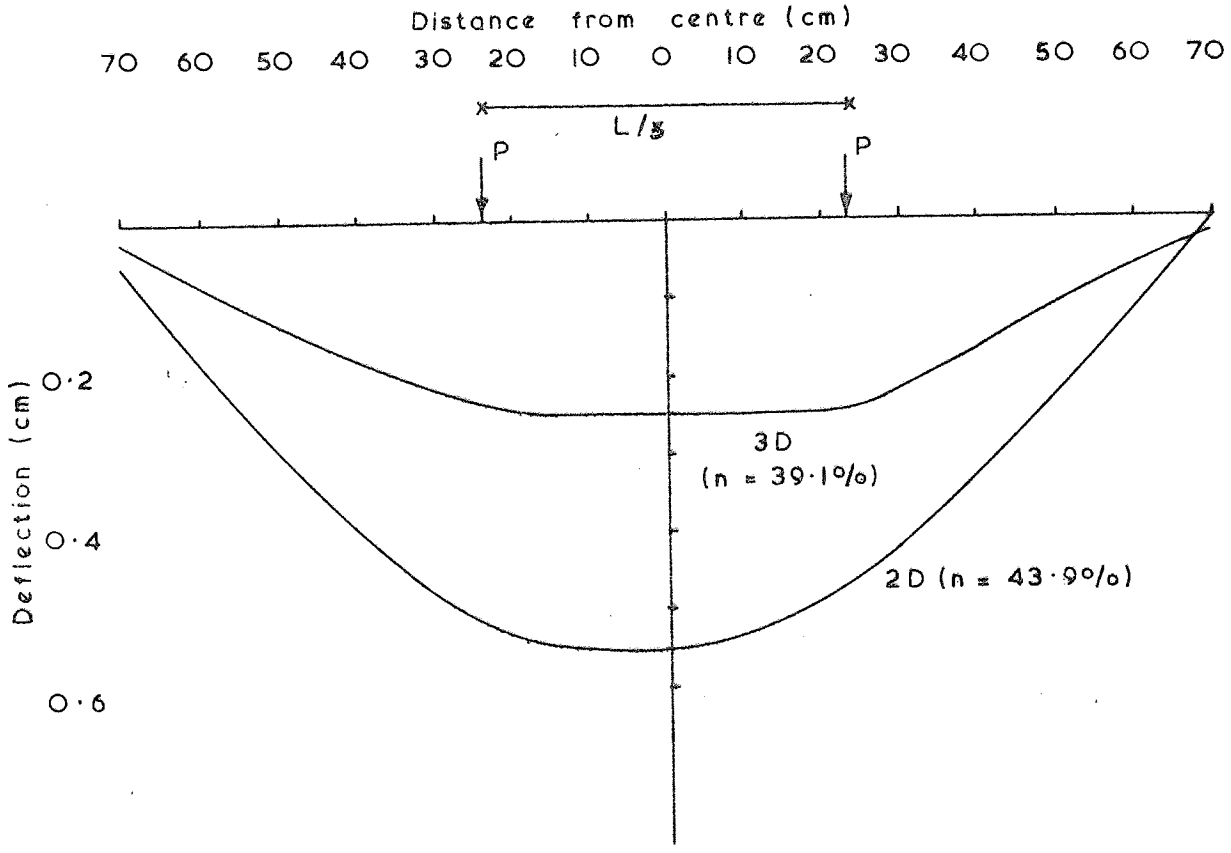

FIG. 6. 3d Flat beam - Deflection curve
P = 300 kg

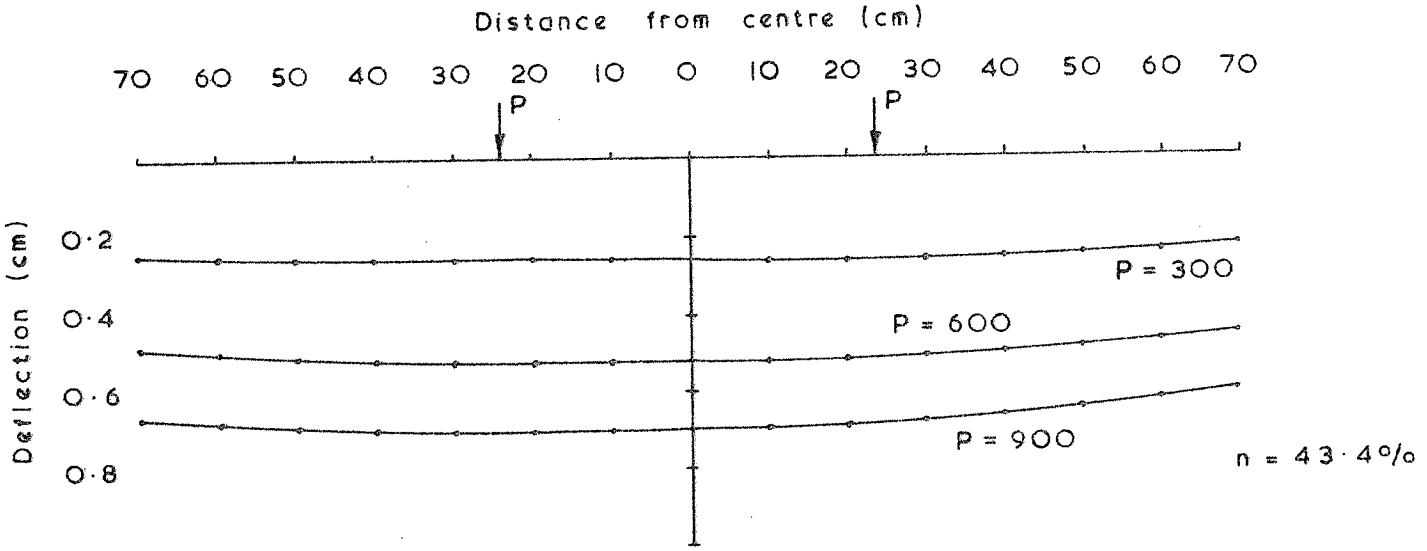

FIG. 6. 3e Channel beam – Deflection curve (Two dimensional)

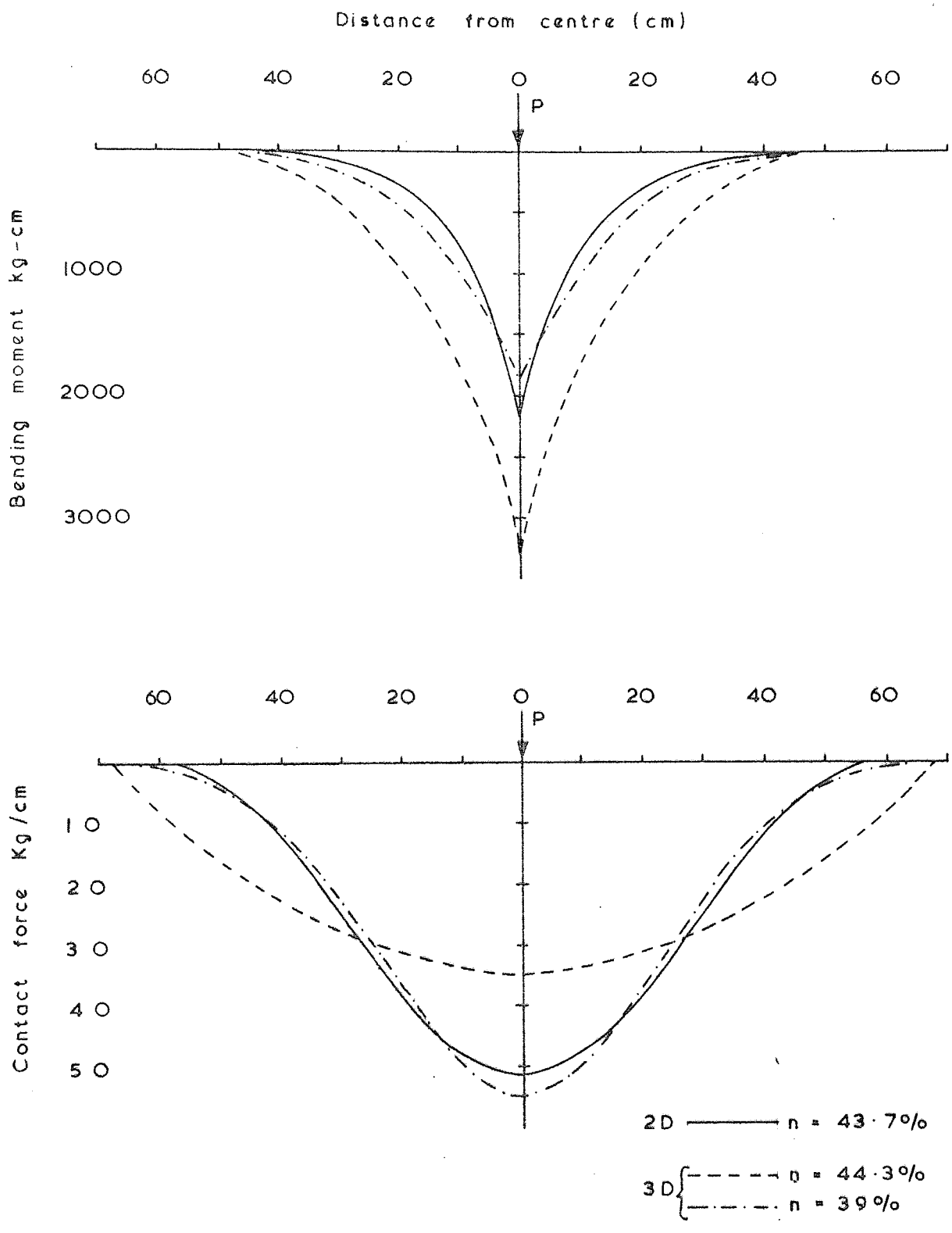

FIG. 6. 4a Flat beam (Single load)

P = 300 kg

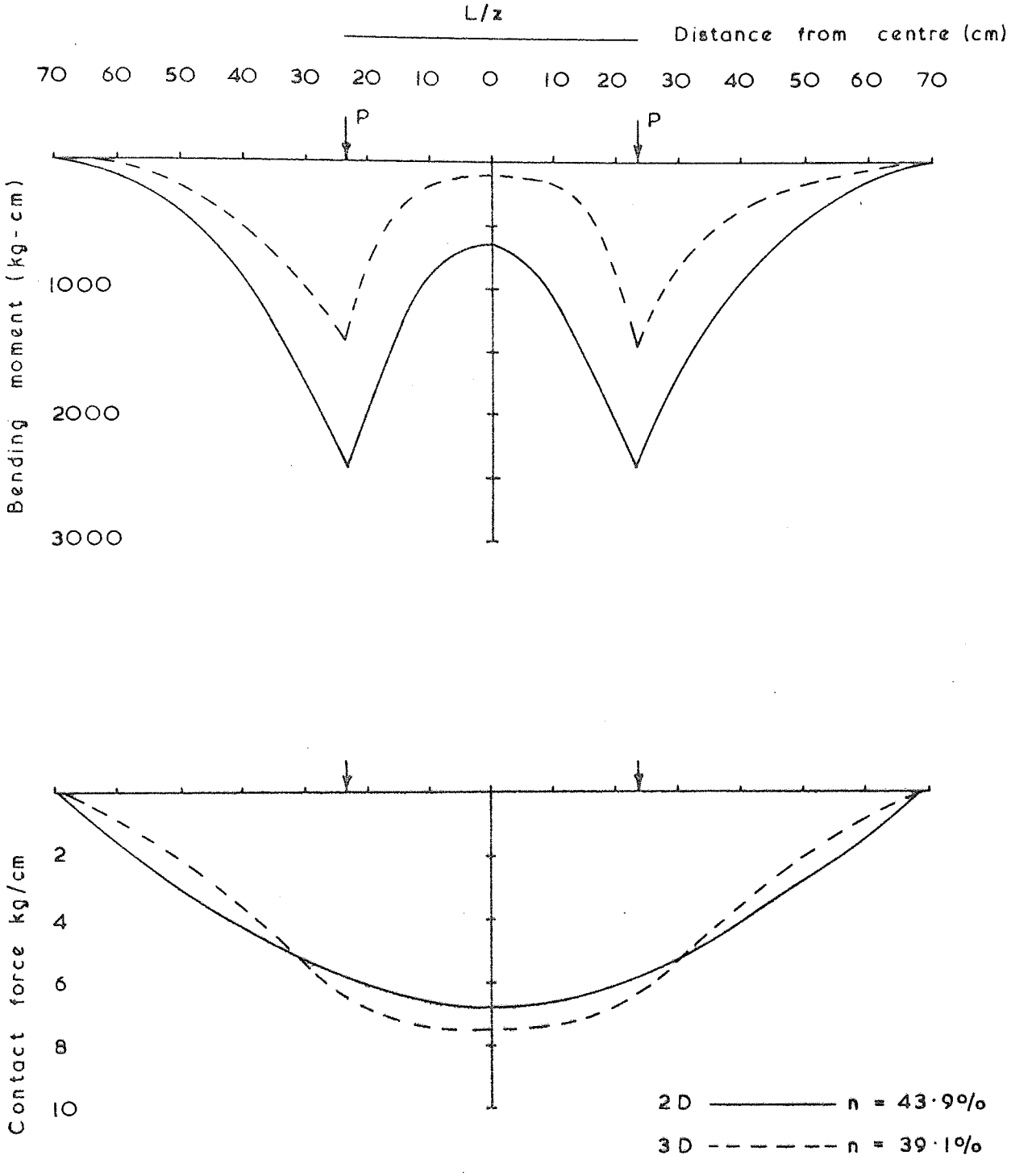

FIG. 6.4b Flat beam (two loads)

P = 300 kg

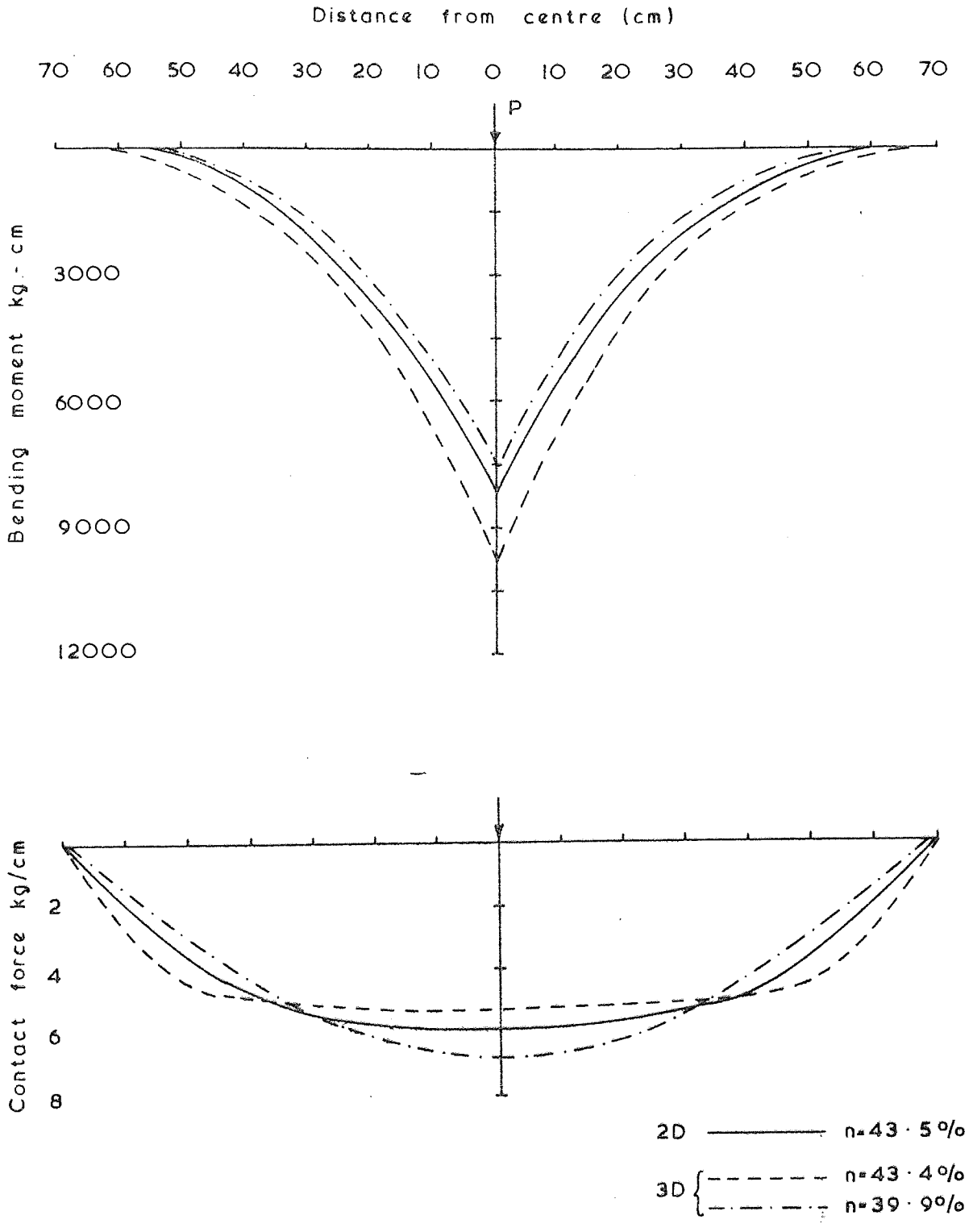

FIG. 6. 4c Channel beam

(P = 600 kg)

6.3 Discussion of the results

The deflection of the box section beam under a single central load, in both the two and three dimensional tests (Figure 6.3c), indicate that the beam behaves as a rigid foundation. The deflection curves for the beams subjected to a concentrated load, show that (Figures 6.3ab) the deflection of the beam under the load relative to the ends of the beam increases as the flexibility increases.

The distribution of contact force (for a single and two loads) under the flat beam (Figures 6.4ab) is similar to the deflection curves (Figures 6.3a and 6.3d). The contact force curve for the channel beam (Figure 6.4c) had the shape of the deflection curve (Figure 6.3b) towards the centre of the beam, and reduced to zero at the ends.

Due to the rigid behavior of the box section beam under point load (Figure 6.3c), and the channel beam (Figure 6.3e) under two loads (two dimensional test) recorded strains along the length at the surfaces of these beams were practically zero; it was therefore not possible to obtain the distribution of contact force beneath the beams. The tests on the box section beam can be considered as plate loading tests, and in Chapter 7 the results of these tests are used to obtain values for K (modulus of subgrade reaction) and the elastic properties of the granular material ($\frac{E}{1-\nu^2}$). To investigate the effect of change in porosity of sand on the maximum deflections, bending moments, and contact forces, the ratios of these values in tests with medium loose sand, and medium dense sand,

for different beams under concentrated load (Figures 6.3a-c, 6.4a and 6.4c) were obtained and given in Table (6.2).

From Table (6.2) it can be seen that an increase in porosity causes a considerable increase in the value of maximum deflection. A 5.3% increase in the porosity of sand causes 2.9 times increase in the maximum deflection of the flat beam under a central load of P = 300Kg. For the channel and box beam the increases are 3.8 and 4.6 times for P = 600Kg. The increase in the porosities are 3.5% for the channel beam and 3.9% for the box beam. It can be concluded that, in the linear range of the load deflection curves (the curves shown as 3D in Figures 6.1a-c), the ratio of $\frac{W_{n1}}{W_{n2}}$ increases as the rigidity of the beam increases.

	FL n_1= 44.3% n_2= 39%	CH n_1= 43.4% n_2= 39.9%	BO n_1= 44.1% n_2= 40.2%
$\frac{W_{n1}}{W_{n2}}$	2.9	3.8	4.6
$\frac{M_{n1}}{M_{n2}}$	1.78	1.30	-
$\frac{Q_{n1}}{Q_{n2}}$	0.64	0.78	-

Table (6.2)

Table (6.2) shows that an increase in porosity of the deposit, increases the maximum bending moment and decreases the maximum contact force. In contrast to the deflection, the effect of change in porosity on the maximum bending moments and contact forces of the flat beam is more than that on the channel beam.

A comparison of the results for deflection (Figures 6.3a-c), bending moments and contact forces (Figures 6.4a and 6.4c) for a single load show that creating a condition of plane strain for the subgrade has the same effect as decreasing the porosity of the sand in the three dimensional test.

The deflection curve of the three dimensional test with the flat beam subjected to two loads (each acting at a distance L/3 from the ends) and resting on medium dense sand (Figure 6.3d) shows that a part of the beam between the applied loads behaves like a rigid beam.

CHAPTER SEVEN

COMPARISON OF EXPERIMENTAL AND THEORETICAL RESULTS

7.1 Introduction

In this chapter we compare the experimental results obtained from model tests with equivalent theoretical results, assuming that the granular medium behaves as (i) a Winkler medium and (ii) an isotropic-homogeneous elastic medium. To carry out such a correlation we require numerical values for the constants describing the Winkler model (K), and the elastic medium (E and ν).

The basic disadvantage of idealizing the response of the soil medium as a Winkler medium is that the constant describing this model is not an intrinsic property of soil. It may, of course, be unique for a particular foundation problem.

With the elastic continuum idealization the constants (E and ν) describing the models are assumed to be characteristic and unique properties of the material. In practice, however, the stress-strain relationships of most soils is non-linear and depends on the type of soil, its moisture content, compaction, axial stress, confining stress, ~~axial stress,~~ confining stress, duration of load application, repetition of load, etc. In reality, it is impossible to determine a modulus of elasticity (E) for a soil. If all the above factors are kept constant and the change in stresses is small (compared to say the yield stress), a tangent modulus can be defined. Similar arguments follow for Poisson's ratio ν.

In the present discussion we shall assume these properties can be determined to a reasonable degree of accuracy, from either laboratory or in situ tests. The determination of constants describing the Winkler model (K) can be approached in the following ways :

(i) the constant K for a particular soil medium may be obtained from in situ plate loading tests.

(ii) the constant can be related to the elastic properties of soil (E and ν) by comparing the solutions to a particular soil foundation interaction problem.

A comprehensive account of the evaluation of the modulus of subgrade reaction from plate loading test, and practical application of the theory of subgrade reaction is given by Terzaghi (1955). The discussion of the factors affecting the determination of modulus of subgrade reaction and further references on the measurement of K is given by Selvadurai (1975).

Using the second approach, Biot (1937) has expressed the modulus of subgrade reaction K in terms of the elastic constants of the soil medium and the flexural property of the beam by equating the maximum bending moments in an infinite beam subjected to a concentrated load P and resting on Winkler and elastic medium.

$$K = 1.23 \left[\frac{1}{C(1-\nu^2)} \quad \frac{Eb^4}{E_b I}\right]^{0.11} \frac{E}{C(1-\nu^2)} \tag{7.1}$$

for the three dimensional problem, and

$$K = 0.710 \left[\frac{1}{(1-\nu^2)} \quad \frac{Eb^4}{E_b I}\right]^{1/3} \frac{E}{(1-\nu^2} \tag{7.2}$$

for the two dimensional plane strain problem.

Expressions similar to (7.1) were obtained (chapter 2, equations 2.62), by equating the maximum deflections, bending moments and contact forces in an infinite beam resting on Winkler and elastic medium, subjected to a concentrated load.

Vesic (1961, 1963) and Barden (1962, 1963) have suggested the following expressions

$$K = \frac{0.65E}{(1-\nu^2)} \left[\frac{Eb^4}{E_b I}\right]^{1/12} \tag{7.3}$$

and

$$K = \frac{0.65E}{1-\nu^2} \tag{7.4}$$

In (7.1) through (7.4), E and ν are elastic properties of the medium, $E_b I$ is flexural rigidity of the beam, b is half width of the beam and C is a factor (C = 1.00 if the distribution of contact stress across the width of the beam is uniform; $1.00 < C < 1.13$ if the deflection across the width of the beam is uniform).

Another interesting interpretation of the modulus of subgrade reaction K was proposed by Gibson (1967). The stresses and displacements in an incompressible non-homogeneous elastic half space, where shear modulus G(z) increases according to

$$G(z) = G(o) + mz$$

were obtained by Gibson. It is found that when G(o) = 0, the surface deflection w(o) is $q_o/2m$ within the loaded area and zero outside the loaded area, where q_o is the stress intensity of the uniform external load. This interpretation suggests that K = 2m.

In order to evaluate the elastic properties (E and ν) and the modulus of subgrade reaction K of the sand subgrade, a series of plate loading tests was performed. It is assumed that the supporting soil medium behaves like an isotropic elastic half space. From the knowledge of the solution of a rigid plate resting on an isotropic elastic half space it is then possible to determine a value for the term $\frac{E}{1-\nu^2}$. This has been carried out for both the plane strain and three dimensional plate loading tests. The values of $\frac{E}{1-\nu^2}$ are then used to obtain values for the modulus of subgrade reaction K for the Winkler model (equation 7.2 for the two dimensional and the second equation of 2.62 for the three dimensional analysis) and the beam-foundation characteristic c (equations 2.28 and 2.29) for the elastic half space model.

7.2 Plate loading tests

7.2.1 Two dimensional plate loading tests

Two sets of plate loading tests were performed. The plates were square, 16cm x 16cm x 1.2cm, and rectangular, 32cm x 16cm x 1.2cm. The experiments on each plate were carried out twice. The load settlement curves for these tests are shown in Figures 7.1 (first set of tests) and 7.2 (second set of tests). The unloading curves (Figure 7.1) show that the settlements were completely irrecoverable. The settlements were proportional to the applied load up to the points A and A' (for the square plate), B and B' (for the rectangular plate). The values of applied load and induced settlements at these points are used to evaluate the term $\frac{E}{1-\nu^2}$ for sand. The loads and settlement corresponding to points A, A', B and B' are as follows :

Square plate first test (point A in Figure 7.1)

$$P = 100 \text{ Kg} \qquad w = 0.819\text{cm} \tag{7.5}$$

Square plate second test (point A' in Figure 7.2)

$$P = 100 \text{ Kg} \qquad w = 0.795\text{cm} \tag{7.6}$$

Rectangular plate first test (point B in Figure 7.2)

$$P = 400 \text{ Kg} \qquad w = 0.925\text{cm} \tag{7.7}$$

Rectangular plate second test (point B' in Figure 7.2)

$$P = 400 \text{ Kg} \qquad w = 0.907\text{cm} \tag{7.8}$$

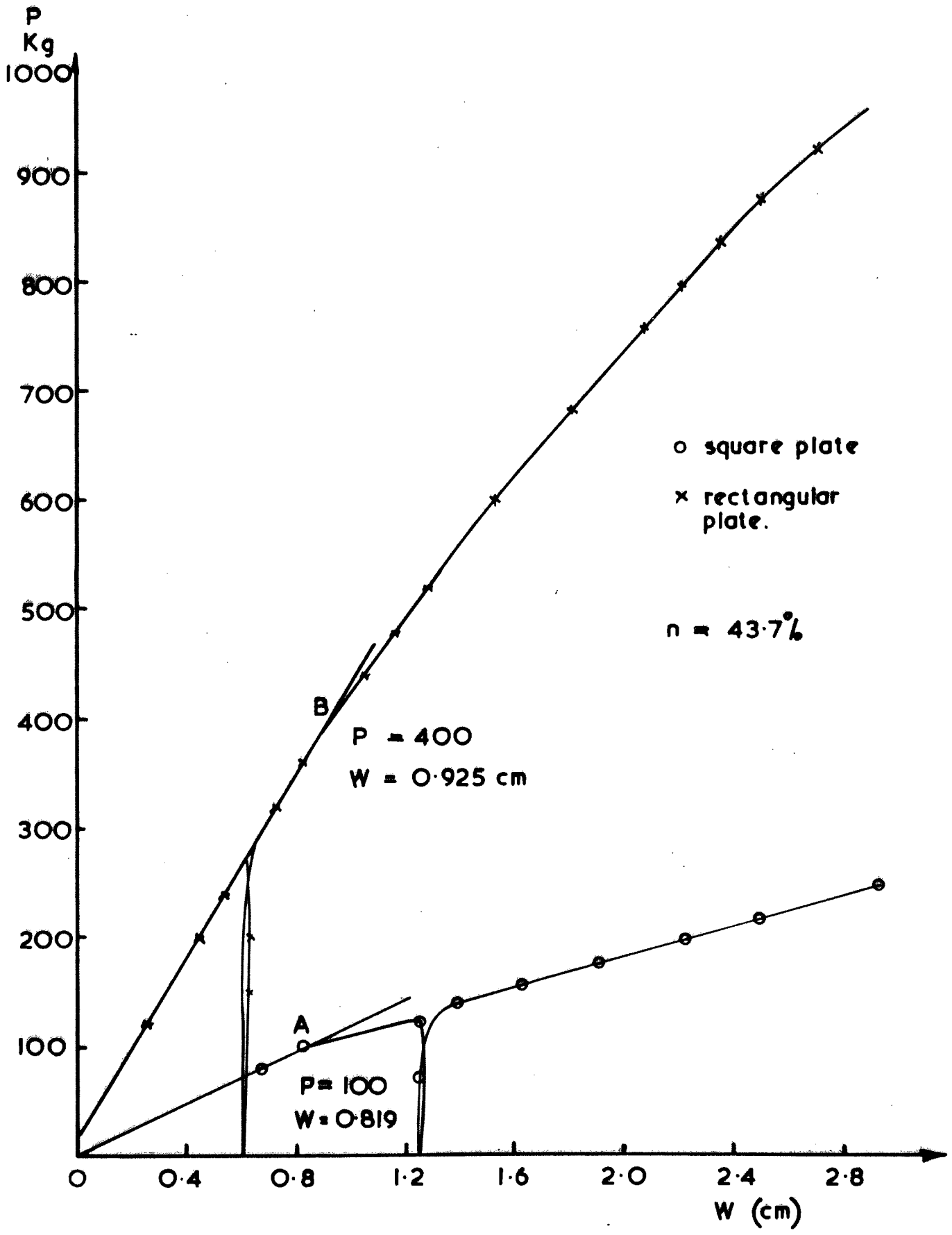

Fig. 7.1 Plate loading test - first set of tests two dimensional

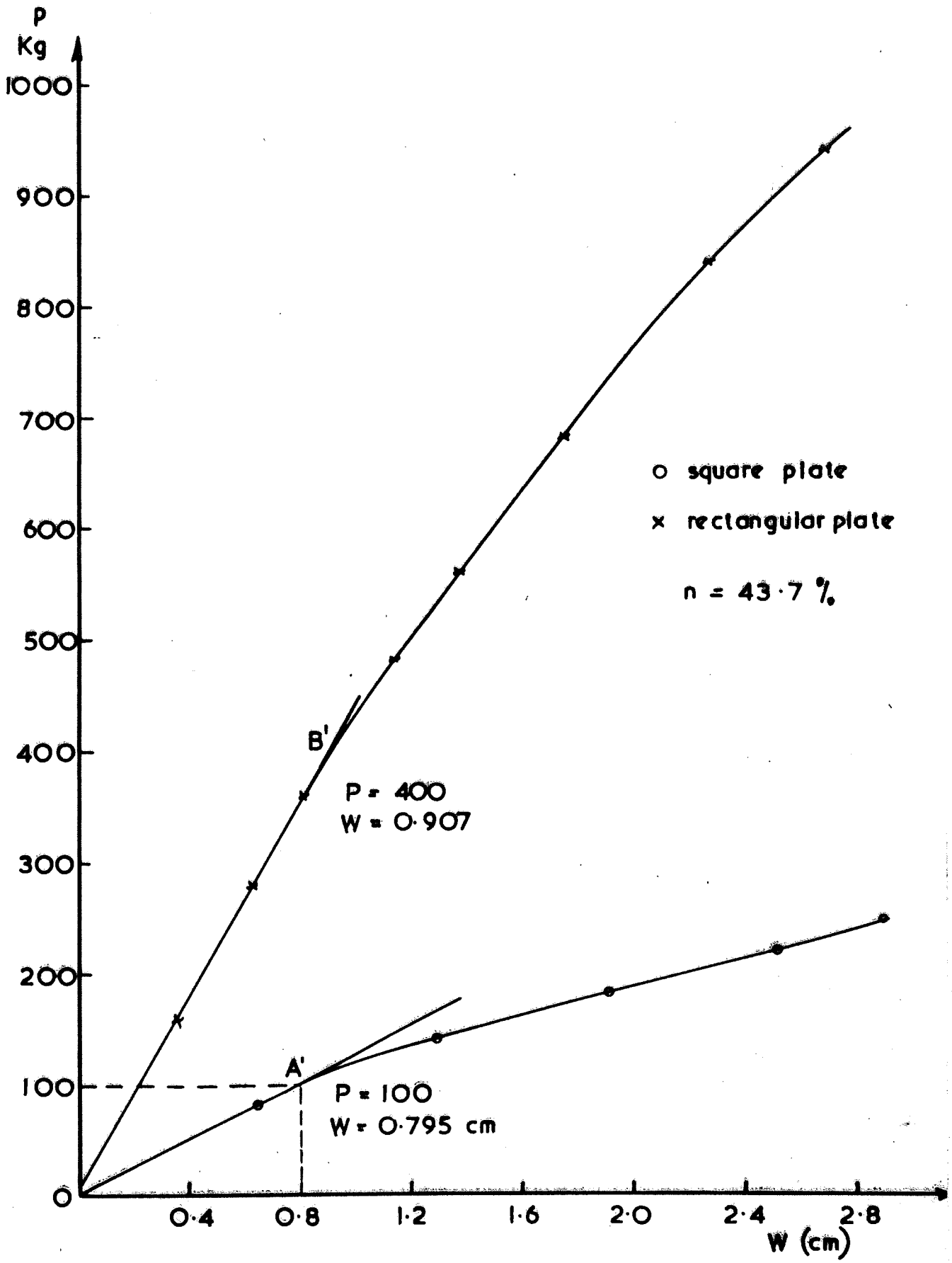

Fig. 7.2 Plate loading test - second set of tests two dimensional

It is assumed that the supporting soil medium is an isotropic homogeneous, linear elastic continuum of semi infinite extend. The settlement of a rigid plate resting on such a medium is given by (see Zeevaert, 1974) :

$$w = \alpha_e B q_a \frac{1-\nu^2}{E_s} \tag{7.9}$$

where q_a is applied load per unit area of the plate, B is the width of the plate and α_e is a constant depending on the ratio of the sides of the plate.

The settlement of the rigid plate in the plane strain problem can be approximated by the settlement of a rectangular rigid plate where the ratio L/B (L is the length of the plate) is large. For example, the deflection of a rigid plate with L/B = 25, is given by (7.9) with $\alpha_e = 2.65$.

$$w = 2.65 B q_a \frac{1-\nu^2}{E} \tag{7.10}$$

By using the values of P and w given by (7.5) through (7.8) we obtain values for $\frac{E}{1-\nu^2}$ as follows :

	Square plate	Rectangular plate
first test	20.2	35.8
second test	20.8	36.5

Values of $\frac{E}{1-\nu^2}$ in Kg/cm^2

The average values of $\frac{E}{1-\nu^2}$ are then

$$\frac{E}{1-\nu^2} = 20.5 \quad Kg/cm^2 \tag{7.11}$$

from the square plate loading test (16cm x 16cm), and

$$\frac{E}{1-\nu^2} = 36.1 \quad Kg/cm^2 \tag{7.12}$$

from the rectangular plate loading test (32cm x 16cm).

From (7.11) and (7.12) it can be seen that the $\frac{E}{1-\nu^2}$ values obtained from the results of square and rectangular plate loading tests are not unique. The two dimensional theoretical analyses are therefore carried out (section 7.3) with K (equation 7.2) and c (equation 2.28) values obtained using both values of $\frac{E}{1-\nu^2}$ given by (7.11) and (7.12).

7.2.2 Three dimensional plate loading tests

The results of three dimensional tests on box section beam resting on medium loose and medium dense deposits and subjected to a central concentrated load (see chapter 6) showed a uniform settlement of the beam along its length. These tests are considered as plate loading tests. The results obtained from these tests are used to obtain a value of $\frac{E}{1-\nu^2}$ for the sand in

the three dimensional tests. The load displacement curve for these tests are shown in Figure (7.3). These tests were performed on deposits of sand with porosities n = 40.2% and n = 44.1%. These porosities correspond to aperture settings 1 and 3 of the hopper (see chapter 5) respectively. At the limit of proportionality of load displacement curves (points C and D in Figure 7.3) we have

$$P = 600 \text{ Kg} \qquad w = 1.11\text{cm} \qquad (7.13)$$

for the test on medium loose deposit (n = 44.1%), and

$$P = 1200 \text{ Kg} \qquad w = 0.43\text{cm} \qquad (7.14)$$

for medium dense deposit (n = 40.2%).

As in the two dimensional plate loading tests, it is assumed that the sand behaves like an isotropic-homogeneous elastic medium. By substituting (7.13) and (7.14) in the expression for the displacement of a rigid stamp resting on an isotropic homogeneous elastic medium (equation 7.9 with $\alpha_e = 2.15$ for L/B = 9) we obtain

$$\frac{E}{1-\nu^2} = 42.8 \quad \text{Kg/cm}^2 \qquad (7.15)$$

for medium dense deposit (n = 40.2%), and

$$\frac{E}{1-\nu^2} = 8.3 \quad \text{Kg/cm}^2 \qquad (7.16)$$

for medium loose deposit (n = 44.1%).

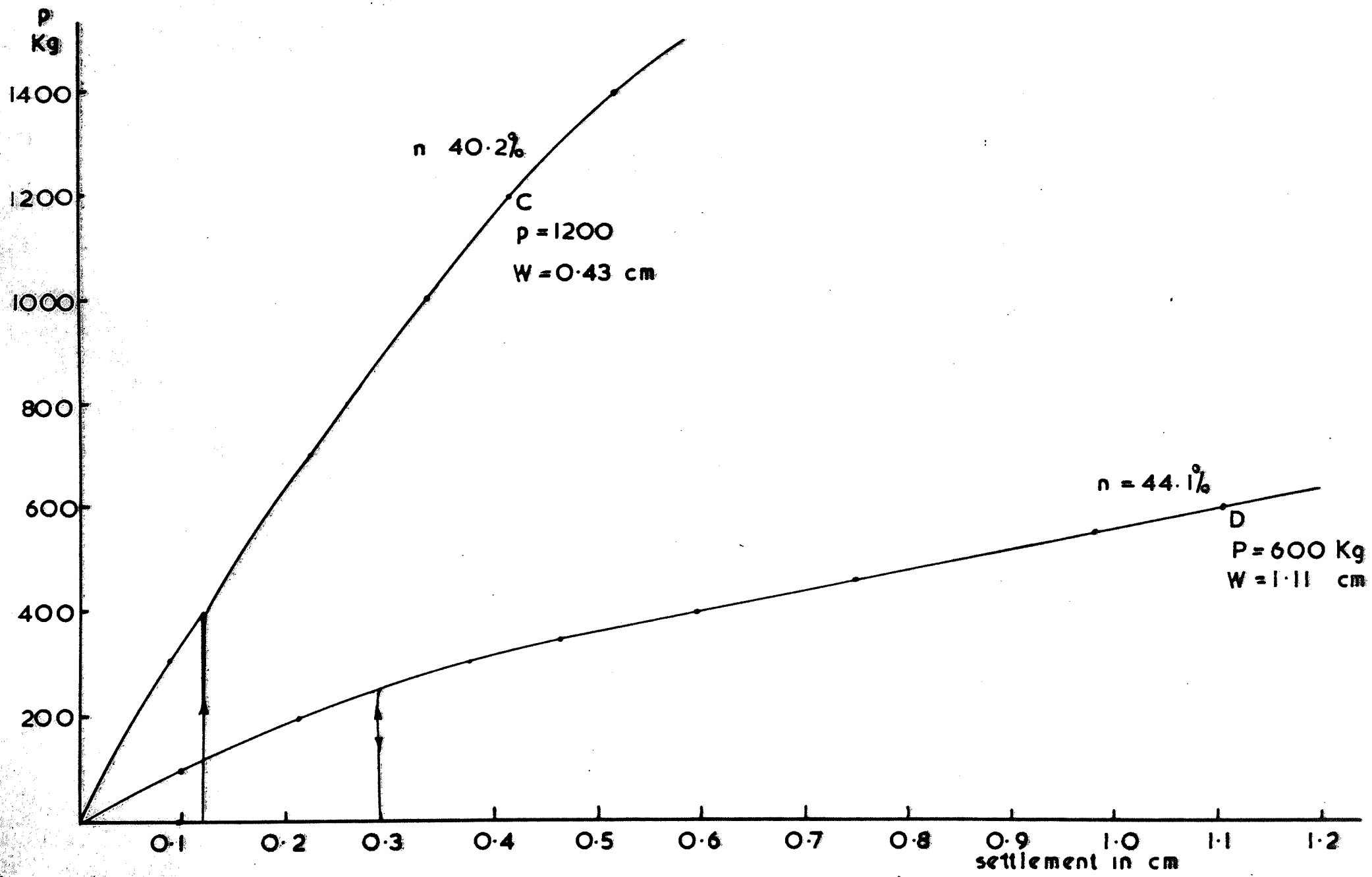

Fig. 7.3 Load settlement curve for box section beam three dimensional

7.3 Theoretical Analysis

In the previous section, from the results of the plate loading tests, values were obtained for the term $\frac{E}{1-\nu^2}$. These values are used to carry out theoretical analyses assuming that the granular subgrade behaves like (i) Winkler medium, (ii) an isotropic homogeneous elastic medium. The two dimensional analysis of the beams are carried out for both $\frac{E}{1-\nu^2}$ values obtained from the square and rectangular plate loading tests. The values of K for the flat and channel beams are obtained by substituting (7.11) and (7.12) in (7.2) and using the corresponding values of I and b (half width of the beam) from Table (5.1). These values are given in Table (7.1) :

	Square plate loading test	Rectangular plate loading test
Flat	3.60	7.65
Channel	1.01	2.14

Table (7.1) Values of K in Kg/cm^2
Two dimensional analyses

The corresponding K values for the three dimensional analyses are obtained by making use of equation 2.62 and the terms $\frac{E}{1-\nu^2}$ given by (7.15) and (7.16). These values for the flat and channel beam resting on medium loose and medium dense sand are given in Table (7.2).

	M D		M L	
	FL	CH	FL	CH
K Kg/cm^2 equation 2.62	32.7	23.8	5.5	4.0

Table (7.2) Values of K in Kg/cm^2

Three dimensional analysis

In the analysis of beams resting on an homogeneous elastic medium, the characteristic of the beam-medium was defined as (see equations 2.28 and 2.29)

$$c = \left[(1-\nu^2)\ \frac{E_b I}{Eb}\right]^{1/3} \qquad (7.17)$$

in the two dimensional analysis, and

$$c = \left[C(1-\nu^2)\ \frac{E_b I}{Eb}\right]^{1/3} \qquad (7.18)$$

in the three dimensional analysis.

By making use of equations (7.17) and (7.18) and the $\frac{E}{1-\nu^2}$ values obtained from plate loading tests, the c values for the two and three dimensional analyses are evaluated and given in Tables (7.3) and (7.4). In (7.18) it is assumed that C = 1 (i.e. the distribution of contact stress across the beam is uniform).

	Square PLT	Rectangular PLT
FL	30.6	25.4
CH	113.3	93.8

Table (7.3) c values for two dimensional analysis

	MD	ML
FL	24.00	41.4
CH	88.7	153.1

Table (7.4) c values for three dimensional analysis

In Table (7.4), MD and ML refer to medium dense and medium loose deposits respectively.

With the knowledge of K and c values given in Tables (7.1) to (7.4), it is now possible to carry out theoretical analyses of the flat and channel beams resting on both Winkler and elastic media. For both types of media the contact forces and bending moment distributions are obtained by assuming that the beams have finite and infinite length. The analyses of the finite and infinite beams resting on an isotropic homogeneous elastic medium, and subjected to a single concentrated load, are given in chapters 2

and 3. For the case of two loadings (flat beam subjected to two loads each acting at a distance L/6 from its centre), the solutions for the finite and infinite beams are obtained by superposition of the solutions for each loading.

The expressions for the contact force and bending moment distribution of an infinite beam resting on Winkler's media and subjected to a concentrated load (Figure 7.4a) are as follows (Hetenyi 1946) :

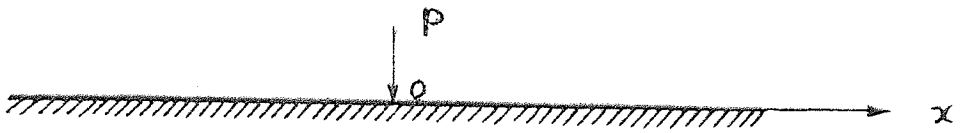

Fig. 7.4a

$$Q = \frac{P\lambda}{2} e^{-\lambda x} (\cos\lambda x + \sin\lambda x) \qquad (7.19a)$$

$$M = \frac{P}{4\lambda} e^{-\lambda x} (\cos\lambda x - \sin\lambda x) \qquad (7.19b)$$

In (7.19a) and (7.19b) λ is given by

$$\lambda = \sqrt[4]{\frac{K}{4EI}} \qquad (7.20)$$

By making use of K values given in Table (7.1) the λ values for two dimensional analyses are evaluated and given in Table (7.5).

	Square PLT	Rectangular PLT
FL	0.0211	0.0255
CH	0.0056	0.0068

Table (7.5) values of λ for the two dimensional analysis

For the three dimensional analyses the values of λ are obtained by using equation (7.20) and the values of K given in Table (7.2).

	MD	ML
FL	0.0366	0.023
CH	0.0125	0.008

Table (7.6) values of λ for three dimensional analyses

The expressions for bending moment and contact force distribution of a finite beam resting on a Winkler medium and subjected to a concentrated load P at its centre (Fig. 7.4b) are (Hetenyi, 1946) :

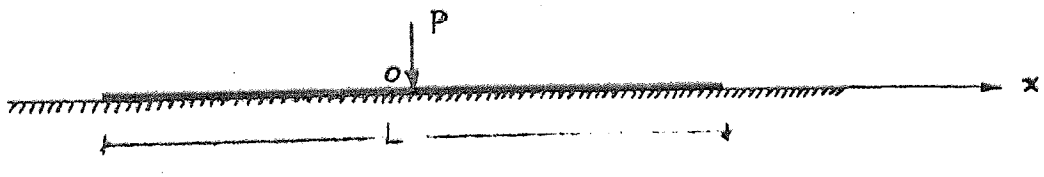

Fig. 7.4b

$$M = \frac{P}{4\lambda} \frac{1}{\mathrm{Sinh}\lambda\ell + \sin\lambda\ell} \{\mathrm{Sinh}\lambda x[\sin\lambda x - \sin\lambda(\ell-x)] -$$

$$- \mathrm{Cosh}\lambda x[\cos\lambda x + \cos\lambda(\ell-x)] +$$

$$+ \sin\lambda x[\mathrm{Sinh}\lambda x - \mathrm{Sinh}\lambda(\ell-x)] + \qquad (7.21)$$

$$+ \cos\lambda x[\mathrm{Cosh}\lambda x + \cosh\lambda(\ell-x)]\}$$

and

$$Q = \frac{P}{2} \frac{1}{\mathrm{Sinh}\lambda\ell + \sin\lambda\ell} \{\mathrm{Cosh}\lambda x[\sin\lambda x - \sin\lambda(\ell-x)] + \qquad (7.22)$$

$$+ \cos\lambda x[\mathrm{Sinh}\lambda x - \mathrm{Sinh}\lambda(\ell-x)]\}$$

The expressions similar to (7.21) and (7.22) for the case of two concentrated loading each acting at a distance L/6 from the centre of the beam as shown in Fig. 7.4c are

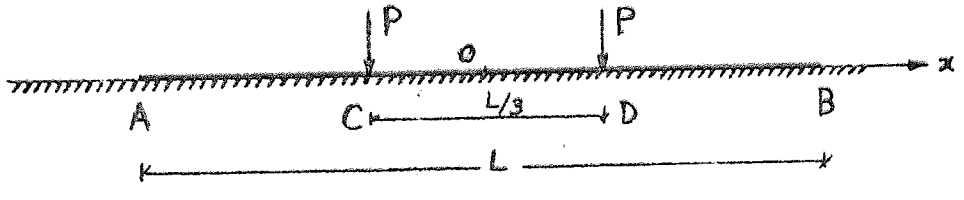

Fig. 7.4c

$$M_{A-c} = \frac{P}{2\lambda} \frac{1}{\text{Sinh}\lambda\ell + \sin\lambda\ell} \{2\text{Sinh}\lambda x \quad \sin\lambda x[\text{Cosh}\lambda(L/3)\cos\lambda(2L/3) +$$

$$+ \text{Cosh}\lambda(2L/3)\cos\lambda(L/3)] + (\text{Cosh}\lambda x \sin\lambda x - \text{Sinh}\lambda x \cos\lambda x)$$

$$[\text{Cosh}\lambda(L/3)\sin\lambda(2L/3) - \text{Sinh}\lambda(L/3)\cos\lambda(2L/3) + \tag{7.23}$$

$$+ \text{Cosh}\lambda(2L/3)\sin\lambda(L/3) - \text{Sinh}\lambda(2L/3)\cos\lambda(L/3)]\}$$

for $L/3 > x > 0$ and

$$M_{c-D} = \left[M_{A-c}\right]_{x>a} - \frac{P}{2\lambda} [\text{Cosh}\lambda(x-L/3)\sin\lambda(x-L/3) +$$

$$+ \text{Sinh}\lambda(x-L/3)\cos\lambda(x-L/3)]$$

for $2L/3 > x > L/3$

$$Q_{A-c} = \frac{1}{\text{Sinh}\lambda\ell + \sin\lambda\ell} \{2\text{Cosh}\lambda x \cos\lambda x[\text{Cosh}\lambda(L/3)\cos\lambda(2L/3)$$

$$+ \text{Cosh}\lambda(2L/3)\cos\lambda(L/3)] + (\text{Cosh}\lambda x \sin\lambda x + \text{Sinh}\lambda x \cos\lambda x)$$

$$[\text{Cosh}\lambda(L/3)\sin\lambda(2L/3) - \text{Sinh}\lambda(L/3)\cos\lambda(2L/3) + \tag{7.24}$$

$$+ \text{Cosh}\lambda(2L/3)\sin\lambda(L/3) - \text{Sinh}\lambda(2L/3)\cos\lambda(L/3)]\}$$

for $L/3 > x > 0$ and

$$Q_{B-c} = \left[Q_{A-B}\right]_{x>L/3} + P\lambda[\text{Cosh}\lambda(x-L/3)\sin\lambda(x-L/3) -$$

$$- \text{Sinh}\lambda(x-L/3)\cos\lambda(x-L/3)] \tag{7.25}$$

for $2L/3 > x > L/3$

Equations (7.19), and (7.21) through (7.25) are used to obtain the distribution of the bending moments and contact forces for both infinite and finite beam analyses of beam on Winkler medium.

The theoretical resuls for the bending moments and contact force distribution of the flat and channel beam assuming the Winkler and elastic behaviour of the subgrade based on both actual dimensions of the beams and infinite beam analyses are shown in Figs.7.5 to 7.10. The results for the infinite and finite beams are referred to as W_i and W_f (for the Winkler medium), E_i and E_f (for the elastic medium). In figs. 7.5 to 7.10 the experimental results are shown in dash lines. It was not possible to show all theoretical results as the graphs would have been too congested. Therefore the maximum values of contact force and bending moments for different theoretical analyses (W_i, W_f, E_i, E_f) together with the experimental results are given in Tables (7.7a-c), for the three dimensional analyses, and Tables (7.8a-c) for the two dimensional analyses. As far as maximum bending moments and contact forces are concerned, from these tables it is possible to make comparisons between the results obtained from experiments and those of theoretical approaches. Figure 7.11 shows the values of K obtained from the results of square, rectangular (for the two dimensional analyses), and box section beam (for the three dimensional analyses). The K values obtained from the experiments (ratio between contact force and deflection) are also shown in this figure.

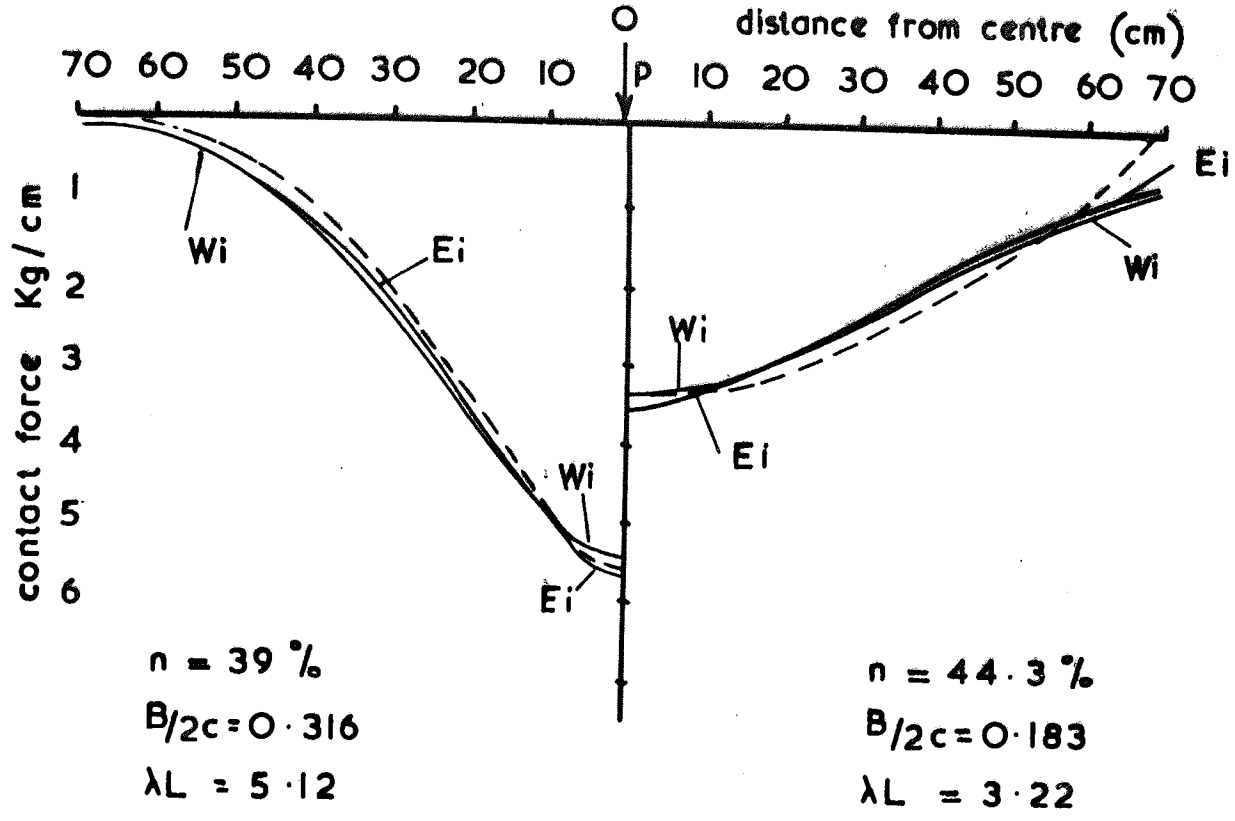

a. Contact force distribution

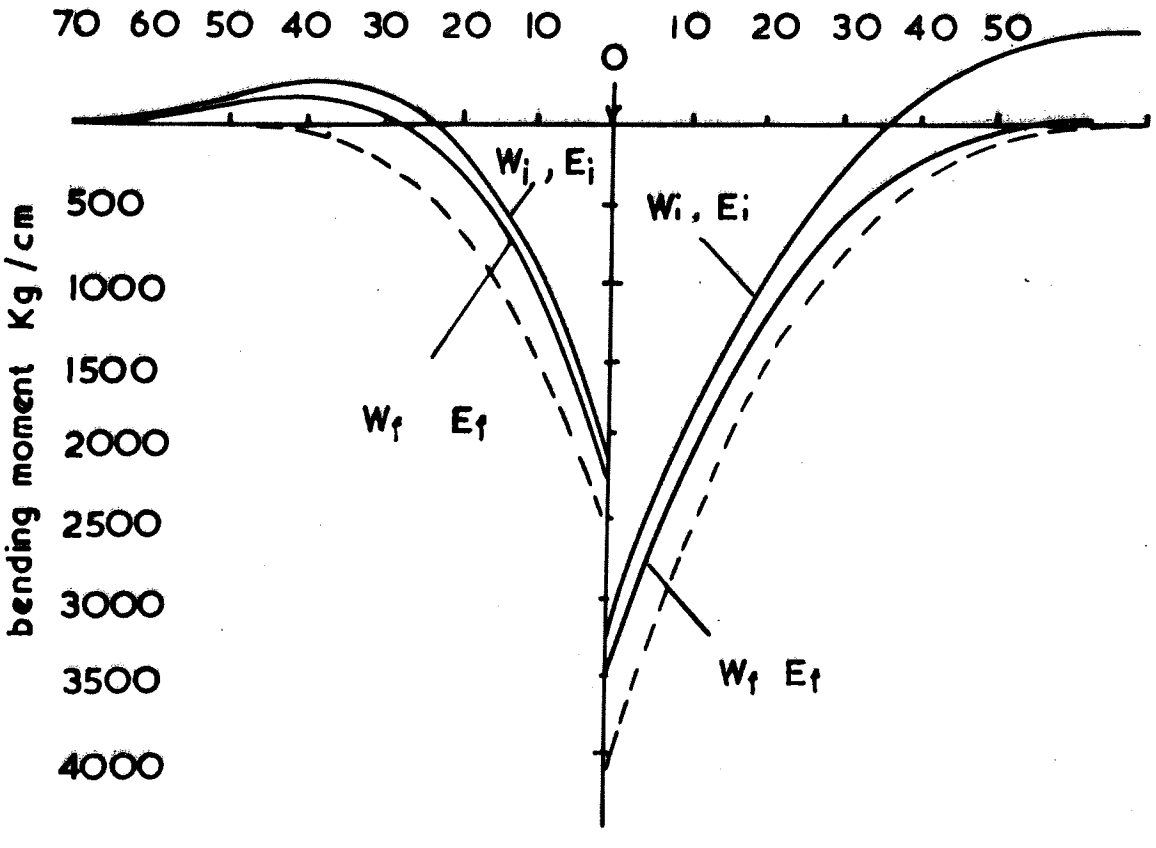

b. Bending moment distributions

Fig. 7.5 Flat beam - Single load

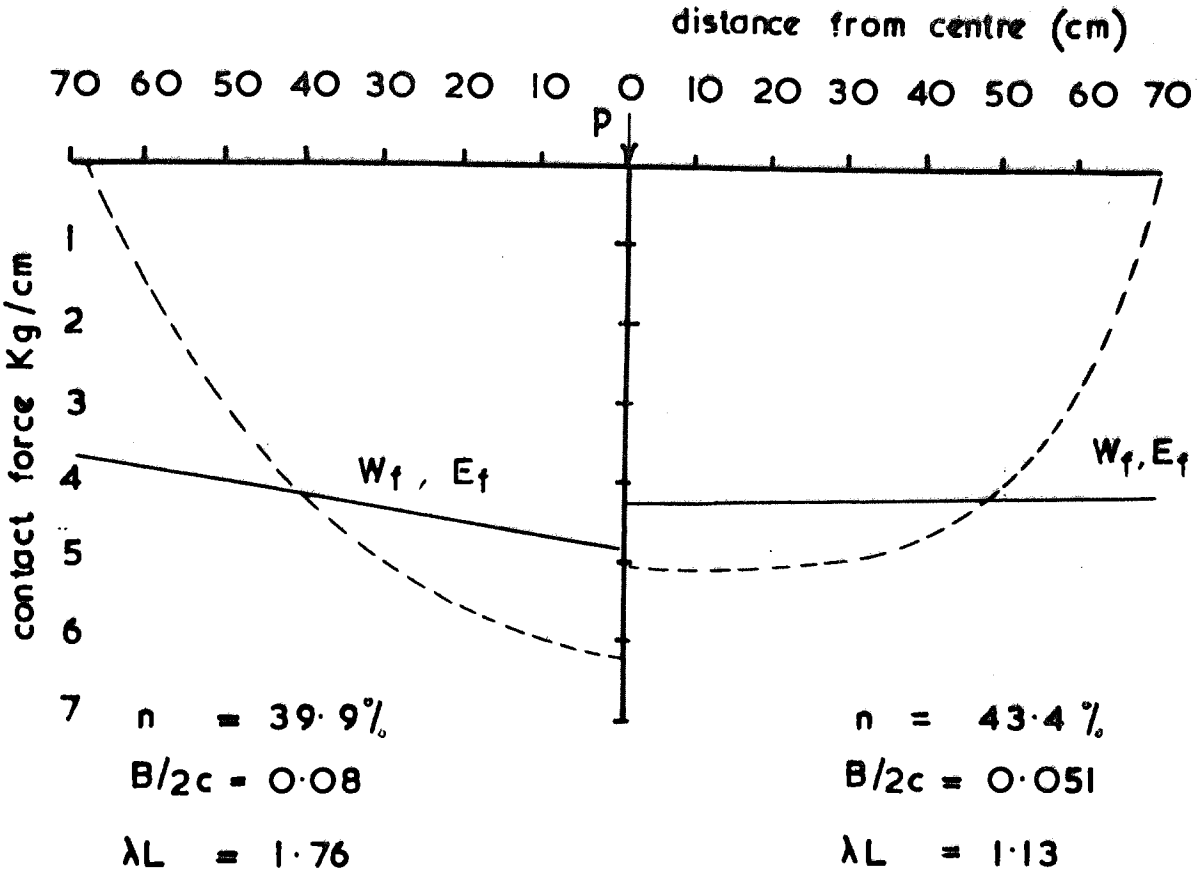

a. Contact force distribution

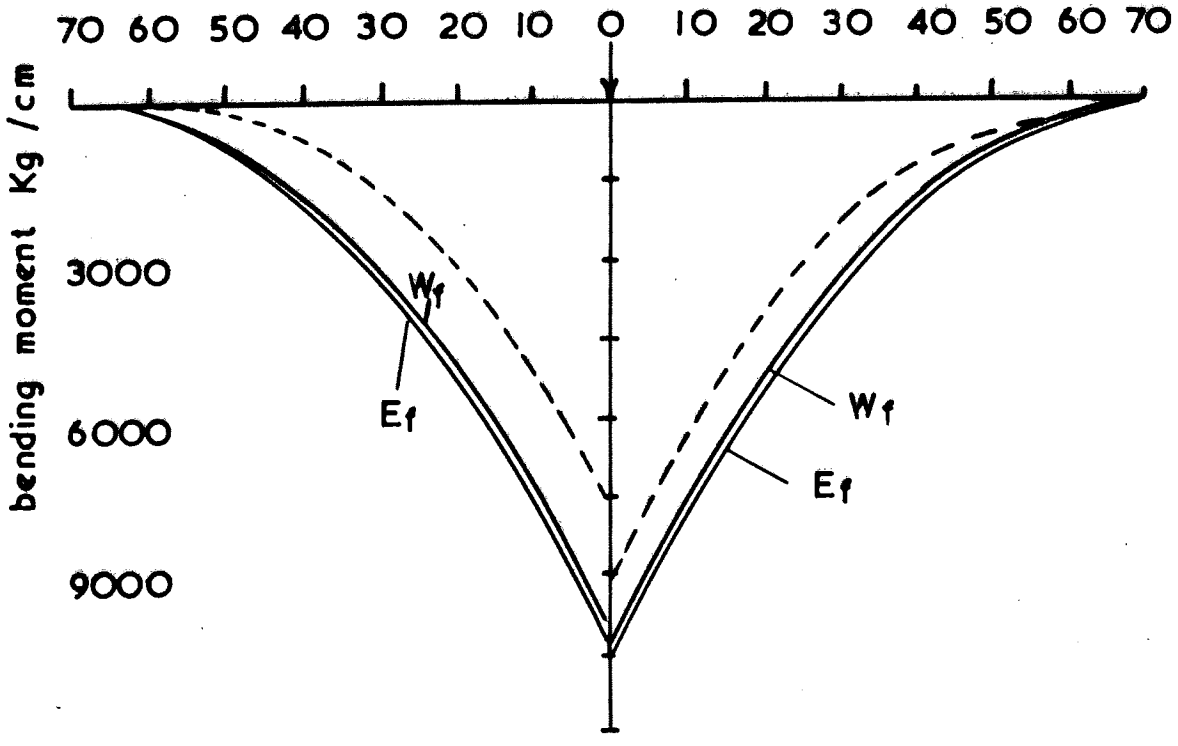

Fig . 7.6 Channel beam - Single load .

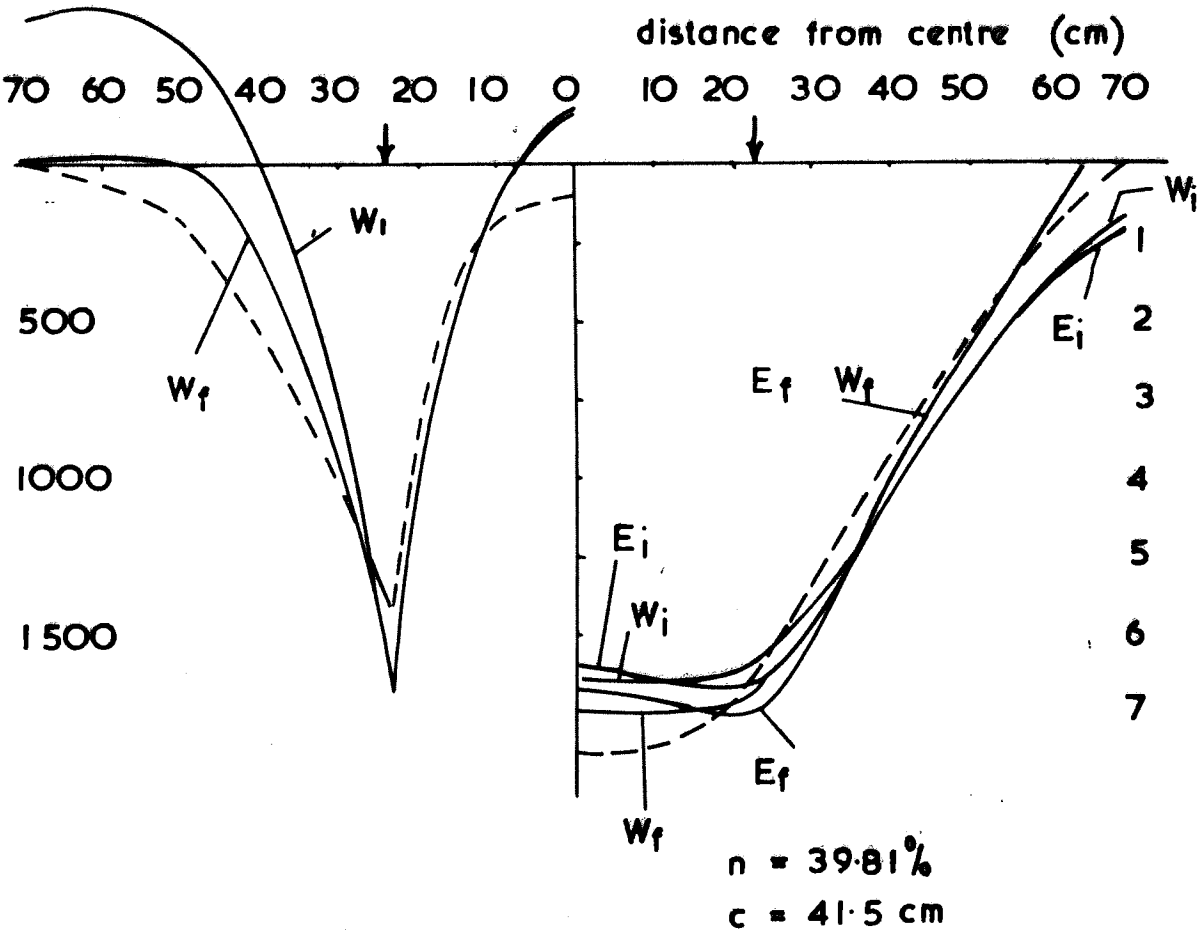

Fig. 7. 7. Flat beam - two loads
three dimensional
P = 300

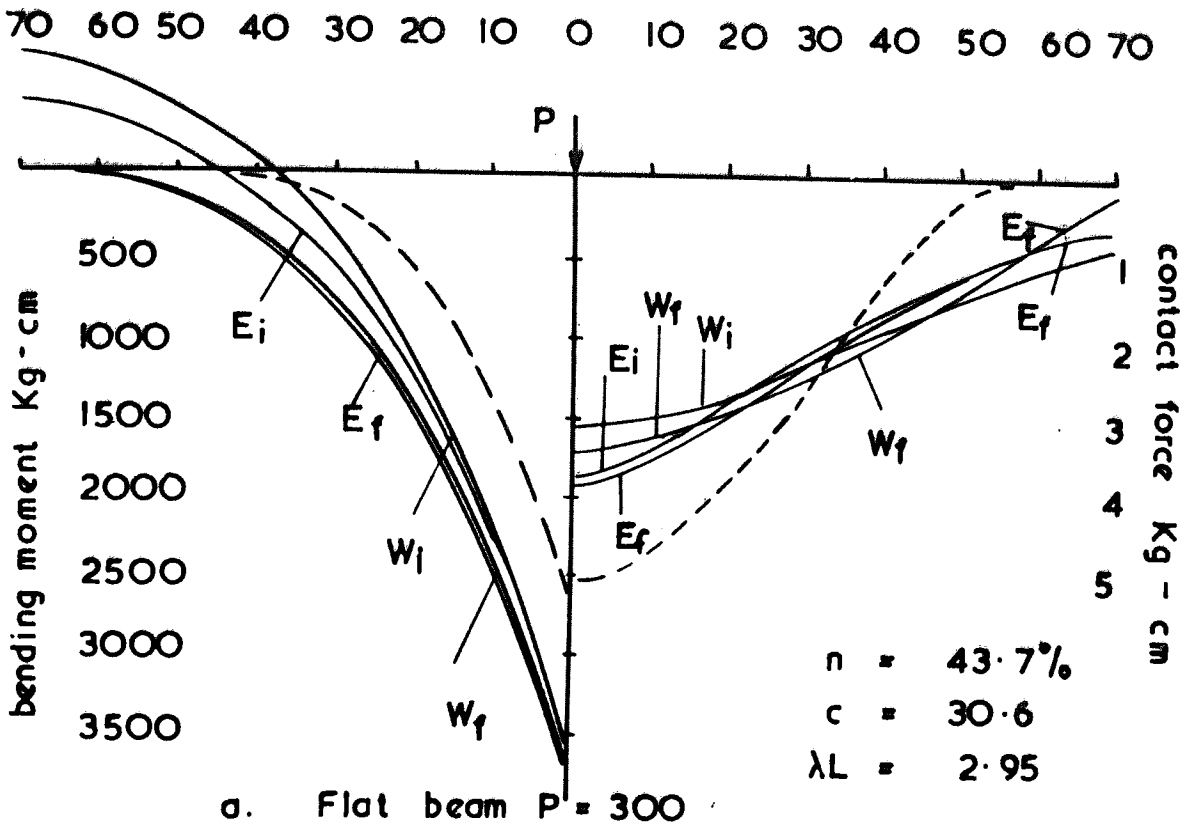

a. Flat beam P = 300

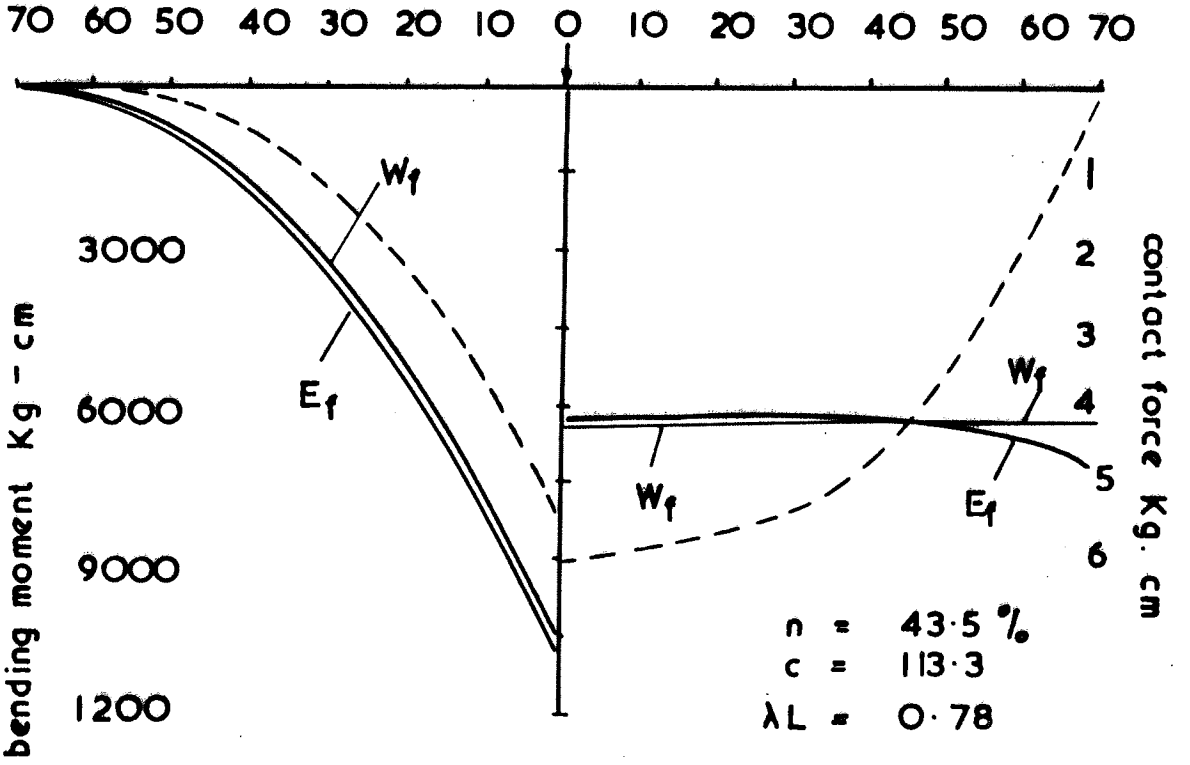

b. Channel beam P = 600

Fig. 7.8 Two dimensional test

$\frac{E}{1-\nu^2}$ from the results of square plate loading test

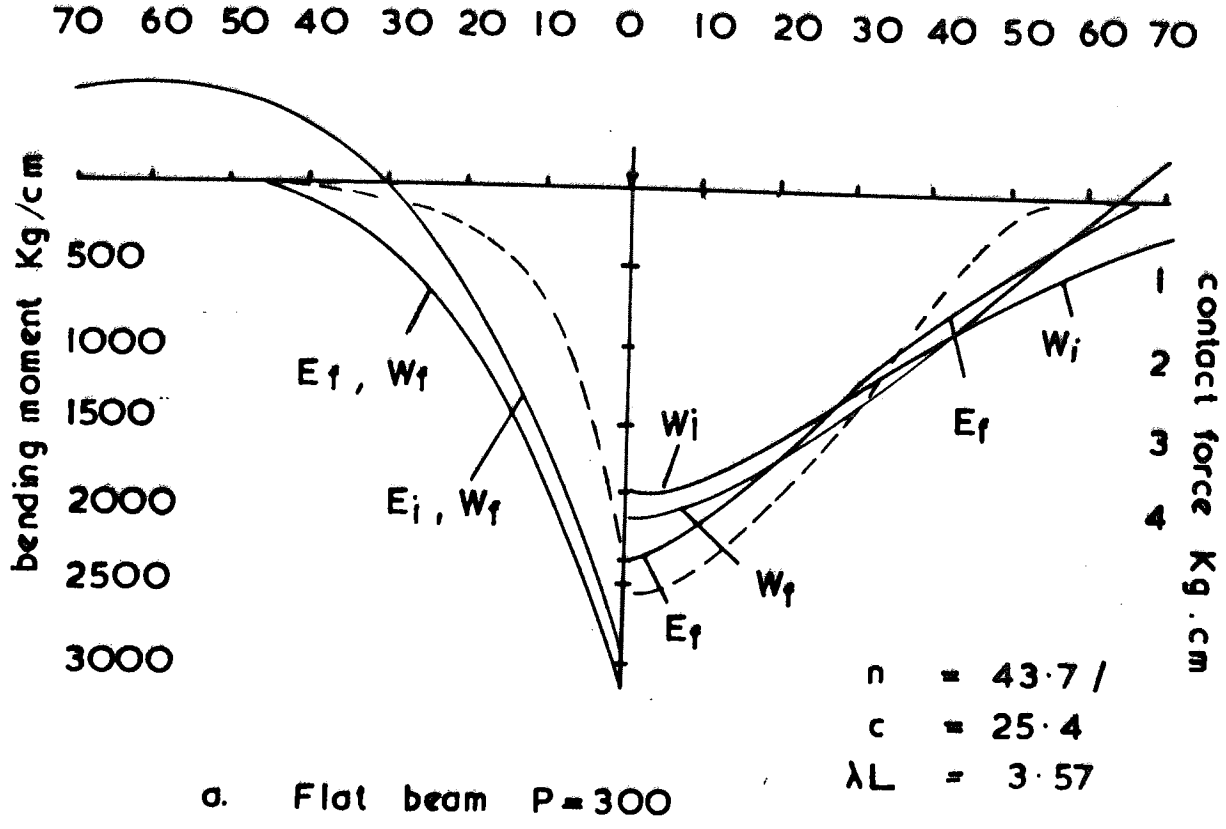

a. Flat beam P=300

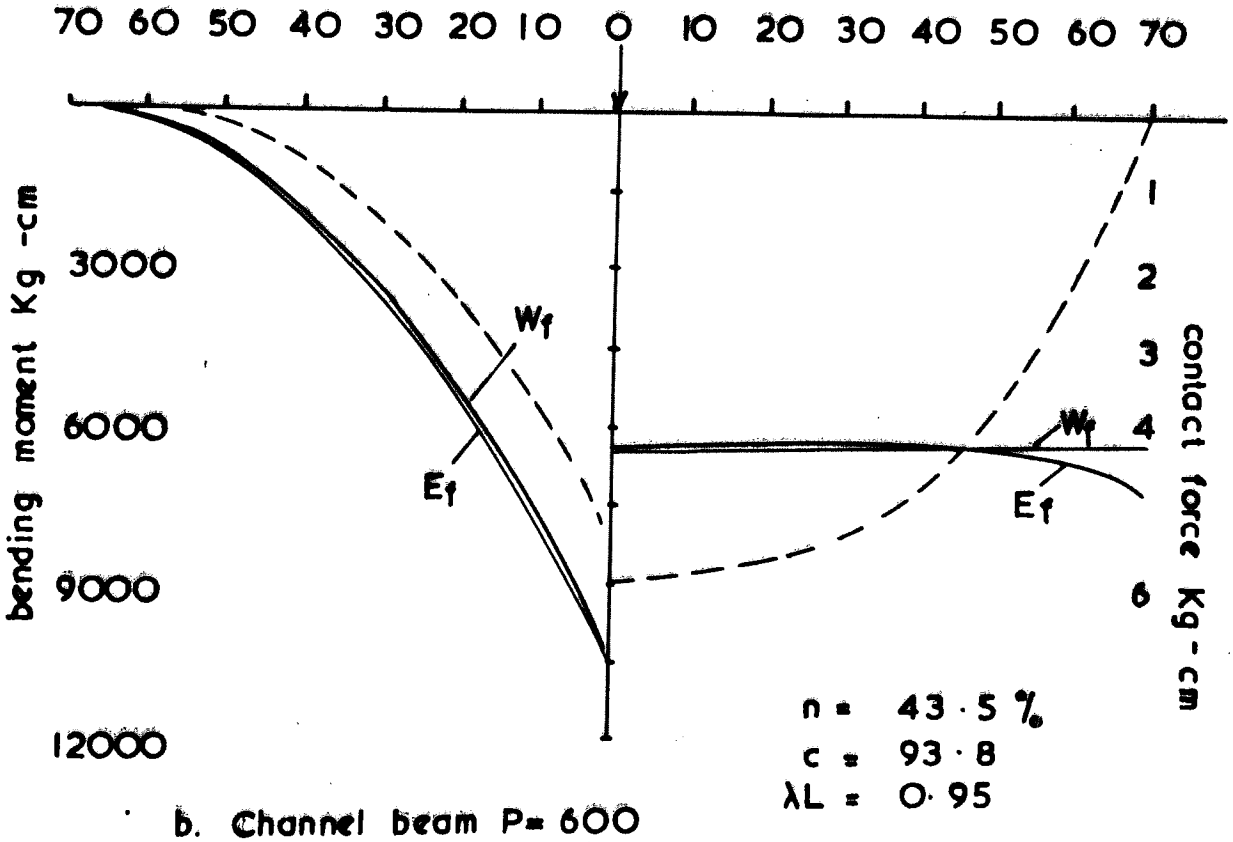

b. Channel beam P= 600

Fig. 7.9 Two dimensional tests

$\frac{E}{1-\nu^2}$ from the results of rectangular plate loading test

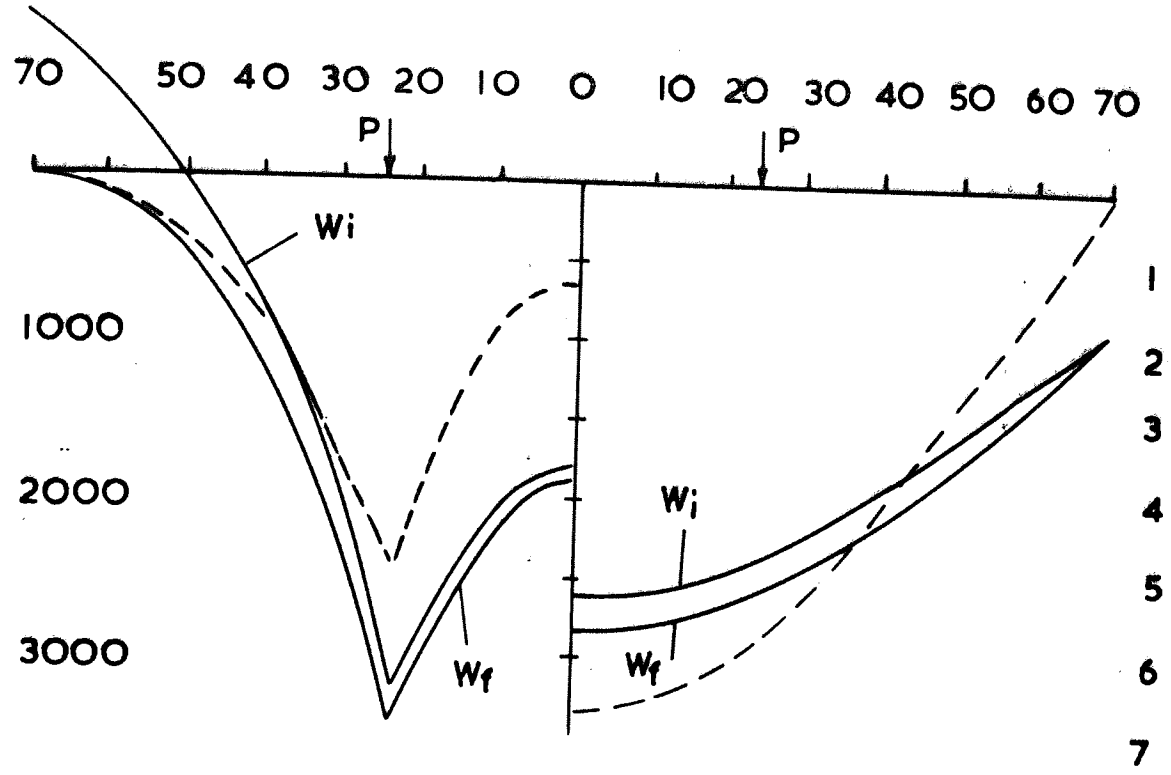

a. $\frac{E}{1-\nu^2}$ values from square P.L.T

n = 43·9 %
c = 41·5 cm

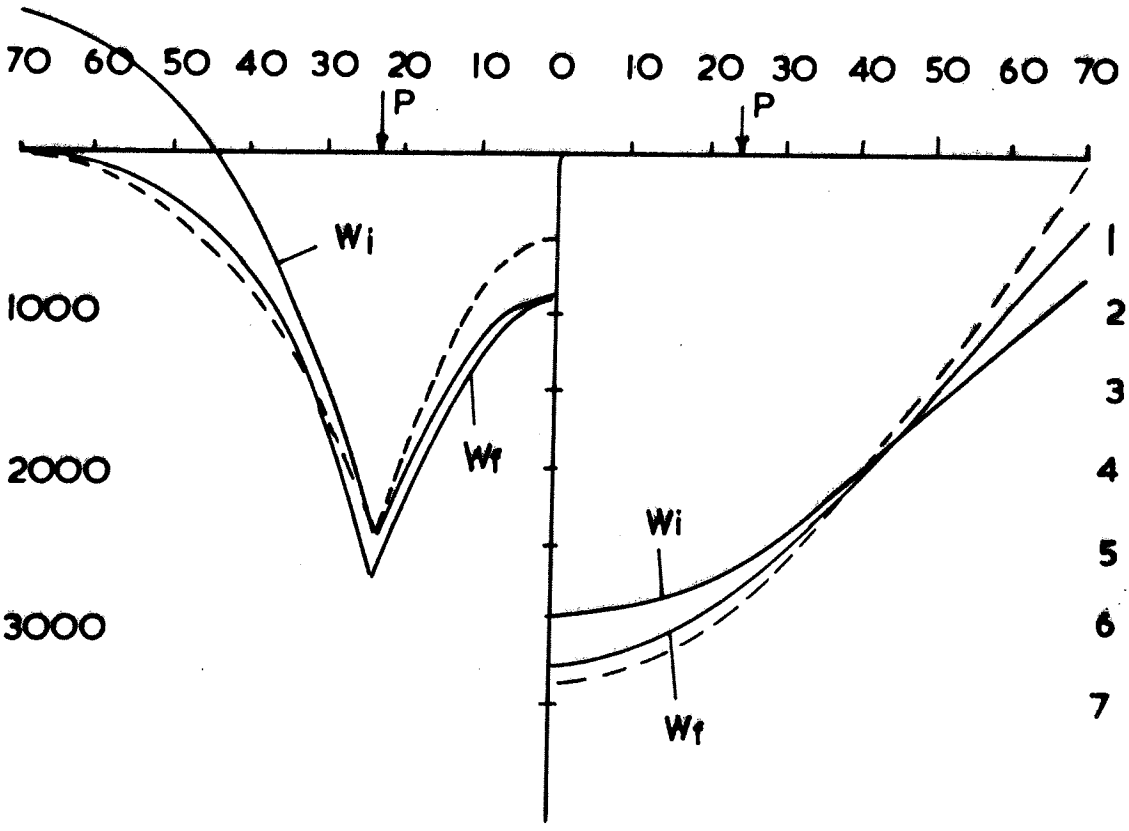

b. $\frac{E}{1-\nu^2}$ values from rectangular P.L.T

Fig. 7.10 Flat beam - two loads -- two dimensional

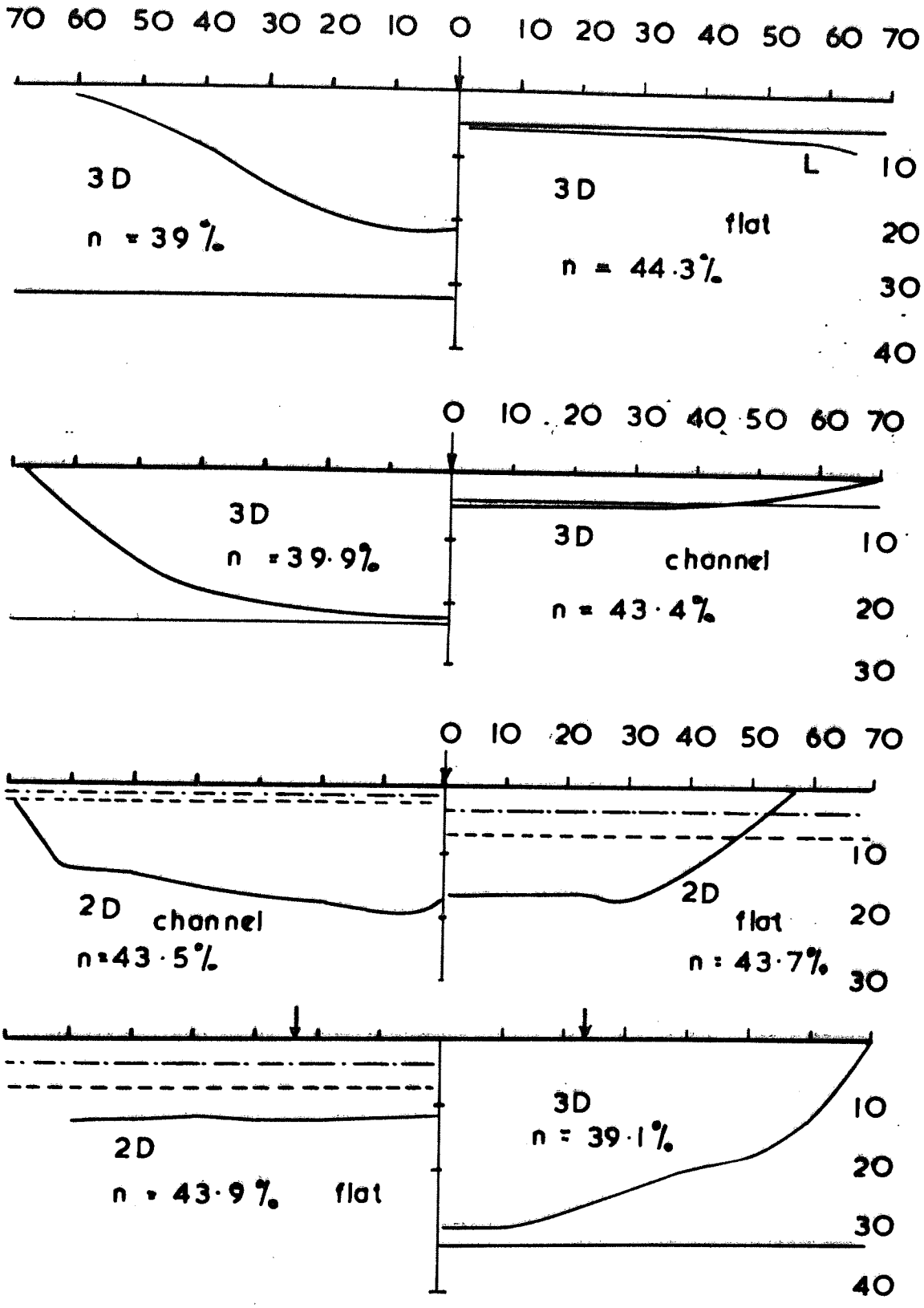

Fig. 7.11 K values from experiment and plate loading tests

2D - two dimensional tests

3D - three " "

3D ——— K from box section beam

2D —·—·— " square plate

2D - - - - - " rectangular plate

(a)

	Ex	W_i	W_f	E_i	E_f
FL	3.46* 5.57+	3.45 5.49	3.76 5.71	3.55 5.71	3.79 5.88
CH	5.12 6.18	2.40 3.75	4.37 2.76	2.39 3.72	4.37 4.79

(b)

	Ex	W_i	W_f	E_i	E_f
FL	4120 2550	3260 2049	3553 2062	3338 2125	3627 2172
CH	9220 7750	18750 12000	10410 9990	19378 12565	10704 10285

(c)

	Ex	W_i	W_f	E_i	E_f
Q	7.50	6.54	6.95	6.74	7.03
M	1400	1630	1717	1858	1281

Tables (7.7a-c) Three dimensional analyses

(a) Maximum contact force - single load (Kg/cm)

(b) Maximum bending moment " " (Kg-cm)

(c) Maximum contact force and bending moment for the flat beam subjected to two loads

* Medium loose

\+ Medium dense

(a)

	Ex	W_i	W_f	E_i	E_f
FL	5.10	3.16* 3.82+	3.45 4.16	3.77 4.55	3.92 4.70
CH	6.02	1.68 2.04	4.31 4.33	2.04 2.46	4.18 4.24

(b)

	Ex	W_i	W_f	E_i	E_f
FL	2700	3554 2941	3864 3171	3533 2934	3678 3078
CH	8400	26785 22058	10476 10452	26165 21662	10683 10635

(c)

	Ex	W_i	W_f	E_i	E_f
FL	6.70	5.24 5.86	5.67 5.71	5.25 5.76	5.41 6.04
CH	2425	3184 2443	3354 2657	3417 2671	3368 2796

Tables (7.8a-c) Two dimensional analyses

(a) Maximum contact force - single load (Kg/cm)

(b) Maximum bending moment " " (Kg-cm)

(c) Maximum contact force and bending moment for the flate beam subjected to two loads

* $\frac{E}{1-\nu^2}$ from square PLT

\+ $\frac{E}{1-\nu^2}$ from rectangular PLT

7.4 Conclusions

The values of modulus of subgrade reaction as calculated from the experimental results are not generally constant. The variation of K along the beams (Figure 7.11) depends on; flexural rigidity of beams (EI), porosity of the subgrade, intensity of loading, and the condition of testing (three or two dimensional).

The results of the plate loading tests show that it is not possible to obtain a unique value of $\frac{E}{1-\nu^2}$ by assuming that the granular material behaves like an elastic medium. The two dimensional plate loading tests suggest that $\frac{E}{1-\nu^2}$ values increase as the width of the plate increases. The comparisons between the theoretical and experimental results are therefore valid for the values of beam-subgrade characteristics (λ for the Winkler, and c for the elastic half space analysis) which are based on the results of a particular plate loading test, i.e. square and rectangular plate loading test (for the two dimensional analyses) and box section beam (for the three dimensional analyses).

The results of the three dimensional tests with flat beam on medium loose sand ($\lambda L = 3.22$) and medium dense sand ($\lambda L = 5.12$) show that the Winkler solution for the infinite beam gives a close approximation of contact force distribution on medium dense and medium loose deposits. Similar conclusion was made by Barden (1963)

for dense sand (for $\lambda L > 2.75$). It may therefore be concluded that a value of non-dimensional parameter λL for a particular porosity of sand can be found such that beyond this value the Winkler solution is valid. Further experimental evidence is required to obtain the variation of this limit with porosity of sand. With the values of λL for the flat and channel beam it is not possible to define a limit for λL beyond which the Winkler solution is applicable. It can only be mentioned that this limit is between $3.22 > \lambda L > 1.13$ for medium loose sand, and between $5.12 > \lambda L > 1.76$ for medium dense sand.

In contrast to the three dimensional tests, the correlation between the experimental results and Winkler solution is less in the two dimensional test on the flat beam. From the results of the two dimensional test on the flat beam (Figures 7.8 and 7.9) good agreement was observed between the experimental and theoretical results, if the beam is assumed to have finite length and resting on elastic medium with the characteristic length c obtained from the results of the rectangular plate loading test.

The results of the two and three dimensional tests on the channel beam show that the Winkler and elastic half space analyses underestimate the maximum contact force and overestimate the maximum bending moments. This is due to the fact that the contact forces at the ends of the beams resting on a granular material tend to be small regardless of the flexural rigidity of the beam.

The results obtained for the flat beam subjected to two loads show that the finite beam analysis on elastic medium gives a close approximation of maximum contact force for both two and three dimensional (see Tables 7.7c, 7.8c and Figures 7.7, 7.10). The analytical results for this beam indicate that the maximum value of contact forces are under the loads (for three dimensional analyses) and at the centre of the beam (for two dimensional analyses). The experimental results for both cases showed the maximum value of contact force at the centre of the beam. The understanding of the behaviour of the beams resting on a granular material and subjected to different types of loading demands performance of several more experiments to investigate the effect of factors like porosity of granular material, stiffness of the beam, type of loading on contact force and bending moment distribution for both two and three dimensional conditions. The sand deposition apparatus for the three dimensional test described in chapter 5 was shown to be capable of forming large uniform beds of sand over almost the complete range of porosity. The apparatus for sand deposition in the two dimensional test was not capable of producing deposits of sand denser than medium dense. The hopper can be modified to produce a range of porosities. This can be achieved by using a technique similar to three dimensional deposition.

For further work the steel model beams with moments of inertia of I = 2.0, 50, 100, 500, 1000, and 1500 are suggested. With the information obtained from the tests with these beams

it would be possible to find for different porosities of sand a limit for λL beyond which the Winkler solution is valid.

The results of tests on these beams would also give information regarding the behaviour of beams with the flexural rigidities intermediate between the flat and channel, channel and box section beams.

Finally, the surface strain is practically zero for the beams which have a uniform displacement due to applied load. It is not therefore possible to obtain contact force distribution for these beams by using strain gauges. The contact force under such beams can only be measured by installing pressure cells (Barden, 1962a), at the beam subgrade interface.

APPENDIX ONE

NUMERICAL RESULTS

A.1.1

Three dimensional analysis

A.1.1a

Numerical values of the integrals $J_{nP}(X)$ for the analysis of infinite beam subjected to a concentrated load or a concentrated couple

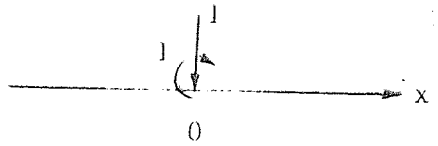

x/B	B/2c	$J_0(x)/\pi$	$J_1(x)/\pi$	$J_2(x)/\pi$	$J_3(x)/\pi$	$J_4(x)/\pi$	$J_5(x)/\pi$
0	0.01	0.02450	0.000	0.14414	0.5000	0.87433	0.0
	0.05	0.07758	"	0.20828	"	0.61601	"
	0.1	0.12422	"	0.24024	"	0.54163	"
	0.2	0.19378	"	0.27280	"	0.48600	"
	1	0.46904	"	0.33726	"	0.41453	"
1	0.01	0.02447	0.00278	0.13432	0.48253	0.87324	0.10881
	0.05	0.07662	0.01843	0.16135	0.43878	0.60537	0.19443
	0.1	0.12005	0.03877	0.15097	0.39368	0.51390	0.23682
	0.2	0.17678	0.07421	0.11053	0.31615	0.41704	0.26550
	1	0.22418	0.12293	-0.05424	0.01573	0.07618	0.10793
2	0.01	0.02439	0.00537	0.12484	0.46510	0.87006	0.20734
	0.05	0.07404	0.03247	0.12046	0.37943	0.57931	0.31784
	0.1	0.10977	0.06175	0.08215	0.29644	0.45536	0.33522
	0.2	0.14120	0.09727	0.01442	0.17213	0.30130	0.29368
	1	0.07836	0.03423	-0.02530	-0.01844	-0.00819	0.00444
3	0.01	0.02426	0.00778	0.11571	0.44774	0.86498	0.29970
	0.05	0.07025	0.04272	0.08536	0.32325	0.54327	0.39702
	0.1	0.09614	0.07284	0.03151	0.21239	0.38411	0.36836
	0.2	0.10268	0.09218	-0.03337	0.07414	0.19185	0.24680
	1	0.04160	0.00935	-0.00448	-0.00410	-0.00406	-0.00321
4	0.01	0.02408	0.01001	0.10693	0.43051	0.85811	0.38587
	0.05	0.06560	0.04972	0.05568	0.27100	0.50084	0.44751
	0.1	0.08120	0.07538	-0.00378	0.14294	0.31061	0.36161
	0.2	0.06908	0.07470	-0.05013	0.01537	0.10653	0.17898
	1	0.02838	0.00491	-0.00111	-0.0044	-0.00049	-0.00065
5	0.01	0.02386	0.01206	0.09849	0.41342	0.84959	0.46544
	0.05	0.06039	0.05402	0.03101	0.22320	0.45456	0.47414
	0.1	0.06637	0.07216	-0.02663	0.08787	0.24113	0.33038
	0.2	0.04328	0.05438	-0.04949	-0.01469	0.04804	0.11522
	1	0.02038	0.00322	-0.00067	-0.00014	-0.00002	-0.00002
6	0.01	0.02360	0.01395	0.09039	0.39653	0.83945	0.53804
	0.05	0.05487	0.05608	0.01088	0.18014	0.40668	0.48067
	0.1	0.05257	0.06537	-0.03981	0.04598	0.17925	0.28680
	0.2	0.02529	0.03616	-0.04086	-0.02613	0.01249	0.06515
	1	0.01510	0.00215	-0.00042	-0.00010	-0.00002	0.00000

x/B	B/2c	$J_o(x)/\pi$	$J_1(x)/\pi$	$J_2(x)/\pi$	$J_3(x)/\pi$	$J_4(x)/\pi$	$J_5(x)/\pi$
7	0.01	0.02330	0.01568	0.08263	0.37984	0.828111	0.60349
	0.05	0.04924	0.05633	-0.00518	0.14187	0.35887	0.47373
	0.1	0.04035	0.05671	-0.04579	0.01555	0.12670	0.23853
	0.2	0.01380	0.02198	-0.03000	-0.02694	-0.00613	0.03046
	1	0.01152	0.00148	-0.00025	-0.00006	-0.00002	-0.00000
8	0.01	0.02297	0.01725	0.07520	0.36340	0.81545	0.66183
	0.05	0.04365	0.05516	-0.01765	0.10832	0.31229	0.45620
	0.1	0.02993	0.04740	-0.04666	-0.00535	0.08385	0.19040
	0.2	0.00714	0.01204	-0.01997	-0.02270	-0.01367	0.00913
	1	0.00900	0.00108	-0.00016	-0.00004	-0.00001	-0.00000
9	0.01	0.2261	0.01869	0.06809	0.34723	0.80169	0.71332
	0.05	0.3824	0.05290	-0.02700	0.07934	0.26792	0.42987
	0.1	0.02137	0.03827	-0.04416	-0.01861	0.05025	-0.14622
	0.2	0.00369	0.00572	-0.01204	-0.01686	-0.01477	-0.00227
	1	0.00712	0.00082	-0.00010	-0.00002	-0.00001	-0.000001
10	0.01	0.02222	0.01998	0.06131	0.33134	0.78696	0.758410
	0.05	0.03310	0.04985	-0.03361	0.05465	0.22647	0.398622
	0.1	0.01458	0.02987	-0.03961	-0.02601	0.02500	0.107461
	0.2	0.00220	0.00209	-0.00644	-0.01130	-0.01271	0.00714
	1	0.00566	0.00065	-0.00007	-0.00001	-0.00001	-0.00000

$$\frac{B}{2c} = \left[\frac{EB^4}{16C(1-\nu^2)E_b I}\right]^{1/3}$$

B = Width of the beam

A.1.1b

Finite beam subjected to a concentrated load

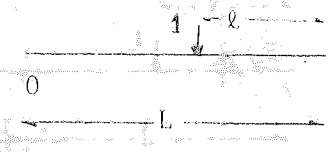

L/B = 5

ℓ = 0

x/B	B/2c	EIW(x)/c^3	M(x)/c	V(x)	cQ(x)
0	0.01	-0.19257	0.0000	0.0000	-8.32392
	0.05	-0.14622	"	"	-1.67841
	0.1	-0.12697	"	"	-0.85311
	0.2	-0.09798	"	"	-0.41232
	1	0.02355	"	"	-0.00293
1	0.01	-0.19256	-0.00310	-0.28528	-8.22420
	0.05	-0.14544	-0.01616	-0.28033	-1.54740
	0.1	-0.12245	-0.03185	-0.27512	-0.75173
	0.2	-0.07473	-0.05540	-0.23990	-0.33999
	1	0.11258	-0.00279	-0.00135	0.00031
2	0.01	0.12395	-0.00951	-0.32764	3.92237
	0.05	0.12955	-0.04804	-0.31526	0.82889
	0.1	0.13070	-0.09421	-0.31054	0.39133
	0.2	0.13311	-0.16621	-0.28324	0.12491
	1	0.15960	-0.00773	-0.00631	-0.00843
3	0.01	0.44046	-0.01449	-0.12759	16.08213
	0.05	0.40501	-0.07140	-0.11711	3.13766
	0.1	0.38757	-0.14094	-0.11854	1.53581
	0.2	0.36728	-0.25614	-0.13114	0.65565
	1	0.25038	-0.05837	-0.05861	-0.05076
4	0.01	0.75698	-0.01294	0.31480	28.22354
	0.05	0.68117	-0.06360	0.31595	5.54865
	0.1	0.64987	-0.12595	0.30877	2.75559
	0.2	0.64102	-0.23886	0.26431	1.35871
	1	0.64068	-0.2425	0.16176	0.01534
5	0.01	1.07350	0.0000	1.0000	40.54464
	0.05	0.95791	"	"	8.23508
	0.1	0.91684	"	"	4.26934
	0.2	0.95006	"	"	2.45829
	1	2.12803	"	"	1.88091

W = Deflection

M = Bending Moment

V = Shearing Force

Q = Contact Force

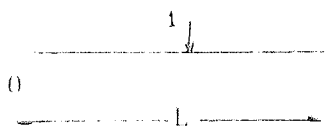

L/B = 5

ℓ = B

x/B	B/2c	EIW(x)/c³	M(x)/c	V(x)	cQ(x)
0	0.01	-0.50907	0.00000	0.00000	-20.54075
	0.05	-0.42025	"	"	- 4.14469
	0.1	-0.37422	"	"	- 2.08171
	0.2	-0.27299	"	"	- 0.92226
	1	0.07671	"	"	- 0.00514
1	0.01	-0.00266	-0.00107	-0.09118	-0.93464
	0.05	0.01889	-0.00568	-0.08801	-0.12978
	0.1	0.02601	-0.01124	-0.08642	-0.05635
	0.2	0.03534	-0.02097	-0.07987	-0.02273
	1	0.03823	-0.00401	-0.00451	-0.00392
2	0.01	0.18725	-0.00255	-0.03659	6.35452
	0.05	0.18406	-0.01280	-0.02918	1.29522
	0.1	0.17944	-0.02498	-0.02783	0.63894
	0.2	0.17206	-0.04610	-0.02424	0.30158
	1	0.07444	-0.02548	-0.01876	-0.00821
3	0.01	0.37716	-0.00151	0.16346	13.65047
	0.05	0.34935	-0.00683	o.16960	2.68246
	0.1	0.33379	-0.01317	0.16905	1.33327
	0.2	0.31551	-0.02263	0.16488	0.65079
	1	0.22038	-0.05453	0.01656	0.07815
4	0.01	0.56707	0.00503	0.50890	20.93419
	0.05	0.51468	0.02584	0.50950	4.13029
	0.1	0.48849	0.05209	0.50755	2.05833
	0.2	0.46119	0.10555	0.50199	1.03852
	1	0.46351	0.34757	0.51299	0.42579
5	0.01	0.75697	0.0000	0.0000	28.32739
	0.05	0.67989	"	"	5.74377
	0.1	0.64216	"	"	2.93340
	0.2	0.59844	"	"	1.51448
	1	0.16188	"	"	0.02121

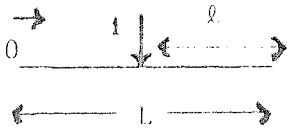

L/B = 5

ℓ = 2.5B

x/B	B/2c	EIW(x)/c^3	M(x)/c	V(x)	cQ(x)
0	0.01	0.28219	0.0000	0.0000	9.95695
	0.05	0.26556	0.0000	0.0000	2.03392
	0.1	0.10323	0.0000	0.0000	0.99148
	0.2	0.19416	0.0000	0.0000	0.40539
	1	0.01181	0.0000	0.0000	-0.04588
1	0.01	0.28220	0.00049	0.09998	9.96602
	0.05	0.26582	0.00251	0.10061	1.98724
	0.1	0.10977	0.00498	0.09948	0.99056
	0.2	0.20918	0.00834	0.08444	0.44555
	1	0.05692	-0.01397	0.02329	-0.01170
2	0.01	0.28220	0.00447	0.29996	9.96809
	0.05	0.26630	0.02258	0.30057	1.98532
	0.1	0.12005	0.04473	0.29838	0.99331
	0.2	0.23700	0.07944	0.27669	0.52436
	1	0.21622	-0.05184	0.01321	0.08004
2.5	0.01	0.28220	0.01247	0.50000	9.96754
	0.05	0.26654	0.06262	"	2.03663
	0.1	0.12422	0.12454	"	1.02509
	0.2	0.25100	0.23397	"	0.57384
	1	0.46235	0.33760	"	0.41266

L/B = 10

ℓ = 0

x/B	B/2c	EIW(x)/c^3	M(x)/c	V(x)	cQ(x)
0	0.01	-0.25031	0.00000	0.00000	-9.91756
	0.05	-0.22185	"	"	-2.01453
	0.1	-0.15857	"	"	-0.81506
	0.2	-0.01176	"	"	-0.07840
	1	0.02252	"	"	-0.00051
1	0.01	-0.09341	-0.0062	-0.27793	-4.01862
	0.05	-0.08064	-0.03135	-0.27224	-0.76067
	0.1	-0.05711	-0.05072	-0.22290	-0.33809
	0.2	-0.00476	-0.02524	-0.06497	-0.09061
	1	0.03711	-0.00060	-0.00014	-0.00003
2	0.01	0.06350	-0.01908	-0.01908	-0.31923
	0.05	0.06192	-0.09342	-0.31071	0.37491
	0.1	0.05318	-0.15594	-0.27506	0.08510
	0.2	0.02148	-0.10836	-0.14418	-0.09851
	1	0.06171	-0.00159	-0.00040	-0.00012
3	0.01	0.22044	-0.02893	-0.11937	0.02443
	0.05	0.20817	-0.14045	-0.12102	1.53167
	0.1	0.18824	-0.24610	-0.14049	0.61573
	0.2	0.12027	-0.24711	-0.18487	0.03987
	1	0.11367	-0.00367	-0.00052	-0.00021
4	0.01	0.37743	-0.02582	0.32180	14.01914
	0.05	0.35984	-0.12591	0.30736	2.76827
	0.1	0.36135	-0.23474	0.24741	1.36860
	0.2	0.35539	-0.33803	0.03175	0.60246
	1	0.25076	-0.05837	-0.05861	-0.05076
5	0.1	0.53446	0.0000	1.00000	19.93967
	0.05	0.51616	"	"	4.23626
	0.1	0.56907	"	"	2.51078
	0.2	0.82536	"	"	2.07098
	1	2.12822	"	"	1.88089

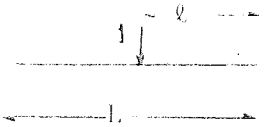

L/B = 10

ℓ = B

x/B	B/2c	$EIW(x)/c^3$	M(x)/c	V(x)	cQ(x)
0	0.01	-0.17189	0.0000	0.0000	-6.93312
	0.05	-0.15231	"	"	-1.42123
	0.1	-0.11313	"	"	-0.60022
	0.2	-0.02101	"	"	-0.09470
	1	0.00621	"	"	-0.00019
2	0.01	-0.04635	-0.00416	-0.18234	-2.21503
	0.05	-0.03830	-0.02124	-0.17925	-0.41223
	0.1	-0.02477	-0.03549	-0.15055	-0.18362
	0.2	0.00223	-0.02449	-0.05643	-0.05494
	1	0.01048	-0.00024	-0.00006	-0.00001
4	0.01	0.07919	-0.01207	-0.17539	2.57299
	0.05	0.07661	-0.05921	-0.16988	0.50503
	0.1	0.06966	-0.10067	-0.15059	0.18901
	0.2	0.04301	-0.08352	-0.08480	-0.00553
	1	0.01878	-0.00063	-0.00013	-0.00002
6	0.01	0.20474	-0.01595	0.02450	7.41937
	0.05	0.19383	-0.07694	0.02354	1.43569
	0.1	0.17979	-0.13462	0.01047	0.63455
	0.2	0.13728	-0.13929	-0.03119	0.17278
	1	0.03880	-0.00442	-0.00414	-0.00412
8	0.01	0.33033	-0.00785	0.41744	12.21553
	0.05	0.31393	-0.03705	0.40797	2.41856
	0.1	0.31010	-0.06523	0.37502	1.21224
	0.2	0.31450	-0.07033	0.26186	0.60944
	1	0.22056	-0.05453	0.01656	0.07815
9	0.01	0.39312	0.00313	-0.31479	14.57167
	0.05	0.37466	0.01668	-0.32393	2.94978
	0.1	0.38000	0.03626	-0.34892	1.55256
	0.2	0.42336	0.09127	-0.43301	0.92030
	1	0.46364	0.34757	-0.48701	0.42579
10	0.01	0.45592	0.0000	0.0000	16.95251
	0.05	0.43536	"	"	3.55870
	0.1	0.44958	"	"	1.97357
	0.2	0.52633	"	"	1.29502
	1	0.16197	"	"	0.02120

L/B = 10

ℓ =2B

x/B	B/2c	EIW(x)/c^3	M(x)/c	V(x)	cQ(x)
0	0.01	-0.09345	0.0000	0.0000	-3.94852
	0.05	-0.08274	"	"	-0.82831
	0.1	-0.06744	"	"	-0.38633
	0.2	-0.02931	"	"	-0.11382
	1	0.00771	"	"	-0.00031
2	0.01	0.00071	-0.00212	-0.08675	-0.41139
	0.05	0.00415	-0.01114	-0.08629	-0.06379
	0.1	0.00823	-0.02029	-0.07828	-0.02872
	0.2	0.01233	-0.02412	-0.04831	-0.01797
4	0.01	0.09487	-0.00505	-0.03154	3.17929
	0.05	0.09150	-0.02500	-0.02902	0.63555
	0.1	0.08722	-0.04541	-0.02585	0.29416
	0.2	0.07000	-0.05863	-0.02353	0.09184
	1	0.02603	-0.00105	-0.00043	-0.00048
6	0.01	0.18905	-0.00296	0.16839	6.81426
	0.05	0.17977	-0.01344	0.16818	1.34013
	0.1	0.17283	-0.02294	0.16220	0.65436
	0.2	0.16192	-0.02831	0.12845	0.31032
	1	0.07411	-0.02518	-0.01845	-0.00822
8	0.01	0.28323	0.01011	-0.48693	10.41184
	0.05	0.26839	0.05184	-0.49137	2.06718
	0.1	0.26072	0.10479	-0.49698	1.05008
	0.2	0.26126	0.20553	-0.50470	0.59350
	1	0.46364	0.34757	-0.48701	0.42579
10	0.01	0.37740	0.0000	0.0000	13.96556
	0.05	0.35600	"	"	2.89008
	0.1	0.34028	"	"	1.47669
	0.2	0.29465	"	"	0.68785
	1	0.16197	"	"	0.02120

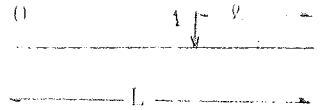

L/B = 10

ℓ = 3B

x/B	B/2c	EIW(x)/c³	M(x)/c	V(x)	cQ(x)
0	0.01	-0.01501	0.0000	0.0000	-0.96370
	0.05	-0.01283	"	"	-0.23339
	0.1	-0.01972	"	"	-0.16531
	0.2	-0.03416	"	"	-0.12929
	1	0.01072	"	"	-0.00053
2	0.01	0.04778	-0.00008	0.00885	1.39232
	0.05	0.04688	-0.00101	0.00696	0.28572
	0.1	0.04277	-0.00461	-0.00385	0.13008
	0.2	0.02823	-0.02195	-0.03494	0.02832
	1	0.02003	-0.00066	-0.00015	-0.00001
4	0.01	0.11057	0.00196	0.11232	3.78554
	0.05	0.10659	0.00930	0.11223	0.76591
	0.1	0.10572	0.01141	0.10193	0.39947
	0.2	0.10366	-0.02430	0.05197	0.20103
	1	0.04110	-0.00447	-0.00410	-0.00406
6	0.01	0.17335	0.01002	0.31224	6.20903
	0.05	0.16582	0.05024	0.31306	1.24267
	0.1	0.16599	0.09137	0.31576	0.66689
	0.2	0.18769	0.10627	0.30688	0.44052
	1	0.22332	-0.05421	0.01573	0.07618
7	0.01	0.20474	0.01755	-0.55151	7.41484
	0.05	0.19480	0.08815	-0.55079	1.47931
	0.1	0.19153	0.16867	-0.53886	0.78184
	0.2	0.21018	0.26698	-0.49784	0.52042
	1	0.46786	0.33728	-0.49999	0.41457
9	0.01	0.26750	0.00206	-0.20741	9.78636
	0.05	0.25087	0.01065	-0.20854	1.95099
	0.1	0.22838	0.01989	-0.19543	0.93059
	0.2	0.17049	0.02467	-0.12944	0.37056
	1	0.07444	-0.02286	0.02039	-0.00734
10	0.01	0.29888	0.0000	0.0000	10.97894
	0.05	0.27857	"	"	2.23637
	0.1	0.24428	"	"	1.03947
	0.2	0.13671	"	"	0.27929
	1	0.02494	"	"	-0.01877

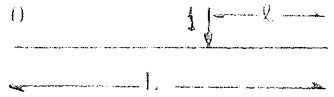

L/B = 10

ℓ = 4B

x/B	B/2c	$EIW(x)/c^3$	M(x)/c	V(x)	cQ(x)
0	0.01	0.06344	0.0000	0.0000	2.02141
	0.05	0.05784	"	"	0.36696
	0.1	0.03255	"	"	0.07463
	0.2	-0.03043	"	"	-0.12683
	1	0.01406	"	"	-0.00088
2	0.01	0.09485	0.00195	0.10445	3.19611
	0.05	0.09003	0.00920	0.10097	0.63736
	0.1	0.07982	0.01225	0.0758	0.29673
	0.2	0.03303	-0.01402	-0.00687	0.09421
	1	0.02824	-0.00110	-0.00046	-0.00046
4	0.01	0.12626	0.00898	0.25617	4.31711
	0.05	0.12177	0.04387	0.25431	0.89500
	0.1	0.12449	0.07185	0.23590	0.50126
	0.2	0.14220	0.03375	0.15694	0.32375
	1	0.07823	-0.02530	-0.01844	-0.00819
6	0.01	0.15766	0.02301	-0.54389	5.60359
	0.05	0.15163	0.11429	-0.54198	1.13819
	0.1	0.15659	0.21106	-0.52943	0.65445
	0.2	0.19873	0.28831	-0.49347	0.51508
	1	0.46887	0.33726	-0.50000	0.41453
8	0.01	0.18903	0.00603	-0.29568	6.80393
	0.05	0.17810	0.03011	-0.29292	1.34943
	0.1	0.16421	0.05253	-0.26291	0.66327
	0.2	0.13921	0.04377	-0.14576	0.31696
	1	0.07807	-0.02527	0.01850	-0.00811
10	0.01	0.22039	0.0000	0.0000	7.99270
	0.05	0.20319	"	"	1.59888
	0.1	0.16202	"	"	0.66488
	0.2	0.04089	"	"	0.03807
	1	0.02547	"	"	-0.00305

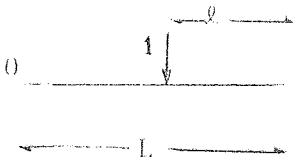

L/B = 10

ℓ = 5B

x/B	B/2c	EIW(x)/c^3	M(x)/c	V(x)	cQ(x)
0	0.01	0.14190	0.0000	0.0000	5.00686
	0.05	0.12971	"	"	0.97655
	0.1	0.0921	"	"	0.34695
	0.2	-0.00955	"	"	-0.08259
	1	0.01887	"	"	-0.00132
1	0.01	0.14192	0.00100	0.10005	5.00167
	0.05	0.13176	0.00488	0.09765	0.97964
	0.1	0.10637	0.00734	0.07552	0.40909
	0.2	0.03991	-0.00223	-0.00177	0.06273
	1	0.02807	-0.00088	-0.00066	-0.00035
2	0.01	0.14194	0.00399	0.20006	4.9999
	0.05	0.13375	0.01956	0.19618	0.99181
	0.1	0.12018	0.03106	0.16384	0.47428
	0.2	0.08959	0.00545	0.04855	0.18915
	1	0.04144	-0.00447	-0.00413	-0.00402
3	0.01	0.14195	0.00899	0.30005	4.99866
	0.05	0.13553	0.04416	0.29612	1.00733
	0.1	0.13268	0.07375	0.26515	0.53806
	0.2	0.13799	0.04346	0.015022	0.31995
	1	0.07823	-0.02530	-0.01844	-0.00819
4	0.01	0.14196	0.01599	0.40003	4.99776
	0.05	0.13687	0.07883	0.39757	1.02054
	0.1	0.14217	0.13792	0.37838	0.59156
	0.2	0.17876	0.13261	0.30397	0.44557
	1	0.22407	-0.05423	0.01574	0.07618
5	0.01	0.14197	0.02499	0.50000	4.99748
	0.05	0.13741	0.12371	0.50000	1.02649
	0.1	0.14605	0.22567	"	0.61754
	0.2	0.19737	0.29241	"	0.51738
	1	0.46887	0.33726	"	0.41453

L/B = 20

ℓ = 0

x/B	B/2c	EIW(x)/c³	M(x)/c	V(x)	cΘ(x)
0	0.01	-0.13283	0.00000	0.00000	-5.02442
	0.05	-0.07628	"	"	-0.66327
	0.1	0.00328	"	"	-0.00446
	0.2	0.00588	"	"	-0.00029
	1.0	-0.01913	"	"	0.00030
4	0.01	-0.04878	-0.01278	-0.27950	-1.97763
	0.05	-0.03436	-0.04313	-0.19364	-0.32423
	0.1	-0.00728	-0.0083	-0.02913	-0.06832
	0.2	0.00924	0.00116	0.00209	0.00207
	1.0	-0.00221	0.00008	-0.00008	-0.00001
8	0.01	0.03061	-0.03829	-0.31779	1.01046
	0.05	0.01523	-0.13794	-0.25759	0.02035
	0.1	-0.01014	-0.06026	-0.10833	-0.12307
	0.2	0.00869	0.00503	-0.00046	-0.01093
	1.0	0.01338	-0.00013	0.00002	-0.00002
12	0.01	0.10983	-0.05733	-0.11954	3.95075
	0.05	0.08687	-0.22722	-0.15450	0.53681
	0.1	0.02952	-0.18393	-0.18975	-0.03343
	0.2	0.00239	-0.03231	-0.06489	-0.07942
	1.0	0.03712	-0.00060	-0.00013	-0.00005
16	0.01	0.19417	-0.05108	0.31738	6.98704
	0.05	0.19361	-0.22623	0.21511	1.37567
	0.1	0.18761	-0.30213	-0.02640	0.57047
	0.2	0.12058	-0.24921	-0.18202	0.03777
	1.0	0.11373	-0.00367	-0.00052	-0.00021
20	0.01	0.27895	0.00000	1.00000	10.09488
	0.05	0.33358	"	"	2.65804
	0.1	0.51825	"	"	2.25975
	0.2	0.82513	"	"	2.06957
	1.0	2.12817	"	"	1.88089

L/B = 20

ℓ = 4B

x/B	B/2c	EIW(x)/c³	M(x)/c	V(x)	cQ(x)
0	0.01	-0.05140	0.00000	0.00000	-2.01757
	0.05	-0.03854	"	"	-0.35381
	0.1	-0.01429	"	"	-0.07976
	0.2	0.00282	"	"	0.00161
	1.0	-0.00021	"	"	-0.00003
4	0.01	-0.00070	-0.00448	-0.08787	-0.18742
	0.05	0.00037	-0.01913	-0.07475	-0.03377
	0.1	0.00084	-0.01871	-0.03973	-0.02360
	0.2	0.00156	-0.00104	-0.00346	-0.00681
	1.0	0.00327	-0.00003	-0.00000	-0.00000
8	0.01	0.04697	-0.01019	-0.03084	1.60718
	0.05	0.04245	-0.04360	-0.02670	0.28092
	0.1	0.02873	-0.05039	-0.02704	0.07156
	0.2	0.00680	-0.02051	-0.02328	-0.01410
	1.0	0.00891	-0.00016	-0.00004	-0.00001
12	0.01	0.09443	-0.00562	0.16830	3.37382
	0.05	0.09092	-0.02231	0.15807	0.65432
	0.1	0.08623	-0.02822	0.11448	0.31164
	0.2	0.07022	-0.05132	0.01616	0.11008
	1.0	0.02832	-0.00111	-0.00044	-0.00049
16	0.01	0.14411	0.02053	0.51070	5.19418
	0.05	0.14152	0.10431	0.50268	1.06498
	0.1	0.15103	0.19940	0.49830	0.62522
	0.2	0.19725	0.28266	0.51675	0.50269
	1.0	0.46890	0.33726	0.50000	0.41453
20	0.01	0.19421	0.00000	0.00000	7.04722
	0.05	0.18384	"	"	1.44511
	0.1	0.15290	"	"	0.62360
	0.2	0.04156	"	"	0.03749
	1.0	0.02548	"	"	-0.00303

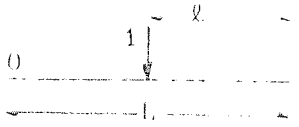

L/B = 20

ℓ = 8B

x/B	B/2c	EIW(x)/c³	M(x)/c	V(x)	cQ(x)
0	0.01	0.03013	0.00000	0.00000	0.99216
	0.05	0.00645	"	"	0.00954
	0.1	-0.02650	"	"	-0.14440
	0.2	-0.00205	"	"	-0.01557
	1.0	0.00323	"	"	-0.00005
4	0.01	0.04745	0.00383	0.10396	1.60437
	0.05	0.03928	0.00837	0.05985	0.28262
	0.1	0.02339	-0.02111	-0.02483	0.07313
	0.2	0.00634	-0.01888	-0.02377	-0.01368
	1.0	0.00892	-0.00016	-0.00004	-0.00001
8	0.01	0.06334	0.01793	0.25635	2.20263
	0.05	0.07018	0.06182	0.22428	0.53530
	0.1	0.08421	0.00785	0.13217	0.33512
	0.2	0.06871	-0.05038	0.01487	0.10706
	1.0	0.02837	-0.00111	-0.00044	-0.00049
12	0.01	0.07966	0.04612	0.45610	2.79272
	0.05	0.09005	0.19994	0.47797	0.70588
	0.1	0.12855	0.25220	0.51234	0.57173
	0.2	0.19412	0.27323	0.50219	0.48975
	1.0	0.46904	0.33726	0.50000	0.41453
16	0.01	0.09572	0.01217	-0.29632	3.39869
	0.05	0.08711	0.04744	-0.24383	0.66028
	0.1	0.07819	0.02634	-0.11300	0.31607
	0.2	0.06695	-0.03903	-0.00345	0.11207
	1.0	0.02835	-0.00111	0.00044	-0.00049
20	0.01	0.11194	0.00000	0.00000	4.01202
	0.05	0.07517	"	"	0.56362
	0.1	0.00022	"	"	-0.04489
	0.2	-0.02763	"	"	-0.10081
	1.0	0.00856	"	"	-0.00033

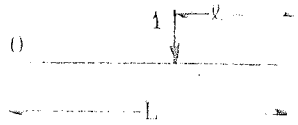

L/B = 20

ℓ = 10B

x/B	B/2c	EIW(x)/c³	M(x)/c	V(x)	cQ(x)
0	0.01	0.07099	0.00000	0.00000	2.50036
	0.05	0.03669	"	"	0.25307
	0.1	-0.02213	"	"	-0.13419
	0.2	-0.01238	"	"	-0.04904
	1.0	0.00539	"	"	-0.00013
2	0.01	0.07133	0.00199	0.10000	2.50106
	0.05	0.04946	0.00573	0.06137	0.35949
	0.1	0.01154	-0.00602	-0.01968	-0.02046
	0.2	0.00167	-0.01181	-0.02600	-0.02046
	1.0	0.00891	-0.00016	-0.00004	-0.00001
4	0.01	0.07157	0.00800	0.40008	2.50123
	0.05	0.06196	0.14366	0.14366	0.46310
	0.1	0.04612	-0.00793	0.01985	0.17258
	0.2	0.02397	-0.03630	-0.03073	0.01408
	1.0	0.01503	0.00024	0.00002	-0.00011
6	0.01	0.07162	0.01800	0.30011	2.49991
	0.05	0.07335	0.06461	0.24628	0.56133
	0.1	0.08160	0.01792	0.11990	0.32959
	0.2	0.06895	-0.04855	0.01267	0.10904
	1.0	0.02837	-0.00111	-0.00044	-0.00049
8	0.01	0.07152	0.03201	0.20006	2.49864
	0.05	0.08209	0.12566	0.36698	0.64130
	0.1	0.11350	0.09653	0.28359	0.48547
	0.2	0.14116	0.01456	0.17109	0.30291
	1.0	0.07835	-0.02530	-0.01844	-0.00819
10	0.01	0.07135	0.05002	0.50000	2.49831
	0.05	0.08571	0.21224	"	0.67834
	0.1	0.12893	0.25201	"	0.57476
	0.2	0.19367	0.27255	"	0.48714
	1.0	0.46904	0.33726	"	0.41453

A.1.1c

Finite beam subjected to a concentrated couple

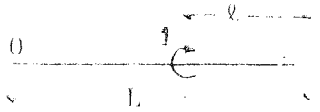

L/B = 5

ℓ = 0

x/B	B/2c	EIW(x)/c²	M(x)	cV(x)	c²Q(x)
0	0.01	-15.8246	0.00000	0.00000	-610.838
	0.05	-2.74006	"	"	-24.6683
	0.1	-1.23623	"	"	-6.15394
	0.2	-0.43786	"	"	-1.29140
	1.0	0.05772	"	"	-0.00370
1	0.01	-9.49465	-0.10166	-9.70469	-364.473
	0.05	-1.64237	-0.10480	-1.92360	-14.1770
	0.1	-0.74013	-0.10317	-0.94465	-3.47894
	0.2	-0.26971	-0.08697	-0.40355	-0.79552
	1.0	0.08361	-0.00152	-0.00006	0.00151
2	0.01	-3.16463	-0.35057	-14.55223	-121.602
	0.05	-0.54352	-0.35247	-2.86109	-4.65930
	0.1	-0.23939	-0.34653	-1.41439	-1.23291
	0.2	-0.08594	-0.30245	-0.64992	-0.43445
	1.0	0.11367	0.00179	0.00289	-0.00059
3	0.01	3.16553	-0.64926	-14.55237	121.590
	0.05	0.55890	-0.64581	-2.86667	4.55641
	0.1	0.27537	-0.63922	-1.43743	1.02119
	0.2	0.14714	-0.58615	-0.73817	0.02517
	1.0	0.13916	-0.01151	-0.03221	-0.05096
4	0.01	9.49595	-0.89835	-9.70497	364.4740
	0.05	1.66774	-0.89445	-1.93500	14.18267
	0.1	0.81557	-0.89031	-0.99198	3.48530
	0.2	0.47392	-0.86170	-0.58833	0.79898
	1.0	0.28533	-0.27542	-0.28647	-0.20314
5	0.01	15.8267	-1.00000	0.00000	610.870
	0.05	2.78540	"	"	24.92588
	0.1	1.39091	"	"	6.71022
	0.2	0.93683	"	"	2.44016
	1.0	1.76430	"	"	1.55939

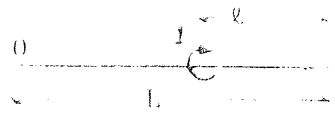

L/B = 5

ℓ = B

x/B	B/2c	EIW(x)/c^2	M(x)	cV(x)	c^{2}Q(x)
0	0.01	-15.82503	0.00000	0.00000	-610.844
	0.05	-2.74099	"	"	-24.65965
	0.1	-1.23797	"	"	-6.13926
	0.2	-0.44258	"	"	-1.27125
	1.0	0.00365	"	"	0.00181
1	0.01	-9.49499	-0.10166	-9.70478	-364.480
	0.05	-1.64450	-0.10476	-1.92314	-14.1767
	0.1	-0.74556	-0.10299	-0.94326	-3.47832
	0.2	-0.28419	-0.08605	-0.40037	-0.79711
	1.0	0.00098	0.00360	0.00416	0.00317
2	0.01	-3.16490	-0.35075	-14.55238	-121.604
	0.05	-0.54684	-0.35239	-2.86103	-4.6668
	0.1	-0.24857	-0.34614	-1.4.403	-1.24249
	0.2	-0.11032	-0.30077	-0.65020	-0.44917
	1.0	-0.02010	0.01758	0.00780	-0.00514
3	0.01	3.16532	-0.64926	-14.55253	121.590
	0.05	0.55439	-0.64579	-2.86732	4.55174
	0.1	0.26243	-0.63897	-1.43931	1.00912
	0.2	0.11262	-0.58592	-0.74525	0.00926
	1.0	-0.10154	-0.02037	-0.08115	-0.11260
4	0.01	9.49581	-0.39834	-9.70510	364.480
	0.05	1.66203	-0.89448	-1.93548	14.19887
	0.1	0.79886	-0.89058	-0.99396	3.51892
	0.2	0.42926	-0.86480	-0.59354	0.86766
	1.0	0.05339	-0.52675	-0.43136	-0.00203
5	0.01	15.82645	0.00000	0.00000	610.871
	0.05	2.77350	"	"	24.87734
	0.1	1.35044	"	"	6.59867
	0.2	0.80240	"	"	2.18023
	1.0	0.31287	"	"	0.27575

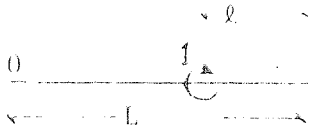

L/B = 5

ℓ = 2B

x/B	B/2c	$EIW(x)/c^2$	M(x)	cV(x)	$c^2Q(x)$
0	0.01	-15.82549	0.00000	0.00000	-610.852
	0.05	-2.74660	"	"	-24.68895
	0.1	-1.25730	"	"	-6.20560
	0.2	-0.50153	"	"	-1.39950
	1.0	0.00483	"	"	0.01735
1	0.01	-9.49533	-0.10166	-9.70490	-364.480
	0.05	-1.64903	-0.10487	-1.92540	-14.19231
	0.1	-0.75975	-0.10406	-0.95275	-3.50750
	0.2	-0.32434	-0.09408	-0.43595	-0.85296
	1.0	-0.03293	0.01617	0.01003	-0.00524
2	0.01	-3.16512	-0.35075	-14.55253	-121.604
	0.05	-0.55030	-0.35280	-2.86383	-4.65957
	0.1	-0.25757	-0.34941	-1.42540	-1.23091
	0.2	-0.13027	-0.32569	-0.69412	-0.43030
	1.0	-0.12475	-0.01599	-0.07581	-0.10826
3	0.01	3.16522	-0.64926	-14.55264	121.597
	0.05	0.55200	-0.64637	-2.86767	4.60227
	0.1	0.25875	-0.64388	-1.44140	1.11360
	0.2	0.11682	-0.62376	-0.75511	0.21012
	1.0	-0.00350	-0.49933	-0.41345	0.00132
4	0.01	9.49563	0.10166	-9.70503	364.484
	0.05	1.65572	-0.10520	-1.93062	14.21340
	0.1	0.78068	-0.10655	-0.97366	3.55240
	0.2	0.38325	0.11293	-0.51461	0.93661
	1.0	0.11322	0.02321	-0.06957	0.11156
5	0.01	15.82599	0.00000	0.00000	610.861
	0.05	2.75828	"	"	24.77163
	0.1	1.29787	"	"	6.37508
	0.2	0.62962	"	"	1.72706
	1.0	-0.01519	"	"	-0.03976

L/B = 5

ℓ = 2.5B

x/B	B/2c	EIW(x)/c^2	M(x)	cV(x)	c^{2}Q(x)
0	0.01	-15.82574	0.00000	0.00000	-610.86
	0.05	-2.75174	"	"	-24.724
	0.1	-1.27519	"	"	-6.27912
	0.2	-0.55748	"	"	-1.53974
	1.0	0.01583	"	"	0.03319
0.5	0.01	-12.66061	-0.02635	-5.46395	-486.10
	0.05	-2.20201	-0.02809	-1.09280	-19.222
	0.1	-1.02265	-0.02857	-0.54770	-4.77538
	0.2	-0.45577	-0.02779	-0.26579	-1.16321
	1.0	-0.01958	0.00890	0.01256	-0.00165
1	0.01	-9.49549	-0.10166	-9.70496	-364.48
	0.05	-1.65221	-0.10502	-1.92777	-14.204
	0.1	-0.76977	-0.10518	-0.96214	-3.53023
	0.2	-0.35279	-0.10237	-0.47117	-0.89644
	1.0	-0.06375	0.01573	-0.00469	-0.03691
1.5	0.01	-6.33035	-0.21386	-12.73431	-243.10
	0.05	-1.10213	-0.21760	-2.51638	-9.35378
	0.1	-0.51582	-0.21701	-1.25625	-2.36053
	0.2	-0.24560	-0.21286	-0.62543	-0.64580
	1.0	-0.12046	-0.01761	-0.07410	-0.10969
2.0	0.01	-3.16519	-0.35075	-14.55260	-121.60
	0.05	-0.55151	-0.35320	-2.86595	-4.64225
	0.1	-0.25968	-0.35254	-1.43428	-1.19795
	0.2	-0.12981	-0.34911	-0.72798	-0.37270
	1.0	-0.15032	-0.16341	-0.23424	-0.20708
2.5	0.01	0.00000	-0.50000	-15.15888	0.00000
	0.05	"	"	-2.98203	"
	0.1	"	"	-1.49504	"
	0.2	"	"	-0.76878	"
	1.0	"	"	-0.41415	"

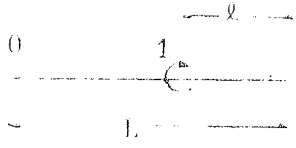

L/B = 10

ℓ = 0

x/B	B/2c	EIW(x)/c^2	M(x)	c V(x)	c^{2}Q(x)
0	0.01	-3.92130	0.0000	0.0000	-149.224
	0.05	-0.69560	"	"	-5.93902
	0.1	-0.22811	"	"	-1.08270
	0.2	0.02351	"	"	0.03620
	1.0	0.01740	"	"	-0.00036
2	0.01	-2.35279	-0.10187	-4.77931	-90.1804
	0.05	-0.42305	-0.10111	-0.93059	-3.48593
	0.1	-0.16108	-0.07666	-0.36376	-0.77444
	0.2	-0.01533	-0.00295	-0.02375	-0.09115
	1.0	0.02860	0.00000	0.00000	-0.00002
4	0.01	-0.78411	-0.35069	-7.19219	-30.3161
	0.05	-0.14599	-0.34233	-1.40894	-1.29855
	0.1	-0.08013	-0.27766	-0.62423	-0.51674
	0.2	-0.04913	-0.06558	-0.15171	-0.23242
	1.0	0.04686	0.00000	0.00000	-0.00010
6	0.01	0.78514	-0.64917	-7.19351	30.255
	0.05	0.14493	-0.63531	-1.44547	0.96415
	0.1	0.04633	-0.55911	-0.75466	-0.08736
	0.2	-0.03306	-0.27519	-0.38565	-0.32697
	1.0	0.08440	0.00000	0.00000	0.00113
8	0.01	2.35543	-0.89807	-4.78195	90.186
	0.05	0.46114	-0.88874	-1.00492	3.50042
	0.1	0.26240	-0.84862	-0.63491	0.78872
	0.2	0.16986	-0.67355	-0.56953	-0.00613
	1.0	0.13943	0.00000	0.00000	-0.05097
10	0.01	3.92713	-1.00000	0.00000	149.366
	0.05	0.81243	"	"	6.78072
	0.1	0.61251	"	"	2.70425
	0.2	0.80250	"	"	2.01184
	1.0	1.76443	"	"	1.55938

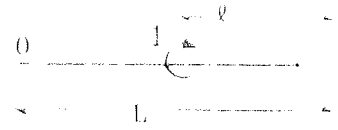

L/B = 10

ℓ = 2B

x/B	B/2c	$EIW(x)/c^2$	M(x)	cV(x)	$c^2Q(x)$
0	0.01	-3.92176	0.0000	0.0000	-149.23
	0.05	-0.69680	"	"	-5.93407
	0.1	-0.23166	"	"	-1.07856
	0.2	0.01796	"	"	0.04745
	1.0	-0.00150	"	"	0.00010
2	0.01	-2.35232	-0.10188	-4.77953	-90.1826
	0.05	-0.42563	-0.10107	-0.93035	-3.48766
	0.1	-0.16802	-0.07666	-0.36444	-0.78086
	0.2	-0.03124	-0.00189	-0.02367	-0.10004
	1.0	-0.00298	0.00012	0.00003	0.00000
4	0.01	-0.78452	-0.35071	-7.19238	-30.3128
	0.05	-0.14995	-0.34233	-1.40979	-1.30579
	0.1	-0.09045	-0.27861	-0.62864	-0.52814
	0.2	-0.07579	-0.06893	-0.16480	-0.25555
	1.0	-0.00628	0.00048	0.00050	0.00066
6	0.01	0.78475	-0.64919	-7.19355	30.259
	0.05	0.13959	-0.63559	-1.44750	0.95886
	0.1	0.03281	-0.56266	-0.76276	-0.09065
	0.2	-0.06755	-0.29693	-0.41796	-0.34458
	1.0	-0.03672	0.01851	0.00819	-0.00446
8	0.01	2.35506	-0.89808	-4.78186	90.19124
	0.05	0.45443	-0.88941	-0.00508	3.54696
	0.1	0.24626	-0.85461	-0.63393	0.88121
	0.2	0.14193	-0.71820	-0.57305	0.17717
	1.0	-0.00462	-0.49931	-0.41346	0.00136
10	0.01	3.92599	0.00000	0.00000	149.35
	0.05	0.78437	"	"	6.61712
	0.1	0.51453	"	"	2.34271
	0.2	0.48446	"	"	1.26371
	1.0	-0.01574	"	"	-0.03972

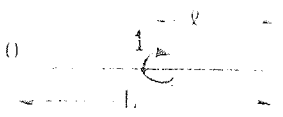

L/B = 10

ℓ = 4B

x/B	B/2c	$EIW(X)/c^2$	M(X)	cV(X)	$c^2Q(X)$
0	0.01	-3.92278	0.00000	0.00000	-149.257
	0.05	-0.71196	"	"	-6.04334
	0.1	-0.27740	"	"	-1.26911
	0.2	-0.02639	"	"	-0.04625
	1.0	-0.00193	"	"	0.00021
2	0.01	-2.35391	-0.10190	-4.78011	-90.1881
	0.05	-0.43416	-0.10279	-0.94539	-3.52953
	0.1	-0.19298	-0.08855	-0.41667	-0.85890
	0.2	-0.07570	-0.03148	-0.09853	-0.19772
	1.0	-0.00493	0.00044	0.00049	0.00065
4	0.01	-0.78485	-0.35074	-7.19289	-30.3046
	0.05	-0.15179	-0.34743	-1.42633	-1.27855
	0.1	-0.09256	-0.31474	-0.68989	-0.48900
	0.2	-0.09811	-0.18879	-0.31122	-0.31679
	1.0	-0.03427	0.01844	0.00819	-0.00444
6	0.01	0.78478	-0.64922	-7.19352	30.2807
	0.05	0.14465	-0.64285	-1.44851	1.10984
	0.1	0.05924	-0.61564	-0.77114	0.18726
	0.2	0.01075	-0.53091	-0.50947	-0.00562
	1.0	-0.00009	-0.50000	-0.41453	-0.00000
8	0.01	2.35464	0.10191	-4.78101	90.1954
	0.05	0.44666	0.10649	-0.97604	3.59018
	0.1	0.22914	0.11485	-0.52594	0.96926
	0.2	0.13953	0.12601	-0.30685	0.35652
	1.0	0.03405	-0.01841	0.00823	0.0049
10	0.01	3.9432	0.00000	0.00000	149.296
	0.05	0.74393	"	"	6.29584
	0.1	0.37860	"	"	1.72387
	0.2	0.17572	"	"	0.43245
	1.0	0.00310	"	"	-0.0026

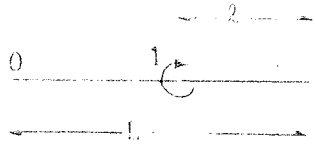

L/B = 10

ℓ = 5B

x/B	B/2c	EIW(x)/c²	M(x)	cV(x)	c²Q(x)
0	0.01	-3.92350	0.00000	0.00000	-149.275
	0.05	-0.72608	"	"	-6.1545
	0.1	-0.32148	"	"	-1.46508
	0.2	-0.08315	"	"	-0.18946
	1.0	-0.00294	"	"	0.00028
1	0.01	-3.13890	-0.02668	-2.68365	-119.601
	0.05	-0.58335	-0.02827	-0.54326	-4.77324
	0.1	-0.26683	-0.02690	-0.25900	-1.1550
	0.2	-0.09697	-0.01607	-0.08306	-0.22940
	1.0	-0.00487	0.00040	0.00053	0.00063
2	0.01	-2.35428	-0.1091	-4.78053	-90.191
	0.05	-0.44029	-0.10446	-0.95931	-3.56049
	0.1	-0.21095	-0.10019	-0.46595	-0.91724
	0.2	-0.10772	-0.06896	-0.18473	-0.27885
	1.0	-0.00933	0.00410	0.00406	0.00320
3	0.01	-1.56963	-0.21396	-6.28621	-60.407
	0.05	-0.29616	-0.21620	-1.25714	-2.40049
	0.1	-0.15095	-0.21017	-0.62598	-0.68007
	0.2	-0.10685	-0.16627	-0.30407	-0.31184
	1.0	-0.03422	0.01844	0.00819	-0.00444
4	0.01	-0.78488	-0.35076	-7.19323	-30.297
	0.05	-0.14984	-0.35201	-1.43871	-1.22529
	0.1	-0.08244	-0.34721	-0.73525	-0.40249
	0.2	-0.07872	-0.31256	-0.42494	-0.27354
	1.0	-0.12293	-0.01574	-0.07618	-0.10793
5	0.01	0.00000	-0.50000	-7.49625	0.00000
	0.05	"	"	-1.50087	"
	0.1	"	"	-0.77949	"
	0.2	"	"	-0.49549	"
	1.0	"	"	-0.41453	"

L/B = 20

ℓ = 0

x/B	B/2c	$EIW(x)/c^2$	M(x)	c V(x)	$c^2\theta(x)$
0	0.01	-1.01635	0.00000	0.00000	-37.5882
	0.05	-0.09402	"	"	-0.77695
	0.1	0.02248	"	"	0.08940
	0.2	0.00427	"	"	-0.00202
	1.0	-0.01704	"	"	0.00018
4	0.01	-0.61113	-0.10378	-2.39549	-22.37434
	0.05	-0.08561	-0.06011	-0.29750	-0.72447
	0.1	-0.00759	-0.01228	0.01226	-0.05414
	0.2	0.00862	0.00049	0.00230	0.00456
	1.0	-0.00265	0.00010	-0.00006	-0.00001
8	0.01	-0.20517	-0.35118	-3.58657	-7.45538
	0.05	-0.06604	-0.23585	-0.57624	-0.64691
	0.1	-0.04362	0.01269	-0.09888	-0.23576
	0.2	0.00923	0.01217	0.01246	0.00372
	1.0	0.01008	-0.00010	0.00002	-0.00002
12	0.01	0.20306	-0.64624	-3.59750	7.20657
	0.05	-0.00737	-0.51151	-0.77866	-0.29090
	0.1	-0.06344	0.18991	-0.37001	-0.42197
	0.2	-0.02175	0.01398	-0.03573	-0.09546
	1.0	0.02863	-0.00042	-0.00009	-0.00003
16	0.01	0.61541	-0.89512	-2.41686	22.4649
	0.05	0.13371	-0.82454	-0.71775	0.75181
	0.1	0.05220	0.61320	-0.64933	-0.10720
	0.2	-0.03217	-0.27298	-0.38997	-0.32126
	1.0	0.08441	-0.00216	0.00054	0.00113
20	0.01	1.03340	-1.00000	0.00000	38.1324
	0.05	0.40502	"	"	3.22505
	0.1	0.56174	"	"	2.44873
	0.2	0.80207	"	"	2.01165
	1.0	1.76443	"	"	1.55938

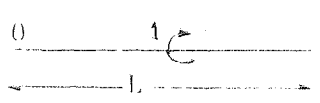

L/B = 20

ℓ = 4B

x/B	B/2c	EIW(x)/c^2	M(x)	cV(x)	c^{2}Q(x)
0	0.01	-1.01670	0.00000	0.00000	-37.590
	0.05	-0.09785	"	"	-0.79491
	0.1	0.02115	"	"	0.09873
	0.2	0.00040	"	"	0.00082
	1.0	-0.00036	"	"	0.00004
4	0.01	-0.61150	-0.10378	-2.39599	-22.384
	0.05	-0.08965	-0.06150	-0.30427	-0.74021
	0.1	-0.01531	0.01245	0.00954	-0.06904
	0.2	0.00155	0.00383	0.00661	0.00758
	1.0	-0.00049	0.00000	0.00000	0.00000
8	0.01	-0.20555	-0.35126	-3.58772	-7.45826
	0.05	-0.07004	-0.24105	-0.58805	-0.65534
	0.1	-0.05732	-0.02175	-0.12191	-0.27006
	0.2	-0.01096	0.02341	0.01381	-0.01022
	1.0	-0.00110	0.00004	0.00001	0.00000
12	0.01	0.20267	-0.64641	-3.59799	7.22598
	0.05	-0.01049	-0.52159	-0.78962	-0.27294
	0.1	-0.07619	-0.22853	-0.41877	-0.43854
	0.2	-0.07478	-0.01861	-0.11398	-0.18891
	1.0	-0.00495	0.00044	0.00049	0.00065
16	0.01	0.61500	-0.89523	-2.41554	22.4286
	0.05	0.13305	-0.83588	-0.70610	0.89223
	0.1	0.06546	-0.68143	-0.64232	0.15970
	0.2	0.01235	-0.53074	-0.51139	-0.00092
	1.0	-0.00009	-0.50000	-0.41453	-0.00000
20	0.01	1.02979	0.00000	0.00000	38.0321
	0.05	0.32839	"	"	2.66946
	0.1	0.31709	"	"	1.41493
	0.2	0.17493	"	"	0.43037
	1.0	0.00310	"	"	-0.00226

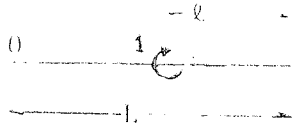

L/B = 20

ℓ = 8B

x/B	B/2c	$EIW(x)/c^2$	M(x)	cV(x)	$c^2Q(x)$
0	0.01	-1.01897	0.00000	0.00000	-37.66944
	0.05	-0.13442	"	"	-1.08189
	0.1	0.00305	"	"	0.03400
	0.2	0.00848	"	"	0.02791
	1.0	-0.00048	"	"	0.00001
4	0.01	-0.61259	-0.10399	-2.40048	-22.41365
	0.05	-0.10716	-0.07963	-0.38403	-0.85971
	0.1	-0.04543	-0.01492	-0.06728	-0.19590
	0.2	-0.01170	0.02006	0.01618	-0.01019
	1.0	-0.00109	0.00004	0.00001	0.00000
8	0.01	-0.20547	-0.35187	-3.59190	-7.41986
	0.05	-0.06534	-0.29608	-0.68056	-0.58882
	0.1	-0.07769	-0.15445	-0.30734	-0.38315
	0.2	-0.07509	-0.01588	-0.10625	-0.17978
	1.0	-0.00492	0.00044	0.00049	0.00065
12	0.01	0.20393	-0.64715	-3.59686	7.31780
	0.05	0.02509	-0.60119	-0.79791	0.14391
	0.1	0.000149	-0.51510	-0.55209	-0.00808
	0.2	0.00055	-0.49980	-0.48435	0.00319
	1.0	-0.00000	-0.50000	-0.41453	0.00000
16	0.01	0.61425	0.10440	-2.40846	22.4420
	0.05	0.13139	0.11868	-0.54618	1.01997
	0.1	0.09057	0.12120	-0.30954	0.40807
	0.2	0.07387	0.02499	-0.09521	0.18579
	1.0	0.00491	-0.00044	0.00049	-0.00065
20	0.01	1.02382	0.00000	0.00000	37.83986
	0.05	0.21653	"	"	1.75064
	0.1	0.08852	"	"	0.36936
	0.2	-0.01739	"	"	-0.06482
	1.0	0.00099	"	"	-0.00009

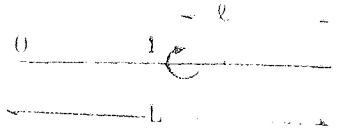

L/B = 20

ℓ = 10B

x/B	B/2c	EIW(x)/c²	M(x)	cV(x)	c²Q(x)
0	0.01	-1.02111	0.00000	0.00000	-37.746
	0.05	-0.16996	"	"	-1.36948
	0.1	-0.02872	"	"	-0.10270
	0.2	0.01734	"	"	0.05621
	1.0	-0.00063	"	"	0.00003
2	0.01	-0.81728	-0.02792	-1.35424	-30.064
	0.05	-0.14541	-0.02565	-0.24891	-1.13761
	0.1	-0.04980	-0.01103	-0.06191	-0.20525
	0.2	-0.00551	0.01078	0.01969	-0.00157
	1.0	-0.00108	0.00004	0.00001	0.00000
4	0.01	-0.61341	-0.10418	-2.40424	-22.430
	0.05	-0.11968	-0.09690	-0.45729	-0.94586
	0.1	-0.06869	-0.05490	-0.16407	-0.30415
	0.2	-0.03520	0.01985	-0.00583	-0.06837
	1.0	-0.00215	0.00011	0.00002	0.00000
6	0.01	-0.40936	-0.21642	-3.14995	-14.843
	0.05	-0.08995	-0.20594	-0.62612	-0.73526
	0.1	-0.07814	-0.14710	-0.30170	-0.37506
	0.2	-0.07520	-0.01756	-0.10304	-0.18286
	1.0	-0.00492	0.00044	0.00049	0.00065
8	0.01	-0.20496	-0.35235	-3.59458	-7.37930
	0.05	-0.05189	-0.34415	-0.74666	-0.45425
	0.1	-0.06326	-0.29796	-0.45060	-0.34231
	0.2	-0.09771	-0.17259	-0.30020	-0.29568
	1.0	-0.03423	0.01844	0.00819	-0.00444
10	0.01	0.00000	-0.50000	-3.74234	0.00000
	0.05	"	"	-0.79695	"
	0.1	"	"	-0.53831	"
	0.2	"	"	-0.48570	"
	1.0	"	"	-0.41453	"

A.1.2

Two dimensional analysis

A.1.2a

Numerical values of integrals $J_{nP}(X)$

x/c	$J_o^*(x)/\pi$	$J_1(x)/\pi$	$J_2(x)/\pi$	$J_3(x)/\pi$	$J_4(x)/\pi$	$J_5(x)/\pi$
0.00	0.0000	0.0000	0.38490	0.50000	0.38490	0.0000
0.25	0.01078	0.08159	0.27178	0.40597	0.36187	0.14489
0.50	0.03867	0.13777	0.18118	0.32056	0.31972	0.18442
0.75	0.07799	0.17385	0.11054	0.24652	0.27235	0.19082
1.00	0.12430	0.19446	0.05693	0.18433	0.22564	0.18097
1.25	0.17425	0.20349	0.01744	0.13340	0.18252	0.16311
1.50	0.22535	0.20413	-0.01062	0.09265	0.14436	0.14189
1.75	0.27584	0.19894	-0.02962	0.06076	0.11162	0.12008
2.00	0.32450	0.18990	-0.04162	0.03639	0.08424	0.09928
2.25	0.37060	0.17856	-0.04833	0.01823	0.06183	0.08036
2.50	0.41369	0.16606	-0.05116	0.00510	0.04387	0.06373
2.75	0.45360	0.15322	-0.05122	-0.00403	0.02976	0.04951
3.00	0.49032	0.14061	-0.04940	-0.01006	0.01892	0.03762
3.25	0.52395	0.12862	-0.04638	-0.01372	0.01077	0.02788
3.50	0.55470	0.11747	-0.04269	-0.01563	0.00482	0.02006
3.75	0.58277	0.10730	-0.03868	-0.01627	0.00061	0.01390
4.00	0.60843	0.09814	-0.03462	-0.01604	-0.00225	0.00914

$$J_o^*(x) = J_o(0) - J_o(x)$$

$$c = \left[\frac{2E_b I(1-\nu^2)}{EB} \right]^{1/3}$$

A.1.2b

Finite beam subjected to a concentrated load

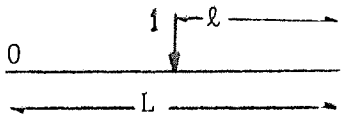

$\ell/L = 0.25$

L/c	x/c	EJW^*/c^3	M(x)/c	V(x)	cQ(x)
0.5	0.0 0.375 0.5	3.54917 0.0 -1.18274	0.0 0.03618 0.0	0.0 0.46357 0.0	-1.19089 3.39061 5.47003
1.0	0.0 0.75 1.0	2.43396 0.0 -0.80860	0.0 0.07324 0.0	0.0 0.45972 0.0	-0.60115 1.67678 2.85404
2.0	0.0 1.5 2.0	1.72383 0.0 -0.55199	0.0 0.14798 0.0	0.0 0.45697 0.0	-0.30082 0.83799 1.49432
4.0	0.0 3.0 4.0	1.22362 0.0 -0.25033	0.0 0.27733 0.0	0.0 0.47091 0.0	-0.15016 0.47270 0.68206

$W^* = W(L - \ell) - W(x)$

$\ell/L = 0.5$

0.5	0.0 0.125 0.25	0.00099 0.00035 0.0	0.0 0.01607 0.06329	0.0 0.25460 0.50000	2.13657 1.98262 1.95443
1.0	0.0 0.25 0.5	0.00803 0.00283 0.0	0.0 0.03264 0.12727	0.0 0.25645 0.50000	1.11313 0.98442 0.97111
2.0	0.0 0.5 1.0	0.06215 0.02199 0.0	0.0 0.06247 0.24844	0.0 0.24693 0.50000	0.53851 0.48861 0.52162
4.0	0.0 1.0 2.0	0.34554 0.12729 0.0	0.0 0.07037 0.38938	0.0 0.16596 0.50000	0.08995 0.24557 0.40230

A.1.2c

Finite beam subjected to a concentrated couple

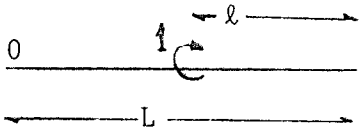

$\ell/L = 0.25$

L/c	x/c	EIW^*/c^2	M(x)	cV(x)	$c^2Q(x)$
0.5	0.0 0.375 0.5	28.40207 0.0 -9.47855	0.0 -0.83897 0.0	0.0 -2.25640 0.0	-26.61204 11.24712 26.70378
1.0	0.0 0.75 1.0	9.74187 0.0 -3.29170	0.0 -0.83618 0.0	0.0 -1.14266 0.0	-6.83692 2.73491 7.04251
2.0	0.0 1.5 2.0	3.40999 0.0 -1.30438	0.0 -0.81710 0.0	0.0 -0.62219 0.0	-1.63075 0.62786 2.08443
4.0	0.0 3.0 4.0	1.05643 0.0 -0.79983	0.0 -0.71479 0.0	0.0 -0.45987 0.0	-0.17878 0.09570 0.89602

$\ell/L = 0.5$

0.5	0.0 0.125 0.25	18.92126 9.46199 0.0	0.0 -0.16070 -0.50000	0.0 -2.25262 -2.94754	-26.63647 -11.26412 0.0
1.0	0.0 0.25 0.5	6.46864 3.23981 0.0	0.0 -0.16100 -0.50000	0.0 -1.12695 -1.47078	-6.89482 -2.77090 0.0
2.0	0.0 0.5 1.0	2.23368 1.13864 0.0	0.0 -0.15960 -0.50000	0.0 -0.55831 -0.74734	-1.76236 -0.70338 0.0
4.0	0.0 1.0 2.0	0.63958 0.39797 0.0	0.0 -0.13736 -0.50000	0.0 -0.25868 -0.43807	-0.35376 -0.22888 0.0

A.1.3d

Finite beam subjected to a concentrated load. Non-homogeneous incompressible medium

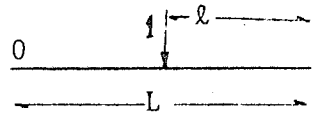

$L/c = 0.5$

$\ell/L = 0.25$

x/c	ρ	EIW*/c³	M(x)/c	V(x)	cQ(x)
0.0 0.375 0.5	0.5	1.61135 0.0 -0.48273	0.0 0.03563 0.0	0.0 0.46643 0.0	-1.10442 3.44482 5.21491
0.0 0.375 0.5	1	1.97425 0.0 -0.61802	0.0 0.03575 0.0	0.0 0.46599 0.0	-1.13378 3.43221 5.27428
0.0 0.375 0.5	2	2.37841 0.0 -0.76483	0.0 0.03586 0.0	0.0 0.46545 0.0	-1.15894 3.41974 5.33172
0.0 0.375 0.5	5	2.86198 0.0 -0.93813	0.0 0.0360 0.0	0.0 0.46475 0.0	-1.17983 3.40672 5.39274
0.0 0.375 0.5	100	3.51883 0.0 -1.17190	0.0 0.03617 0.0	0.0 0.46367 0.0	-1.19310 3.39106 5.46699

$\ell/L = 0.5$ $\qquad \rho = \frac{G(0)}{m}$

0.0 0.125 0.25	0.5	0.04863 0.01237 0.0	0.0 0.01579 0.06278	0.0 0.25165 0.50000	2.05096 1.99309 1.98442
0.0 0.125 0.25	1	0.03664 0.00933 0.0	0.0 0.01584 0.06280	0.0 0.25217 0.50000	2.06662 1.99122 1.97907
0.0 0.125 0.25	2	0.02620 0.00669 0.0	0.0 0.01589 0.06297	0.0 0.25273 0.0	2.08310 1.98921 1.97339
0.0 0.125 0.25	5	0.01539 0.00397 0.0	0.0 0.01596 0.06309	0.0 0.25344 0.50000	2.10336 1.98680 1.96607
0.0 0.125 0.25	100	0.00171 0.00053 0.0	0.0 0.01606 0.06327	0.0 0.25450 0.50000	2.13395 1.98295 1.95541

$\ell/L = 0.25$

$L/c = 1$

x/c	ρ	EIW*/c³	M(x)/c	V(x)	cQ(x)
0.0 0.75 1.0	0.5	+1.33185 0.0 -0.32948	0.0 0.07135 0.0	0.0 0.46592 0.0	-0.55299 1.72285 2.63608
0.0 0.75 1.0	1	-1.49490 0.0 -0.41160	0.0 0.07171 0.0	0.0 0.46486 0.0	-0.56897 1.71309 2.68057
0.0 0.75 1.0	2	-1.70301 0.0 -0.50541	0.0 0.07208 0.0	0.0 0.46373 0.0	-0.58392 1.70320 2.72608
0.0 0.75 1.0	5	1.98312 0.0 -0.62416	0.0 0.07253 0.0	0.0 0.46230 0.0	-0.59713 1.69154 2.77870
0.0 0.75 1.0	100	2.41171 0.0 -0.79944	0.0 0.07319 0.0	0.0 0.45997 0.0	-0.60400 1.67742 2.84982

$\ell/L = 0.5$

0.0 0.25 0.5	0.5	0.09834 0.02606 0.0	0.0 0.03130 0.12495	0.0 0.24964 0.50000	1.01847 0.99526 1.00623
0.0 0.25 0.5	1	0.07754 0.02061 0.0	0.0 0.03159 0.12545	0.0 0.25114 0.50000	1.03754 0.99329 0.99823
0.0 0.25 0.5	2	0.05842 0.01567 0.0	0.0 0.03184 0.12589	0.0 0.25244 0.50000	1.05537 0.99130 0.99150
0.0 0.25 0.5	5	0.03766 0.01035 0.0	0.0 0.03214 0.12640	0.0 0.25393 0.50000	1.07662 0.98880 0.98382
0.0 0.25 0.5	100	0.00971 0.00325 0.0	0.0 0.03259 0.12718	0.0 0.25620 0.50000	1.10965 0.98485 0.97239

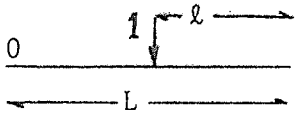

$\ell/L = 0.25$ $L/c = 2$

x/c	ρ	EIW^*/c^3	M(x)/c	V(x)	cQ(x)
0.0 1.5 2.0	0.5	1.21814 0.0 -0.18697	0.0 0.14014 0.0	0.0 0.47040 0.0	-0.28036 0.88461 1.28377
0.0 1.5 2.0	1	1.27444 0.0 -0.24798	0.0 0.14189 0.0	0.0 0.46745 0.0	-0.28694 0.87309 1.32843
0.0 1.5 2.0	2	1.35329 0.0 -0.31490	0.0 0.14340 0.0	0.0 0.46497 0.0	-0.29427 0.86345 1.37002
0.0 1.5 2.0	5	1.47747 0.0 -0.40201	0.0 0.14512 0.0	0.0 0.46213 0.0	-0.30160 0.85303 1.41825
0.0 1.5 2.0	100	1.70732 0.0 -0.54233	0.0 0.14768 0.0	0.0 0.45763 0.0	-0.30414 0.83898 1.48820

$\ell/L = 0.5$

0.0 0.5 1.0	0.5	0.20393 0.06246 0.0	0.0 0.05230 0.23012	0.0 0.21960 0.50000	0.38084 0.50362 0.59842
0.0 0.5 1.0	1	0.17408 0.05268 0.0	0.0 0.05572 0.23644	0.0 0.22913 0.50000	0.42883 0.49972 0.57056
0.0 0.5 1.0	2	0.14603 0.04441 0.0	0.0 0.05797 0.24053	0.0 0.23527 0.50000	0.46242 0.49671 0.55306
0.0 0.5 1.0	5	0.11362 0.03541 0.0	0.0 0.05990 0.24398	0.0 0.24039 0.50000	0.49355 0.49362 0.53887
0.0 0.5 1.0	100	0.06573 0.02289 0.0	0.0 0.06223 0.24803	0.0 0.24633 0.50000	0.53414 0.48915 0.52314

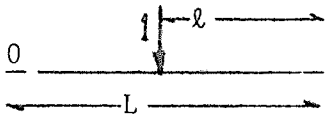

L/c = 4

ℓ/L = 0.25

x/c	ρ	EIW*/c³	M(x)/c	V(x)	cQ(x)
0.0	0.5	0.93402	0.0	0.0	-0.11220
3.0		0.0	0.23605	0.50029	0.56163
4.0		0.09768	0.0	0.0	0.42043
0.0	1	1.00341	0.0	0.0	-0.12911
3.0		0.0	0.24817	0.49293	0.52955
4.0		0.02466	0.0	0.0	0.49218
0.0	2	1.05859	0.0	0.0	-0.13972
3.0		0.0	0.25724	0.48667	0.50875
4.0		-0.04165	0.0	0.0	0.54784
0.0	5	1.11757	0.0	0.0	-0.14791
3.0		0.0	0.26572	0.48037	0.49177
4.0		-0.11868	0.0	0.0	0.60289
0.0	100	1.21312	0.0	0.0	-0.15181
3.0		0.0	0.27621	0.47199	0.47401
4.0		-0.23956	0.0	0.0	0.67500

ℓ/L = 0.5

0.0	0.5	0.53505	0.0	0.0	-0.10927
1.0		0.21748	0.00969	0.07743	0.25147
2.0		0.0	0.27209	0.50000	0.54692
0.0	1	0.48074	0.0	0.0	-0.05912
1.0		0.18572	0.02716	0.10441	0.25341
2.0		0.0	0.30761	0.50000	0.49861
0.0	2	0.43946	0.0	0.0	-0.01282
1.0		0.16398	0.04192	0.12623	0.25246
2.0		0.0	0.33640	0.50000	0.46257
0.0	5	0.40072	0.0	0.0	0.03310
1.0		0.14647	0.05548	0.14563	0.25008
2.0		0.0	0.36212	0.50000	0.43222
0.0	100	0.34954	0.0	0.0	0.08623
1.0		0.12825	0.06960	0.16504	0.24604
2.0		0.0	0.38810	0.50000	0.40343

A.1.3e

Finite beam subjected to a concentrated couple. Non-homogeneous incompressible medium

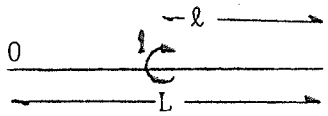

L/c = 0.5

ℓ/L = 0.25

x/c	ρ	EIW*/c²	M(x)	cV(x)	c²Q(x)
0.0 0.375 0.5	0.5	12.48964 0.0 -4.11919	0.0 -0.84103 0.0	0.0 -2.25746 0.0	-25.22907 11.59438 25.35945
0.0 0.375 0.5	1	15.50332 0.0 -5.14394	0.0 -0.84054 0.0	0.0 -2.25672 0.0	-25.59228 11.50990 25.70299
0.0 0.375 0.5	2	18.82839 0.0 -6.26638	0.0 -0.84005 0.0	0.0 -2.25642 0.0	-25.92705 11.42688 26.02765
0.0 0.375 0.5	5	22.78809 0.0 -7.59741	0.0 -0.83954 0.0	0.0 -2.25629 0.0	-26.25725 11.34239 26.35196
0.0 0.375 0.5	100	28.15367 0.0 -9.39569	0.0 -0.83897 0.0	0.0 -2.25639 0.0	-26.60880 11.24815 26.70034

ℓ/L = 0.5

0.0 0.125 0.25	0.5	8.29332 4.18665 0.0	0.0 -0.15853 -0.5	0.0 -2.25252 -2.97209	-25.26851 -11.61591 0.0
0.0 0.125 0.25	1	10.31172 5.18181 0.0	0.0 -0.15907 -0.5	0.0 -2.25237 -2.96613	-25.62425 -11.52909 0.0
0.0 0.125 0.25	2	12.53397 6.28303 0.0	0.0 -0.15959 -0.50000	0.0 -2.25236 -2.96028	-25.95507 -11.44490 0.0
0.0 0.125 0.25	5	15.17717 7.59679 0.0	0.0 -0.16010 -0.5	0.0 -2.25242 -2.95431	-26.28297 -11.35970 0.0
0.0 0.125 0.25	100	18.75582 9.37930 0.0	0.0 -0.16069 -0.5	0.0 -2.25262 -2.94762	-26.63313 -11.26514 0.0

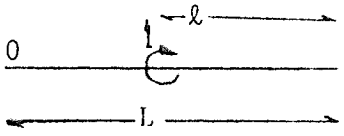

L/c = 1

ℓ/L = 0.25

x/c	ρ	EIW*/c²	M(x)	cV(x)	c²Q(x)
0.0 0.75 1.0	0.5	1.98326 0.0 -0.64963	0.0 -0.83751 0.0	0.0 -1.14935 0.0	-2.86261 2.86261 6.59597
0.0 0.75 1.0	1	5.63144 0.0 -1.85259	0.0 -0.83765 0.0	0.0 -1.14551 0.0	-2.83806 2.83806 6.67422
0.0 0.75 1.0	2	6.56716 0.0 -2.19022	0.0 -0.83741 0.0	0.0 -1.14371 0.0	-6.53057 2.80982 6.77279
0.0 0.75 1.0	5	7.79454 0.0 -2.62121	0.0 -0.83692 0.0	0.0 -1.14283 0.0	-6.67246 2.77517 6.89111
0.0 0.75 1.0	100	9.64496 0.0 -3.25905	0.0 -0.83620 0.0	0.0 -1.14262 0.0	-6.83455 2.73578 7.03934

ℓ/L = 0.5

0.0 0.25 0.5	0.5	3.17046 1.65125 0.0	0.0 -0.15792 -0.5	0.0 -1.12431 -1.49156	-6.35687 -2.91713 0.0
0.0 0.25 0.5	1	3.70496 1.89891 0.0	0.0 -0.15863 -0.5	0.0 -1.12502 -1.48663	-6.48081 -2.88331 0.0
0.0 0.25 0.5	2	4.34121 2.20191 0.0	0.0 -0.15933 -0.5	0.0 -1.12563 -1.48193	-6.60321 -2.85029 0.0
0.0 0.25 0.5	5	5.16726 2.60177 0.0	0.0 -0.16010 -0.5	0.0 -1.12622 -1.47691	-6.73569 -2.81287 0.0
0.0 0.25 0.5	100	6.40443 3.20780 0.0	0.0 -0.16098 -0.5	0.0 -1.12693 -1.47089	-6.89208 -2.77172 0.0

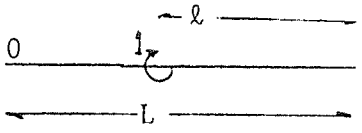

ℓ/L = 0.25 L/c = 2

x/c	ρ	EIW*/c²	M(x)	cV(x)	c²Q(x)
0.0 1.5 2.0	0.5	1.98326 0.0 -0.64963	0.0 -0.80097 0.0	0.0 -0.67846 0.0	-1.19953 0.64262 2.13921
0.0 1.5 2.0	1	2.17208 0.0 -0.76111	0.0 -0.80967 0.0	0.0 -0.65208 0.0	-1.34204 0.65068 2.05631
0.0 1.5 2.0	2	2.41215 0.0 -0.88308	0.0 -0.81413 0.0	0.0 -0.63739 0.0	-1.44367 0.64992 2.03020
0.0 1.5 2.0	5	2.76012 0.0 -1.03976	0.0 -0.81647 0.0	0.0 -0.62804 0.0	-1.53400 0.64305 2.03788
0.0 1.5 2.0	100	3.36584 0.0 -1.28775	0.0 -0.81725 0.0	0.0 -0.62197 0.0	-1.62920 0.62888 2.08014

ℓ/L = 0.5

0.0 0.5 1.0	0.5	1.15464 0.66138 0.0	0.0 -0.15260 -0.5	0.0 -0.55313 -0.77392	-1.50814 -0.78411 0.0
0.0 0.5 1.0	1	1.33513 0.73752 0.0	0.0 -0.15467 -0.5	0.0 -0.55520 -0.76540	-1.57096 -0.76061 0.0
0.0 0.5 1.0	2	1.53002 0.82050 0.0	0.0 -0.15623 -0.5	0.0 -0.55644 -0.75939	-1.62592 -0.74272 0.0
0.0 0.5 1.0	5	1.78621 0.93313 0.0	0.0 -0.15 74 -0.5	0.0 -0.55740 -0.75383	-1.68507 -0.72513 0.0
0.0 0.5 1.0	100	2.20509 1.12464 0.0	0.0 -0.15954 -0.5	0.0 -0.55828 -0.74757	-1.75962 -0.70418 0.0

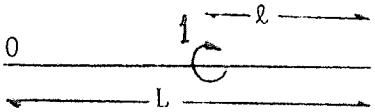

L/c = 4

ℓ/L = 0.25

x/c	ρ	EIW*/c²	M(x)	cV(x)	c²Q(x)
0.0	0.5	0.63029	0.0	0.0	-0.06842
3.0		0.0	-0.62974	-0.59534	0.06170
4.0		-0.42607	0.0	0.0	1.06393
0.0	1	0.69223	0.0	0.0	-0.00976
3.0		0.0	-0.65954	-0.54748	0.07868
4.0		-0.48843	0.0	0.0	0.99621
0.0	2	0.75727	0.0	0.0	-0.04983
3.0		0.0	-0.68272	-0.51200	0.08937
4.0		-0.55251	0.0	0.0	0.94388
0.0	5	0.85002	0.0	0.0	-0.11135
3.0		0.0	-0.70120	-0.48326	0.09560
4.0		-0.63996	0.0	0.0	0.90651
0.0	100	1.03253	0.0	0.0	-0.17676
3.0		0.0	-0.71533	-0.45958	0.09684
4.0		-0.78541	0.0	0.0	0.89126

ℓ/L = 0.5

0.0	0.5	0.09404	0.0	0.0	-0.14760
1.0		0.11596	-0.10289	-0.23562	-0.32225
2.0		0.0	-0.5	-0.51771	0.0
0.0	1	0.21915	0.0	0.0	-0.21644
1.0		0.19076	-0.11632	-0.24573	-0.28672
2.0		0.0	-0.5	-0.48502	0.0
0.0	2	0.33055	0.0	0.0	-0.26472
1.0		0.25170	-0.12482	-0.25162	-0.26373
2.0		0.0	-0.5	-0.46516	0.0
0.0	5	0.45169	0.0	0.0	-0.30655
1.0		0.31185	-0.13128	-0.25561	-0.24595
2.0		0.0	-0.5	-0.45073	0.0
0.0	100	0.62522	0.0	0.0	-0.35141
1.0		0.39130	-0.13714	-0.25864	-0.22955
2.0		0.0	-0.5	-0.43844	0.0

APPENDIX TWO

OHDE'S METHOD OF EVALUATION OF CONTACT STRESS DISTRIBUTION

Ohde's method of evaluation of contact stress distribution

The method is based on the assumption that the supporting medium behaves as a semi infinite homogeneous isotropic elastic continuum. The contact stress at the beam elastic continuum interface is assumed to be made up from a number of blocks of uniformly distributed loads $p_1, p_2 \ldots p_n$ per unit area of contact (Fig.A.2.1b). We denote by $W_1, W_2, W_3 \ldots W_n$ the deflections at the centre of each block (Fig. A.2.1a). The deflections $W_1, W_2 \ldots W_n$ at the centre of the blocks are related to $p_1, p_2, p_3 \ldots p_n$ by following n equations (see Terzaghi, 1943).

$$W_1 = (c_1p_1 + c_2p_2 + c_3p_3 + \ldots c_np_n) \frac{a(1-\nu^2)}{E},$$

$$W_2 = (c_2p_1 + c_1p_2 + c_2p_3 + \ldots c_{n-1}p_n) \frac{a(1-\nu^2)}{E},$$

$$W_n = (c_np_1 + c_{n-1}p_2 + c_{n-3}p_3 + \ldots c_1p_n) \frac{a(1-\nu^2)}{E}$$

(A.2.1)

Where $c_1, c_2, c_3 \ldots c_n$ are influence coefficients for the settlement of point 1 due to a unit load uniformly distributed over the elemental areas, 1, 2, 3, 4 ..... n. They can be obtained by integrating the Boussinesq solution for displacement under a concentrated load (see Terzaghi, 1943). In (A.2.1) E is Young's modulus of the elastic medium, ν is Poisson's ratio of the elastic medium and a = L/n. Where L is the length of the beam and n is the number of blocks of contact stress.

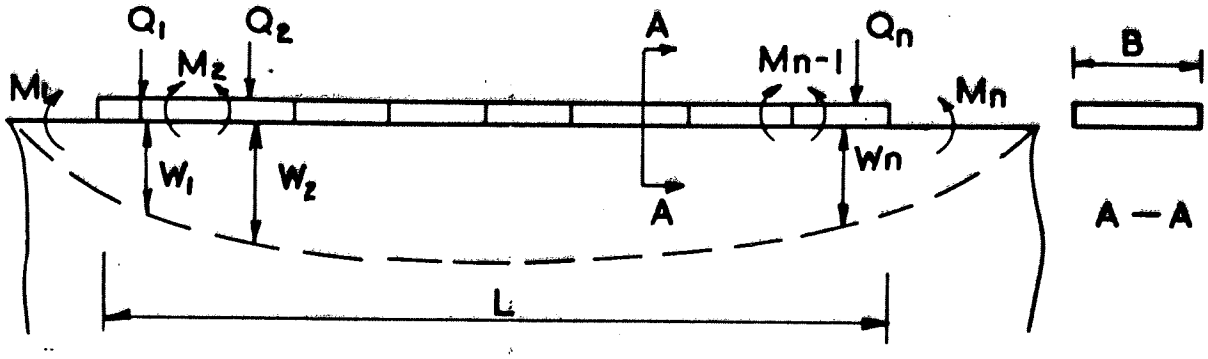

a. Deflected shape of the beam

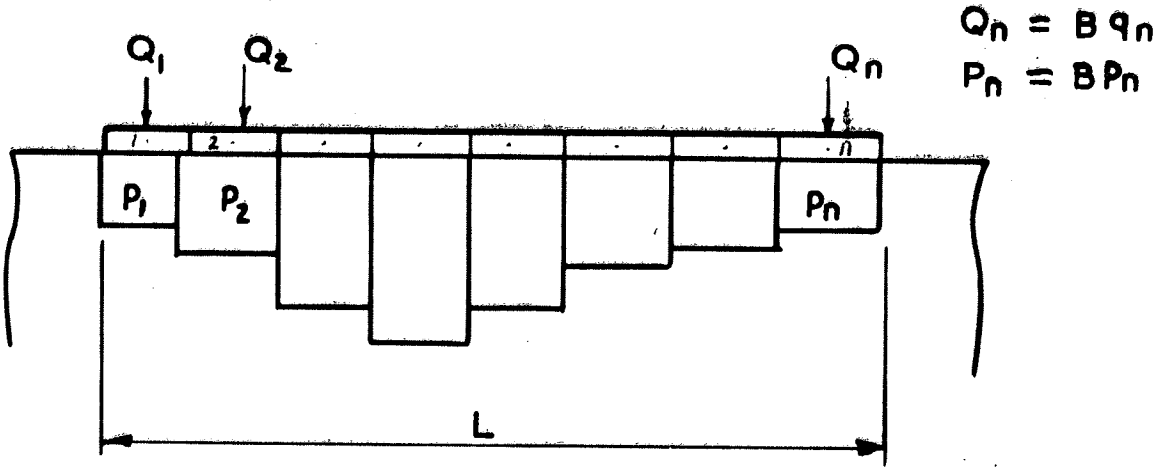

b. Blocks of contact forces

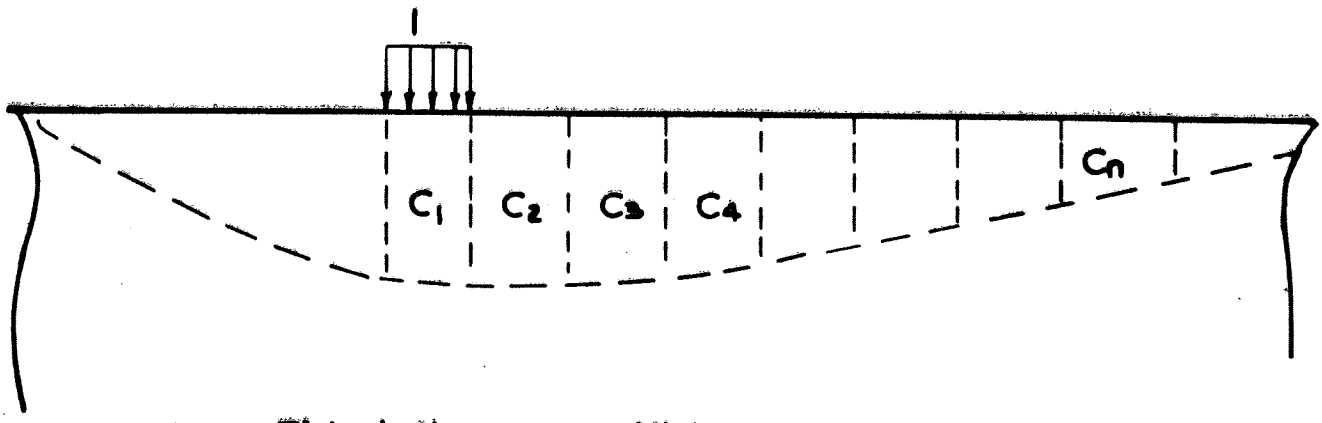

c. The influence coefficients

Fig A 2.1 Ohde's method of analysis of beams resting on an isotropic homogeneous elastic medium.

By making use of Clapeyron's theorem of three moments (see Timoshenko, 1965), the requirement of continuity of slope of the beam is given by the following n-1 equations

$$M_1 + 4M_2 + M_3 = \frac{6EI}{a^2}(-W_1 + 2W_2 - W_3)$$

$$M_2 + 4M_3 + M_4 = \frac{6EI}{a^2}(-W_2 + 2W_3 - W_4) \qquad (A.2.2)$$

$$2M_{n-1} + 4M_n = \frac{6EI}{a^2}(-2W_{n-1} + 2W_n)$$

Where M_1, M_2 ..... M_n are bending moments at the centre of each beam element (Fig. A.2.1) given by

$$M_2 = M_1 + (P_1 - Q_1)a$$

$$M_3 = M_1 + (P_1 - Q_1)2a + (P_2 - Q_2)a \qquad (A.2.3)$$

$$M_n = M_1 + (P_1 - Q_1)na + (P_2 - Q_2)(n-1)a + ... (P_n - Q_n)a.$$

In (A.2.3) Q_1, Q_2 ..... Q_n are external loads and P_1, P_2 ..... P_n are contact loads [(contact stress) a.B], acting at the centre of blocks 1, 2, 3 ..... n. By substituting (A.2.3) and (A.2.4) in (A.2.2) the following n-1 equations are obtained.

$$(C_2 + \beta)p_1 + (C_1 + \beta/6)p_2 + C_2p_3 + \ldots\ldots C_{n-1} \ldots p_n$$

$$= \beta(q_1 + q_2/6 - m_1)$$

$$(C_3 + 2\beta)p_1 + (C_2 + \beta)p_2 + (C_1 + \beta/6)p_3 + C_2p_4 + C_3p_5 + \ldots\ldots$$

$$C_{n-1}p_n = \beta(2q_1 + q_2 + q_{3/6} - m_1)$$

$$(C_4 + 3\beta)p_1 + (C_3 + 2\beta)p_2 + (C_2 + \beta)p_3 + (C_1 + \beta/6)p_4 + C_2p_5 + C_3p_6 + \ldots$$

$$C_{n-2}p_n = \beta(3q_1 + 2q_2 + q_3 + q_{4/6} - m_1)$$

(A.2 .4)

$$[C_n + (n-1)\beta]p_1 + [C_{n-1} + (n-2)\beta]p_2 + \ldots\ldots [C_1 + \beta/6]p_n$$

$$= \beta[nq_1 + (n-1)q_2 + \ldots\ldots q_{n-1} + q_{n/6}]$$

Where

$$C_1 = 2(c_1 - c_2), \quad C_2 = c_1 - 2c_2 + c_3,$$

$$C_3 = c_2 - 2c_3 + c_4, \quad C_n = c_{n-1} - 2c_n + c_{n+1}, \qquad \text{(A.2 .5)}$$

$$\beta = \frac{a^3BE}{E_bI(1-\nu^2)}, \qquad \text{(A.2 .6)}$$

$q_1, q_2 \ldots\ldots q_n = (Q_1, Q_2 \ldots\ldots Q_n)/B$, and $m_1 = \dfrac{M_1}{a^2B}$

The n-1 equations given by (A. .4) together with the conditions of vertical equilibrium,

$$a.B(p_1 + p_2 + \ldots\ldots p_n) = a.B(q_1 + q_2 + \ldots\ldots q_n)$$

give n equations to solve for n unknown contact stresses p_1, p_2 $\ldots\ldots p_n$.

Ohde's method was applied to obtain the influence coefficients for contact stress distribution of beams with L/B = 5, 10, 20, subjected to a concentrated unit load in their centres. In table A.1.1 the influence coefficients c_n and C_n (see equations A.2.1 and A.2.5) are given. Tables (A.2.2 a-c) give the values of p_1/q_m, p_2/q_m, ... p_n/q_m (q_m is the average stress on beam elastic continuum interface due to applied unit load) for different values of $\beta\left(\beta = \frac{a^3BE}{E_b I(1-\nu^2)}\right)$. The values of Barden's coefficients $\left(10^4\phi = \frac{\pi EL^4}{4E_b I(1-\nu^2)}\right)$ corresponding to β values are also given.

Table A.2.1 - The values of coefficients C_n and c_n (number of elemental areas n = 10)

L/B	5	10	20
c_1	0.76589	1.12223	1.53179
C_1	-0.94007	-1.5836	-2.37528
c_2	0.29586	0.033043	0.34415
C_2	0.33010	0.62215	1.00563
c_3	0.15593	0.16078	0.16214
C_3	0.08914	0.11546	0.12685
c_4	0.10513	0.10659	0.10698
C_4	0.02483	0.02738	0.02813
c_5	0.07917	0.07979	0.07994
C_5	0.1025	0.01079	0.01094
c_6	0.06345	0.06377	0.06385
C_6	0.00519	0.00536	0.00541
c_7	0.05293	0.05311	0.05316
C_7	0.00299	0.00305	0.00307
c_8	0.04540	0.04551	0.04554
C_8	0.00187	0.00190	0.00191
c_9	0.03974	0.03982	0.03984
C_9	0.00125	0.00127	0.00127
c_{10}	0.03533	0.03539	0.03540
C_{10}	0.00881	0.00886	0.00887

L/B = 5 (a)

$10^4\,\phi$	β	p_1/q_m	p_2/q_m	p_3/q_m	p_4/q_m	p_5/q_m
0	0	1.44022	0.94566	0.89607	0.86515	0.85290
10	0.0025	1.30818	0.91845	0.91460	0.92244	0.93633
50	0.0127	0.89788	0.83065	0.96856	1.10049	1.20243
100	0.0255	0.55539	0.75147	1.00703	1.24907	1.43704
300	0.0764	-0.06614	0.57211	1.03645	1.51759	1.93998
500	0.1273	-0.28630	0.47116	1.00350	1.61005	2.20159
700	0.1782	-0.38250	0.39864	0.95523	1.64695	2.38169
1000	0.2546	-0.43741	0.31609	0.87720	1.66072	2.58340
5000	1.2733	-0.23254	-0.05169	0.24296	1.31369	3.72757
10000	2.5465	-0.09880	-0.10436	-0.02019	0.91491	4.30845

L/B = 10 (b)

10^4	β	p_1/q_m	p_2/q_m	p_3/q_m	p_4/q_m	p_5/q_m
0	0	1.31719	0.97441	0.92415	0.89755	0.88669
10	0.0013	1.27307	0.96276	0.93002	0.91781	0.91635
50	0.0064	1.11238	0.91988	0.95090	0.99160	1.02524
100	0.0127	0.94142	0.87339	0.97214	1.07013	1.14292
300	0.0382	0.47269	0.73871	1.02226	1.28561	1.48072
500	0.0637	0.19618	0.65023	1.04161	1.41283	1.69914
700	0.0891	0.01715	0.5856	1.04573	1.49517	1.85636
1000	0.1273	-0.15328	0.51326	1.03719	1.57331	2.02951
5000	0.6367	-0.43159	0.14631	0.71589	1.66650	2.90289
10000	1.2733	-0.31557	-0.01487	0.42376	1.52396	3.38272

L/B = 20 (c)

$10^4\phi$	β	p_1/q_m	p_2/q_m	p_3/q_m	p_4/q_m	p_5/q_m
0	0	1.23514	0.9113	0.94318	0.92007	0.91049
10	0.0006	1.21924	0.98621	0.94518	0.92768	0.92169
50	0.0032	1.15783	0.96716	0.95284	0.95707	0.96510
100	0.0064	1.08583	0.94470	0.96168	0.99153	1.01626
300	0.0191	0.84162	0.86724	0.99021	1.10849	1.19244
500	0.0318	0.65077	0.80490	1.01047	1.19996	1.33389
700	0.0446	0.49795	0.75337	1.02486	1.27328	1.45053
1000	0.0637	0.31911	0.69046	1.03873	1.35916	1.59254
5000	0.3183	-0.36843	0.35028	0.97726	1.68879	2.35210
10000	0.6367	-0.44339	0.19001	0.81942	1.71407	2.71989

Tables A.2.2 a-c Influence coefficients for the contact stress distribution, using Ohde's method

(The number of elemental areas n = 10)

(a) L/B = 5

(b) L/B = 10

(c) L/B = 20

REFERENCES

[1] BARDEN, L (1962). 'Distribution of Contact Pressure Under Foundations'. Geotechnique, Vol. 12, pp. 181-197.

[2] BARDEN, L (1962a). PhD Thesis, University of Liverpool. 'The distribution of contact pressure under foundation'.

[3] BARDEN, L (1963). 'The Winkler model and its application to soil'. Structural Engineer, Vol. 41, No. 9.

[4] BIOT, M A (1937). 'Bending of an infinite beam on an elastic foundation'. Journal of Applied Mechanics, Transactions, Amer. Soc. of Mech. Engrs. Vol. 59, pp A1-A7.

[5] BOUSSINESQ, J (1885). 'Applications des Potentiels à l'Étude de l'Équilibre et du Monnement des Solides Élastiques', Paris, Gauthier-Villard.

[6] BURLAND, J B and LORD, J A (1969). 'The load-deformation behaviour of middle chalk at Mundford, Norfolk'. Proc of Institution of Civil Engineering Conf., London 1969.

[7] CUNNELL, M D (1974). PhD Thesis, University of Aston in Birmingham.

[8] DRAPKIN, B (1955). 'Grillage beams on elastic foundations', Proc, ASCE, Proc - separate No. 771, Vol. 81.

[9] FEDA, J (1961). 'Research on the Bearing Capacity of Loose Soil', Proc 5th Int. Conf. Soil Mech, Paris, Vol. 1, pp. 635-642.

[10] FILONENKO-BORODICH, M M (1940). 'Some Approximate Theories of the Elastic Foundations' (in Russian) Uchenyie Zapiski Moskovskogo Gosudarstuennogo Universiteta Mekhanica, No. 46.

[11] GIBSON, R E (1967). 'Some results concerning displacements and stresses in a non-homogeneous elastic half-space'. Geotechnique, 17, pp. 58-67.

[12] GIBSON, R E and SILLS, G C (1971). 'Some results concerning the plane deformation of a non-homogeneous elastic half-space'. Roscoe Memorial Symp., Cambridge.

[13] HETENYI, M (1946). 'Beams on elastic foundations', Univ. of Michigan Press, Ann Arbor.

[14] HETENYI, M (1950). 'A General Solution for the Bending of Beams on an Elastic Foundation of Arbitrary Continuity'. Journal of Applied Physics, Vol. 21, pp 55-58.

[15] JAMES, R M F (1967). PhD Thesis, University of Manchester.

[16] KERR, A D (1964). 'Elastic and Viscoelastic Foundation Models'. Applied Mech. Div. ASME, Paper No. 64

[17] KOLBUSZEWSKI, J J (1948). 'An experimental study of the maximum and minimum porosities of sands'. Proc. 2nd Inter. Conf. Soil Mech. Vol. 1, pp. 158-165.

[18] KOLBUSZEWSKI, J J and JONES, R H (1961). 'The preparation of sand samples for Laboratory Testing'. Proc. Midland S M F E Soc. Vol. 4, pp. 107-123.

[19] LOVE, A E H (1944). 'A treatise on the mathematical theory of elasticity'. Dover publications, Inc., New York.

[20] MARSLAND, A (1971). 'Large in-situ tests to measure the properties of stiff fissured clays'. Pro. First Australian-New Zealand Conf. on Geomechanics, Vol. 1.

[21] N A G (1974). Nottingham Algarithms Group ICL 1900 System N A G Library Manual.

[22] OHDE, J (1942). 'Die Berechnung der Sohldruckuerteilung unter Gründungskörpen'. Der Baningenieur, Vol. 23, pp 99-107.

[23] PASTERNAK, P L (1954). 'On a New Method of Analysis of an Elastic Foundation by Means of Two Foundation Constants' (in Russian), Gosudarstvennoe Izdatelstro Literaturi Po Stroitelstvu i Arkhitekture, Moscow, USSR.

[24] REISSNER, E (1958). 'A Note on Deflections of Plates on a Viscoelastic Foundation'. Jour. of Applied Mech. Vol 25, Trans. ASME, Vol. 80.

[25] SELVADURAI, A P S (1975). 'Elastic Analysis of Soil-Foundation Interaction'. Surrey University Press (in press).

[26] SELVADURAI, A P S (1975). 'Combined Foundations'. Chapter 5 in 'Design and Construction of Engineering Foundations', Chapman and Hall, London (in press).

[27] SIMONS, N E (1971). 'The stress path method of settlement analysis applied to London clay'. Roscoe Memorial Symp., Cambridge.

[28] TERZAGHI, K (1955). 'Evaluation of coefficient of subgrade reaction'. Geotechnique Vol. 5, pp. 297 - 326

[29] TERZAGHI, K (1943). 'Theoretical Soil Mechanics'. Wiley, New York.

[30] TIMOSHENKO, S P and GOODIER, J N (1961). 'Theory of elasticity', New York McGraw-Hill.

[31] TIMOSHENKO, S P (1965). Theory of Structures. New York, McGraw-Hill.

[32] VESIC, A B (1961). 'Bending of beams resting on isotropic elastic solid'. Journal of the Eng. Mech. Div., Proc. of the Amer. Soc. of Civil Eng., EM2, pp. 35 - 55.

[33] VESIC, A B (1963). 'Model studies of beams resting on a silt subgrade'. Journal of SMFD Proc. of the ASCE, SM1, pp 1-28.

[34] VLASOV, V Z (1949). 'Structural Mechanics of Thin Walled Three Dimensional Systems' (in Russian). Stroizdat.

[35] VLASOV, V Z and LEONTIEV, N N (1960). 'Beams, Plates and Shells on an Elastic Foundation' (in Russian). Fizmatgiz, Moscow, USSR.

[36] WALKER, B P and WHITAKER, T (1967). 'Apparatus for Forming Uniform Beds of Sand for Model Foundation Tests'. Geotechnique 17, pp. 161 - 167.

[37] WATSON, G N (1924). 'Treatise on the theory of Bessel functions'. Cambridge University Press, London.

[38] WINKLER, E (1867). 'Die Lehre von der Elasticitaet und Festigkeit'. Prag. Dominicus.

[39] WROTH, C P (1971). 'Some aspects of the elastic behaviour of overconsolidated clay'. Roscoe Memorial Symp., Cambridge.

[40] ZEEVAERT, L (1972). 'Foundation Engineering for Difficult Subsoil Conditions'. New York, VAN, Nostrand Reinhald.

REFERENCES NOT REFERRED TO IN THE TEXT

[41] BREBNER, A and WRIGHT, W (1952). 'An Experimental Investigation to Determine the Variation of Sub-grade modulus of sand loaded by plates of different breadths'. Geotechnique, Vol. 3, pp. 307 - 311.

[42] CONVERSE, F J (1933). 'The Distribution of Pressure Under a Footing'. Civil Engineering, No. 3, pp. 207 - 209.

[43] DE BEER, E (1948). 'Computation of Beams Resting on Soil'. 2nd Inter. Conf. on Soil Mechanics and Foundation Engrg., Rotterdam, Vol. 1, pp. 119 - 122.

[44] DE BEER, E (1948). 'Tests for the Determination of the Distribution of Soil Reactions Underneath Beams Resting on Soil'. 2nd Inter. Conf. on Soil Mechanics and Foundation Engrg., Rotterdam, Vol. 2, pp. 142 - 148.

[45] FABER, O (1933). 'Pressure Distribution Under Bases and Stability of Foundations'. Structural Engineer, Vol. 11, pp. 116 - 125.

[46] HETENYI, M (1966). 'Beams and Plates on Elastic Foundations and Related Problems'. Applied Mech. Rev. Vol. 19, No. 2.

[47] HO, M M K (1969). 'Contact Pressure of A Rigid Circular Foundation'. Proc. ASCE, SMFD, SM3, pp. 791 - 802.

[48] SCHULTZE, E (1961). 'Distribution of Stress Beneath a Rigid Foundation'. Proc. 5th Inter. Conf. on Soil Mechanics and Foundation Engrg., Paris, Vol. 1, pp. 807 - 818.

[49] SUTHERLAND, H B and LINDSAY, J A (1961). 'The Measurement of Load Distribution under Two Adjacent Column Footings'. 5th Inter. Conf. on Soil Mechanics and Foundation Engrg., Paris, Vol. 1, pp. 829 - 835.

[50] TENG, C Y (1949). Determination of the Contact Pressure Against a Large Raft Foundation'. Geotechnique, Vol. 1, pp. 222 - 228.